

**Quantitative genetic analysis of
temperature entrainment in the
Arabidopsis thaliana circadian clock**

Inaugural-Dissertation

Zur

Erlangung des Doktorgrades
der Mathematisch-Naturwissenschaftlichen Fakultät
der Universität zu Köln

vorgelegt von

Eleni Boikoglou

aus Thessaloniki, Griechenland

Köln 2008

Die vorliegende Arbeit wurde am Max-Planck-Institut für Züchtungsforschung Köln,
in der Arbeitsgruppe von Dr. Seth J. Davis, Abteilung für Entwicklungsbiologie der
Pflanzen (Direktor Prof. Dr. George Coupland) angefertigt.

Berichterstatter: Prof. Dr. George Coupland
Prof. Dr. Ute Höcker

Prüfungsvorsitzender: Prof. Dr. Wolfgang Werr

Tag der mündlichen Prüfung: 22 April 2008

“Time is the wisest of all counselors”

Plutarch

ABSTRACT

The circadian clock is an internal mechanism that measures external time and generates overt rhythms. About 90% of the transcripts in the *Arabidopsis thaliana* genome are rhythmically expressed (Michael et al., 2008). Thus, all cellular process can be clock controlled to generate rhythmic physiological responses. Mathematical modeling predicted that the basic clock framework that generates various rhythmic outputs is comprised of three interlocking-feedback loops. The 24-hour rhythms are generated by the main *CCA1/LHY-TOC1* feedback loop (Alabadi et al., 2001). Other genes, such as *PRR7/PRR9* and *GI*, were shown to participate in morning or evening loops to fine tune rhythmicity (Locke et al., 2006; Zeilinger et al., 2006). This model takes in account experimental data generated under light-dark cycles. From this model, we can now hope to add environmental inputs, such as light and temperature entrainment, as integrated mechanisms within the circadian oscillator. What is relevant here is that in addition to light, temperature can also entrain the circadian oscillator. Whereas some understandings of light effects are known, it remains unclear how temperature sets the plant-circadian clock.

In this thesis, I investigated temperature entrainment, as compared to light-dark entrainment, on the *Arabidopsis thaliana* circadian clock. For this, natural variation present in two Recombinant Inbred Lines (RILs) was exploited. The RILs were transformed with a circadian controlled and temperature regulated promoter::reporter construct. Period analysis of this *CCR2* reporter after both entrainments revealed a number of Quantitative Trait Loci (QTL) for each collection assayed. The findings suggested that the circadian clockwork after light-dark and temperature entrainment is controlled by both the same, as well as by different, QTLs. Additionally, it was shown that significant allelic interactions modify the period of *CCR2*. A QTL that was detected, specifically, after temperature entrainment was delineated by fine-mapping procedure.

Previous natural-variation studies in the vast majority of pre-existing RILs exploited the variation of two diverse ecotypes, of otherwise rarely used genetic backgrounds. This caveat restricts QTL fine mapping. To confront this disadvantage, six new RILs were generated by pairwise crosses between the four most commonly lab accessions: Columbia, C24, Landsberg *erecta*, and Wassilewskija. The latter two

accessions were previously transformed with *CCR2::LUC* and used as pollen donor on the other three as a female recipient. All RIL populations were selected for short or long period of *CCR2* after light-dark entrainment. Assessment of flowering-time variation under inductive long days, and circadian rhythmicity of *CCR2::LUC* was measured after light-dark and temperature entrainment. QTL mapping led to the identification of QTLs controlling these two processes. The traits shared some correlations.

The majority of the above described QTLs under these two entrainments co-localized with already known components of the circadian oscillator. An alternative approach to physiologically map the role of already known clock genes after temperature-entrainment was thus taken. The transcriptional kinetics of *CAB2*, *CCA1*, *LHY*, *TOC1*, *CCR2*, *GI*, *ELF3*, and *ELF4* were assayed under various light-dark and temperature entrainment protocols. Each promoter displayed unique responses to the different protocols assessed. This suggested that the circadian oscillator is a dynamic mechanism that is able to respond at a variety of signal changes within the ambient environment. The key role of two evening expressed genes, *TOC1* and *GI*, was further defined through the use of genetics, in response to temperature entrainment. A model for *GI* as a light resettor and *TOC1* as a thermal resettor was proposed.

ZUSAMMENFASSUNG

Der circadiane Rhythmus ist ein innerer Mechanismus, der äußere Zeitgeber misst und einen offenen Rhythmus erzeugt. Etwa 90% der Transkripte des *Arabidopsis thaliana* Genoms sind rhythmisch expremiert (Michael et al., 2008). Somit können alle zellulären Prozesse durch die innere Uhr kontrolliert werden, um rhythmische physiologische Antworten zu generieren. Mathematische Modelle sagen voraus, dass das Grundgerüst der inneren Uhr, das verschiedene rhythmische Leistungen hervorbringt, aus drei ineinander greifenden Rückkopplungsschleifen besteht. Die 24-Stunden-Rhythmen werden durch die Hauptrückkopplungsschleife *CCA1/LHY-TOC1* erzeugt (Alabadi et al., 2001). Für andere Gene, wie *PRR7/PRR9* und *GI*, wurde gezeigt, dass sie Teil der Morgen- oder Abend-Schleifen sind, um die Rhythmik fein abzustimmen (Locke et al., 2006; Zeilinger et al., 2006). Dieses Modell berücksichtigt experimentelle Daten, die unter Licht-Dunkel-Zyklen gewonnen wurden. Basierend auf diesem Modell können wir jetzt hoffen, Umwelteinflüsse wie Licht- und Temperaturabstimmung als integrierte Mechanismen innerhalb des circadianen Oszillators hinzuzufügen. Hierbei relevant ist, dass zusätzlich zum Licht auch die Temperatur den circadianen Oszillator modifizieren kann. Während bereits einige Kenntnisse über die Lichteffekte existieren, bleibt es unklar, wie die Temperatur die innere Uhr der Pflanzen justiert.

In dieser Doktorarbeit habe ich die Temperaturanpassung im Vergleich zur Licht-Dunkel-Anpassung der inneren Uhr von *Arabidopsis thaliana* untersucht. Dafür wurden natürliche Variationen zwischen zwei rekombinanten Inzuchtlinien (Recombinant Inbred Lines, RILs) ausgenutzt. Die Inzuchtlinien wurden mit einem circadian kontrollierten und temperaturregulierten Promotor::Reporter Konstrukt transformiert. Die Analyse der Periode dieses *CCR2* Reporters nach beiden Abstimmungen zeigte eine Reihe von QTLs (Quantitative Trait Loci) auf, die für diese Kollektion untersucht wurden. Die Befunde weisen darauf hin, das die circadiane Uhr nach Licht-Dunkel- und Temperatur-Anpassung von sowohl denselben, als auch von verschiedenen QTLs kontrolliert wird. Zusätzlich wurde gezeigt, dass signifikante Interaktionen zwischen den Allelen die Periode von *CCR2*

modifizieren. Ein QTL wurde speziell nach Temperatur-Anpassung identifiziert und durch Fein-Kartierung abgegrenzt.

Vorangehende Studien über natürliche Variation der großen Mehrheit bereits existierender RILs nutzte die Variation zweier verschiedener Ökotypen mit einem selten genutzten genetischen Hintergrund. Dieser Vorbehalt schränkte die QTL-Feinkartierung ein. Um diesem Nachteil entgegenzuwirken, wurden sechs neue RILs durch paarweises Kreuzen zwischen den vier häufigsten Labor-Ökotypen, Columbia, C24, Landberg *erecta*, und Wassilewskija, generiert. Die beiden letzteren wurden zuvor mit *CCR2::LUC* transformiert und als Pollenspende für die anderen drei weiblichen Empfänger genutzt. Alle RIL Populationen wurden für kurze oder lange Perioden des *CCR2* nach Licht-Dunkel-Anpassung ausgewählt. Die Bestimmung von Blühzeitpunktvariationen unter induktiven Langtagbedingungen und die circadiane Rhythmik von *CCR2::LUC* wurden nach Licht-Dunkel und Temperatur-Anpassung gemessen. QTL Kartierung führte zur Identifikation von QTLs, die diese beiden Prozesse kontrollieren. Beide Merkmale teilten einige Korrelationen.

Die Mehrzahl der oben beschriebenen QTLs unter diesen zwei Anpassungen colokalisierte mit bereits bekannten Komponenten des circadianen Oszillators. Deshalb wurde ein alternativer Ansatz unternommen, um die Rolle von bereits bekannten Uhr-Genen nach Temperatur-Anpassung physiologisch zu entschlüsseln. Die Transkriptionskinetik von *CAB2*, *CCA1*, *LHY*, *TOC1*, *CCR2*, *GI*, *ELF3*, und *ELF4* wurde unter verschiedenen Licht-Dunkel- und Temperatur-Anpassungsprotokollen untersucht. Jeder Promotor zeigte einzigartige Antworten auf die verschiedenen, angewendeten Protokolle. Dies deutet an, dass der circadiane Oszillator ein dynamischer Mechanismus ist, der in der Lage ist, auf eine Vielfalt von Signaländerungen in der umgebenden Umwelt zu antworten. Die Schlüsselrolle zweier abends exprimierter Gene, *TOC1* und *GI*, wurde weiter durch den Gebrauch von Genetik in Reaktion auf Temperatur-Anpassung bestimmt. Ein Modell für *GI* als Licht-Rücksetzer und *TOC1* als Temperatur-Rücksetzer wurde vorgeschlagen.

TABLE OF CONTENTS

ABSTRACT.....	i
ZUSAMMENFASSUNG.....	iii
TABLE OF CONTENTS.....	v
LIST OF FIGURE ELEMENTS.....	vii
ABBREVIATIONS.....	xii
1 INTRODUCTION REVIEW	1
1.1 THE CIRCADIAN CLOCK.....	1
1.2 CIRCADIAN CLOCK MODEL OF VARIOUS ORGANISMS	7
1.2.1 <i>DROSOPHILA MELANOGASTER</i>	7
1.2.2 <i>NEUROSPORA CRASSA</i>	8
1.2.3 <i>DARIO NERIO</i>	10
1.2.4 GENETIC FRAMEWORK FOR <i>ARABIDOPSIS THALIANA</i>	11
1.3 ENTRAINMENT	17
1.3.1 Light regulation of the circadian clock.....	18
1.3.2 Temperature regulation of the circadian clock.....	19
1.4 NATURAL VARIATION	22
2 MATERIALS AND METHODS.....	26
2.1 MATERIALS.....	26
2.1.1 Antibiotics.....	26
2.1.2 Bacterial strains.....	26
2.1.3 Plant material.....	26
2.1.4 Enzymes.....	29
2.1.5 Oligonucleotides.....	29
2.1.6 Media.....	31
2.1.7 Buffers and solutions.....	32
2.1.8 Software, databases, and other internet resources.....	34
2.1.9 Materials for luciferase imaging.....	34
2.2 METHODS.....	35
2.2.1 Agrobacterium-mediated transformation of Arabidopsis plants.....	35
2.2.2 Plant material treatments.....	36
2.2.3 DNA extraction.....	38
2.2.4 PCR.....	38
2.2.5 Restriction digestion.....	39
2.2.6 Flowering time assays with new Recombinant Inbred Lines.....	39
2.2.7 Plant growth conditions.....	39
2.2.8 Determination of clock phenotypes with promoter-luciferase assays.....	41
2.2.9 Software for analysis of circadian rhythms.....	42
2.2.10 QTL mapping.....	43
2.2.11 Statistical analysis.....	43
3 QUANTITATIVE ANALYSIS OF LIGHT-DARK vs TEMPERATURE ENTRAINMENT	45
INTRODUCTION	45
3.1 Light dark vs temperature entrainment of Cvi/Ler RIL.....	47

3.1.1	Period differences after light-dark and temperature entrainment of the Cvi/Ler population.....	50
3.1.2	Statistic analysis of mean period after LD vs. tmp entrainment in the CvL RIL	53
3.1.3	QTL mapping of periodicity in the CvL collection.....	56
3.1.4	Allelic interactions	62
3.2	Light dark vs temperature entrainment of Bay/Sha RIL	69
3.2.1	Period differences after LD or tmp entrainment of the BxS population.....	72
3.2.2	Statistic analysis of mean period after LD vs. tmp entrainment in the BxS RIL	73
3.2.3	QTL mapping of BxS.....	76
3.2.4	Allelic interactions in BxS	80
3.3	Temperature entrainment in constant darkness: etiolated tissue QTLs	84
3.3.1	Non-normal distribution of period in etiolated periodicity	87
3.3.2	QTL mapping results of CvL in temperature cycles in constant darkness	89
3.3.3	Allelic interactions in CvL after the temperature entrainment in constant darkness.....	93
4	GENERATION OF NEW RILS COLLECTIONS.....	96
	INTRODUCTION	96
4.1	Generation of new Recombinant Inbred Lines (nRILS)	97
4.2	Determination of the genotype WSC24 RIL lines	98
4.3	Determination of two continuous traits in the C24WS RILS.....	101
4.3.1	Flowering-time assays of C24WS RIL under inductive long days.....	101
4.3.2	Circadian rhythm assays under light-dark and temperature cycles.....	120
4.4	Conclusions-Remarks.....	126
5	PHYSIOLOGICAL ANALYSIS OF VARIOUS CLOCK MARKERS.....	127
5.1	Light vs. temperature entrainment of various clock markers	128
5.2	IN-OUT of phase experiments of various clock reporter genes	133
5.3	Light vs. temperature: driven or entrained rhythms	137
5.4	Study of <i>GI</i> and <i>TOC1</i> under light and temperature entrainment.....	143
5.5	Light vs. temperature: driven or entrained rhythms	148
5.6	Conclusions-Remarks.....	153
6	GENERAL CONCLUSIONS AND DISCUSSION.....	156
6.1	GENERAL CONCLUSIONS - FUTURE PERSPECTIVES	156
6.2	DISCUSSION	173
7	REFERENCES.....	179
	APPENDIX 1.....	A
	ACKNOWLEDGMENTS.....	H

LIST OF FIGURE ELEMENTS

Figure 1.1 A simplified version of the circadian clock.....	6
Figure 1.2 The multiple feedback loop of the <i>Arabidopsis thaliana</i> circadian clock	15
Figure 2.1 Crosses performed to generate six new RIL collections, each harboring the <i>CCR2::LUC</i> transgene	37
Figure 2.2 INOUT entrainment protocols.....	40
Figure 3.1 Period differences of rhythmic plants within genotypes of the CvL RIL collection of temperature-entrained versus light-dark entrained plants.....	50
Figure 3.2 Variation of period after entrainment to the two different protocols between two representative RILs: CvL 6 and CvL 47.....	52
Figure 3.3 The continuous distribution of period for 39 CvL Recombinant Inbred Lines.....	53
Figure 3.4 MapQTL for the light-dark entrainment of the CvL population	60
Figure 3.5 MapQTL for the temperature entrainment of the CvL population.....	61
Figure 3.6 Period variation due to allelic variation of the first chromosome QTL at PW4 locus after the light-dark entrainment in the CvL population.....	64
Figure 3.7 eriod variation due to allelic variation of the fifth chromosome QTL at BH.107L-Col locus after the light-dark entrainment in the CvL population...	64
Figure 3.8 Period variation due to allelic variation of the fifth chromosome QTL at CC.262C locus after the light-dark entrainment in the CvL population.....	65
Figure 3.9 Period variation due to interaction of two QTLs at chromosome 1 at locus PW4 and chromosome 5 at locus CC.262C after the light-dark entrainment in the CvL population	65
Figure 3.10 Period variation due to allelic variation of the first chromosome QTL at CH.160L-Col locus after the temperature entrainment in the CvL population	66
Figure 3.11 Period variation due to allelic variation of the fifth chromosome QTL at CC.262C locus after the temperature entrainment in the CvL population ...	66
Figure 3.12 Period variation due to interaction of two QTLs at chromosome 1 at locus CH.160L-Col and chromosome 5 at locus CC.262C after the temperature entrainment in the CvL population	67
Figure 3.13 Period differences of rhythmic plants of BxS RIL collection of temperature-entrained versus light-dark entrained plants.....	72
Figure 3.14 The continuous distribution of period for 69 BxS Recombinant Inbred Lines.....	73
Figure 3.15 MapQTL for the light-dark entrainment of the BxS population	78
Figure 3.16 MapQTL for the temperature entrainment of the BxS population.....	79
Figure 3.17 Period variation due to allelic variation of the second chromosome QTL at locus MSAT2-41 after the light-dark entrainment in the BxS population....	81
Figure 3.18 Period variation due to allelic variation of the fourth chromosome QTL at locus MSAT4-37 after the light-dark entrainment in the BxS population....	81
Figure 3.19 Period variation due to allelic variation of the fourth chromosome QTL at locus MSAT2-41 after the temperature entrainment in the BxS population	82

Figure 3.20 Period variation due to allelic variation of the fourth chromosome QTL at locus MSAT4-37 after the temperature entrainment in the BxS population	82
Figure 3.21 <i>CCR2</i> expression under constant darkness as reported by luciferase in various CvL independent lines after temperature cycles in constant darkness	86
Figure 3.22 Continuous distribution of period of 34 CvL RILs after temperature entrainment in constant darkness	88
Figure 3.23 Normal Q-Q plot to test for normality of continuous distribution of period for 34 CvL Recombinant Inbred Lines	88
Figure 3.24 Kruskal Wallis application of MapQTL for QTL detection after entrainment to temperature cycles in constant darkness of the CvL population	91
Figure 3.25 MQM output of MapQTL for QTL detection after entrainment to temperature cycles in constant darkness of the CvL population.....	92
Figure 3.26 Period variation due to allelic variation of the main effect QTL at the first chromosome at locus CH.160L-Col identified for temperature entrainment in constant darkness in the CvL population	94
Figure 3.27 Period variation due to allelic variation of the main effect QTL at the first chromosome at locus HH.143C identified for temperature entrainment in constant darkness in the CvL population	94
Figure 4.1 The continuous distribution of total leaf number for 80 out of 85 C24WS Recombinant Inbred Lines	103
Figure 4.2 MapQTL for flowering time under long days of the long period selected C24WS RIL lines.....	106
Figure 4.3 MapQTL for flowering time under long days of the short period selected C24WS RIL lines.....	107
Figure 4.4 MapQTL for flowering time under long days of the total number of C24WS RIL lines.....	108
Figure 4.5 Flowering time variation in the long period selected lines due to allelic variation of the first chromosome QTL at locus NGA59	110
Figure 4.6 Flowering time variation in the long period selected lines due to allelic variation of the fourth chromosome QTL at locus FRI	110
Figure 4.7 Flowering time variation in the long period selected lines due to allelic variation of the fifth chromosome QTL at locus NGA106.....	111
Figure 4.8 Flowering time variation in the long period selected lines due to interaction of two QTLs at chromosome 1 at locus SO392 and chromosome 5 at locus NGA106.....	111
Figure 4.9 Flowering time variation in the short-period selected lines due to allelic variation of the fifth chromosome QTL at locus NGA106.....	113
Figure 4.10 Flowering time variation in the short-period selected lines due to allelic variation of the fifth chromosome QTL at locus NGA76.....	113
Figure 4.11 Flowering time variation in the short-period selected lines due to allelic variation of the fourth chromosome QTL at locus FRI	114
Figure 4.12 Flowering time variation in the short-period selected lines due to interaction of two QTLs at chromosome 4 at locus FRI and chromosome 5 at locus NGA76	114
Figure 4.13 Flowering time variation in all RILs of the C24WS population due to allelic variation of the fifth chromosome QTL at locus NGA106.....	116

Figure 4.14 Flowering time variation in all RILs of the C24WS population due to allelic variation of the fourth chromosome QTL at locus FRI in the C24WS population	116
Figure 4.15 Flowering time variation in all RILs of the C24WS population due to allelic variation of the first chromosome QTL at locus NGA59	117
Figure 4.16 Flowering time variation in all RILs of the C24WS population due to interaction of two QTLs at chromosome 1 at locus SO392 and chromosome 5 at locus NGA76.....	117
Figure 4.17 Flowering time variation in all RILs of the C24WS population due to interaction of two QTLs at chromosome 4 at locus FRI and chromosome 5 at locus NGA106	118
Figure 4.18 Period differences of rhythmic plants within genotypes of the C24WS RIL collection of temperature-entrained versus light-dark entrained plants	123
Figure 4.19 MapQTL for the light-dark entrainment of the C24WS population....	124
Figure 4.20 MapQTL for the temperature entrainment of the C24WS population.....	125
Figure 5.1 <i>GI::LUC</i> rhythms after light-dark entrainment to 14 hours light::10 hours darkness, 10 hours light::14 hours darkness, and temperature entrainment to 14 hours warm::10 hours cool, 10 hours warm::14 hours cool.....	130
Figure 5.2 <i>CCR2::LUC</i> rhythms after light-dark entrainment to 14 hours light::10 hours darkness, 10 hours light::14 hours darkness, and temperature entrainment to 14 hours warm::10 hours cool, 10 hours warm::14 hours cool.....	131
Figure 5.3 <i>TOC1::LUC</i> rhythms after light-dark entrainment to 14 hours light::10 hours darkness, 10 hours light::14 hours darkness, and temperature entrainment to 14 hours warm::10 hours cool, 10 hours warm::14 hours cool.....	132
Figure 5.4 <i>CCA1::LUC</i> rhythms after the light-dark entrainment (LD) and synchronous entrainment of light dark and temperature cycles, where IN denotes onset of warm temperatures in the middle of the light period and OUT the onset of cool temperatures in the middle of the light period.....	135
Figure 5.5 <i>TOC1::LUC</i> rhythms after the light-dark entrainment (LD) and synchronous entrainment of light dark and temperature cycles, where IN denotes onset of warm temperatures in the middle of the light period and OUT the onset of cool temperatures in the middle of the light period.....	136
Figure 5.6 <i>TOC1::LUC</i> rhythms after entrainment in T-cycles of 14 hours of light::14 hours of darkness, 10 hours of light::10 hours of darkness for the light-dark entrainment, and 14 hours of warm::14 hours of cool, 10 hours of warm::10 hours of cool for the temperature entrainment.....	140
Figure 5.7 <i>CCR2::LUC</i> rhythms after entrainment in T-cycles of 14 hours of light::14 hours of darkness, 10 hours of light::10 hours of darkness for the light-dark entrainment, and 14 hours of warm::14 hours of cool, 10 hours of warm::10 hours of cool for the temperature entrainment.....	141

Figure 5.8 *GI::LUC* rhythms after entrainment in T-cycles of 14 hours of light::14 hours of darkness, 10 hours of light::10 hours of darkness for the light-dark entrainment, and 14 hours of warm::14 hours of cool, 10 hours of warm::10 hours of cool for the temperature entrainment.....142

Figure 5.9 *CCR2::LUC* rhythms in the *gi-11* mutant after light-dark entrainment to 14 hours light::10 hours darkness, 10 hours light::14 hours darkness, and temperature entrainment to 14 hours warm::10 hours cool, 10 hours warm::14 hours cool.....145

Figure 5.10 *CCR2::LUC* rhythms in the *toc1-21* mutant after light-dark entrainment to 14 hours light::10 hours darkness, 10 hours light::14 hours darkness, and temperature entrainment to 14 hours warm::10 hours cool, 10 hours warm::14 hours cool.....146

Figure 5.11 *CCR2::LUC* rhythms in the double mutant *gi-11 toc1-21* mutant after light-dark entrainment to 14 hours light::10 hours darkness, 10 hours light::14 hours darkness, and temperature entrainment to 14 hours warm::10 hours cool, 10 hours warm::14 hours cool.....147

Figure 5.12 *CCR2::LUC* rhythms in *gi-11* after entrainment in T-cycles of 14 hours of light::14 hours of darkness, 10 hours of light::10 hours of darkness for the light-dark entrainment, and 14 hours of warm::14 hours of cool, 10 hours of warm::10 hours of cool for the temperature entrainment.....150

Figure 5.13 *CCR2::LUC* rhythms in *toc1-21* after entrainment in T-cycles of 14 hours of light::14 hours of darkness, 10 hours of light::10 hours of darkness for the light-dark entrainment, and 14 hours of warm::14 hours of cool, 10 hours of warm::10 hours of cool for the temperature entrainment..... 151

Figure 5.14 *CCR2::LUC* rhythms in the double mutant *gi-11 toc1-21* after entrainment in T-cycles of 14 hours of light::14 hours of darkness, 10 hours of light::10 hours of darkness for the light-dark entrainment, and 14 hours of warm::14 hours of cool, 10 hours of warm::10 hours of cool for the temperature entrainment.....152

Table 2.1 Bayreuth-0/Shakdara RIL lines that were transformed with <i>CCR2::LUC</i> mediated by <i>A. tumefaciens</i>	28
Table 2.2 <i>Cvi/Ler</i> RIL lines that were transformed with <i>CCR2::LUC</i> mediated by <i>A. tumefaciens</i>	28
Table 2.3 SSLPs/CAPS/derived CAPS markers used for mapping the 1 st chromosome QTL of the <i>CvL</i> population	29
Table 2.4 SSLPs/CAPS primers used for genotyping the C24WS RIL population	30
Table 3.1 The free-running period of the <i>Cvi/Ler</i> RIL collection under constant light after entrainment to 12 hours light followed by 12 hours dark.....	48
Table 3.2 The free-running period of the <i>Cvi/Ler</i> RIL collection under constant light after entrainment in temperature cycles of 12 hours at 22°C followed by 12 hours at 16°C in constant light	49
Table 3.3 Statistic analysis of the <i>CvL</i> lines used for QTL mapping	55
Table 3.4 ANOVA analysis depicts significant genotype by environment interaction for the two different entrainments.....	55
Table 3.5 Concentrated results for the QTL identified in the <i>CvL</i> population after light dark or after temperature entrainment.....	68
Table 3.6 The free-running period of the Bay/Shal RIL collection under constant light after entrainment to 12 hours light followed by 12 hours dark.....	70
Table 3.7 The free running period of the Bay/Shal RIL collection under constant light after entrainment to 12 hours at 22°C followed by 12 hours at 16°C.....	71
Table 3.8 Statistic analysis of the BxS RIL lines used for QTL mapping showed that the period average for light and temperature are marginally different for 95% of confidence interval.....	75
Table 3.9 ANOVA analysis shows significant genotype by environment interaction for the two different entrainments.....	75
Table 3.10 Concentrated results for the QTL identified in the BxS population after light dark or after temperature entrainment	83
Table 3.11 The free running period of the <i>Cvi/Ler</i> RIL collection in constant darkness, after entrainment in temperature cycles in constant darkness	85
Table 3.12 Concentrated results for the QTL identified in the <i>Cvi/Ler</i> population after temperature entrainment in constant darkness.....	95
Table 4.1 Allelic frequencies at various loci in the first chromosome for the long and short period selected lines.....	100
Table 4.2 Flowering time variation of the WSC24 RIL collection grown in 16 hours light:8 hours darkness in greenhouse.....	102
Table 4.3 Concentrated results for the QTL identified in the C24WS population for flowering time in inductive long days.....	119
Table 4.4 The free-running period of the C24WS RIL collection after light-dark entrainment under constant 22°C (LD) or after entrainment in temperature cycles of 12 hours at 22°C followed by 12 hours at 16°C under constant light (TMP).....	122

ABBREVIATIONS

AEQ AEQUORIN
ANOVA ANALYSIS OF VARIANCE
APRR ARABIDOPSIS PSEUDO RESPONSE REGULATOR
AtGRP7 ARABIDOPSIS THALIANA GLYCINE RICH PROTEIN 7
BxS BAYREUTH-0 / SHAKDARA RIL
CAB2 CHLOROPHYLL A/B BINDING 2
CAPS CLEAVED AMPLIFIED POLYMORPHIC SEQUENCE
CAT3 CATALASE 3
CBF C-REPEAT BINDING FACTOR
CCA1 CIRCADIAN CLOCK-ASSOCIATED 1
CCR1 COLD AND CIRCADIAN REGULATED 1
CCR2 COLD AND CIRCADIAN REGULATED 2
CLK CLOCK
CO CONSTANS
CRY CRYPTOCHROME
CRY2 CRYPTOCHROME 2
CvL CAPE VERDE ISLANDS / LANDSBERG *ERECTA* RIL
CYC CYCLE
DCAPS DERIVED CLEAVED AMPLIFIED POLYMORPHIC SEQUENCE
DD CONTINUOUS DARKNESS
ELF3 EARLY FLOWERING 3
ELF4 EARLY FLOWERING 4
EPR1 EARLY-PHYTOCHROME-RESPONSIVE 1
FLC FLOWERING LOCUS C
FLM FLOWERING LOCUS M
FRI FRIGIDA
FLO FREQUENCY-LESS OSCILLATOR
FRQ FREQUENCY
FT FLOWERING LOCUS T
GI GIGANTEA

GLM GENERAL LINEAR MODEL
ICE INDUCER OF *CBF* EXPRESSION
IM INTERVAL MAPPING
LD LONG DAY
LHY LATE ELONGATED HYPOCOTYL
LL CONTINUOUS LIGHT (RED AND BLUE LIGHT)
LOD LIKELIHOOD OF ODDS
LUC LUCIFERASE
LUX LUX ARRHYTHMO
MQM MULTIPLE QTL MAPPING
NILS NEAR ISOGENIC LINES
PER PERIOD
PHOT PHOTOTROPIN
PHY PHYTOCHROME
QTL QUANTITATIVE TRAIT LOCUS
R.A.E. RELATIVE AMPLITUDE OF ERROR
RILS RECOMBINANT INBRED LINES
SD SEGREGATION DISTORTION
SRR1 SENSITIVITY TO RED LIGHT REDUCED1
SSLP SIMPLE SEQUENCE LENGTH POLYMORPHISM
TIC TIME FOR COFFEE
TIM TIMELESS
TOC1 TIMING OF *CAB* EXPRESSION1
ZTL ZEITLUPE

1 INTRODUCTORY REVIEW

1.1 THE CIRCADIAN CLOCK

Most organisms experience dramatic changes in light and temperature during a daily and seasonal timescale. Seasonal changes in photoperiod and temperature affect many physiological processes during their life cycle. However, the most dramatic changes generally occur under diurnal conditions, during both light and dark, and of warm and cool cycles (Barak et al., 2000). Specifically, during the light period, temperatures are generally warmer, whereas during the night period, temperatures are generally cooler. These concerted changes take place essentially every day during the rotation of Earth around its axis of 24 hours. To anticipate these rhythmic changes, many organisms have evolved an internal-timing mechanism, called a circadian clock, from the latin *circa* and *dian*, meaning ‘about a day’. In this way, the circadian clock generates rhythms used in anticipation of the ever changing light and temperature environment.

Circadian rhythms are manifest from cyanobacteria to mammals to plants. The first report of diurnal rhythmicity was made in the fourth century BC, when Androsthene described that tamarind plants open and close their leaves periodically in course of 24 hours (Bretzl, 1903). However, the first experiments to directly test for circadian rhythms were recorded in 1729 by a French astronomer, de Mairan, who observed that the leaf movements of the plant *Mimosa pudica* were rhythmic in the absence of a changing environment. He thus conclusively demonstrated that an internal mechanism was involved (de Mairan, 1729). In early 1930s, Bünning and Stern studied leaf movements in bean plants and realized that exposure to brief dim red light was able to synchronize the circadian clock. When these experiments were performed in constant darkness, they observed that the period of leaf movement was not 24 hours, but extended to a periodicity of 25.5 hours. Therefore, the plants were not synchronized to a 24-hour period and were free running (Bünning, 1931). The persistence in the absence of environmental cues is then considered one of the key defining hallmarks of circadian rhythms.

Genetic studies in the mid 20th century were performed in the fruitfly *Drosophila melanogaster* by one of the two intellectual founders of circadian

rhythms, Colin Pittendrigh. The result of those studies led to the proposal that the circadian clock is a mechanism that measures the duration of light, which is termed photoperiod (Pittendrigh, 1964). To explain the photoperiodic phenomena, two different models were introduced called the external-and the internal-coincidence model. There are two basic differences between the two models. The internal model accepted that two or more oscillators are involved that may be coupled to inductive signals such as dawn or dusk. This suggested that while photoperiod changes, the phase relationship also changes. In contrast, the external-coincidence model accepted that there is one oscillator and that the external inductive signal has differential effect that varies with the steady-state of the oscillator (Pittendrigh, 1964). Indirectly, this led to the study of a phenomenon called entrainment. To date, those two models are still robustly debated in the scientific community.

Every circadian organism has its own endogenous period that may deviate from 24 hours. As one example, the mean periodicity in beans was found to be 25.5 hours (Buening, 1931). The only way for organisms to have rhythms of exactly 24 hours is for them to be synchronized every day to the changes of external environment. Studies in plants have shown that only when the internal and the external period match, enhanced fitness is conferred (Michael et al., 2003b; Dodd et al., 2005). To match these two periods, a synchronization process that is also called entrainment is obviously an absolute requirement. The main cues for this are changes in light and temperature.

The period of the entrained rhythms should remain the same for a range of temperatures. Unlike other processes, which are affected by temperature increases or decreases, circadian rhythms are temperature compensated. This temperature compensation, which is another defining hallmark of circadian rhythms, is a buffering mechanism of the circadian clock against long-term temperature variations (Gould et al., 2006). If the period of the clock is not temperature compensated then in two successive days, for example a warm one followed by a cool one, the oscillator would incorrectly entrain differentially. The clock in the warm day would run faster, therefore, will have a short period, whereas, in the cool day it would run slower, therefore, it would have a long period. Then the oscillator would be inappropriately at different state between these two successive dawns. Therefore, the adaptive significance of temperature-compensated period is that the clock has a preserved phase relationship to the environment, and thereby set all processes in good time.

The generated circadian rhythms have a characteristic waveform, described by peaks and troughs (Figure 1.1). These rhythms are defined by three key parameters named in the chronobiological community as period, phase, and amplitude, (Barak et al., 2000) (Figure 1.1). Amplitude is the half magnitude of the circadian oscillation from peak to trough. Period is the time an oscillation needs to progress a complete cycle with the end point of one cycle as the beginning of the next cycle, and it is approximately 24 hours. Phase is a time relative to a reference time point, usually the reference point is taken as the last onset of lights. Moreover, a recently added fourth parameter is precision-robustness of the rhythms, considered as an atypical parameter; it is measured by Relative Amplitude Error (RAE) (McWatters et al., 2007). RAE is defined as the ratio of the measured, or observed, amplitude error in relation to the most probable, or expected, amplitude error. This means that RAE is a measure of how well the actual data fit to the cosine curve generated by the least squares method. Of all four parameters, period is the most studied example from plants (Swarup et al., 1999; Michael et al., 2003b; Edwards et al., 2005).

The basis of the circadian clock in most organisms studied consists of a negative transcriptional/translational feedback loop. This loop has a positive and a negative part (Figure 1.1). The positive part of the loop induces the expression of the negative, and in turn, the negative part suppresses expression of the positive. To be a component of the feedback loop, certain requirements should be fulfilled. First, morning and evening expressed components, and their products, should oscillate in a circadian manner. Additionally, constitutive expression or loss of expression of a core clock component might cause arrhythmic behaviors (Wang and Tobin, 1998; Barak et al., 2000) (Aronson et al., 1994), although this is not always the case (Green and Tobin, 1999; Barak et al., 2000). Especially in the plant-circadian system, mutations in any of the core-oscillator genes results in a short-period rhythmic phenotype, whereas constitutive expression of some of any of these genes has been shown to be able to result in arrhythmic phenotypes (Wang and Tobin, 1998; Strayer et al., 2000). Obviously, any changes in the level of a core clock component can, thereby, set the various outputs.

The onset and offset of light is the main synchronization cue of the circadian clock. For some organisms, a dedicated photoreceptor mediates entrainment (Emery et al., 1998; Stanewsky et al., 1998; Emery et al., 2000). In contrast to a variety of organisms that detect only one wavelength of light, or do not differentiate between

different light intensities, plants can detect variations in light intensity, and wavelength, and set their physiology according to these changes (Fankhauser and Staiger, 2002; Nagy and Schafer, 2002). All these changes have a variable effect in the entrainment of the oscillator (Somers et al., 1998a; Yanovsky et al., 2001).

During the day-night cycle, dramatic changes in temperature in addition to light, occur over the 24 hour day, with light period thus coincides with warmer temperatures and dark period with cooler temperatures. The mechanistic effect on temperature on the circadian clock of several organisms has started to emerge (Diernfellner et al., 2005; Boothroyd et al., 2007; Busza et al., 2007). However, in what way temperature sets the plant circadian clock is not as known as light. However, changes in both signals, light and temperature, are able to synchronize the core oscillator and thereby sets the proper timing of gene expression, and temporal regulation of many output rhythms (Millar, 2004). These different outputs oscillate with the same 24-hour period, but they occur at different phases (Figure 1.1). For example, when two oscillations have a phase difference of 180 degrees, they are in antiphase.

Circadian clocks in various organisms are far more complicated than the oversimplified core oscillator (Figure 1.1). In the majority of eukaryotic model organisms, the core oscillator is comprised of multiple interlocking transcriptional/translational feedback loops of circadian controlled RNA and proteins. However, there are fundamental differences among key elements of the Arabidopsis circadian clock, the mammalian/Drosophila, and the Neurospora circadian clock. For example, sequence comparison between Arabidopsis clock genes compared to clock genes of other organisms revealed low to no conservation, supporting the notion that the plant-circadian clock has independent evolutionary origin. Apart from this, in mammals and Drosophila, the changes in the environmental signals are perceived by the eye, where photoreceptors are localized, and the signal is then transmitted to the central pacemaker, which is located in the Supra Chiasmatic Nuclei (SCN) in the brain, and thereby sets the phase of the various rhythmic outputs (Ashmore and Sehgal, 2003). In plants, the organization is not as hierarchical as in animals (Thain et al., 2002). A basic difference is that self-sustained core oscillators are not located in one organ, but are instead present in all parts of the plant. In plants, slave oscillators exist instead of peripheral oscillators (Heintzen et al., 1997; Kreps and Simon, 1997; Barak et al., 2000). Though, these oscillators are not able on their own to generate

rhythms in the manner peripheral oscillators do in mammals (Barak et al., 2000). Collectively, the plant-circadian machinery involves the core oscillator that generates rhythms, which then are fine tuned by slave oscillators. What follow is a comparison of the circadian clock of various organisms, in terms of molecular organization and function, and further emphasis will be given in the entrainment process of the *A. thaliana* circadian clock.

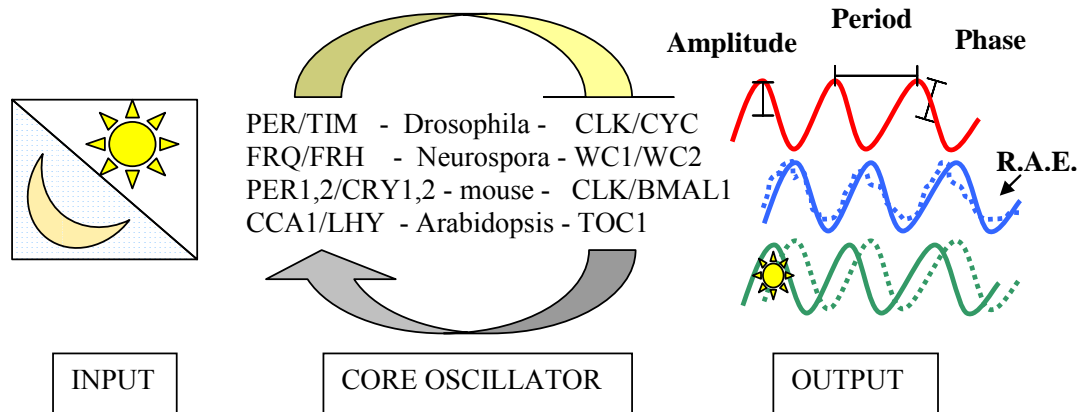


Figure 1.1 A simplified version of the circadian clock

The input pathway is represented by light dark and temperature cycles. The core oscillator is comprised by transcriptional-translational feedback loop. Here, the positive and negative elements of *Drosophila melanogaster*, *Neurospora crassa*, *Mus musculus*, and *Arabidopsis thaliana* are shown, respectively. The output pathway can be many diverse processes. The red and blue output oscillations correspond to two rhythmic outputs that are in antiphase (180 degrees difference between the two outputs), whereas blue and green has a phase shift, less than 180 degrees difference. The green dotted line represents the phase shifting effect of a light pulse at a certain time point, compared to the non pulsed solid green line. The dotted blue line represents an observed rhythmic output with high R.A.E, whereas the solid blue line represents an observed rhythmic output with low R.A.E.

1.2 CIRCADIAN CLOCK MODEL OF VARIOUS ORGANISMS

In this section, the circadian oscillator of various eukaryotic model organisms will be described and compared, with regard to similarities and basic differences, in synchronization to light versus temperature, and natural-variation studies. Comparison of a vertebrate animal, a fungus, an invertebrate animal and a model plant species will be assessed. First, the animal circadian clock will be reviewed using *Drosophila melanogaster* as a model.

1.2.1 DROSOPHILA MELANOGASTER

The most advanced studied eukaryotic organism with regard to its circadian clock is the fruitfly *Drosophila melanogaster*. The identification of *D. melanogaster* oscillator genes that comprise the central pacemaker has been based on mutagenesis screens (Konopka and Benzer, 1971). The circadian organization involves not only the neuronal circadian pacemaker that is comprised by interlocking negative feedback loops, but also peripheral clocks that exist in most tested organs (Plautz, J. D., 1997). Interestingly, these peripheral oscillators are unable to entrain themselves. This means that they are largely dependent on the central pacemaker for synchronization. As soon as they are synchronized, they are then able to maintain a stable phase (Hardin et al., 2003). Another difference to the fundamental properties of circadian clock is that wild-type flies in constant light and constant temperature are arrhythmic. This difference is in contrast to the key defining property of the circadian rhythms that explicitly states that circadian rhythms persist in absence of cues such as light or temperature. However, under constant light, temperature driven cycles wild-type flies were rhythmic, suggesting that the temperature cycles 'gate' light transduction to allow *D. melanogaster* clock to continue through out the day (Glaser and Stanewsky, 2005).

Drosophila's circadian clock is comprised by three interlocking feedback loops. The main loop consists of two reciprocally regulated genes named PERIOD (PER) and TIMELESS (TIM) (Hardin et al., 1990; Sehgal et al., 1995; Hardin, 2000). Together with PER and TIM, two other genes named CYCLE (CYC) and dCLOCK

(dCLK) comprise the primary negative feedback loop of *Drosophila*'s circadian clock, where PER/TIM form a heterodimer that represses dCLK and CYC, which in turn induce *per* and *tim* mRNA expression (Glossop et al., 1999)(Figure 1.1). Light input to *Drosophila* pacemaker is mediated through a blue light photoreceptor called Cryptochrome (CRY), where upon light induction, CRY forms complex with PER and TIM proteins (Emery et al., 1998; Stanewsky et al., 1998).

Temperature entrainment is mediated at the posttranscriptional level by the oscillations of the two central pacemaker components PER and TIM (Glaser and Stanewsky, 2005). Additionally, temporal analysis of genome-wide transcriptional profiles during temperature cycles, or light-dark cycles, and also in constant conditions after the synchronizing cycles in wild types and in TIM knockout-mutant flies, led to the conclusion that the organization of the temperature-entrained clock is very similar to the light entrained, since most of the clock genes oscillate in phase (Glaser and Stanewsky, 2005). Interestingly, in temperature entrainment, the *per* and *tim* genes display a temporal expression that is differential due to an advance of the *per*, and delay of *tim* mRNA expression, whereas in light entrainment these two genes have the same temporal expression under all entraining protocols tested (Boothroyd et al., 2007). The involvement of *per* and *tim* in light-dark and also in temperature entrainment suggest that thermoperception drives the clock in a similar way as photoperception. Although the most feasible scenario is that a gene can be a master controller of both entrainment processes, data indicate the existence of a specialized thermoreceptor in *D. melanogaster*. Potentially, in *D. melanogaster*, light and temperature information could be integrated in to the same clock, using the same, and also, specialized pathways. Though, the second impact role of temperature, as to temperature compensation, is mediated through PER protein, and polymorphisms in the number of Thr-Gly repeats indicate a latitudinal cline of these repeats, suggesting that selective pressure is present leading to ecological adaptation (Sawyer et al., 1997). All these collective findings suggest that PER and TIM play a central role in both light and in temperature entrainment.

1.2.2 NEUROSPORA CRASSA

Neurospora crassa is a filamentous fungus particularly interesting for molecular geneticists due to its haploid life cycle. Therefore, it is not a surprise that

the *Neurospora* circadian system is well defined. Approximately 19% of *Neurospora* transcripts cycle over circadian time, a number certainly higher than that of other higher eukaryotic organisms (Correa et al., 2003). Its circadian clock does not share similarities to *Drosophila*, due to its small and simple organization. Only few components are required for fungal circadian oscillator (Correa et al., 2003). The central component of the oscillator is the FREQUENCY (FRQ) gene, to which multiple roles and functions have been assigned (Gardner and Feldman, 1980; Dunlap et al., 1995). The FRQ-based oscillator is light dependent, since *FRQ* mRNA is rapidly induced by a light treatment (Crosthwaite et al., 1995). In addition to FRQ, the circadian clock of *Neurospora* is comprised of an interplay of four genes over the 24 hour cycle (Lee et al., 2000) (Figure 1.1). Specifically, FRQ interacts with an FRQ helicase (FRH), and they form a feedback loop with two White Collar (WC) genes, named WC1 and WC2 (Collett et al., 2001; Denault et al., 2001; Lee et al., 2003). The WC gene products physically interact and form the White Collar complex (WCC) (Cheng et al., 2002). In addition, temperature can synchronize the *Neurospora* circadian clock and this also through FRQ. FRQ is differentially spliced, giving rise to a long and short form of the FRQ. The ratio of the long and short forms of FRQ is temperature dependent. In higher temperatures the full length, or long form, predominate the short form (Diernfellner et al., 2007). The accumulation of the short form seems to be unaffected by temperature. Thus, the accumulation of long versus short form mediates temperature inputs.

Irrespective of how the FRQ-based oscillator works, micro-array analysis of *frq* null mutant strains after light-dark entrainment have identified three genes that have short period in constant darkness, supporting the notion of an oscillator independent of FRQ. Data indicate that a temperature-entrained oscillator independent of FRQ exists (Merrow et al., 1999). Whether temperature-entrained FRQ-less oscillator (FLO) is the same or different as to the micro-array detected light-dark entrained FLO oscillator, and what the components of the FLO are, remains to be elucidated. These findings suggest that the circadian clock of *Neurospora* is a multi-oscillatory system (Correa et al., 2003). At the moment, it is poorly understood how the multiple oscillators function to regulate rhythmic outputs. Some of these issues are being resolved with the first published natural-variation studies after light dark entrainment, in which a high number of period and phase QTLs was revealed,

including already known and novel loci (Kim et al., 2007a). These novel loci could lead to the identification of the components of the multi-oscillatory system.

1.2.3 *DARIO NERIO*

Dario nerio (zebrafish) became an attractive model in the last decade to study circadian rhythms in a vertebrate (Lopez-Olmeda, 2006). However, most circadian genes of the fish isolated resulted from reverse-genetic screens, based on comparative studies with their animal counterparts (Pando and Sassone-Corsi, 2002). This genetic work showed that the circadian organization of zebrafish resembles more to that of *Drosophila* than any other organism. In both organisms, almost every organ possesses a self-sustained circadian pacemaker. Furthermore, it was found that in the fish, heart cells not only contained a circadian clock, but that this clock is directly responsive to light (Whitmore et al., 2000). These studies were extended to the most organs of zebrafish (Whitmore et al., 2000). This suggests that in contrast to mammalian counterparts, where the light input to the clock goes through the retina, in *Drosophila* and in zebrafish, each organ is capable of detecting light and synchronizing the underlying clock (Whitmore et al., 2000). Though, currently no concrete genetic model of the circadian clock exists for the fish.

Zebrafish is an ectotherm organism and therefore represents an ideal vertebrate organism to study temperature effects on the circadian clock. Successful survival is dependent on adaptation of this organism to the environment by subtle changes of body temperature. Temperature cycles with even 2 degrees difference were able to entrain the circadian clock of zebrafish (Lahiri et al., 2005). This is not true for the mouse or human circadian clock. Many zebrafish circadian-clock genes are rhythmically expressed under light-dark cycles and are also rhythmically expressed in temperature cycles, although peak expression could be shifted, suggesting differential regulation of clock gene expression by temperature compared to light (Kaneko and Cahill, 2005). All these collective findings suggest that temperature entrainment of the fish is a fascinating field for the future.

1.2.4 GENETIC FRAMEWORK FOR *ARABIDOPSIS THALIANA*

1.2.4.1 The core oscillator machinery

Previously, three organisms were compared with regard to the circadian oscillator, its organization, and light versus temperature entrainment. *Neurospora* has the smaller genome size from all three organisms compared; therefore the circadian organization is simpler. The FRQ-based oscillator is the best studied; however, the interest would be to identify the components of the FRQ-less oscillator. The other two organisms compared, *Drosophila* and zebrafish, share many similarities in terms of circadian organization (Pando and Sassone-Corsi, 2002). However, the oscillatory model in light-dark entrainment differs, because a number of genes although they are orthologues, they have different functions in the oscillator (Barak et al., 2000). Moreover, the emerged temperature entrainment studies on these model organisms suggest that there are no similarities. It is noteworthy if these differences also exist in the plant kingdom.

Arabidopsis thaliana has been the best clock model organism for plants. Its genome sequence was defined and annotated, and it became publicly available in 2000 (Initiative, 2000). The small genome size, and the extensive genetic and physical maps, all ease the cloning of clock genes. Moreover, the efficient transformation utilizing *Agrobacterium tumefaciens* gave rise to a large number of circadian-defective lines. This availability of a rapidly increasing number of natural accessions allowed the assessment of natural genetic variants and the development of high throughput techniques, such as micro-arrays, has given a great boost to plant circadian research, compared to just ten years ago.

The first micro-arrays experiment regarding circadian clock was published in 2000, where it was shown that approximately 10% of the *Arabidopsis thaliana* genome is under circadian control (Harmer et al., 2000). Recently, Michael et al., have shown that the number of diurnally regulated genes is up to 90%, in at least one of the conditions tested (Michael et al., 2008). Thus, the rhythmic habitat of plants can control essentially every biological process. In this, genetic components of several physiological processes are included. Some processes governed by circadian clock are hypocotyl growth, flowering induction, calcium uptake, stomata opening, and

photosynthesis, floral petal movements (Sweeney, 1987; Dowson-Day and Millar, 1999; van Doorn and Van Meeteren, 2003). A great number of genes that coordinate these physiological outputs serve as markers that can be used to answer various genetic and physiological questions.

The most studied molecular output of the plant circadian clock is the transcript accumulation of *Chlorophyll a/b-binding protein 2* (*CAB2*). *CAB2* is an essential protein of the photosynthetic machinery expressed in the midday. The generation of transgenic *A.thaliana* plants expressing luciferase gene fused to *CAB2* promoter (Millar et al., 1995). The luciferase gene serves as a "reporter" in that it encodes a protein that produces bioluminescence as a result of the expression of the regulating promoter. If a circadian regulated promoter is used, the resulting bioluminescence of transgenic plants is rhythmic. This technology is suited for precise measurements of the marker, and it is suited for high throughput for detection of clock outputs. Forward-genetic screens of mutagenized *CAB2::LUC* transgenic plants led to the identification of many circadian genes, and consequently to the current understanding of the circadian rhythms (Millar et al., 1995).

Alabadi *et al.* proposed back in 2001 the basic framework of *A.thaliana* clock. They presented a model that was comprised by three genes, two closely related Myb transcription factors *Circadian Clock-Associated 1* (*CCA1*) and *Late elongated Hypocotyl* (*LHY*), and a pioneer protein called *Timing of CAB expression 1* (*TOC1*) (Alabadi et al., 2001). Constitutive expression of any of these three genes can cause arrhythmicity of *CAB2::LUC*, whereas null mutants of any of them exhibit short-period phenotype of *CAB2::LUC* (Wang and Tobin, 1998; Strayer et al., 2000). Single loss of function *cca1* and *lhy* mutants exhibit similar phenotypes under all conditions tested, and the *cca1 lhy* double mutant is more extreme in period phenotypes, supporting the notion of redundancy between these sequence related factors (Alabadi et al., 2002). Under a 24 hours diurnal cycle, *CCA1* and *LHY* are maximally expressed at early to mid morning. Their encoding proteins repress *TOC1* transcription by direct binding to the evening element (EE) present in the *TOC1* promoter (Alabadi et al., 2001). In contrast to other circadian-model organisms, where the repressive elements form heterodimers to suppress the positive elements of the clock, in *A. thaliana*, *CCA1* and *LHY* bind separately on *TOC1* promoter (Yu et al., 2006). By suppressing *TOC1* expression, they indirectly reduce their own expression since *TOC1* promotes their expression. When *CCA1/LHY* levels reduce to release repression, *TOC1* mRNA

levels progressively increase. Eventually, TOC1 protein levels are expressed to peak levels in the evening. Since TOC1 is an activator of *CCA1/LHY*, an increase of TOC1 levels subsequently cause increase in *CCA1/LHY* levels. When TOC1 protein levels reduce, with a mechanism that will be described later, at just before dawn, TOC1 reaches its minimum, and this way the loop closes and a new cycle begins (Alabadi et al., 2001). However, there are several phenotypes that cannot be explained by the single-loop model. First off, all three single mutants display a short-period phenotype, and not an arrhythmic phenotype, as it is expected for a core clock gene (Wang and Tobin, 1998). Further, the triple mutant *cca1 lhy toc1* was found to be partially rhythmic for a cycle after both light-dark and temperature entrainment (Alabadi et al., 2001; Ding et al., 2007b). Moreover, overexpressor TOC1 did not affect mean levels of *CCA1/LHY* expression (Makino et al., 2002). Collectively, the *CCA1/LHY-TOC1* loop readily explains most, but not all, aspects of the experimentally defined circadian behavior in *A. thaliana*.

Experimental validation with computational methods by two independent research groups suggested that the plant circadian clock is comprised of at least three interconnected feedback loops (Locke et al., 2005; Locke et al., 2006; Zeilinger et al., 2006). The main loop described just above is responsible for generating rhythms during the 24 hours day-night cycle, whereas the two additional loops are specialized for morning or evening specific fine tuning, respectively. The morning loop is comprised by *CCA1/LHY* and *PRR9* and *PRR7*. *TOC1*, also termed *PPR1*, together with *PRR7* and *PRR9* genes are members of a gene family, called pseudo-response regulator (*PRR*). It was shown that *CCA1* and *LHY* bind to promoter elements of *PRR9* and *PRR7*, in similar way to the *TOC1* promoter (Farre et al., 2005). Interestingly, the two Myb transcription factors have opposite effects on the different members of the *PRR* family. In contrast to the above described repression, *CCA1/LHY* genetically function to activate *PRR9* and *PRR7* (Farre et al., 2005). Conversely, *PRR9* and *PRR7* genetically function to repress *LHY/CCA1* (Farre et al., 2005). In addition to the morning loop, a specialized evening loop also exists. This loop is comprised by the interaction of *TOC1* and a "Y" factor that its phenotype is largely explained by *GIGANTEA* (*GI*) (Locke et al., 2005). Several studies showed that *GI* is involved in light input to the circadian clock (Martin-Tryon et al., 2007). Furthermore, *GI* shows an acute light induction as it was shown by simulation studies (Locke et al., 2005). This acute peak, and the circadian peak of *GI*, might explain the

biphasic expression of *TOC1*, since it was shown mathematically that these two genes form a loop. Specifically, it was predicted that *GI* activates *TOC1*, and *TOC1* represses *GI* (Locke et al., 2005). Additionally, it was mathematically predicted that an "X" factor is required for *CCA1/LHY* induction at dawn (Locke et al., 2006). This factor remains hypothetical to date. The above mathematical model has been confirmed by Ding et al. The three loop model is summarized in Figure 1.2.

It was mentioned earlier that *TOC1* is not the only positive element of the core oscillator. This suggests that another gene(s) might be responsible for the direct activation of *CCA1/LHY* (Figure 1.2). In this respect, other evening expressed genes, such as *LUX* and *ELF4*, have been implicated as part of the oscillator (Hazen et al., 2005; Kikis et al., 2005; Onai and Ishiura, 2005; McWatters et al., 2007). It was shown that in *elf4-1* mutant the expression of *CCA1/LHY* and *TOC1* was retained for a cycle and then turned to arrhythmic, in constant light conditions, suggesting that *ELF4* is required to sustain rhythmicity in the *CCA1/LHY-TOC1* loop (McWatters et al., 2007). *ELF4* was shown to be required for red-light mediated induction of *CCA1/LHY* (Kikis et al., 2005). Moreover, *CCA1/LHY* and *ELF4* genetically interact reciprocally, where *CCA1/LHY* suppress *ELF4* (Kikis et al., 2005). The second gene that could probably fit as the X factor in the three loop model, although this has not been tested in the mathematical models, is *LUX*. Specifically, it was shown that *LUX* genetically suppresses *TOC1*, and activates *CCA1* and *LHY* (Hazen et al., 2005). Further, *CCA1* and *LHY* bind to the evening element of the *LUX* promoter and this correlates with suppression of *LUX* transcript accumulation in a manner similar to *TOC1* repression (Hazen et al., 2005). *LUX* can thus be considered as a core-clock component since it satisfied many of the properties of the circadian clock (Hazen et al., 2005; Onai and Ishiura, 2005).

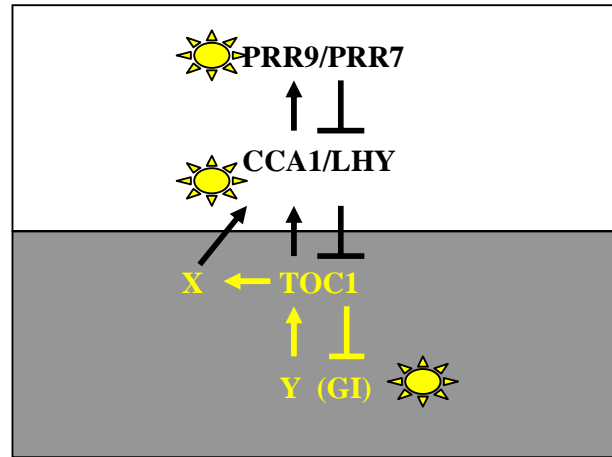


Figure 1.2 The multiple feedback loop of the *Arabidopsis thaliana* circadian clock

The three-loop model as it was computationally generated by fitting current experimental data under constant light conditions, after light dark entrainment. The core oscillator is comprised by transcriptional-translational feedback loop of the genes indicated. The genes appear next to the sun, are light activated. The letters Y and X, represent hypothetical genes. Arrows indicate promotion of activity, whereas \perp indicates repression of activity. White box represent day and grey box represents night.

Adapted from Locke *et al.* 2006, Zeilinger *et al.* 2006

1.2.4.2 Slave oscillators

Slave oscillator components possess two properties (Barak et al., 2000). First, when they are constitutively expressed, they repress accumulation of their own endogenous transcript and thereby regulate their own expression through a negative-feedback loop. Additionally, some slave-oscillator components are able to regulate the expression of other transcripts. Second, the slave oscillator is downstream of the core oscillator and its rhythm is highly dependent on the core oscillator. A typical example of a slave oscillator is a novel MYB protein Early-Phytochrome-Responsive 1 (EPR1). EPR1 regulates its own expression and other downstream genes, such as *CAB2*, but not the parameters of core-oscillator genes (Kuno, 2003). Therefore, slave oscillators work as intermediates between the core oscillator and the output pathway, perhaps contributing to proper phase maintenance.

A classical example of slave-oscillator gene is *Cold and Circadian Regulated 2 (CCR2)*, also named *AtGRP7* for *A. thaliana* Glycine-Rich Protein 7. In *A. thaliana*, CCR2 is an RNA binding protein whose expression is induced by cold temperatures. It is considered as part of a slave oscillator since it regulates its own expression by binding to its own RNA (Staiger et al., 2003a). This binding might be responsible for producing an early stop codon in its endogenous transcript, preventing in this way its translation into a functional CCR2 protein (Staiger et al., 2003a). Additionally, it was found that CCR2 suppresses the rhythmic expression of a related RNA binding protein called *AtGRP8*, also named CCR1 (Heintzen et al., 1997). Importantly, when CCR2 is overexpressed, core-clock genes are normal. So, CCR2 represents a slave oscillator that obtains timing information from the core oscillator, retains the rhythmicity through its negative feedback, and then transduces this rhythmicity, to thereby regulate a subset of clock-controlled transcripts, such as *CCR1*. *CCR2* transcription is regulated by the clock in a circadian manner, with peak time 8-12 hours after onset of illumination, whereas CCR2 protein oscillates with a delay of 4 hours after the respective mRNA peak expression (Heintzen et al., 1997). In independent research, it was found that expression of *CCR2*, and the related *CCR1*, is up regulated under stress conditions, such as chilling cold (Carpenter et al., 1994). Thus, CCR2 is also an output of the temperature pathway. *CCR2* transcription serves as an ideal tool to probe the oscillator function due to the robust rhythmicity under a wide range of conditions. Another main reason that I decided to use it as a reporter

gene in my research was its temperature regulation. Exploiting its temperature regulation, one can map temperature entrainment QTLs by using *CCR2* fusion to luciferase (Chapters 3 and 4).

1.3 ENTRAINMENT

The circadian oscillator generates rhythmic outputs by using timing information given by the external environment, such as light and temperature onset. The process through which the oscillator synchronizes to the environment is called entrainment (Barak et al., 2000). Characteristic of an entrained oscillator is that it must have a stable phase regarding to the entraining cycle (Morrow, 2006). This can be tested in cycles with length different than 24 hours of which the amount of light versus dark or warm versus cold is the same. This type of entrainment is called symmetrical T cycles. In *Neurospora*, such experiments revealed that the FRQ-based rhythms are driven, since onset of conidiation occurred at the same time, 7 hours after dark, regardless of the cycle length (Morrow, 2006). This strongly suggests that the light is able to mask entrained rhythms, meaning that light can affect rhythms without entraining the underlying oscillator. Therefore, masking could be due to strong stimulus intensity or to a weak oscillator (Morrow, 2006).

One can appreciate the importance of entrainment when flying over many time zones. It takes several days in the new time zone for the human circadian clock to gradually reset to the local environmental signals (Waterhouse, 2007). Therefore, one can study entrainment by applying such experiments to the plants grown in controlled conditions. For this, a phase shift between the old and new entrainment protocol is required. Plants with a functionally entrained oscillator would gradually reset to the new entrainment protocol, and thereby attain a phase angle then the phase of the rhythms would show a stable shift equal to the difference of the onset of the two signals. This would indicate that these rhythms are entrained to the new environment. Moreover, by synchronizing plants to two synchronous, but phase shifted, entrainment protocols one could determine preference to one of the two protocols. To conclude, the performance of each of these different protocols in temperature cycles, could discriminate whether temperature is driving or entraining the circadian clock.

1.3.1 Light regulation of the circadian clock

At the molecular level, light is perceived by proteins called photoreceptors (Somers et al., 1998a; Franklin and Whitelam, 2004). To be a photoreceptor, several criteria must be fulfilled. Mutants lacking such a protein should have aberrant phenotypes compared to wild-type plants in light-regulated processes, such as hypocotyl elongation, flowering time, and circadian rhythms. Additionally, the protein should show that it binds to a chromophore, and that it undergoes certain photochemistry under specific fluence and wavelengths of light. Plants, compared to other organisms, can detect a broad range of wavelengths of the visible-light spectrum (Fankhauser and Staiger, 2002; Chen et al., 2004). As a contrast *Neurospora* only detects blue light (Froehlich et al., 2002; Dunlap and Loros, 2004). To exploit the available light, a suite of photoreceptors in plants are used to monitor changes in light duration, quantity, and quality (Murtas and Millar, 2000). Depending on the quality of the detected light, photoreceptors are subdivided in three classes. Red/farred light is perceived by phytochromes. Five phytochromes have been identified so far, and named PHYA-E (Devlin, 2001). Blue light is mainly absorbed by cryptochromes (CRY1-2), and phototropins (PHOT1-2) (Devlin and Kay, 2000). However, phototropins are as of yet not connected to the circadian-clock. Apparently, recruitment of the appropriate photoreceptor upon different light environments enables advantageous resetting of the clock under these environments. Moreover, photoreceptors affect period length of the clock in a fluence dependent manner (Somers et al., 1998a). However, the double, *cry1 cry2*, and the quadruple *phyA phyB cry1 cry2* mutant retains rhythmicity suggesting that other photoreceptors mediate light input to the clock (Yanovsky et al., 2000).

Intermediate light signaling genes are involved in the input pathway. ELF3 plays such a key role in the photo-transduction pathway to the clock. Under continuous light, *elf3* mutants become rapidly arrhythmic, but in constant darkness remain rhythmic (Hicks et al., 1996; Covington et al., 2001). Additionally, overexpression of ELF3 shows long-period phenotype in constant light, but no period effect in constant darkness (Covington et al., 2001). These phenotypes suggest that ELF3 functions in the light input, by gating light during subjective night (McWatters et al., 2000). Moreover, yeast-two hybrid and in vitro pull down assays shows that ELF3 interacts with PHYB, therefore linking ELF3 to the phytochrome signal

transduction (Liu et al., 2001). All these suggest a role of ELF3 to mediate light input to circadian clock.

In addition to *ELF3*, the *TIME FOR COFFEE (TIC)* gene is a potential photo-entrainment intermediate that works close to the oscillator. However, TIC and ELF3 function at different phases of the circadian cycle. Therefore, it was foreseen that the *elf3 tic* double mutants would have a completely arrhythmic phenotype (Hall et al., 2003). Surprisingly, and in contrast to ELF3, neither *TIC*'s mRNA nor its protein is circadian expressed. Ding *et al.*, have shown that TIC affects the clock by promoting transcriptional induction of *LHY*, rather than *CCA1* (Ding et al., 2007a). This is the further evidence of an uncoupling function of the *CCA1* and *LHY*, otherwise, redundant transcription factors (Ding et al., 2007a). How *TIC* mediates light input has not yet resolved.

Other clock components are also involved in light transmission to the clock. Specifically, mutations in *PRR7* and *PRR9* lengthen the period of *CCR2* under constant light, whereas *CCR2* period is unaffected in constant darkness (Farre et al., 2005). The evening gene *GI* is light induced (Locke et al., 2005). Genes such as *CCA1*, *LHY*, and *PRR9*, have been found to mediate red and also in blue light to the clock. Furthermore, GI protein stabilizes ZTL protein accumulation (Kim et al., 2007b). ZTL is a putative blue-light photoreceptor that regulates its own protein expression in a circadian manner (Kim et al., 2003b). This ZTL-dependent degradation of TOC1 in darkness is probably indirectly mediated by the stabilization of ZTL by GI under blue light (Kim et al., 2007b).

1.3.2 Temperature regulation of the circadian clock

Over 24 hours, plants experience not only a light-dark cycle, but also a warm-cool cycle, where warm coincides in time with light and cool with darkness. Although light is the major factor responsible for the resetting of the circadian oscillator, temperature oscillations can as well reset the oscillator (Barak et al., 2000; McClung, 2006) Temperature can affect the oscillator differentially. Entrainment occurs after changes in ambient temperatures and not by extreme stress temperatures, such as chilling or heat shock. In experiments performed at ambient temperature cycles, the existence of two oscillators with differential response to the environmental entrainment cues was reported, since two genes are shown preference to either light

dark or temperature entrainment (Michael et al., 2003a). However, our knowledge of temperature perception and oscillator resetting is fairly poor. So far, two members of the PRR family in Arabidopsis, PRR7 and PRR9, have been suggested to play a role in temperature entrainment, since the *prp7 prp9* double mutant when subjected to temperature cycles under constant light failed to be entrained (Salome and McClung, 2005). Though, when they perform similar experiments where the double mutant plants were entrained to temperature cycles, but in constant darkness, expression of *CCA1* and *LHY* was rhythmic. This suggests that additional gene(s) other than PRR7 and PRR9 are involved to maintain residual rhythmicity in temperature cycles in the absence of light. To conclude, temperature cycles can entrain the oscillator, and PRR7 and PRR9 are two components of the temperature entrained oscillator.

Temperature cycles can entrain the circadian oscillator, but the circadian oscillator is temperature compensated, being buffered from mean temperature differences. Temperature compensation studies in other model organisms - *e.g.* *Drosophila* and *Neurospora* - have shown that clock components identified under light - dark entrainment are also play a role in temperature compensation, and surprisingly, also in temperature entrainment (Diernfellner et al., 2005; Glaser and Stanewsky, 2005). In comparisons to other model organisms, one could expect that some of the genetic components involved in temperature compensation of *A. thaliana*, would be also involved in temperature entrainment of the circadian clock. An example in *A. thaliana* is the gene *GI*, which according to circadian modeling, is part of a three-loop light entrained oscillator (Locke et al., 2006; Zeilinger et al., 2006). Additionally, *GI* plays a role in temperature compensation in the circadian clock, especially, in higher and lower mean temperatures (Gould et al., 2006). Whether *GI* is part of thermal entrainment is not yet established.

Another gene involved in the temperature compensation of the circadian clock is *FLC* (Edwards et al., 2006). Specifically, *FLC* is a factor that maintain the same period over moderate temperature ranges, although the period is altered at 27°C. Additionally, a dose-dependent effect of *FLC* on circadian period after light-dark entrainment was shown (Salathia, BMC2006). The classical role of *FLC* is in repression of flowering time (Michaels and Amasino, 1999). High levels of *FLC* suppress expression of downstream - flowering integrator - genes (Searle et al., 2006). After extended low temperatures, *FLC* is down-regulated, so the downstream positive regulators are activated and flowering is promoted (Bastow et al., 2004; Mylne et al.,

2006). The relationship of FLC to the clock appears to involve the LUX gene (Edwards et al., 2006). How FLC regulates LUX is unknown.

In addition to low temperatures, moderate temperatures affect flowering. It was shown that in either 16°C or 23°C photoreceptors genes, such as PHYB, PHYD, PHYE, CRY1 and CRY2, display a differential flowering (Blazquez et al., 2003; Halliday et al., 2003). The differential control of flowering at various temperatures by these genes, and especially the exaggerated phenotype of CRY2, prompt us to think that photoreceptors could be also involved in temperature perception, as well as in light perception. It is intriguing that this light and temperature connection could extend to the entrainment of the clock. It is currently untested if photoreceptors mutants in *A. thaliana* have temperature dependent clock phenotypes.

Temperature signaling and resetting of the oscillator could be rather complicated to resolve because many biochemical reactions are temperature sensitive. Normally, increases of 10 degrees will double the speed of metabolic reactions (McClung, 2006). At very high temperatures biochemical reactions are affected by heat shock proteins that are activated on these stressful temperatures (Rensing and Monnerjahn, 1996). At low temperatures, plant growth and development is influenced, through direct inhibition of metabolism, and/or indirect induction of other stress responses (Strand et al., 1999; Stitt and Hurry, 2002). The biophysical nature of a thermal reset of the oscillator can thus not be predicted.

At chilling temperatures, almost 4% of the *A. thaliana* genome is transcriptionally induced or suppressed. Three transcription factors, called C-repeat Binding Factors (CBF), are part of this cold-acclimation pathway in *A. thaliana*. They are rapidly induced upon cool temperatures (Gilmour et al., 1998; Medina et al., 1999). Interestingly, *CBF1* and *CBF3* transcripts are circadian expressed, peaking at ZT6 (Gong et al., 2002). Recently, the most upstream element of this pathway, Inducer of CBFs Expression 1 (*ICE1*), was identified (Chinnusamy et al., 2003). Microarray data performed at wild type and *ice-1* mutant where the plants were subjected for 0, 3, 6, 24 hours in 0°C (Lee et al., 2005). In this study, among almost 1000 of genes, four genes involved in circadian clock were upregulated by cold temperature. Three of them, *TOC1*, *TIC* and *CRY2* are late induced, after 6 hours of cold, whereas *PRR5*, another member of *TOC1* family, is early continuously upregulated by chilling cold. However, lack of more time points makes difficult to determine the effect of cold temperatures in the expression of these circadian genes.

As an interesting example in chestnut, the homologs of *A. thaliana* *LHY* and *TOC1* were expressed but not oscillating in either long days or short days at 4°C, suggesting an alteration in clock function at low temperatures (Ramos et al., 2005). Similarly, in *A. thaliana*, period is affected by vernalization treatment partially independent of *FLC* (Salathia et al., 2006). Moreover, evidence in *A. thaliana* show that the induction of *CBF* by cold is gated by the circadian clock (Fowler et al., 2005). Whether *TOC1* and *LHY* are part of the oscillator at chilling low temperatures, or other components as of yet unidentified or known, remains to be elucidated. Interestingly, changes in *GI* were not found in these microarrays, although molecular data exist for *GI* functions in cold acclimation mediating freezing tolerance through a *CBF*-independent pathway (Cao et al., 2005).

Chilling cold temperatures are sensed in plants through membranes, since it was shown that, upon cold stress, in mutants lacking fatty acid desaturases, the plasma membrane was rapidly rigidified (Vaultier et al., 2006). Additionally, calcium ions are increased in cold temperatures in the cytosol (Knight et al., 1996). So, it is possible that cold-stress signaling is mediated by calcium and phospholipids signaling. Therefore, temperature is expected to affect the circadian clock both directly through entrainment, also indirectly through other temperature-regulated processes, such as affecting calcium influx, changes in hormone levels, and protein phosphorylation.

1.4 NATURAL VARIATION

In nature, *A. thaliana* grows in a wide range of environments, distributed over the Northern Hemisphere at latitudes from the tropics to the arctic cycle, and at altitudes from sea level up to 3500 m in the mountains of central Asia (Loudet et al., 2002; Koornneef et al., 2004). To date, more than 600 accessions have been collected from various places all over world. Each accession is presumed to be adapted to the local environment rendering the best plant performance. This adaptation is reflected by selection upon genetic variation. Relevant to the clock, this genetic variation can be strongly selected by rhythmic environmental factors, such as light and temperature. This selection thus generates a useful genetic resource *via* natural resources. Often, genetic variation of multiple genes control continuous traits. Continuous traits are of a quantitative nature, and this is why they also called quantitative traits. Quantitative

traits are under the control of several loci called quantitative trait loci (QTL). So, by scoring differences in quantitative traits, one can map allelic variation. Here, QTLs of light and temperature regulation of the clock can be explored.

In addition to natural accessions, for QTL analysis in *A. thaliana*, “immortal” mapping populations, such as Recombinant Inbred Lines (RILs), can be used. RILs are generated by the cross of two accessions that originate from ecologically distinct environments (Koornneef et al., 2004; Alonso-Blanco et al., 2005). Several rounds of self fertilization generations until F8 will produce lines that are a homozygote mosaic of the two parents, for 98% of the genome. RILs can be used in replicate experiments under various environments to map QTLs for several traits (Koornneef et al., 2004). In this case, the direct comparison of map positions (genetic location) of genes encoding for these different traits is allowed. To fine map the detected QTLs Near Isogenic Lines (NILs) are used. NILs are generated by repeated backcrosses resulting to introgressions of a part of the genome of one parent into the gene pool of the second parent. At the moment, various RILs have been generated and are publicly available for natural variation studies.

Assessment of natural variation and subsequent QTL analysis facilitates the unraveling of the genetics of quantitative traits, such as hypocotyl length, clock parameters, and flowering time (Alonso-Blanco et al., 1998; Swarup et al., 1999; Maloof et al., 2001; Fankhauser and Staiger, 2002; Edwards et al., 2005; Balasubramanian et al., 2006). The analysis of variation in flowering time in naturally late-flowering accessions and RILs was used particularly to identify repressors of the floral transition. Most of the phenotypic variation in flowering time is resulted from natural variation of various loci, such as *FLC*, *FRI*, *PHYC*, *CRY2*, *HUA*, and *FLM* (Johanson et al., 2000; El-Din El-Assal et al., 2001; Doyle et al., 2005; Shindo et al., 2005; Werner et al., 2005; Balasubramanian et al., 2006). Existing RILs can thus be exploited to uncover individual genes that coordinate particular processes of investigation.

Several QTL studies have been performed on a number of accessions and RILs for clock parameters control. This was done by either assaying leaf movement or luciferase expression as a reporter for clock controlled genes (Swarup et al., 1999; Michael et al., 2003b; Edwards et al., 2005; Darrah et al., 2006). The most informative RIL population has been the one generated by the cross of Cvi to *Ler* (CvL). CvL RILs transformed with *CAB2::LUC* have identified a first chromosome

QTL for circadian phase of plants entrained in short day photoperiods (Darrah et al., 2006). Although *GI* is localized in that area, from this analysis, it turned out that *GI* was not candidate for this phase QTL, suggesting another, yet unidentified, loci is responsible for this phenotype. However, period QTL of leaf movement of 48 CvL lines for temperature compensation at 12°C, 22°C, and 27°C, implicate *GI* as a temperature-responsive gene, and thus as candidate gene for temperature compensation at 27°C (Edwards et al., 2005). Sequence analysis of the *Ler* *GI* and *Cvi* *GI* identify two changes that encode for amino-acid changes, however since the domain structure of *GI* is unknown, no assumptions could be made on the functional consequences of these substitutions. Additionally, it was shown that period length was shorter if a NIL was carrying the *Cvi* allele for the narrow area containing *GI* than the broader area containing *GI*, suggesting that the difference in period for the different NILs could be due to the presence of two interacting QTLs (Edwards et al., 2005). From these two studies, it can be concluded that at least two different QTL exist in the first chromosome, from 15-40cM (Edwards et al., 2005; Darrah et al., 2006). That finding is also in agreement of Swarup *et al.* in the first attempt to map allelic variation responsible for period variation of the circadian clock, for leaf movement of CvL RILs in light dark entrainment (Swarup et al., 1999). However, molecular studies using *GI* null mutant concluded that *GI* plays a role on maintaining rhythmicity in temperature ranges outside of 17-22C (Gould et al., 2006). To recapitulate, the null mutant data are in conflict with the natural-variation data concerning the role of *GI* at a range of 17-22C, meaning that another gene should take over the role of *GI* in this range of temperatures. Moreover, variation in more than one QTL close to *GI* might be involved for phase and period control of the circadian clock (Edwards et al., 2005; Darrah et al., 2006).

All the above QTL studies were performed after light-dark cycles of 24 hours length. However, temperature changes also occur during a natural 24 hours. So, the main question of my thesis work has been on how temperature changes synchronize the oscillator. This main question can be divided in several sub-parts: How are these temperature changes signaled to the oscillator? Does the oscillator responds differential to changes in cooler compared to changes in warmer temperatures? Though, the ultimate question is how the oscillator(s) is entrained by both light and temperature changes, in reality these often occur at the same time. Thus, the two input signals converge to one oscillator or many different oscillators are in coupled phase?

Are there times of the day that one input is stronger than the other? Finally, are environmental entrainment cues targets for natural and artificial selection? The present thesis study focuses on the identification of temperature-entrainment loci by assaying clock parameters using available natural genetic resources. This is a step towards answering the above questions.

2 MATERIALS AND METHODS

2.1 MATERIALS

2.1.1 Antibiotics

Antibiotics used for selection of *CCR2::LUC* transformed plants

Hygromycin (2000x): 30 mg/ml in H₂O. Filter sterilize. Use at 15 µg/ml final concentration

Stock solution and working solutions were stored at –20°C

Antibiotics used for *Agrobacterium tumefaciens* selection

Carbenicillin (2000x): Stock solution 100 mg/ml in 100% ethanol. Use at 50 µg/ml

Chloramphenicol (1000x): Stock solution 10 mg/ml in 100% Ethanol. Use at 10 µg/ml

Rifampicin (1000x): Stock solution 25 mg/ml in methanol. Use at 12.5 µg/ml

Streptomycin (1000x): Stock solution 50 mg/ml in H₂O. Filter sterilize. Use at 50 µg/ml

Stock solutions and working solutions were stored at –20°C

2.1.2 Bacterial strains

For *Agrobacterium tumefaciens* mediated transformation, the strain bearing *CCR2::LUC*, described by Doyle *et al.* 2002, was used (Doyle *et al.*, 2002).

2.1.3 Plant material

Two existing populations of Recombinant Inbred Lines (RIL) were used. One was generated by crossing the accessions Landsberg *erecta* (*Ler*) and Cape Verde Islands (*Cvi*) (Alonso-Blanco, 1998), and the other one was generated by crossing the accessions Bayreuth-0 (*Bay*) and Shakhara (*Sha*) (Loudet *et al.*, 2002). Progeny of F8 generation of the *Cvi* x *Ler* collection was donated by M. Koornneef, whereas the core population of *Bay*-0 x *Shakhara* at F8 seeds was obtained from Nottingham

Arabidopsis Stock Centre (NASC, UK). T0 transgenic *CCR2::LUC* reporter lines were obtained by floral dipped. T1 plants were selected on hydroponic rock-wool growing media containing $\frac{1}{4}$ Muraskige and Skoog and hygromycin 15 μ g/ml. Between one to four independent transformed T1 plants resistant to hygromycin, and possessing luciferase activity, were transferred to soil to allow self-fertilization. T2 plants were used for circadian-rhythms experiments. The selected individuals from these populations transformed with *CCR2::LUC* for the two RIL populations are shown at Table 2.1 and Table 2.2. The derived Near Isogenic Lines used for QTL mapping were introgressions of Cvi genome into *Ler* background (Keurentjes et al., 2007), donated by M. Koornneef.

BXS RILs lines						
BXS007		BXS118		BXS179		BXS262
BXS013		BXS126		BXS186		BXS264
BXS015		BXS127		BXS187		BXS273
BXS030		BXS129		BXS190		BXS289
BXS037		BXS131		BXS191		BXS298
BXS045		BXS133		BXS194		BXS300
BXS053		BXS134		BXS195		BXS320
BXS059		BXS135		BXS198		BXS325
BXS061		BXS136		BXS199		BXS329
BXS067		BXS137		BXS200		BXS363
BXS070		BXS140		BXS210		BXS364
BXS078		BXS143		BXS211		BXS365
BXS083		BXS146		BXS214		BXS368
BXS092		BXS147		BXS220		BXS376
BXS098		BXS155		BXS232		BXS379
BXS111		BXS162		BXS234		BXS387
BXS112		BXS165		BXS240		BXS394
BXS114		BXS173		BXS252		

Table 2.1 Bayreuth-0/Shakdara RIL lines that were transformed with *CCR2::LUC* mediated by *A. tumefaciens*

CvL RIL lines						
CvL5		CvL44		CvL103		CvL150
CvL6		CvL47		CvL105		CvL151
CvL11		CvL48		CvL114		CvL153
CvL12		CvL49		CvL116		CvL154
CvL13		CvL50		CvL125		CvL156
CvL16		CvL54		CvL131		CvL164
CvL19		CvL59		CvL140		CvL175
CvL20		CvL61		CvL141		CvL183
CvL27		CvL65		CvL145		CvL187
CvL36		CvL69		CvL149		CvL193
CvL38		CvL72				

Table 2.2 Cvi/Ler RIL lines that were transformed with *CCR2::LUC* mediated by *A. tumefaciens*

2.1.4 Enzymes

- Restriction enzymes were purchased from New England Biolabs (Boston, USA), and Fermentas (Lithuania)
- Taq Polymerase was purchased from Peqlab, Erlangen

2.1.5 Oligonucleotides

All oligonucleotides were synthesized by Invitrogen, Karlsruhe. Oligonucleotides were obtained after desalted purification, at 0.05 μ mol scale.

Marker name	Forward marker 5-->3	Products (bp) for Ler/Cvi	Restriction enzyme
	Reverse marker 5-->3		
IND79	GAAACCCTGCCGGAGGAAGT	40/119bp	
	AGCTTTTCAGATATGTAGATC		
X47	GAGGTTATACTTGC GGCTGGGG	47/88	
	CGAAATCATTGAGATGATTCTCGGG		
X5.48	TTGAAGTTGCTTTTGTGGTTGTCC	26+75/101	SmaI
	CGGTTTGGCCAAAGAAGTGT		
F309	GTCGATTATTTTCATTATAATGAA	40/73	
	ATCAACAAAAATACGTTAAACA		
X5.5	TTGGGAATAGTTTTTCATTTACTTTT	49/126	
	AAGTTGCTCGTTAAAGACACAAT		
X5.8	CAAAGTTCTGTTCTCCAAGGACTTCATCGG	30+112/142	BamHI
	CGTGATGATATTGATGTACGCT		
F20D23	TCCTCGTCTCCGCATCTTAATCATT	160/183	
	AATGAAGAATTCAGAAAGCAACAGACTT		
X6.1	GGTCATTGCAGTGGCAACTCA	188/18+170	DdeI
	CCGTGCTTCCAGAATAGCCTC		
CAT3	CAGATGCAATGGCATCGTGGAG	790+185/973	HINCII
	CGGTGGTGTCCAGTCTCCAAC		
X7.3	ATACGAAGATCTTCGTACCATAAGCT	140/125+15	HindIII
	TTACCGATTCTAGGCTGAGGTCT		
X7.5	CTAGACATGACTTCCAAGAGAAAAGCTA	29_96/125	DdeI
	GCCTCGTATCTCTATCCGTTCTT		
X7.8	GAGAGAGAAAATTTGTTCTGATTAATGAAAGGATC	31+131/162	BamHI
	CGTCACAATATCACGTCACTAAAGAAA		
m235	GAATCTGTTTCGCCTAACGC	534/309+225	HindIII
	AGTCCACAACAATTGCAGCC		
XR1GI	AAAAGTAGGAATGTCAAGGGACAGGGACCTGA	32+124/156	DdeI
	ATAGTTCCAGCCACGGCAGAATTGGAAAAGT		
F3I6-1	AACTAATGGAGGATATTCAAG	177/201	
	TTTAATTATTCACTTTTTATTG		
SO392	GTTGTTGATCGCAGCTTGATAAG	156/142	
	TTTGGAGTTAGACACGGATCTG		

Table 2.3 SSLPs/CAPS/derived CAPS markers used for mapping the 1st chromosome QTL of the CvL population

The 'derived' nucleotide base is underlined

CHR	Marker	Forward marker 5 -->3	Reverse marker 5--> 3
1	NGA59	TTAATACATTAGCCCAGACCCG	GCATCTGTGTTCACTCGCC
1	NGA63	AACCAAGGCACAGAAGCG	ACCCAAGTGATCGCCACC
1	MSAT1.10	ATGGTGAGATACTGAGATTAT	CGAGAAGGTCTAAAGGTA
1	ATHS0392	TTTGGAGTTAGACACGGATCTG	GTTGATCGCAGCTTGATAAGC
1	T27K12	GGAGGCTATACGAATCTTGACA	GGACAACGTCTCAAACGGTT
1	CIW1	ACATTTTCTCAATCCTTACTC	GAGAGCTTCTTTATTTGTGAT
1	NGA128	GGTCTGTTGATGTCGTAAGTCG	ATCTTGAAACCTTTAGGGAGGG
1	NGA111	TGTTTTTTAGGACAAATGGCG	CTCCAGTTGGAAGCTAAAGGG
2	RGA*	TTCGATTCAAGTTCGGTTTAG	GTTTAAGCAAGCGAGTATGC
2	MSAT2.28	AATAGAAATGGAGTTCGACG	TGAACTTGTTGTGAGCTTTG
2	MSAT2.11	GATTTAAAAGTCCGACCTA	CCAAAGAGTTGTGCAA
2	MSAT2.41	GACTGTTTCATCGGATCCAT	ACAAACCATTGTTGGTCGTG
2	NGA361	AAAGAGATGAGAATTTGGAC	ACATATCAATATATTAAGTAGC
2	MSAT2.22	CGATCCAATCGGTCTCTCT	TGGTAACATCCCGAAGTTC
3	NGA172	CATCCGAATGCCATTGTTT	AGCTGCTTCCTTATAGCGTCC
3	NGA162	CATGCAATTTGCATCTGAGG	CTCTGTCACCTTTTCTCTGG
3	MSAT3.19	TAATTCGATCCAATTGACAT	TGGCTTGGCACAAC
3	MSAT3.28	TACAAGTCATAATAGAGGC	GGGTTTAGCATTTAGC
3	NGA6	ATGGAGAAGCTTACACTGATC	TGGATTTCTCCTCTCTTCAC
4	FRI	GAACCGTTACATTTGACTAC- AAAGTAA	ACAAACAAATAAATGTATAAAA- TGAGCTT
4	T3H13	TTTGGTGGGTCAAGAGTCAAG	GCAAAAGTCATTACGGACAATAC
4	MSAT4.16	AGGTGGAGATTGTTCTTGTT	CGTTGCGTTCTCTATCCTC
4	MSAT4.15	TTTCTTGCTTTTCCCCTGAA	GACGAAGAAGGAGACGAAAA
4	CIW7	AATTTGGAGATTAGCTGGAAT	CCATGTTGATGATAAGCACAA
4	MSAT4.12	AAAGGAAGAAGAAGACTGTT	AGAAGAAGAAGCGAGATT
4	MSAT4.28	GAAGCTCCGCGTGAC	TGAATTGATGTCGCAATCAG
5	NGA158	ACCTGAACCATCCTCCGTC	TCATTTTGGCCGACTTAGC
5	NGA106	GTTATGGAGTTTCTAGGGCACG	TGCCCCATTTTGTCTTCTC
5	MSAT5.14	AACAACCCTATCTTCTCTG	TGTGACCCCTTACTCAATA
5	NGA76	GGAGAAAATGTCACTCTCCACC	AGGCATGGGAGACATTTACG
5	MSAT5.22	AGAACAAGTTAGGTGGCT	GGGACAAGAATGGAGT
5	ATHS0191	TGATGTTGATGGAGATGGTCA	CTCCACCAATCATGCAAATG
5	MSAT5.9	CGTCATTTTTCGCCGCTCT	CATGGTGGCGGTAGCTTA
5	JV61/62	CGCTTTCCTTGTGTCATTC	AAATGCAAATATTGATGTGTGAAA

Table 2.4 SSLPs/CAPS primers used for genotyping the C24WS RIL population

CHR denotes chromosome * indicates that the RGA marker is a CAPS marker digested with RSAI restriction enzyme

2.1.6 Media

Media for plants

Muraskige and Skoog Basal Salt (MS), containing 3% sucrose (MS3), liquid medium

In 800mL of distilled water add:

- 4.4g of Muraskige and Skoog Basal Salt (MS) (SIGMA M5524-10L, Seelze)
- 30g of sucrose
- 0.5g of 2-(*N*-morpholino) ethanesulfonic acid (MES)

Adjust pH to 5.7 with potassium hydroxide (KOH)

Add distilled water to final volume 1000mL

For Muraskige and Skoog Basal Salt (MS), containing 3% sucrose MS3 solid media, add 15g/L Phytoagar (DUCHEFA, Haarlem)

Autoclave in 120°C for 20 minutes

For transgenic plant selection, hygromycin in 15µg/ml was supplemented

¼ Muraskige and Skoog Basal Salt (MS) (MS0), liquid medium

In 800mL of distilled water add

- 1.1g of Muraskige and Skoog Basal Salt (MS)
- 0.5g MES

Adjust pH to 5.7 with KOH

Add distilled water to final volume 1000mL

For ¼ MS0 solid media, add 15g/L Phytoagar

Autoclave in 120°C for 20 minutes

For transgenic plant selection, hygromycin in 15µg/ml was supplemented

Media for bacteriaLuria-Bertani (LB), liquid medium

In 800mL of distilled water add:

-5g yeast extract (ROTH, Karlsruhe)

-10g bactotryptone (Beckton Dickenson, Le Pont de Claix)

-10g sodium chloride (NaCl)

Adjust pH to 7.5 with KOH

Add distilled water to final volume 1000mL

Autoclave in 120°C for 20 minutes

YEBS, liquid medium

In In 800mL of distilled water add

-1g yeast extract (ROTH, Karlsruhe)

-5g beef extract (SIGMA, Steinheim)

-5g peptone (Beckton Dickenson, Le Pont de Claix)

-5g sucrose

-0.5g MgSO₄

Adjust pH to 7.0 with sodium hydroxide (NaOH)

Add distilled water to final volume 1000mL

Autoclave in 120°C for 20 minutes

2.1.7 Buffers and solutions0.1M Triphosphate Buffer for Luciferin

In 180ml of distilled H₂O add

-3.56g of Na₂HPO₄

-2.76g of NaH₂PO₄

Adjust pH to 8.0 with NaH₂PO₄

Fill in to final volume of 200mL with distilled water

50mM Luciferin stock solution

71.3mL of 0.1M of the triphosphate Buffer pH 8.0 was used to dissolve 1g of firefly D-luciferin (D-[4,5-dihydro-2-(6-hydroxy-2-benzothiazolyl)-4-thiazole-carboxylic acid]) (LABTECH INTERNATIONAL, UK) to give 50mM of luciferin stock solution

Aliquot into 1.5mL Eppendorf tubes

Store at -80°C

0.01% Triton X-100

Add 100µL of Triton X-100 into a Liter of distilled water

5mM Luciferin working solution

Dilute 1.5mL of luciferin stock into 13.5mL of Triton-X solution

Filter sterilize

Bleach solution

In 100mL of water add:

-33ml of Klorix Bleach (commercial sodium hypochlorite solution)

-20µL Triton X-100

DNA Extraction Buffer (DEB)

In 800mL of distilled water add:

-24.2g of 2-amino-2-hydroxymethyl-1,3-propanediol (Tris)

-14.02g of NaCl

-50mL of Ethylene Diamine Tetraacetic Acid (EDTA)

-10g of Sodium Dodecyl Sulfate (SDS)

Adjust pH to 8.0 with KOH

Add distilled water to 1000mL

2.1.8 Software, databases, and other internet resources

Databases for genomic sequences of *Arabidopsis thaliana*:

<http://www.arabidopsis.org>

<http://www.tigr.org/tdb/e2k1/ath1/ath1.shtml>

<http://www.ncbi.nlm.nih.gov/gquery/gquery.fcgi>

Searching for simple sequence length polymorphism (SSLP) and Cleaved Amplified Polymorphic Sequence (CAPS) markers:

<http://helix.wustl.edu/dcaps/dcaps.html> (Neff, 2002)

<http://www.arabidopsis.org>

<http://www2.mpiz-koeln.mpg.de/masc/> (Schmid, 2003; Toerjek, 2003)

<http://www.arabidopsis.org/Cereon/> (Jander et al., 2002)

Primer design:

DNAMAN version 4.0, Lynnon BioSoft 1994-1998

Software for RIL mapping:

MapQTL5.0, Kyasma (<http://www.kyazma.nl/index.php/mc.MapQTL/>)

2.1.9 Materials for luciferase imaging

Packard Top Count Scintillation Counter

Sterile OptiPlate -96F (Black, 96-well, pinch bar design) (6005270)

MS agar containing 3% sucrose media

Strips of Light-Emitting Diodes (LEDs) with Red, Blue, and Far red (for continuous light assayed plates) (MD ELECTRONICS, UK)

Reflector plates used to mirror light from the LEDs to the plants (custom made)

Top Seal Microplate Press-On Adhesive Sealing Film (Packard 6005185)

2.2 METHODS

2.2.1 Agrobacterium-mediated transformation of Arabidopsis plants

Floral dip transformation of Arabidopsis plants (Clough and Bent, 1998)

1. A starting culture of the *Agrobacterium* strain bearing *CCR2::LUC* reporter was made in a 3-5 mL YEBS media in which carbenicillin and rifampicin were added for selection of both the Ti and the T-DNA plasmid. The starting culture was incubated for 2-3 days at 28°C while shaking at approximately 200rpm
2. 200 mL of YEBS media containing the selection antibiotics were inoculated with the starting culture and incubated for 16 hours at 28°C while shaking at approximately 200rpm
3. 5% of sucrose was added to the culture and mixed until dissolved
4. Additionally 300 µL of Silwet-77 was added to the bacterial culture
5. After adding 400 mL of YEBS, the culture was further incubated at room temperature while shaking until OD reaches 0.6
6. Arabidopsis RIL plants grown in greenhouse until flowers were visible
7. Inflorescences bearing young flowers were submerged for about 30 seconds into the bacterial solution
8. The dipped plants were put in sealed plastic bags for two days to ensure high humidity
9. Plants were allowed to set seeds and harvested.

Selection of independent transformed Arabidopsis plants

The bulked seeds were sown on hydroponic rock wool growing media as it was described in Hadi *et al* (Hadi, 2002). T1 plants were selected on rock wool containing ¼ MS0 and hygromycin 15µg/mL. Two weeks later, T1 plants were sprayed with 1mM luciferin and imaged for bioluminescence in a Lumi-imager camera for 10 minutes with 2x2 binning of the exposure (Boehringer Mannheim). Only plants that harbored the full-length construct, as assessed by being resistant were resistant against the antibiotic and luminescent, were selected for transfer to soil. T2 progeny were harvested for experimentation.

2.2.2 Plant material treatments

2.2.1.1 Crosses

Surface sterilized forceps before crossing

Select appropriate stage of flower

For the female parent, the three outer whorls of the flower were dissected, keeping only the carpel. For the male parent, anthers with mature pollen were dissected to be used for the cross to the stigma of the female parent. Approximately after 3 weeks siliques containing F1 seed can be harvested

2.2.1.2 Seed sterilization

Surface sterilize the seed by washing with 100% ethanol

Wash the seed with 33% Klorix bleach for up to 5 minutes

Rinse twice with sterile distilled water

Suspend seeds in 0.15% sterile agar/water

Sow individual seed in MS plates containing 3% sucrose. Avoid seed clumping

Seal the lid to the plate with parafilm to prevent evaporation and infection

Stratify for 2-4 days before transferring to the desired light regime

2.2.1.3 Generation of new Recombinant Inbred Lines

Six new Recombinant Inbred Lines were constructed. Pair-wise crosses of two parental accessions to four laboratory strains were the foundation for these new RILs. One of the parents -P2- was transformed with the promoter-reporter *CCR2::LUC*. A T1 transgenic was backcrossed to P1. This “clears up” the genome from multiple transgene insertions and residual mutations. A single insert line was isolated, and crossed to a divergent ecotype. The resulting F1 was repeatedly crossed with the respective P1 parent to generate many BC1 lines (Figure 2.4). At this BC1 stage, 6 long and 6 short period lines were selected from approximately 100 seedlings, based on *CCR2* period analysis. At the BC1F2 stage, *CCR2::LUC* rhythms of the progeny of the 6 long and 6 short period BC1 genotypes were assayed, and from each genotype, 8 individuals with either shorter period compared to their short period parent or longer compared to their long period parent were selected. In total, each RIL

set is comprised of 48 short period selected lines and 48 long period selected lines. Consequently, all RILs of one collection bearing the same reporter insert. These BC1F2 lines were then progressively self-fertilized. At the moment, the nRILs are at the BC1F5 generation. Assumingly, the homozygosity throughout their genome is about 96.875%. Single-seed descent will continue until BC1F6. BC1F7 bulk progeny will be genotyped.

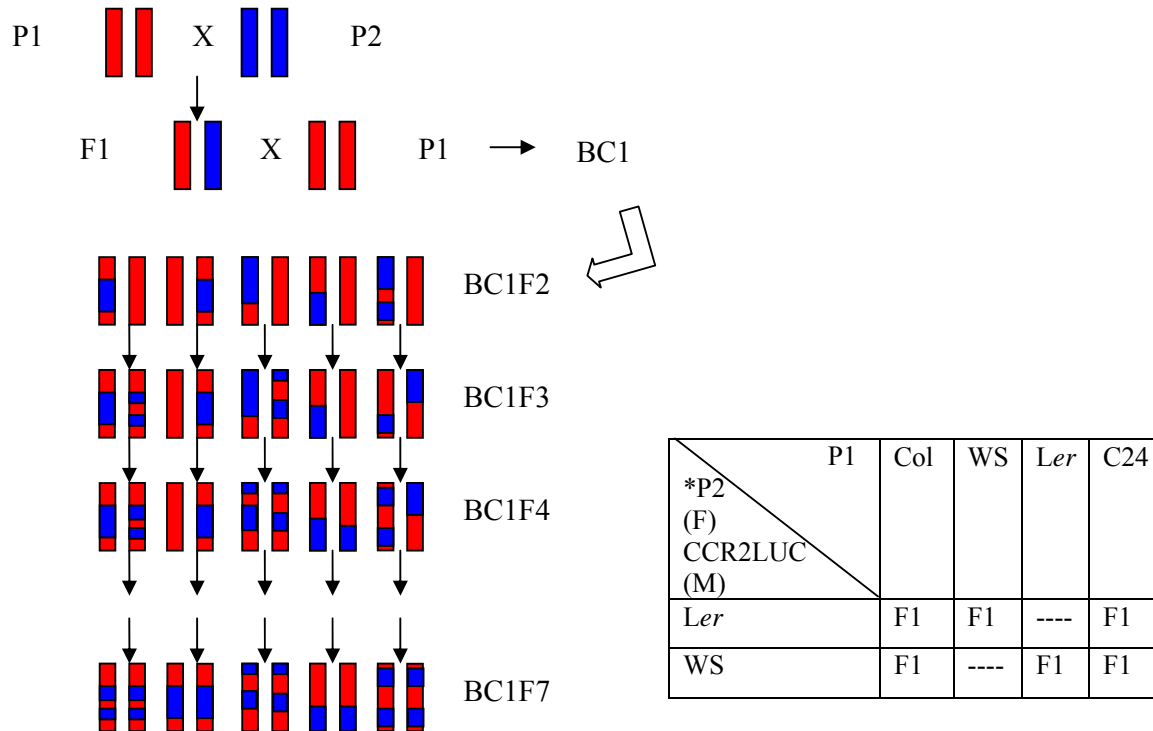


Figure 2.1 Crosses performed to generate six new RIL collections, each harboring the *CCR2::LUC* transgene

A represents the scheme used to generate the RILs during this project, and B represents the parents used in the crosses. * means that P2 was transformed with *CCR2::LUC*. T1 transformed plants were back crossed to P2, and afterwards were used for crossing P1 plants. M stands for male parent and F stands for female parent. ---- indicates crosses not made.

2.2.3 DNA extraction

1. Place seedlings, young leaves, or floral buds into Eppendorf tube and label
2. Add 500 μ l DEB to tube and disrupt tissues with a drill head holding a glass rod (model IKA RW16)
3. Add 75 μ l Chloroform
4. Close tubes tightly and vortex for 5 minutes
5. Centrifuge tubes at max for 5-10 minutes
6. Whilst centrifuging, label new tubes and add 350 μ l Isopropanol
7. When centrifuge is finished, carefully pipette 350 μ l upper DEB layer and add to new tube of Isopropanol, close tube, and invert gently four times
8. Centrifuge at max for 10 minutes
9. Decant supernatant
10. Add 500 μ l 70% Ethanol, invert and centrifuge for 5 minutes
11. Decant, carefully pipette residual and air dry
12. Add 100 μ l TE, flick vigorously, wait ~10 minutes, and centrifuge at max (16K) for 5 minutes
13. Whilst centrifuging, label new tubes
14. When centrifuge is finished, pipette 90 μ l DNA solution into new tube

2.2.4 PCR

For the genotyping of the new Recombinant Inbred Lines the following PCR protocol was followed for most of the mapping primers

94°C x 5min
94°C x 30sec
52°C x 30sec
72°C x 30sec
72°C x 10min

} x 39 cycles

2.2.5 Restriction digestion

PCR products were digested by adding 1.2 μl H₂O, 1.2 μl 10x restriction nuclease buffer and 0.2 μl restriction enzyme per 10 μl PCR product volume. The reaction were incubated for 5-6 h or over-night at the appropriate temperature and the reaction products were subsequently resolved on 4% TBE-agarose gels.

2.2.6 Flowering time assays with new Recombinant Inbred Lines

The flowering-time experiments were performed in the greenhouse supplemented with artificial lighting at Max Planck Institute for Plant Breeding Research (MPIZ) during the end of autumn and winter 2007. The average temperature was 16°C and the typical photoperiod was 14 hours light:: 10 hours darkness. The seeds of the C24 cross to WS bearing *CCR2::LUC*, and backcrossed to C24 were sown on a moistured filter paper, and kept in 4°C for 48 hours. Then five stratified seeds were placed in a 8cm*8cm*7cm pots filled with soil. The first experiment was started 15 November 2007 and the second on 02 December 2007. Upon germination, only one plant per pot was kept for the flowering-time assay. Total leaf number was measured including rosette and cauline leaves at the time of the bolting (Domagalska et al., 2007).

2.2.7 Plant growth conditions

2.2.7.1 For light dark entrainment (LD):

Plants were grown on MS-containing 3% sucrose plates under a 12 hours light-12 hours dark cycles, at 22°C. Onset of illumination was 9:00am. Light intensity in the growth cabinet was 35 $\mu\text{mol m}^{-2}\text{sec}^{-1}$.

2.2.7.2 For temperature entrainment (TMP):

Plants were grown on MS-containing 3% sucrose plates under a 12 hours at 22°C-12 hours at 16°C cycles, at constant light. Onset of warm temperatures was 9:00am. Light intensity in the growth cabinet was 35 $\mu\text{mol m}^{-2}\text{sec}^{-1}$.

2.2.7.3 For light-dark / temperature cycles experiments:

Plants were grown on MS-containing 3% sucrose plates under 12 hours light-12 hours dark cycles, at 22°C, for 5 days and then transferred to 2 days in 12 hours at 22°C-12 hours at 16°C cycles, the onset of illumination was 9:00am for 12 hours light-12 hours dark cycles and the onset of warm temperatures was set at: A) 03:00pm called IN, or B) 03:00am called OUT.

In separate experiments, plants were grown in MS-containing 3% sucrose plates in 12 hours light-12 hours dark cycles, at 22°C, for 5 days and then for 2 days in 12 hours at 22°C-12 hours at 12°C cycles, at 12 hours light-12 hours dark cycles. In all cases light intensity in the growth cabinet was $35\mu\text{mol m}^{-2}\text{sec}^{-1}$.

2.2.7.1: LD



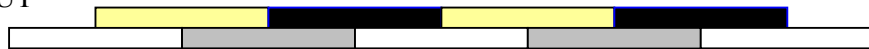
2.2.7.2: TMP



2.2.7.3A: IN



2.2.7.3B: OUT

**Figure 2.2 INOUT entrainment protocols**

Yellow bars represent light period, black represents dark period, white represents warm period, and grey represents cold period. In all cases light intensity was $35\mu\text{mol m}^{-2}\text{sec}^{-1}$.

2.2.8 Determination of clock phenotypes with promoter-luciferase assays

2.2.8.1 Luminometer assays for bioluminescence

1. Prepare the 96-well assay plates: Surface sterilize with ethanol, and air dry ethanol. After drying, add 200 μ l of MS3 in each well
2. Transfer plants grown for 7 days at light dark cycles at 22°C to 96-well microtiter plates containing MS3
3. Filter sterilize 5mM luciferin
4. Add 15 μ l of filter sterilized 5mM of luciferin to each plant
5. Cover the plate with Top Seal
6. Poke a hole on the Top Seal with a surgical needle in each well to allow air exchange for the oxidation of luciferin to oxyluciferin, and therefore enable the luminescence detection
7. Let the plates to synchronize for another entrainment cycle by returning them to the previous entrainment conditions
8. Transfer the 96-well plates to Packard Top Count Scintillation for the luminescence detection. The light emission measurements were performed with the use of 6 synchronized photomultipliers, and measured as counts per second

2.2.8.2 Liquid nitrogen Cooled Digital camera (CCD) assays for bioluminescence

1. Prepare the 96-well assay plates: Surface sterilize with ethanol the cryo boxes (ROTH Karlsruhe), and air dry ethanol. After drying, add 1ml of MS3 in each well
2. Sterilize 100 seeds of each independent transformed line
3. Divide the amount of the seeds in equal portions, and sow them directly to the cryo boxes
4. Stratify sown seeds in the sterile box for 2 days at dark at 4°C
5. Transfer the box with the seeds to a growth cabinet for 7 days at either light dark at 22°C or 22-16°C cycle at constant light
6. Filter sterilize 5mM luciferin.
7. Add 15 μ l of filter sterilized 5mM of luciferin to each plant

8. Cover the plate with Top Seal
9. Poke a hole on the Top Seal with a surgical needle in each well to allow for air exchange for the oxidation of luciferin to oxyluciferin, and therefore enable the luminescence detection
10. Let the plates to synchronize for another entrainment cycle
11. Transfer the 96-well plates to ROPER VersArray ST-133 CCD camera for the luminescence detection. Camera exposure was set at 15 minutes, images were taken once every hour

2.2.9 Software for analysis of circadian rhythms

2.2.9.1 For analysis of luminescence output of Top Count scintillation counter

The data obtained by TopCount were processed with TopTempII, a Microsoft Excel macro (Braun *et al.*, 2002) to analyze circadian parameters of light-dark and temperature entrained plants. Period, amplitude, and phase estimates were performed using a Microsoft Excel macros suite termed Biological Rhythms Analysis Software System (BRASS), generated by Southern and Millar, 2005, that includes the FAST FOURIER TRANSFORMATION NONLINEAR LEAST SQUARES (FFT-NLLS) method (Plautz, 1997). A time window corresponding to at least three periods (>72 h) was used for FFT-NLLS analysis, normally this time window was from ZT30-120. The period limits used were 15-35 h, and the parameter confidence probability was 95%. Rhythms were assessed by comparison of relative amplitude of error (R.A.E.)-weighted means of the period lengths calculated by BRASS. This was in addition to comparisons of individual period and of R.A.E. values. R.A.E. is the ratio of amplitude of error estimate in relation to the estimate of the most probable amplitude that describes the fit of the actual data to the theoretical cosine curve. Therefore, R.A.E. is a measure for the degree of rhythmicity. For example, R.A.E. = 0 the trace is perfectly rhythmic (precise) compared to the theoretical curve and when R.A.E. = 1 the trace is completely arrhythmic. In this study, R.A.E. < 0.4 is considered rhythmic. For luminescence data, phase was determined as the first period acrophase of the cosine curve, unless otherwise stated.

2.2.9.2 CCD Camera data analysis

Luminescence images were taken with Roper VersArray ST-133 CCD camera with one image every one hour. Plants were kept in constant red and blue light for 40 minutes, and then imaged in an intervening dark period for 20 minutes. The resultant images were stacked using METAMORPH software (Universal Imaging Corporation). All imaging with this CCD setup was performed and analyzed as Gould *et al.* (Gould et al., 2006).

2.2.10 QTL mapping

The statistical package used to map QTLs in this study was MapQTL 5.0 (Kyazma BV). Three input files were generated containing information such as the quantitative data (phenotype), the loci (genotype of each RIL), and the map information (marker location). Interval mapping (IM), and consequently MQM mapping were performed for period for each entrainment. During IM, each position of the genome was checked for the presence of a segregating QTL. However, MQM is more accurate than IM, because in addition to the genome scanning of a single segregating QTL it also fits the effect of nearby markers, cofactors, therefore reducing the residual variance, and potentially revealing other close by QTL.

A measure of QTL significance was defined by the Likelihood of Odds (LOD). The higher the LOD score, the more statistically significant was the presence of a QTL in the genomic interval detected. LOD score is a 10-base logarithm of the quotient of two likelihoods H_1 , and H_0 . H_1 is the likelihood of having a segregating QTL at a specific locus, whereas H_0 is the likelihood of having no segregating QTL at the respective locus. After performing one thousand permutation tests repeatedly, the averaged genome wide LOD for 95% significance was taken as a threshold. Additionally, the estimated percentage of explained variance of each QTL was calculated by MapQTL 5.0 during MQM.

2.2.11 Statistical analysis

For the statistical analysis, the package SPSS version 11.0.0 was used (SPSS Inc., Chicago, IL). Univariate analysis was preferred because it allows calculating uni- but also multi-variate F-tests, in contrast to one way ANOVA that can perform F-test for only one factor. For the GLM Univariate analysis, period was used as a dependent

variable and RIL and environment as fixed factors. The null hypotheses of the test were that the mean period is the same across RILs or different environments, and there was no RIL by environment interaction. Additionally, it calculated the R^2 (R squared). R^2 represents a goodness of fit measure. It described how well the variation in period can be accounted for by RILs (genotype) or LD or TMP entrainment (environment). It ranged from 0 to 1, where small values indicate that the data do not fit well model. Two-way interactions among the QTLs identified for period, were tested by ANOVA using the corresponding two markers as fixed factors and the period as dependent variable, using the general linear model (GLM). Heritability (broad sense) was estimated as the proportion of variance explained by between-line differences and among line differences calculated by using the GLM module of the statistical package of SPSS.

3 QUANTITATIVE ANALYSIS OF LIGHT-DARK vs TEMPERATURE ENTRAINMENT

INTRODUCTION

Natural variation on circadian-clock parameters was previously assayed successfully in the past to map QTLs for circadian rhythmicity (Swarup et al., 1999; Edwards et al., 2005; Darrah et al., 2006). To study such genetic variation several accessions and Recombinant Inbred Lines (RILs) were used. The most informative RIL for circadian studies has been the collection generated by crossing *Ler* to Cape Verde Islands. Cvi was collected in a tropical environment close to the equator, where daylength does not change as much as in northern temperate climates, where *Ler* is originated. As one circadian QTL example, Darrah, *et al.* used transformed CvL RILs with *CAB2::LUC*, to identify loci that contribute to daylength measurement by assaying circadian phase of *CAB2* (Darrah et al., 2006). Multiple QTLs were detected. Since natural variation is an established method for studying circadian rhythmicity, I decided to exploit this natural-genetic variation to study the effect of temperature entrainment, as compared to light-dark entrainment.

The daily rotation of the earth provides two sets of stimuli for organisms to synchronize to external time. In addition to light, temperature cycles are also able to reset the circadian clock (McClung, 2006). It was shown that *A. thaliana* can be entrained when as little as 4°C temperature variation is present (Somers et al., 1998b; Michael and McClung, 2002). A major finding regarding temperature entrainment was that two oscillators can be distinguished based on differential sensitivity to temperature (Michael et al., 2003a). This was concluded from experiments that mapped the effect of four hours temperature pulses in the expression of *TOC1*, *CAB2*, and *CAT3* (Michael et al., 2003a). Though it was not clear from this work if there are two unlinked primary oscillators, two primary oscillators that are coupled, or a primary oscillator that sets the rhythms to a secondary (slave) oscillator. Moreover, it cannot yet be resolved if there is one oscillator that is primarily for light-dark entrainment, and another one for temperature entrainment, because the expression of

clock genes after light pulses was not conducted. Regardless, the circadian clock(s) have differential sensitivity to light versus temperature inputs.

Molecularly, the temperature effect on the entrainment of the oscillator has been examined in the mutant background of two PRR family members, *PRR9* and *PRR7*. Although the single mutants have no phenotype after light-dark entrainment, the cotyledon-movement phenotype in the double mutant, and the expression *CCA1*, *LHY*, and *TOC1* in the same background was found to be extremely long period. Surprisingly, the double mutant was unresponsive to temperature cycles, as indicated by the dampened phenotype of the *CCA1::LUC* or *LHY::LUC*. However, *TOC1* expression, as reported by luciferase, is more variable. In some cases, *TOC1* in *prp9 prp7* double mutant peaks in antiphase compared to the wild type, whereas in other cases is completely arrhythmic. All these results suggested that *PRR9* and *PRR7* are indispensable for thermal-entrainment inputs, although it is not clear that they function as integrators of temperature signal or purely as oscillator components that when lost resulting a clock without the ability to respond to temperature cycles. Genetics can resolve this physiological discrepancy.

This chapter study will provide a description of natural variation present when comparing circadian parameters after temperature to light-dark entrainment, respectively. A natural-variation approach was chosen, instead of a mutant screen, on the basis that the genetic variation reflects adaptation of a certain genotype to the specific ecological environment. In this chapter, the identification of novel and identified loci will be described using two RIL population generated by four different parental accessions. Circadian-period variation was used as a trait to study temperature entrainment in both RIL populations.

3.1 Light dark vs temperature entrainment of Cvi/Ler RIL

To investigate natural-variation effects on temperature, I modified a population suited for a circadian study. The existing *Cvi/Ler* (hereafter CvL) RIL population is one of the most informative collection to date to study natural variation of the circadian clock (Swarup et al., 1999; Edwards et al., 2005; Darrah et al., 2006). By measuring clock traits, various loci have been mapped (Edwards et al., 2005; Darrah et al., 2006). Further, gene expression assayed with a promoter::luciferase construct has been previously described as a robust method to measure an expression QTL (eQTL) (Darrah et al., 2006). Therefore, I transformed a number of *Cvi/Ler* RILs with a temperature responsive and circadian-regulated reporter *CCR2::LUC*. *CCR2* was also chosen amongst other clock marker genes due to its temperature entrainability and to its robust rhythmicity under a wide range of conditions (Heintzen et al., 1997). So, by using the luciferase platform, I was able to kinetically monitor luciferase expression driven by the *CCR2* promoter under constant light, after entrainment by 12-hours light followed by 12-hours darkness at 22°C, or by entrainment with temperature cycles of 12 hours at 22°C followed by 12 hours at 16°C under constant light. Luciferase monitoring of T2 plants was performed under free running constant light, for at least five days. Period length of *CCR2* rhythms was estimated by FFT-NLLS analysis (see 2.2.9.1), where circadian data was fit to cosine curves. The designated RILs, and the averaged period of after light-dark entrainment, and the standard deviation, and standard error of the mean, are showed in Table 3.1. Additionally, in Table 3.2, the free-running-period phenotype under constant light of the same CvL population, and the standard deviation and the standard error of the mean, are showed after temperature entrainment under constant light. The two tables show that there are differences between different RILs regarding period within, as well as between, in response to different entrainment protocols. Thus, a variety of kinetic parameters of the *CCR2::LUC* could be detected.

RIL NAME	LD PERIOD	SD	SE	RIL NAME	LD PERIOD	SD	SE
5	27.760	0.373	0.215	72	25.467	0.397	0.120
6	24.903	0.703	0.212	103	24.650	0.423	0.244
11	26.287	0.831	0.372	105	26.011	0.721	0.180
12	26.420	0.946	0.273	114	24.807	0.808	0.172
13	27.480	0.652	0.112	116	26.867	0.837	0.144
16	25.055	0.714	0.173	125	28.536	0.885	0.313
19	27.548	1.028	0.343	131	25.701	1.226	0.433
20	25.705	0.647	0.216	140	26.181	1.305	0.227
27	26.576	1.139	0.431	141	27.087	0.282	0.199
36	25.120	1.074	0.287	145	25.784	0.734	0.300
38	26.656	0.410	0.155	149	25.190	0.380	0.134
44	25.414	1.006	0.318	150	25.676	1.082	0.167
47	28.220	0.529	0.167	151	25.386	1.367	0.395
48	24.223	0.784	0.296	153	26.588	0.696	0.156
49	27.874	0.933	0.467	154	25.474	0.843	0.204
50	25.212	0.730	0.177	156	25.503	0.381	0.171
54	25.395	1.023	0.324	164	24.783	0.537	0.203
59	24.014	0.979	0.489	175	24.520	0.648	0.265
61	25.036	1.198	0.599	183	25.633	1.450	0.302
65	25.171	0.520	0.212	187	26.489	0.894	0.258
69	25.430	0.556	0.393	193	25.014	1.224	0.170

Table 3.1 The free-running period of the Cvi/Ler RIL collection under constant light after entrainment to 12 hours light followed by 12 hours dark

RIL NAME corresponds to the arbitrary name as given in Alonso-Blanco *et al.* for the CvL population (Alonso-Blanco, 1998), LD period corresponds to averaged period after light-dark entrainment. SD is the standard deviation of the period and SE is the standard error of the mean period.

RIL NAME	TMP PERIOD	SD	SE	RIL NAME	TMP PERIOD	SD	SE
5	27.718	0.617	0.159	105	25.040	0.553	0.175
6	24.553	1.162	0.439	114	23.980	0.605	0.349
11	25.280	0.468	0.085	116	26.064	0.677	0.128
12	24.930	0.471	0.192	125	27.721	0.895	0.316
13	26.296	0.631	0.093	131	25.660	0.727	0.188
16	24.278	0.692	0.148	140	25.176	0.855	0.137
19	27.632	0.598	0.166	141	24.674	0.874	0.291
20	25.419	0.893	0.231	145	25.376	0.493	0.156
27	25.222	0.569	0.152	149	24.194	0.533	0.161
36	24.799	0.712	0.197	150	25.047	0.932	0.132
38	26.823	0.689	0.308	151	24.483	0.678	0.226
44	24.947	0.893	0.231	153	25.418	1.063	0.320
47	27.291	0.814	0.308	154	24.927	0.700	0.181
48	23.763	0.561	0.169	156	24.037	0.803	0.242
49	27.094	0.553	0.196	164	24.333	0.224	0.158
50	25.341	0.802	0.214	175	23.286	0.706	0.182
54	23.885	0.923	0.292	183	25.105	0.861	0.230
65	24.486	0.446	0.158	187	25.464	1.301	0.492
72	23.848	0.549	0.246	193	24.012	1.103	0.349

Table 3.2 The free-running period of the Cvi/Ler RIL collection under constant light after entrainment in temperature cycles of 12 hours at 22°C followed by 12 hours at 16°C in constant light

RIL NAME corresponds to the arbitrary name as given in Alonso-Blanco *et al.* for the CvL population (Alonso-Blanco, 1998), TMP period corresponds to averaged period after temperature entrainment. SD is the standard deviation of the period and SE is the standard error of the mean period.

3.1.1 Period differences after light-dark and temperature entrainment of the CvL/Ler population

Previously I found that there was a period variation in the CvL RILs after entrainment to 12 hours light::12 hours darkness at 22°C, compared to entrainment to 12 hours at 22°C and 12 hours in 16°C at constant light (Tables 3.1 and 3.2). The differences in the period between the two protocols were plotted against each other in the overlay plot as shown in Figure 3.1, using the JMP4 software. Interestingly, the period in the majority of the CvL RILs is significantly longer after the light-dark entrainment compared to after the temperature entrainment (Figure 3.1). In those few lines that had a slightly longer period after temperature entrainment, this difference was not significantly different. Thus, the heritability of periodicity was dependent on the preceding entrainment. The details of these phenomena will be described later (see 3.1.4).

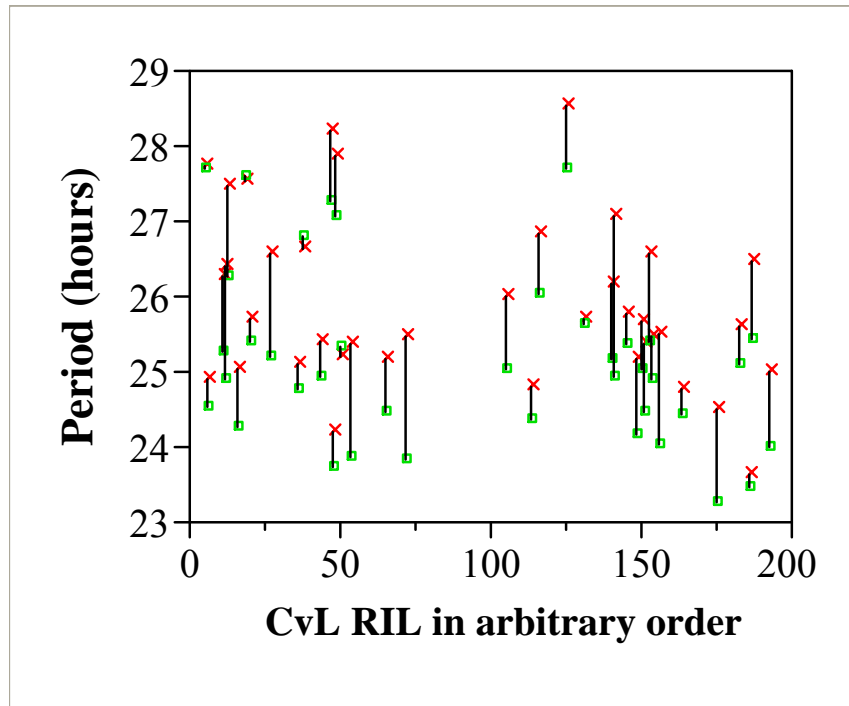


Figure 3.1 Period differences of rhythmic plants within genotypes of the CvL RIL collection of temperature-entrained versus light-dark entrained plants

X axis represents the CvL RIL number, and Y axis represents period. ■ represents the period of temperature entrained plants, × represents the period of the light-dark entrained plants.

Two RILs, CvL 47 and CvL 6, were further chosen to illustrate the differences shown in Figure 3.1. The RILS were entrained in light dark or temperature cycles, as described in the beginning of this session. The graphical depiction of the circadian rhythmicity of luciferase driven by the *CCR2* promoter is showed in Figure 3.2. Of these two lines, CvL 6 displayed a period difference of about half an hour, when comparing the period after the light-dark and after temperature entrainment. CvL 47 displayed after light-dark entrainment a longer period, when compared to the temperature-entrainment protocol. These results are in agreement with the results of Figure 3.1 in establishing the quantitative and differential kinetic effect of *CCR2* rhythms dependent on the preceding entrainment.

More detailed analysis of Figure 3.2 suggests that phase also varies differentially after the two entrainments in these two RILs. Specifically, CvL 6 showed not only small period variation, when compared after the light dark and temperature entrainment, but also minor differences in phase. Whereas CvL 47 after light-dark entrainment showed earlier phase and longer period compared to the effect after the temperature entrainment. Furthermore, CvL 6 was found to have a shorter period, and earlier phase, compared to CvL 47 in both entrainments. The evident phenotypic variation of period, after the different entrainment protocols, could be due to the different genetic background and/or due a preferential response to either of the two environmental inputs. The test of this hypothesis will be described by statistical analysis in the subsequent section.

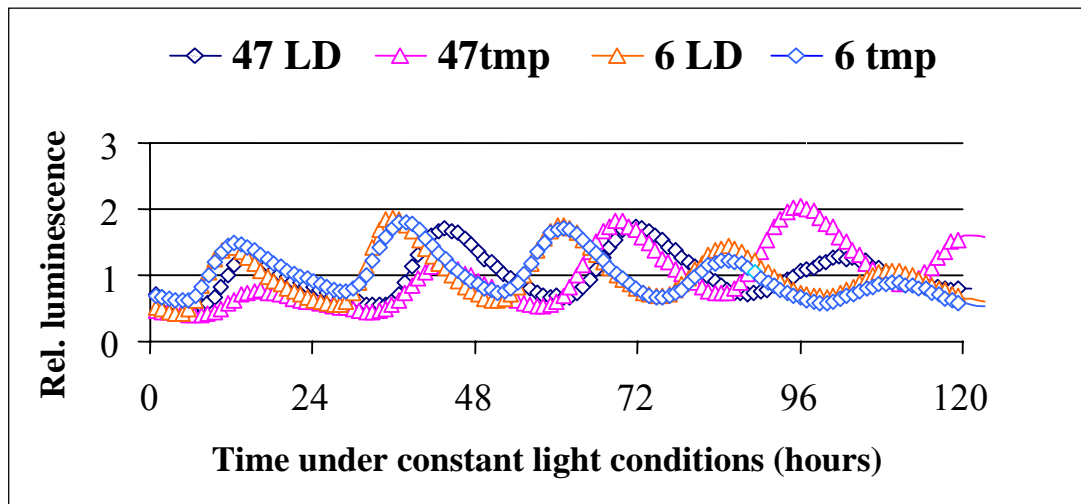


Figure 3.2 Variation of period after entrainment to the two different protocols between two representative RILs: CvL 6 and CvL 47

LD denotes the free running rhythmicity of luminescence driven from the *CCR2* promoter after light dark entrainment, and tmp denotes the free-running rhythmicity after temperature entrainment. Relative luminescence was depicted as a ratio of the actual luminescence of each time point divided by the average luminescence over the time course of the experiment. Assay started at time 0, and is the onset of lights for light-dark entrainment, or the onset of warm temperature for temperature entrainment. Note that CvL6 has smaller differences in free running period than the CvL 47 after the two entrainment protocols.

3.1.2 Statistic analysis of mean period after LD vs. tmp entrainment in the CvL RIL

Variation of traits fall into two categories: continuous or distinct. I found earlier that period varies between various RILs after the entrainment in the two different protocols, but period varies also after entrainment in the same protocol (Tables 3.1 and 3.2, Figure 3.1). However, whether the variation in period was continuously distributed, and, if so, whether it was normally distributed, will determine the QTL mapping model. Therefore, the averaged period of *CCR2::LUC* for each transformed CvL line, as measured after the two different entrainments, was binned in one hour intervals. The binned period was then plotted against how frequently period values were fall into each one hour interval, as it is represented in Figure 3.3.

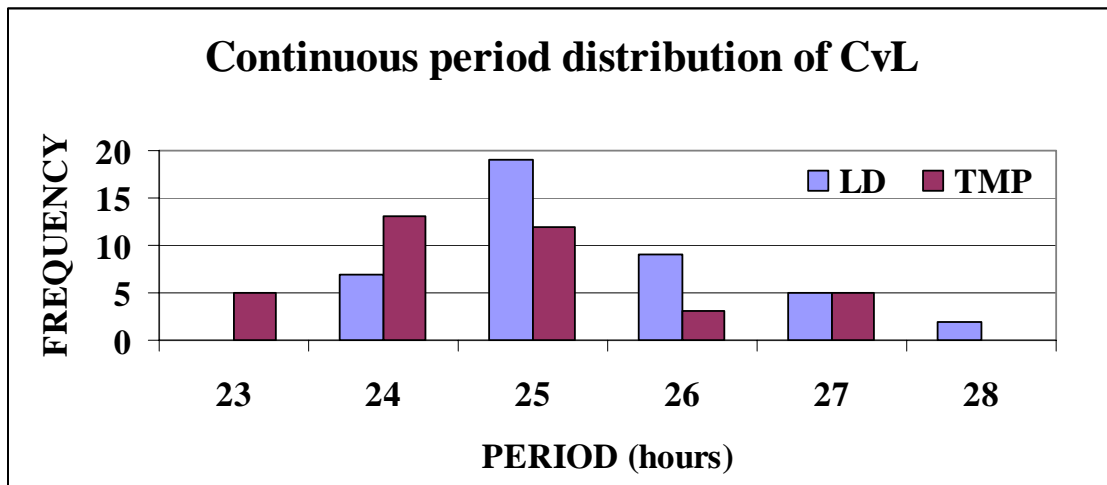


Figure 3.3 The continuous distribution of period for 39 CvL Recombinant Inbred Lines X-axis is period measured in hours and Y axis represents number of CvL RILs with a certain period. The period was binned in 1 hour interval.

The free running period of each averaged RILs after the entrainment to either light-dark cycles or temperature cycles was found to be continuously, and normally, distributed (Figure 3.3). Since the data were normally distributed, Analysis of Variance (ANOVA) could be used to compare the population period mean for the two entrainments. Confidence interval (CI) is a measure of spread of the period means of the various RILs per environment, therefore 95% of CI means that 95% of the period means of the different RILS falls between the upper and lower bounds. For 95% of confidence interval, the lower bound of mean period after light-dark entrainment, which is 25.696 hours, was not found to overlap with the upper bound of the mean period after the temperature entrainment, which was 25.251 hours (Table 3.3). The standard error of the mean indicates how much the mean period varies from RIL to RIL, within each environment, as they deviated from the overall mean calculated for each environment. The standard error after each entrainment was found to be low (Table 3.3). Therefore, by taking the modified population period mean measured after each entrainment protocol, as calculated for the 95% of period values and adding/subtracting the standard error of each respective entrainment, the period was found to be statistically different. All these data confirm that there were significant period differences within genotypes of the population after the two entrainment protocols.

Further analysis for the contribution of the genotypes, environment and the genotype by environment interactions, to the phenotype (period) was performed by GLM Univariate analysis of variance. Details about the performance of the test can be found in session 2.2.11. A key value of the resulted analysis seen in Table 3.4 is the F value. The F value calculated by the test, for either the main effect of RIL and ENVIRONMENT or their interaction effect, was higher than the F value found in tables for the respective degrees of freedom (df). Therefore, these results rejected the null hypothesis, which was that the mean of period after the light-dark entrainment is the same after the temperature entrainment, or that the mean periods of various RILs did not differ. Furthermore it rejected the null hypothesis that there was no interaction between the two factors. Moreover, the adjusted R^2 indicated that about 60% of the mean period variation can be explained by genotype, environment, or genotype-by-environment interactions. Strong statistical support affirmed that the preceding entrainment protocol differentially directs the free-running periodicity under identical

assay conditions.

	Mean	Std. Error	95% Confidence Interval	
Environment			Lower Bound	Upper Bound
LD	25.792 ^a	0.049	25.696	25.887
TMP	25.161 ^a	0.046	25.071	25.251

^a Based on modified population marginal mean.

Table 3.3 Statistic analysis of the CvL lines used for QTL mapping

The mean period after light or temperature entrainment is calculated based on the 95% of the measurements. Environment indicates the different entrainment protocols. LD stands for the light-dark entrainment and TMP for the temperature entrainment. The two bounds for 95% of confidence interval suggest that 95% of the mean period measured in various RILs falls within the lower and upper bound, and the rest 5% is outside of these intervals. Standard error of a mean is a measure of the variation and it is dependent on the sample size. ^a denotes the modified population marginal mean for the 95% Confidence Interval.

Source	SS	df	MS	F	Sig.
Corrected Model	999.351 ^a	56	17.846	26.693	0.000
Intercept	370584.652	1	370584.652	554317.010	0.000
RIL	828.310	37	22.387	33.486	0.000
ENVIRONMENT	60.448	1	60.448	90.417	0.000
RIL * ENVIRONMENT	30.002	18	1.667	2.493	0.001
Error	615.059	920	0.669		
Total	637295.809	977			
Corrected Total	1614.410	976			

^a R Squared = .619 (Adjusted R Squared = .596)

Table 3.4 ANOVA analysis depicts significant genotype by environment interaction for the two different entrainments

RIL denotes the genotypic effect, ENVIRONMENT denotes the different entrainments and RIL*ENVIRONMENT denotes the interaction of the genotypes to the different entrainments. SS is the sum of squares. df are the degrees of freedom. MS is the mean square calculated by dividing the SS by df. F is the F-ratio calculated by dividing MS by the error. Significance level was set to .05. Significance of ≤ 0.001 means highly significant differences or highly significant interactions. * denotes the testing for an interaction between two factors.

3.1.3 QTL mapping of periodicity in the CvL collection

The CvL RILs transformed with *CCR2::LUC* were successfully assayed for period under constant light after two different entrainments; after light-dark at constant warm temperature, and after warm-cold cycles under constant light. Here, approximately 40 genotypes were phenotypically characterized for clock period (Tables 3.1 and 3.2). The averaged period of these lines revealed that overall temperature-entrained plants have a shorter period mean than light-entrained plants (Table 3.3). As I could identify that some RILs that respond differentially to the one entrainment over the other (Tables 3.1 and 3.2), this supports my hypothesis of the existence of specific loci controlling the two different entrainment inputs. To test this, I applied QTL mapping to the data.

Since circadian period varied continuously between the different genotypes of a *Cvi/Ler* RIL population, I could analyze it as a quantitative trait. Once the period is scored, and the genotype of the RILs is known, one can use available statistical packages to map genomic regions containing significant natural genetic variation that accounts for genetic variation to temperature or light-dark entrainment. The statistical package used in this case was MapQTL 5.0. A measure of QTL significance is the Likelihood of Odds (LOD). Whenever, the LOD score exceeds the threshold obtained by the permutation tests, this supports the detection of a segregating QTL at that location. The identified loci were thus mapped. Another important measure given by the analysis is the percentage of explained variance of the respective QTL. The higher this percentage, the larger the effect the QTL supplies the trait.

Quantitative analysis was performed for each entrainment protocol using two different data sets of genotypes. The first data set includes RILs that the averaged value of period meets the following three criteria. The period of at least 10 plants were averaged, the standard deviation was found to be less than 1 hour, and the standard error of the mean period was less than 0.25 hours (Tables 3.1 and 3.2). The period was assessed separately for either light dark, and for temperature entrainment. Note that in this set that both the same, and different RILS were included for the two entrainments. The second data set includes exactly the same lines, 43 in total, for the temperature and light entrainment. However, some lines of these 43 show intraline variation, and/or the number of individuals assayed for one of the two entrainments

was low (Tables 3.1 and 3.2). The second set was used as a control to distinguish between genotypic or environmental effect. Analysis performed in the second set identifies a QTL at the same location, suggesting strongly that there is a genetic component involved. However, a difference in the LOD score was observed for the light dark versus the temperature entrainment. When analyzing the first set, in which some lines show more robust phenotype in one of the two different entrainments, different segregating QTLs were identified for different physiological entrainments. As well, common QTLs were also detected (Figures 3.4 and 3.5).

For the light-dark entrainment, the MQM mapping application detected only one main effect periodicity QTLs at chromosome five at 17-24cM. The explained variance of this QTL was found to be more than 45%. No main QTL was identified at the first chromosome. All the other QTLs shown in Figure 3.4 are interacting QTLs. At the top of 1 chromosome, at 0-10cM, the interacting QTL overlaps with *LHY*, a core-clock gene, *CRY2* a blue light photoreceptor, and also with *PHYA* a red-farred light receptor. All are thus gene candidates for this locus. At 50-60 cM of the first chromosome, a locus not previously identified exists. At the bottom of chromosome five at 90-100cM, another interacting QTL was identified. *TOC1*, *PRR3*, and *SRR1* are located within this area. At the top arm of chromosome 4, another interacting QTL was identified at 0-20cM. *FRIGIDA (FRI)*, a positive regulator of *Flowering Locus C (FLC)* transcription factor is localized at that proximity. These known genes might be candidates, however, the presence of novel genes that represent those QTLs cannot be excluded. In Figure 3.4, the main and interacting QTLs and their effects are represented.

For the temperature entrainment, three main periodicity QTLs were detected through MQM analysis, one at the first chromosome and two at the fifth chromosome. The main effect QTL detected at chromosome 1 at position 24-40cM explains about 40% of the phenotype. This QTL co-localized to a known circadian oscillator gene named *GIGANTEA (GI)*. The two QTLs at chromosome 5 are located at the top arm at position 20-30cM and at the bottom arm at 90-100cM. QTLs at the top and bottom of chromosome 5 explain 35% and 25% of the phenotype respectively. However, interacting QTLs modified the effect of the three main QTLs. Especially, the QTL at chromosome 3 had a positive effect on the phenotype of QTL in chromosome 1, and the same for the bottom QTL in chromosome 5. This QTL was not previously

identified from other circadian studies. Also, no known clock gene is localized at this area. At chromosome 5, two loci were identified to have differential effect at location 0-9 cM, and at 17-24cM. Specifically, the effect the first QTL had a positive effect on the main QTLs and the second had a negative effect. The chromosome five QTL localized at 0-9cM is in an interval with a member of the *TOCI* family called *PRR7*. The second QTL of fifth chromosome at 17-24cM co-localizes with *FLC*, a flowering time regulator in response to cool temperatures that can affect periodicity. Finally, the QTL localized at the end of chromosome 4 showed minor effects on QTL at chromosome 1, but it had a great positive effect on the main QTL at the bottom arm of chromosome 5. In the bottom of chromosome 4, no clock gene has been identified so far. The chromosome 2 QTL has a small effect in chromosome 1 and chromosome 5 main QTLs. All the above described positive or negative effects suggest that the identified QTLs are epistatic. An expansion of the epistatic effects will follow in the session 3.1.4.

To conclude, I found QTL for light and temperature that both were co-localized and others that map to distinct positions. The chromosome 1 main effect QTL found at 0-10cM, and the interacting QTL at 60cM were both specific for the light entrainment, whereas the first chromosome main effect QTL found at 24-40cM seemed to be specific to the temperature entrainment. The chromosome 2 and 3 interacting QTL were specific for temperature entrainment. The top arm of chromosome 4 interacting QTL seemed to be specific for light-dark entrainment, whereas the bottom arm interacting QTL of chromosome 4 was specific for temperature entrainment. The top arm chromosome five main effect QTL locus was shared component for both entrainments. Therefore, light and temperature entrainment seemed to use the both same and also different components.

I found with MQM mapping that several loci contributed to the control of periodicity after light-dark or temperature entrainment. But what was the effect of this genotypic variation that brings on the total phenotypic variation? To answer that, I estimated the broad sense heritability of the trait. The broad sense heritability was 0.82 for the light-dark entrainment and 0.85 for the temperature entrainment (Table 3.5). These results suggested that the phenotypic variation can be assigned largely, but not totally, to the genetic variation. However, it is wrong to extrapolate that if an individual has 25 hours period after the light-dark entrainment the 85 %, which

CHAPTER 3 Quantitative analysis of light-dark vs temperature entrainment

accounts for 20.5 hours, is due to genes and the rest 15%, which equals to 4.5 hours due to environment. In general, the phenotype of an individual is a consequence of the interaction between its genes and its environment. Gene interaction will be extensively described in the next session for the light-dark and temperature entrainment.

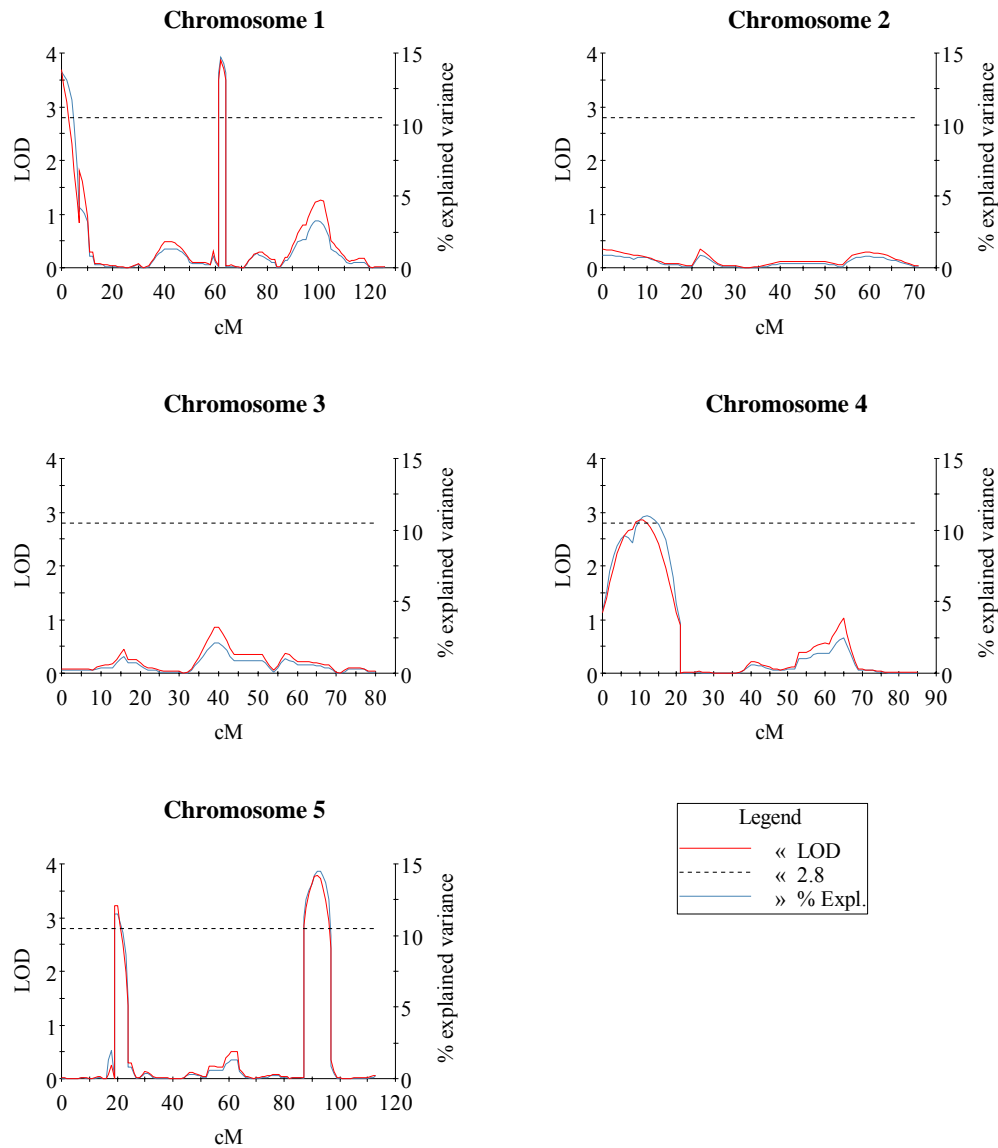


Figure 3.4 MapQTL for the light-dark entrainment of the CvL population

X axis represents the chromosome location, measured in cM, left Y axis represents the LOD score, and right Y axis represents the % of explained variance. This percentage is a measure of the effect of the QTL that supplies to the phenotype. The dotted line represents the LOD score threshold. It was set to 2.8 after calculation of 1000 permutations, for 95% significance level.

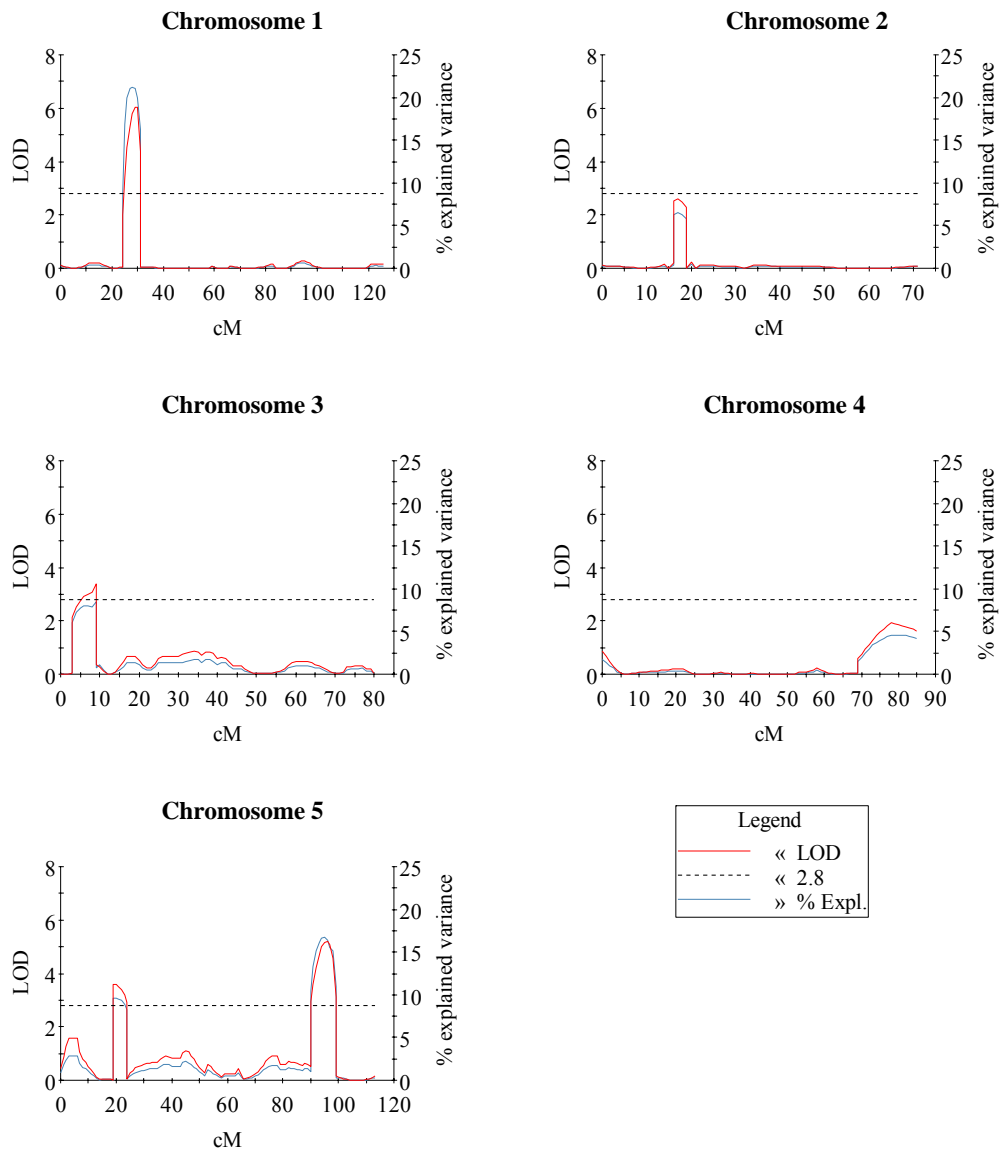


Figure 3.5 MapQTL for the temperature entrainment of the CvL population

X axis represents the chromosome location, measured in cM, left Y axis represents the LOD score, and right Y axis represents the % of explained variance. This percentage is a measure of the effect of the QTL that supplies to the phenotype. The dotted line represents the LOD score threshold. It was set to 2.8 after calculation of 1000 permutations, for 95% significance level.

3.1.4 Allelic interactions

ANOVA analysis has shown both significant RIL x Environment interactions and significant genetic differences among RILs (Tables 3.3 and 3.4). Common, but also different, periodicity QTLs after the two entrainments were identified. Further, I could investigate how each allele at a specific locus contributes to the phenotype, and thereby find additive effects by deducing the effect of the two allelic forms of each locus. Moreover, in the case of QTL interactions, I could study allelic effects of interacting QTLs, and find epistatic relationships among different allelic combinations. The epistatic relationships between allelic forms of the respective QTLs identified for the different entrainment conditions, and their additive effect on period are represented in the following graphs (Figures 3.6-3.12). The analysis was performed by SPSS through GLM Univariate using period as a dependent variable, and using markers, and marker interactions as factors. The title on each graph represents the QTL location at which chromosome and the superscripted letter represent marker name where the QTL was identified. *Ler* and *Cvi* are the allelic forms of each QTL. In case of QTL interactions, the first code letter stands for the first QTL, the second letter code stands for the second QTL. Figures 3.6-3.9 represent interactions for light-dark entrainment QTLs and Figures 3.10-3.12 for temperature-entrainment QTLs. An extensive description of allele specific effects of each QTL or interactions of QTL for each entrainment will be described below.

For the light-dark entrainment, the chromosome 1 QTL at PW4 locus shown in Figure 3.6 has an additive effect of 1.131 hours after light-dark entrainment, with *Ler* allele being longer period than the *Cvi* allele (Figure 3.6, Table 3.5). This period QTL was found to have the largest effect for this entrainment. According to the applied F-test, by ANOVA, the probability value is <0.001, therefore it was found to be highly significant QTL. The fifth chromosome QTL at marker locus BH.107L-Col has an additive effect of 0.838 hours, with *Cvi* allele showing a longer period compared to the *Ler* allele (Figure 3.7, Table 3.5). The P-value for this QTL is 0.001. The contribution of the *Cvi* allele of the fifth chromosome QTL at locus CC.262C was 0.466 hours (Figure 3.8, Table 3.5). Although the additive effect of this QTL in the phenotype was smaller than the two previous QTLs, the P-value is <0.001 therefore was highly significant. ANOVA application for the interaction between two

QTLs, those of chromosome 1 at PW4 locus and chromosome 5 at CC.262C locus, was highly significant for $P < 0.001$ (Figure 3.9, Table 3.5). The interaction of the *Ler* alleles of the QTL at PW4 locus to the *Cvi* allele at the CC.262C locus showed a long-period phenotype that was significantly different from the other allelic combinations.

For the temperature-entrainment protocol, the additive effect of the *Ler* allele of the main QTL at chromosome 1 at locus CH.160L-Col was 1.094 hours (Figure 3.10, Table 3.5). This was a highly significant QTL for $P = 0.001$, as being processed by ANOVA. The *Cvi* allele of the second main QTL in chromosome five at locus CC.262C had an additive effect of 0.539 hours (Figure 3.11, Table 3.5). The interaction of these two QTLs was significant. The period of the interaction of *Ler* allele at CH.160L-Col and the *Cvi* allele of the CC.262C was longer than the period length of either of the single alleles (Figure 3.12, Table 3.5).

Collectively, it was described that light and temperature input into the circadian oscillator are mediated by both the same and by different QTLs. Many of the QTLs co-localize with already known circadian genes, although some are novel QTL. This includes the third chromosome QTL at the EG.75L locus. In the future, studies should focus on the confirmation of the phenotype, to the cloning of QTLs, and to complementation of the phenotype by transgression of the *Ler* allele into the *Cvi* genome.

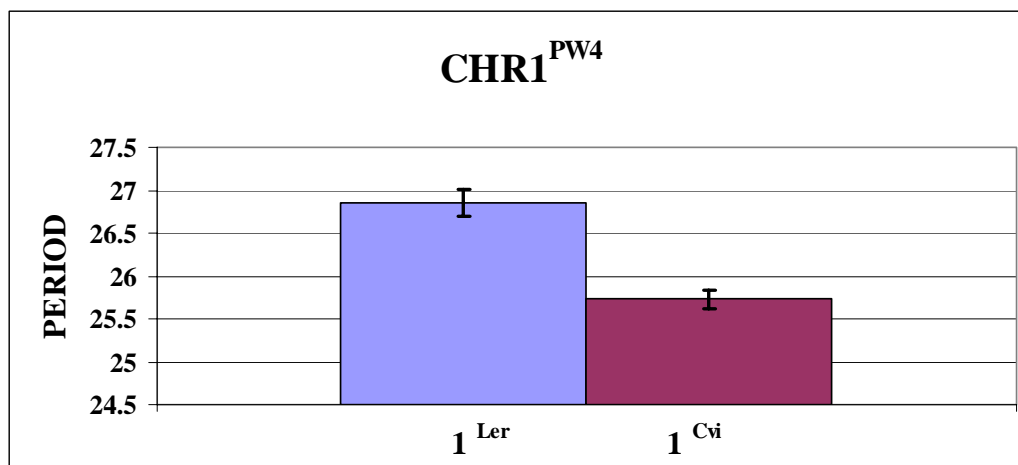


Figure 3.6 Period variation due to allelic variation of the first chromosome QTL at PW4 locus after the light-dark entrainment in the CvL population

In X-axis the number represents the chromosome number and the superscripted *Ler* and *Cvi* are designated for the Landsberg *erecta* and Cape verde islands allele respectively. Bars represent standard error.

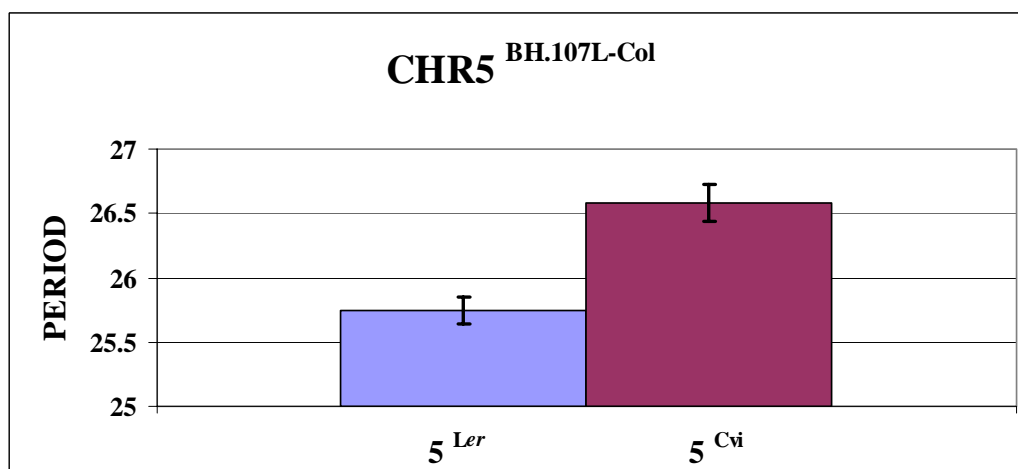


Figure 3.7 Period variation due to allelic variation of the fifth chromosome QTL at BH.107L-Col locus after the light-dark entrainment in the CvL population

In X-axis the number represents the chromosome number and the superscripted *Ler* and *Cvi* are designated for the Landsberg *erecta* and Cape verde islands allele respectively. Bars represent standard error.

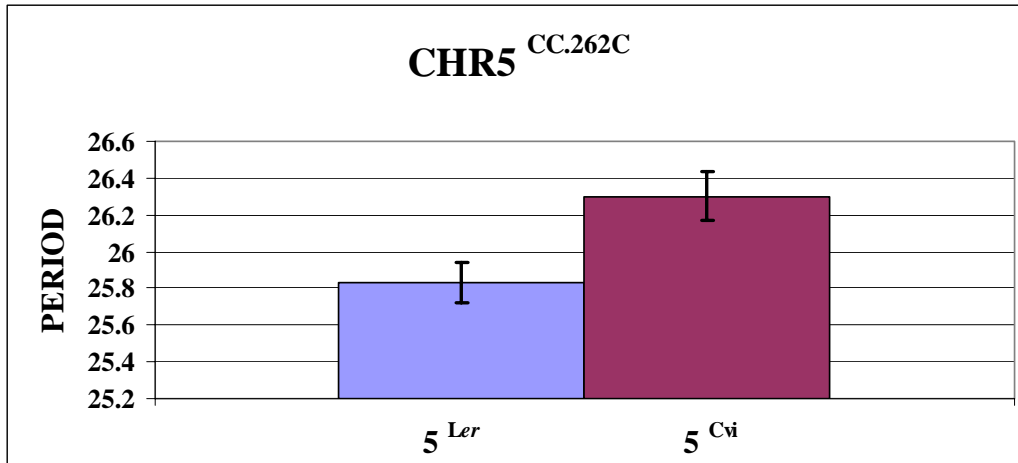


Figure 3.8 Period variation due to allelic variation of the fifth chromosome QTL at **CC.262C** locus after the light-dark entrainment in the CvL population

In X-axis the number represents the chromosome number and the superscripted *Ler* and *Cvi* are designated for the Landsberg *erecta* and Cape verde islands allele respectively. Bars represent standard error.

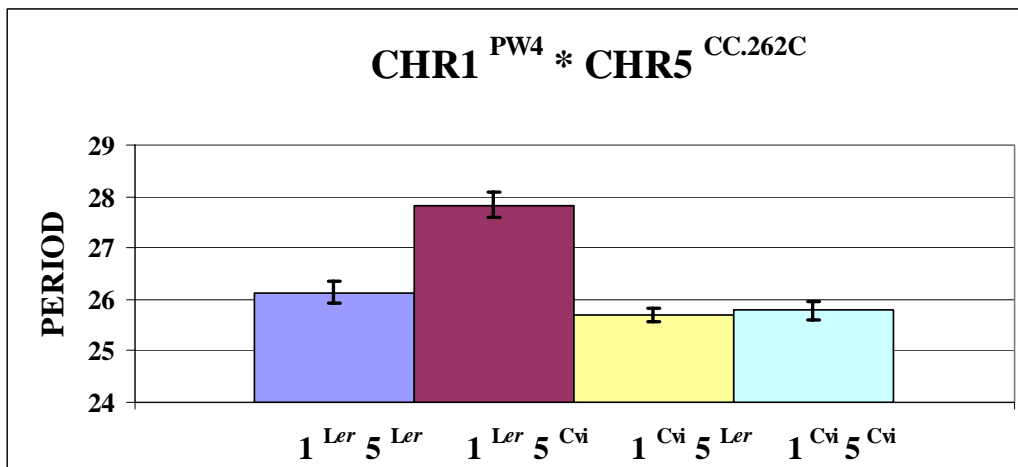


Figure 3.9 Period variation due to interaction of two QTLs at chromosome 1 at locus **PW4** and chromosome 5 at locus **CC.262C** after the light-dark entrainment in the CvL population

In X-axis the number represents the chromosome number and the superscripted *Ler* and *Cvi* are designated for the Landsberg *erecta* and Cape verde islands allele respectively. Bars represent standard error.

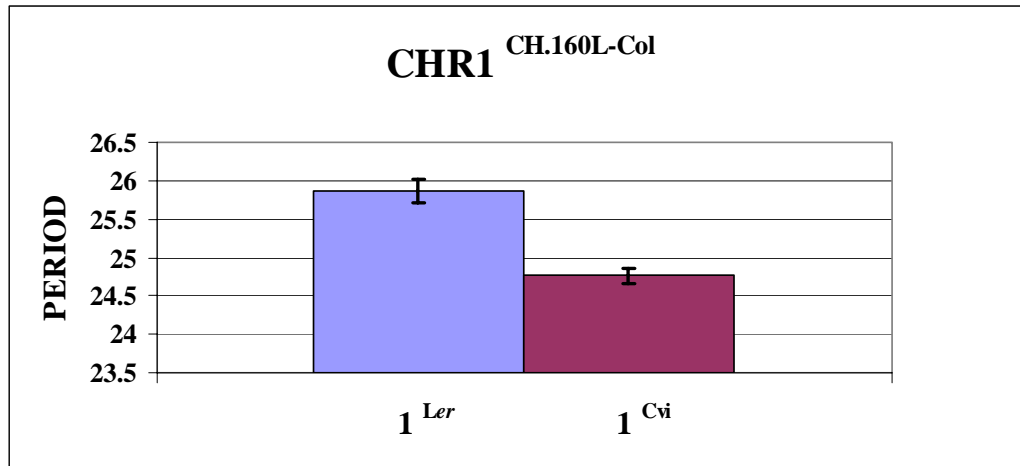


Figure 3.10 Period variation due to allelic variation of the first chromosome QTL at CH.160L-Col locus after the temperature entrainment in the CvL population

In X-axis the number represents the chromosome number and the superscripted *Ler* and *Cvi* are designated for the Landsberg *erecta* and Cape verde islands allele respectively. Bars represent standard error.

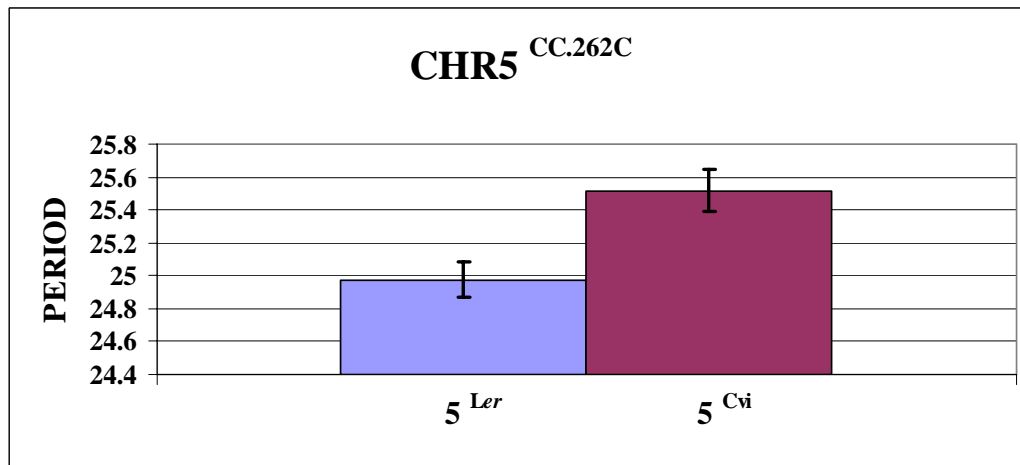


Figure 3.11 Period variation due to allelic variation of the fifth chromosome QTL at CC.262C locus after the temperature entrainment in the CvL population

In X-axis the number represents the chromosome number and the superscripted *Ler* and *Cvi* are designated for the Landsberg *erecta* and Cape verde islands allele respectively. Bars represent standard error.

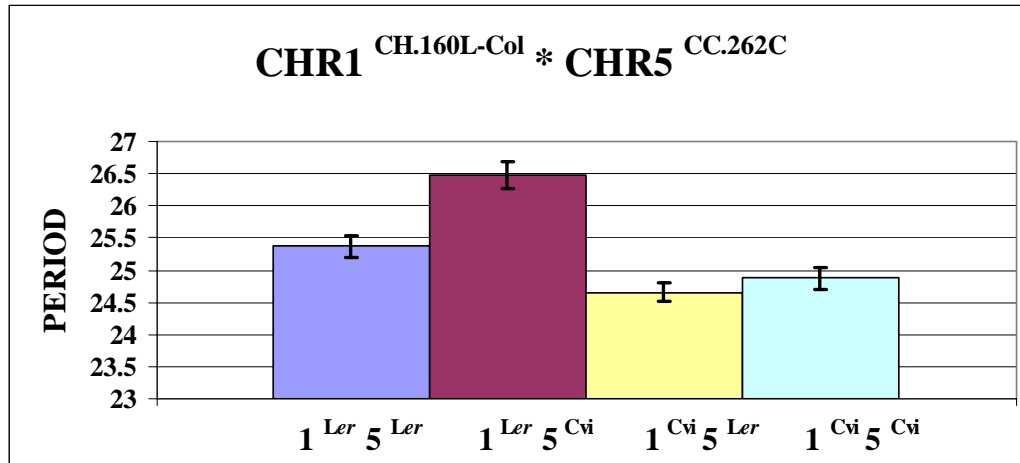


Figure 3.12 Period variation due to interaction of two QTLs at chromosome 1 at locus CH.160L-Col and chromosome 5 at locus CC.262C after the temperature entrainment in the CvL population

In X-axis the number represents the chromosome number and the superscripted *Ler* and *Cvi* are designated for the Landsberg *erecta* and Cape verde islands allele respectively. Bars represent standard error.

CHAPTER 3 Quantitative analysis of light-dark vs temperature entrainment

Trait	Environment	h^2	Marker	Chromosome	Position	F	P value	2a
(cM)								(h)
PER	LD	0.82						
			PVV4	I	0	17.270	<0.001	1.131
			BH.107L-Col	V	20	13.418	0.001	0.838
			CC.262C	V	92	28.449	<0.001	0.466
			PVV4 *					
			CC262C	I*V	0*92	26.488	<0.001	-
PER	TMP	0.85						
			CH.160L-Col	I	31	8.929	0.001	1.094
			CC.262C	V	92	11.379	0.002	0.539
			CH.160L-Col *					
			CC.262C	I*V	31*92	4.629	0.040	-

Table 3.5 Concentrated results for the QTL identified in the CvL population after light dark or after temperature entrainment

h^2 denotes the heritability of the trait for a specific environment. Marker, chromosome and position describe the exact location of the QTL identified. F is the value of the F-test calculated by ANOVA. P value is the probability value. <0.001 indicates very highly significant QTLs. 2a is the additive effect of the QTL calculated as the difference of the two alleles, and it is measured in hours.

3.2 Light dark vs temperature entrainment of Bay/Sha RIL

In the previous sub-chapter (3.1.3), the natural variation present in the CvL collection was used as a successful tool to map temperature entrainment QTLs. Here, the same trait, circadian rhythmicity, was assessed in a second RIL population generated by the cross of Bayreuth-0 to Shakdara, hereafter BxS. This RIL population was selected because the two accessions, Bay-0 and Shakdara, originate from distinct altitude environments. Bayreuth-0 originated from Germany, and is a fallow land habitat at 350 meters, whereas Shakdara collected in Tadjikistan at 3.500 meter altitude. At this altitude, plants generally confront higher light intensities and colder temperatures. Therefore, it was of interest to study circadian rhythmicity in this genetic background, and compare the findings to the CvL collection. As with the CvL collection, the existing BxS RIL population was also transformed with *CCR2::LUC*. For most of these lines, multiple plants derived from independent transformants were assayed under constant light after light dark, or after temperature entrainment. The arbitrary number of BxS RILs, as given by Loudet *et al.*, the circadian period, the standard deviation per RIL line, and the standard error of the mean of the individuals of each RIL line after light-dark or temperature entrainment in constant light are showed in the Tables 3.6 and 3.7, respectively. It should be noted that the intraline variation was found to be higher in the BxS population (Tables 3.6 and 3.7) compared to CvL (Tables 3.1 and 3.2). Therefore, a larger number of plants in the BxS experiments were used for averages to obtain more statistically accurate period estimates to process with QTL mapping.

RIL NAME	LD PERIOD	SD	SE	RIL NAME	LD PERIOD	SD	SE
7	26.733	1.953	0.564	146	25.995	0.943	0.164
13	25.998	0.758	0.165	147	25.749	0.943	0.155
15	23.592	0.587	0.142	155	26.657	1.250	0.273
30	27.143	1.615	0.417	157	28.705	1.410	0.425
37	26.057	1.120	0.354	162	26.500	1.602	0.303
45	27.075	1.846	0.331	165	26.487	0.869	0.149
53	26.053	1.495	0.283	173	25.799	1.184	0.296
55	25.544	1.368	0.432	175	27.031	1.420	0.367
59	25.135	1.305	0.299	176	27.471	1.033	0.225
61	28.028	1.385	0.462	179	27.861	0.841	0.146
67	26.107	0.707	0.213	183	25.792	1.451	0.484
70	24.784	0.990	0.313	186	26.908	1.269	0.232
78	25.544	0.979	0.225	187	26.310	1.496	0.234
83	26.090	1.377	0.316	190	27.653	2.133	0.410
92	24.145	0.486	0.154	191	27.598	2.391	0.416
98	25.400	1.079	0.225	194	25.689	0.672	0.168
99	25.371	1.287	0.388	195	26.486	0.941	0.140
102	26.354	1.707	0.402	200	28.191	0.884	0.280
106	26.449	1.602	0.414	210	26.836	0.702	0.234
111	27.045	1.084	0.209	211	27.730	0.601	0.227
112	25.585	1.483	0.332	214	27.976	0.563	0.213
114	27.763	1.393	0.360	234	27.869	1.005	0.251
123	26.382	1.739	0.371	240	28.695	1.806	0.414
126	25.391	1.017	0.384	252	28.567	1.364	0.341
127	26.711	0.951	0.218	262	27.423	1.028	0.265
129	26.005	0.788	0.161	264	27.787	2.050	0.775
131	25.574	1.148	0.271	298	25.986	1.109	0.237
133	26.263	1.318	0.229	300	26.238	1.010	0.337
134	27.416	0.948	0.202	320	27.596	0.627	0.157
135	26.587	0.922	0.141	325	27.305	1.056	0.318
136	26.798	1.734	0.481	329	27.733	1.329	0.343
137	26.609	1.448	0.374	364	26.119	0.805	0.268
140	27.537	0.837	0.136	368	28.049	0.927	0.328
143	28.064	1.016	0.272	394	26.607	1.368	0.353

Table 3.6 The free-running period of the Bay/Sha RIL collection under constant light after entrainment to 12 hours light followed by 12 hours dark

RIL NAME corresponds to the arbitrary name as given in Loudet *et al.* for the BxS population (Loudet et al., 2002). LD period corresponds to averaged period after light-dark entrainment. SD is the standard deviation of the period and SE is the standard error of the mean period.

RIL NAME	TMP PERIOD	SD	SE		RIL NAME	TMP PERIOD	SD	SE
7	25.399	0.800	0.253		165	26.326	1.187	0.233
30	26.025	1.159	0.273		173	25.619	0.523	0.131
37	25.481	1.016	0.233		179	27.066	1.414	0.243
45	25.882	0.373	0.124		186	26.195	1.079	0.279
53	26.225	0.978	0.173		187	26.989	1.147	0.234
59	23.982	1.366	0.268		190	25.825	1.513	0.323
61	27.082	1.155	0.289		191	26.384	1.032	0.258
83	25.447	0.885	0.215		194	25.271	0.894	0.211
92	23.867	0.952	0.317		195	26.362	1.412	0.223
98	24.934	0.836	0.192		198	26.615	0.613	0.217
111	27.082	1.106	0.179		199	26.345	0.622	0.254
112	25.443	1.668	0.327		200	27.576	0.811	0.244
114	27.623	1.187	0.265		210	26.136	0.518	0.232
118	26.300	1.156	0.366		211	27.986	1.467	0.464
126	26.175	2.002	0.472		214	27.763	0.811	0.331
127	26.054	0.822	0.155		220	26.438	0.476	0.194
129	25.807	0.793	0.153		232	27.511	0.644	0.215
131	25.150	1.095	0.234		234	26.970	0.893	0.269
133	25.947	0.999	0.169		240	26.991	0.920	0.223
134	27.518	1.162	0.260		252	26.482	0.772	0.345
135	26.192	1.621	0.286		262	26.839	0.686	0.259
136	25.809	0.708	0.224		264	26.233	1.394	0.805
137	25.169	0.598	0.166		273	26.873	0.202	0.117
140	27.508	0.797	0.123		289	26.440	0.745	0.373
143	26.646	0.910	0.199		298	25.197	0.739	0.165
146	25.956	1.004	0.161		300	25.035	0.439	0.166
147	25.989	1.144	0.181		325	26.460	0.593	0.210
155	26.562	1.186	0.233		329	27.070	0.652	0.188
162	26.309	0.775	0.183		365	26.278	0.562	0.230

Table 3.7 The free running period of the Bay/Sha RIL collection under constant light after entrainment to 12 hours at 22°C followed by 12 hours at 16°C

RIL NAME corresponds to the arbitrary name as given in Loudet *et al.* for the BxS population (Loudet et al., 2002). TMP period corresponds to averaged period after temperature entrainment. SD is the standard deviation of the period and SE is the standard error of the mean period.

3.2.1 Period differences after LD or tmp entrainment of the BxS population

As was seen with the CvL population, the differences of period in the two different entrainment conditions within one genotype were overlay plotted for BxS population (Figure 3.13). The period in most of the lines was significantly longer after light-dark entrainment compared to temperature entrainment. However, a reverse response was observed in the BxS population more often than in the CvL population. Furthermore, the majority of the BxS lines had a longer period than was seen with the majority of CvL lines. This might have an ecological meaning, since the parents of the two RIL populations are from drastically distinct environments.

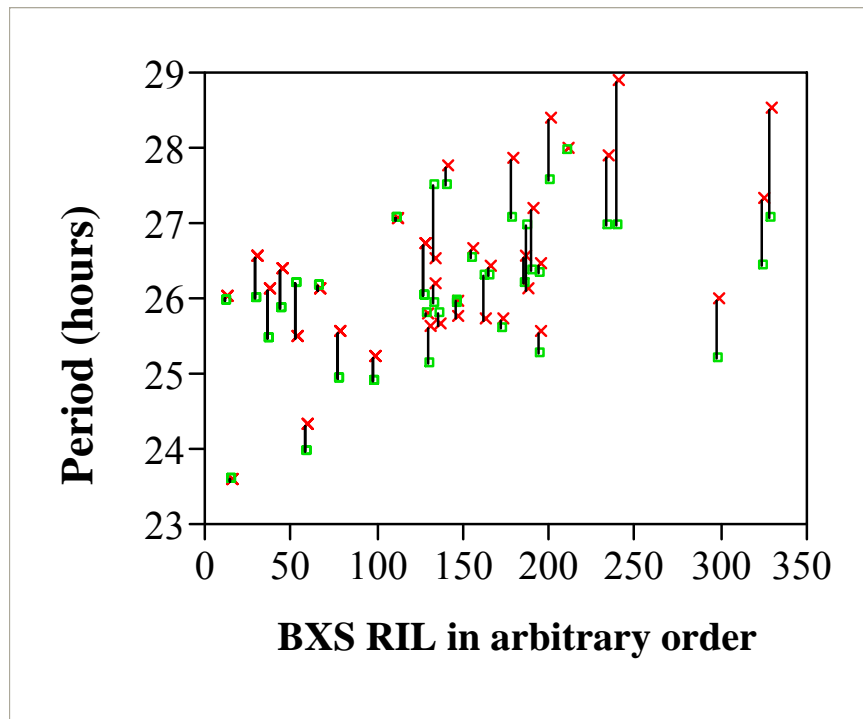


Figure 3.13 Period differences of rhythmic plants of BxS RIL collection of temperature-entrained versus light-dark entrained plants

X axis represents the arbitrary number of BxS RIL (Loudet et al., 2002), and Y axis represents period. ■ represents the period of temperature entrained plants, × represents the period of the light-dark entrained plants.

3.2.2 Statistic analysis of mean period after LD vs. tmp entrainment in the BxS RIL

The circadian periodicity of the BxS collection varied similarly to was seen with the CvL collection. One difference was that the overall mean period of the BxS population after either light dark or temperature entrainment was longer than the respective mean period of the CvL collection (Tables 3.3 and 3.8). To test whether the averaged period of transformed BxS RILs for the two different entrainments was continuously distributed, the period was categorized in hour intervals, and then it was plotted against frequency. The plotting resulted in a continuous distribution of period after the two different entrainment protocols, as represented in Figure 3.14. Moreover, the free-running period of each averaged RILs after the entrainment to either light-dark cycles or temperature cycles not only varied continuously, but was found to be normally distributed. When compared with the Figure 3.3, the BxS mean period seems to be longer than the CvL mean period after both entrainments.

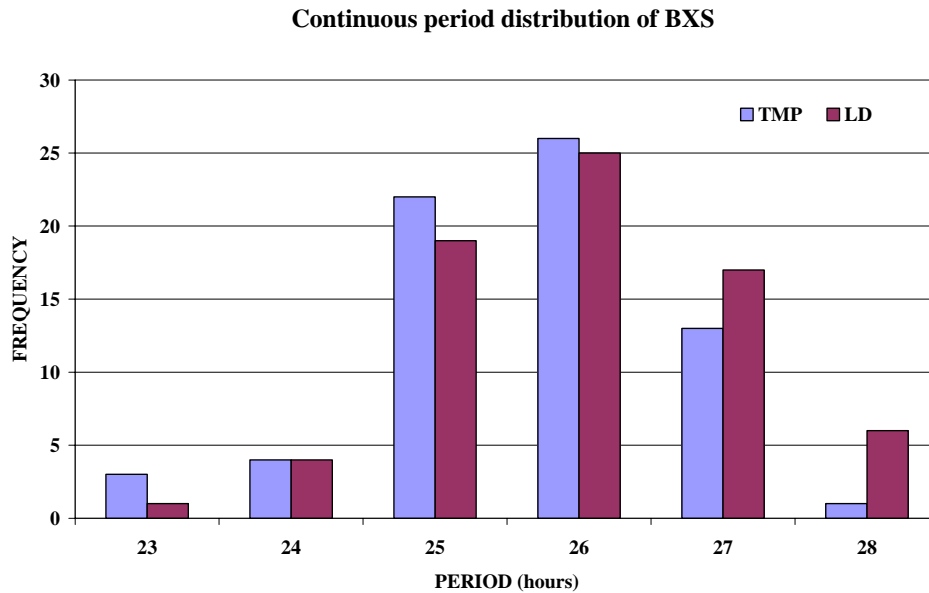


Figure 3.14 The continuous distribution of period for 69 BxS Recombinant Inbred Lines.

X-axis is period measured in hours and Y-axis represents number of BxS RILs with a certain period. The period was binned in 1 hour interval as of 23.0-23.9. TMP denotes temperature entrainment and LD light-dark entrainment.

Since period was normally distributed, all assumptions of ANOVA are fulfilled, and therefore, I could compare the mean period after the two entrainments. The upper and lower values for period for 95 % of the means fall into these bounds was calculated (Table 3.8). For 95% of confidence interval, the lower bound of mean period after light-dark entrainment did not overlap with the upper bound of the mean period after the temperature entrainment (Table 3.8). Moreover, the standard error of the mean was calculated and this is a measure of how much the mean period from RIL to RIL, within each environment, may vary from the overall mean calculated of each environment. Therefore the period after the two entrainment protocols was different.

GLM Univariate analysis of variance was performed, using period as a dependent variable, to test for the main effect of the genotypes, environment and the environment by RIL interactions to the dependent variable. RIL and environment were used as fixed factors. Like for the CvL collection, the null hypotheses of the test were that the mean period is the same across RILs or different environments, and there was no RIL by environment interaction. R^2 was used as a measure of how much the actual period data fit to the expected data. I found that the null hypothesis could be rejected (Table 3.9). This means that the mean of period after the two entrainment protocols did not differ either among different RILS or between the different environments. Furthermore it rejected the null hypothesis that there was no interaction between the two genotypes and environments. Moreover, the adjusted R^2 indicated that about 40% of the mean period variation could be explained by genotype, environment or genotype by environment interaction.

Environment	Mean	Std. Error	95% Confidence Interval	
			Lower Bound	Upper Bound
LD	26.640 ^a	0.046	26.550	26.730
TMP	26.213 ^a	0.044	26.126	26.300

^a Based on modified population marginal mean.

Table 3.8 Statistic analysis of the BxS RIL lines used for QTL mapping showed that the period average for light and temperature are marginally different for 95% of confidence interval

As environment, I consider the different entrainment protocols. The two bounds for 95% of confidence interval suggest that for the 95% of the RILS the mean period falls within the lower and upper bound, and the rest 5% is outside of these intervals. Standard error of a mean is a measure of the variation and it is dependent on the sample size. ^a denotes the modified population marginal mean for the 95% Confidence Interval.

Source	SS	df	MS	F	Sig.
Corrected Model	2367.045 ^a	164	14.433	9.690	0.000
Intercept	894504.347	1	894504.347	600517.3	0.000
RIL	1929.917	87	22.183	14.892	0.000
ENVIRONMENT	79.492	1	79.492	53.367	0.000
RIL * ENVIRONMENT	205.399	76	2.703	1.814	0.000
Error	3795.389	2548	1.490		
Total	1899758.869	2713			
Corrected Total	6162.434	2712			

^a R Squared = .384 (Adjusted R Squared = .344)

Table 3.9 ANOVA analysis shows significant genotype by environment interaction for the two different entrainments

SS is the sum of squares. df are the degrees of freedom. MS is the mean square calculated by dividing the SS by df. F is the F-ratio calculated by dividing MS by the error. Significance level was set to .05. Significance of ≤ 0.001 means highly significant differences or highly significant interactions. * denotes the testing for an interaction between two factors.

3.2.3 QTL mapping of BxS

Circadian rhythmicity of the transformed with *CCR2::LUC* BxS RILs were successfully assayed for period in two different entrainments; after light-dark at constant warm temperature 22°C, and after warm-cold cycles of 12 hours at 22°C and 12 hours at 12°C under constant light. Approximately 70 lines were phenotypically characterized for clock period, and it was found that the overall temperature-entrained plants have a shorter period mean than light-entrained plants (Table 3.8).

As with the CvL collection, the circadian period of the BxS collection could be analyzed as a quantitative trait, since it was continuously and normally distributed. The statistical package MapQTL 5.0 was used to predict map genomic regions containing significant natural genetic variation that accounts for temperature or light-dark entrainment. Interval mapping (IM), and consequently MQM mapping were performed for period separately in each entrainment. The procedure and assumptions of the MapQTL were the same as described in the CvL part at section 3.1.4.

The QTL mapping of the BxS collection resulted in the identification of the same QTLs for the two entrainments (Figures 3.15 and 3.16). The QTL mapping revealed that QTLs localized at the chromosome 2 and 4 were mediating by both light and temperature entrainment (Figures 3.15 and 3.16). Though, the identified QTLs explained more of the phenotype in the light dark than in the temperature entrainment. Additionally, at some loci, a bimodal QTL was observed. For example at chromosome 2, I could not distinguish whether there was one or two QTLs at these loci since there is a restriction in the number of markers I could take as cofactors. Further statistic analysis of the QTL effects and possible interactions and their heritability will be described in the next session.

For the light-dark entrainment, a QTL at chromosome two at 30-40cM was identified. The explained variance this QTL was about 30%. The second QTL shown in Figure 3.17 localizes at the bottom of the fourth chromosome, at 60-70cM. The explained variance of this QTL was 30%. At 50-60 cM of the first chromosome, a yet as unidentified locus exists. The chromosome two and four QTLs were also identified for the temperature entrainment. Furthermore, the second and fourth chromosome identified main QTLs for either the light-dark or the temperature entrainment in the BxS collection, were also identified as an interacting QTLs for the temperature

entrainment in the CvL collection; this QTL might be a shared component between these two populations. At the second chromosome, at the area where the QTL was identified two circadian clock genes localized. One of these two genes was *ELF3* and it was involved in gating light input to the clock, whereas the other gene, *ELF4*, is considered to form a feedback loop with *CCA1* (Kikis et al., 2005). All these suggested that in the BxS population light-dark entrainment was mediated by the same loci as with temperature entrainment.

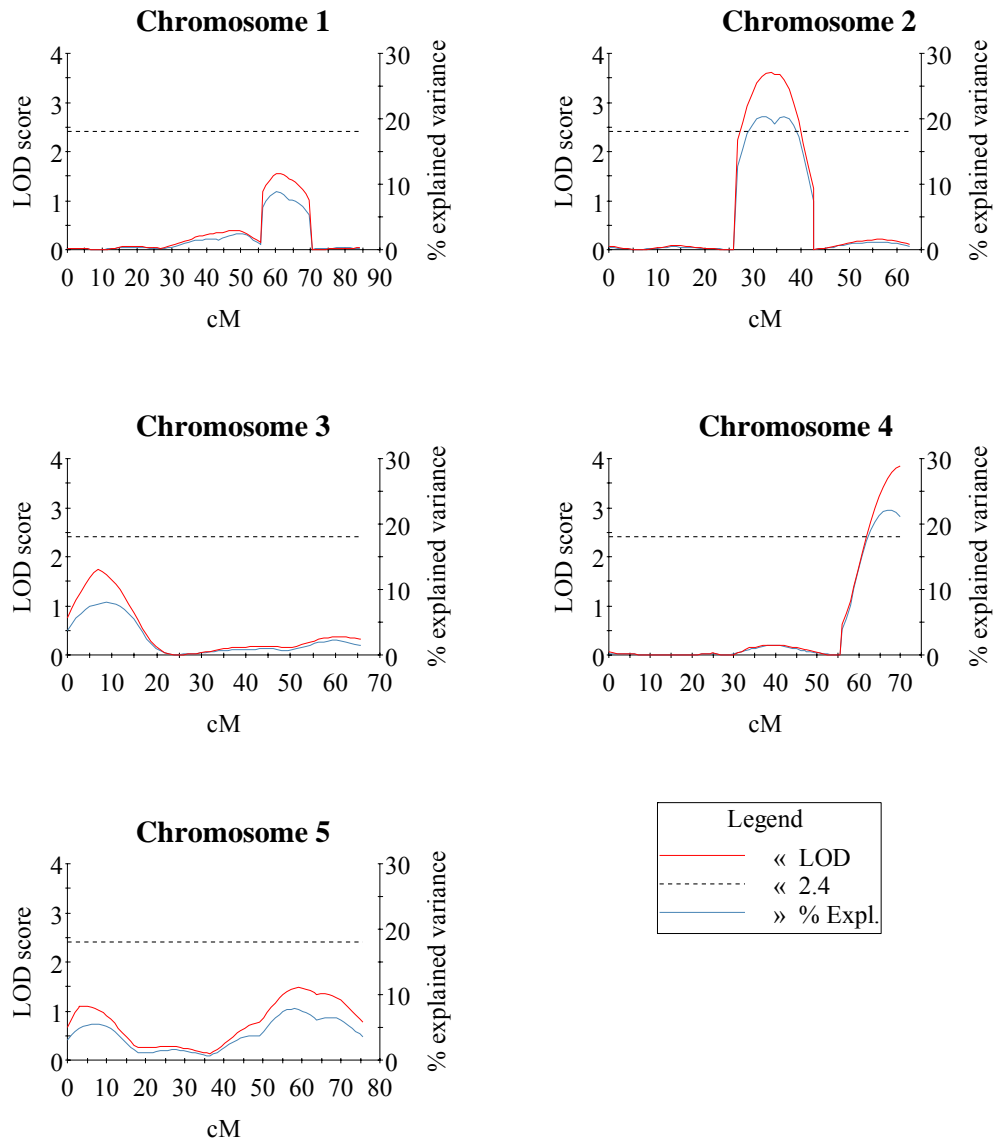


Figure 3.15 MapQTL for the light-dark entrainment of the BxS population

Left Y axis represents the LOD score, and right Y axis represents the % of explained variance. This percentage is a measure of the effect of the QTL that supplies to the phenotype. The dotted line represents the LOD score threshold. It was set to 2.4 after calculation of 1000 permutations, for 95% significance level.

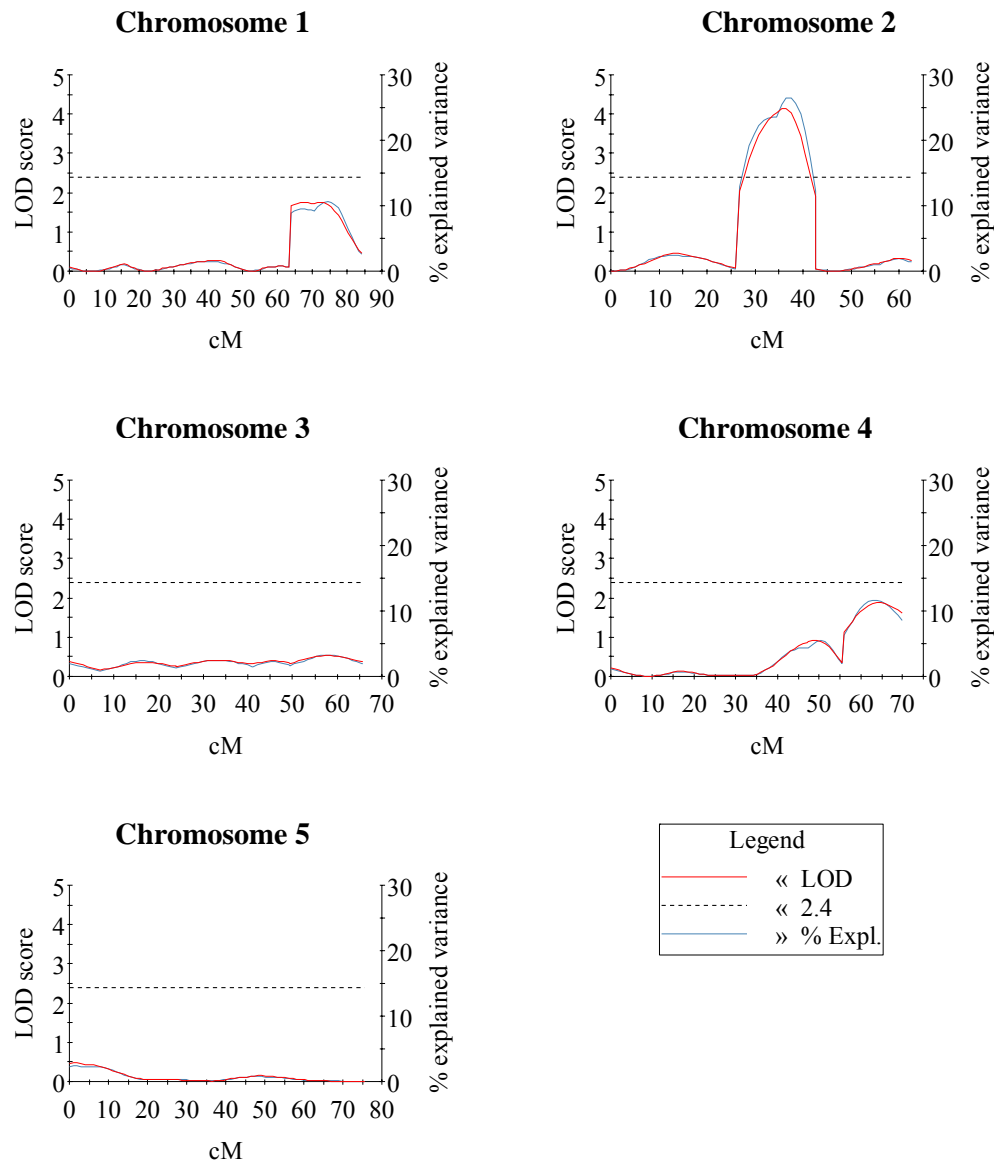


Figure 3.16 MapQTL for the temperature entrainment of the BxS population

X axis represents the chromosome location, measured in cM, left Y axis represents the LOD score, and right Y axis represents the % of explained variance. This percentage is a measure of the effect of the QTL that supplies to the phenotype. The dotted line represents the LOD score threshold. It was set to 2.4 after calculation of 1000 permutations, for 95% significance level.

3.2.4 Allelic interactions in BxS

Allelic interactions were tested for the QTLs identified in the BxS population for the two entrainments. There were not significant interactions between the identified QTLs for either of the two conditions. For the light-dark entrainment, the Bayreuth-0 allele of the second chromosome QTL at the locus MSAT2-41 was by 0.834 hours longer than the Shakdara allele (Figure 3.17, Table 3.10). Additionally, the Bayreuth-0 allele of the fourth chromosome QTL at the MSAT4-37 locus has a longer period of 0.972 hours than the Shakdara allele (Figure 3.18, Table 3.10). Both QTLs were highly significant for $P < 0.001$ (Table 3.10).

For the temperature entrainment, QTLs at the same locations were identified as with the light-dark entrainment. The allelic differences in the mean period at a single QTL at MSAT-2.41 locus was about an hour with Bayreuth-0 allele having longer period than the Shakdara allele. This QTL was highly significant for $P < 0.001$ (Figure 3.19, Table 3.10). Moreover, the mean period difference of the fourth chromosome QTL at the locus MSAT-4.37 was approximately half an hour, with the Bayreuth-0 allele being longer than the Shakdara. This QTL was significant for $P < 0.05$ (Figure 3.20, Table 3.10)

Collectively, for the light-dark entrainment, two QTLs were found that were highly significant. These were located in chromosome 2 and 4. The chromosome 2 QTL was highly significant for the temperature entrainment, but it has a smaller effect than in the light-dark entrainment. All the information described for BxS population is recapitulated in Table 3.10. To conclude, it seemed that the temperature entrainment in BxS was mediated by the same QTLs as for the light-dark entrainment. However, by comparing the two RILs populations, used in this study, in either light-dark or temperature entrainment, different QTL were identified for the different entrainment protocols, in the two different RILs populations. This suggests that the different genes may be involved in the circadian clock of these four ecotypes.

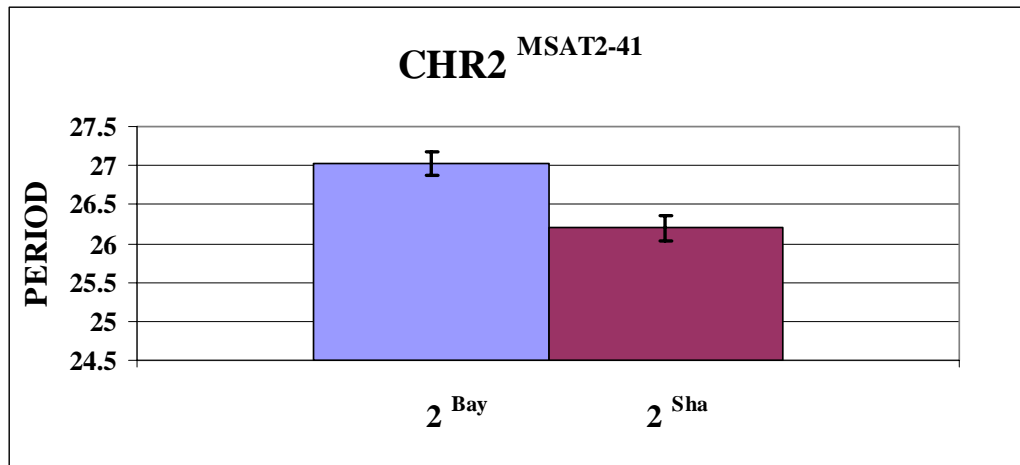


Figure 3.17 Period variation due to allelic variation of the second chromosome QTL at locus MSAT2-41 after the light-dark entrainment in the BxS population

In X-axis the number represents the chromosome number and the superscripted Bay and Sha are designated for the Bayreuth-0 and Shakdara allele respectively. Bars represent standard error.

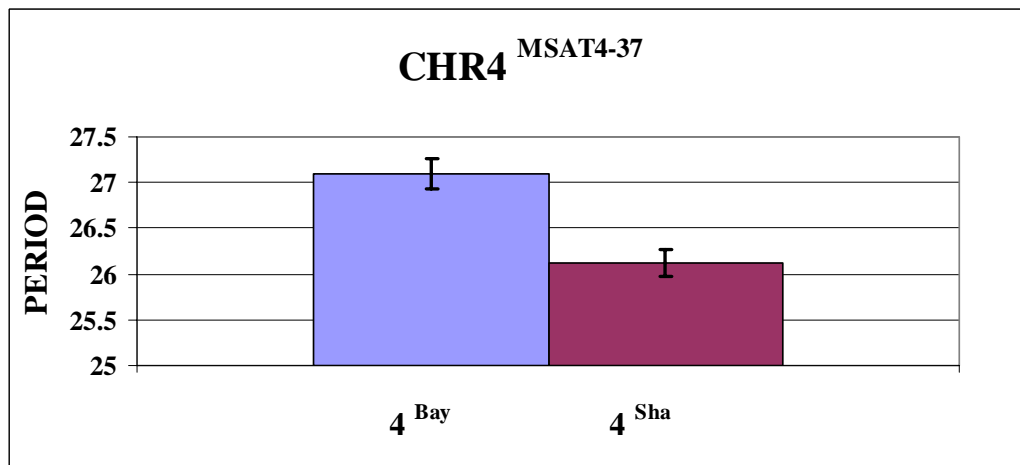


Figure 3.18 Period variation due to allelic variation of the fourth chromosome QTL at locus MSAT4-37 after the light-dark entrainment in the BxS population

In X-axis the number represents the chromosome number and the superscripted Bay and Sha are designated for the Bayreuth-0 and Shakdara allele respectively. Bars represent standard error.

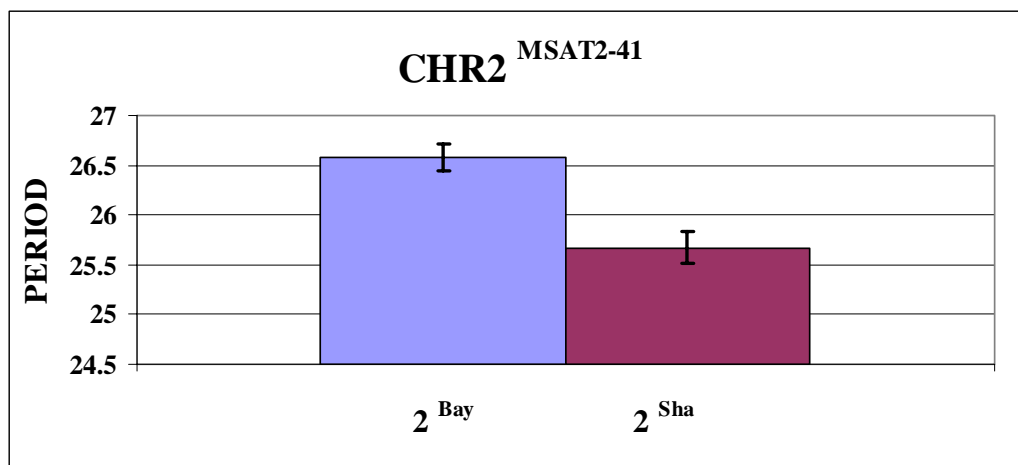


Figure 3.19 Period variation due to allelic variation of the fourth chromosome QTL at locus MSAT2-41 after the temperature entrainment in the BxS population

In X-axis the number represents the chromosome number and the superscripted Bay and Sha are designated for the Bayreuth-0 and Shakdara allele respectively. Bars represent standard error.

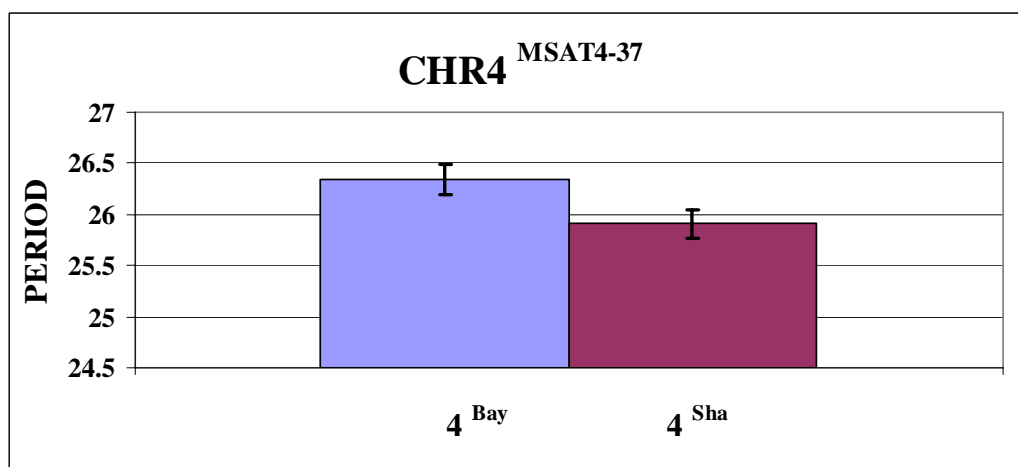


Figure 3.20 Period variation due to allelic variation of the fourth chromosome QTL at locus MSAT4-37 after the temperature entrainment in the BxS population

In X-axis the number represents the chromosome number and the superscripted Bay and Sha are designated for the Bayreuth-0 and Shakdara allele respectively. Bars represent standard error.

Trait	Environment	h^2	Marker	Chromosome	Position	F	P value	2a
					(cM)			(h)
PERIOD	LD	0.75						
			MSAT2_41	II	34.5	14.246	<0.001	0.834
			MSAT4_37	IV	69.9	18.971	<0.001	0.972
PERIOD	TMP	0.76						
			MSAT2_41	II	34.5	18.277	<0.001	0.905
			MSAT4_37	IV	69.9	4.332	0.042	0.438

Table 3.10 Concentrated results for the QTL identified in the BxS population after light dark or after temperature entrainment

h^2 denotes the heritability of the trait for a specific environment. Marker, chromosome and position describe the exact location of the QTL identified. F is the value of the F-test calculated by ANOVA. P value is the probability value. <0.001 indicates very highly significant QTLs. 2a is the additive effect of the QTL calculated as the difference of the two alleles, and it is measured in hours.

3.3 Temperature entrainment in constant darkness: etiolated tissue QTLs

To remove the confounding effect of light from the response of temperature entrainment, as was performed for the CvL and BxS collections under constant light, plants were synchronized in temperature cycles in the absence of light, free run in constant darkness, and circadian period measurement were made. For this, a different experimental set up was required. The seed for these experiments was plated in clusters of 100 seeds for each genotype and not as individuals as it was for the other two entrainments. Furthermore, a set of CvL RILS was tested for period in constant darkness after they have been entrained for a week with temperature cycles in constant darkness, or in temperature cycles under constant light. The total number of lines assayed for period is showed in Table 3.11.

The circadian rhythms of the light-entrained plants in temperature cycles displayed ‘disturbed’ rhythms when the free run was assayed in constant darkness. This was as compared to the robustness of rhythms of the dark grown plants, as it was indicated by relative amplitude error (R.A.E.) (Figure 3.21). RAE is a measure of rhythmicity that take values from 0-1 where 0 is highly rhythmic and 1 is arrhythmic. The light-grown plants had on average R.A.E. of 0.42, whereas the dark grown plants had on average R.A.E. of 0.15. Due to the high R.A.E., I decided to process with QTL mapping only on the dark-grown plants. All genotypes that grew in darkness and temperature cycles displayed a lengthening in period of 2-5hours compared to the light-grown plants. Another interesting observation was that light-grown plants show higher *CCR2* expression than the dark grown plants (Figure 3.21).

CvL RIL	PERIOD	CvL RIL	PERIOD	CvL RIL	PERIOD
5	32.497	47	30.864	142	27.965
6	25.510	48	28.943	150	26.430
11	26.044	49	31.050	151	27.263
12	30.158	50	26.932	153	33.710
13	28.973	61	28.178	156	28.320
16	25.554	64	28.860	174	31.240
19	32.773	66	26.940	175	26.220
20	29.907	72	25.334	183	29.530
27	28.255	114	28.478	187	25.830
31	33.890	116	25.895	193	29.084
36	25.228	131	28.240		
44	27.017	140	26.496		

Table 3.11 The free running period of the Cvi/Ler RIL collection in constant darkness, after entrainment in temperature cycles in constant darkness

CvL RIL corresponds to the arbitrary number as given in Alonso-Blanco et al (Alonso-Blanco, 1998). Period corresponds to measurement of a cluster of 100 seedlings.

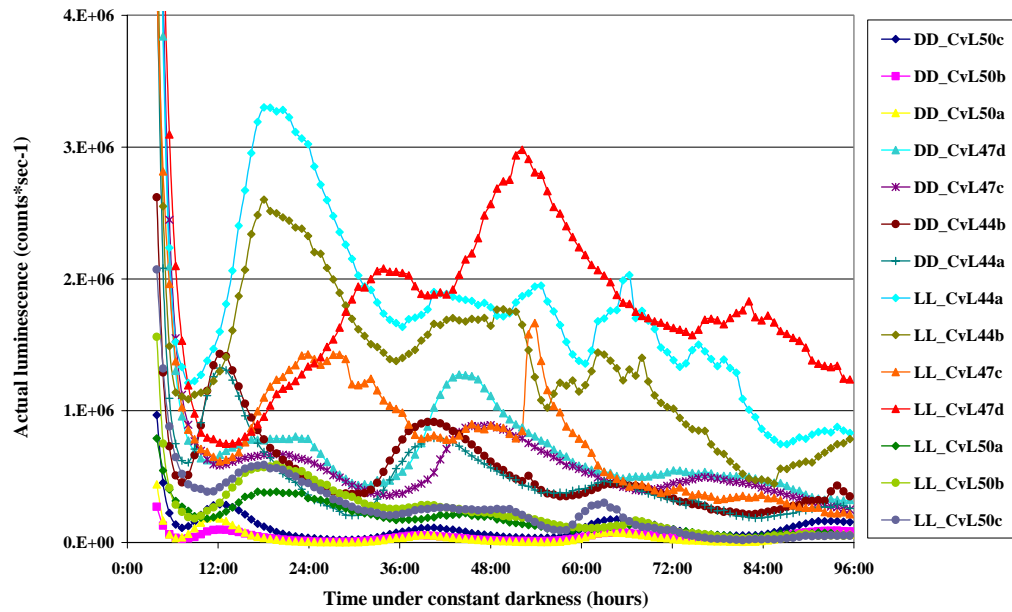


Figure 3.21 *CCR2* expression under constant darkness as reported by luciferase in various CvL independent lines after temperature cycles in constant darkness

DD symbolizes temperature entrainment under constant darkness, and LL symbolizes temperature entrainment under constant light. a, b, c denoted independent transformants of a respective CvL RIL. 44, 47, and 50 denoted different CvL RILs.

3.3.1 Non-normal distribution of period in etiolated periodicity

The mean period of the CvL population, after temperature entrainment in constant darkness, was estimated and plotted against frequency to study whether the distribution of the data was normal. In Figure 3.22, the frequency distribution of CvL period after temperature entrainment in constant darkness was graphed. The period of the CvL lines assayed in constant darkness, after temperature entrainment in constant darkness, ranged from 25 to 33 hours, with most lines displaying approximately 28 hour periodicity (Figure 3.22). Here, it was found that period is continuously distributed, but not in a normal manner. This finding modified the QTL-identification process, compared to the temperature entrainment in constant light.

To further statistically determine whether the distribution of the period matches the normal distribution, a probability Q-Q plot was performed. Probability plots are generally used to determine whether the distribution of a variable matches a given distribution. If the selected variable matches the test distribution, the points cluster around a straight line. In this test, the quantiles of the measured (observed) period distribution is plotted against the quantiles of any of a number of test distributions (expected). The expected normal period is depicted in the Y-axis, whereas the observed normal period is depicted in the X-axis. Thus, the data are not normal (Figure 3.23).

According to the Q-Q plot in Figure 3.23, the period values of most of the CvL lines fit close to the straight line. However, some outlier lines exist. In these outlier lines, the observed period was longer than the expected period. Recall that the period in this experiment represents the averaged period of a cluster of 100 seeds. This was different than in the other experiments where individual seedlings were measured for period. Therefore, further statistic analysis such as ANOVA could not be performed because the set up of the experiment did not allow the measurement of period of individual seedlings. In that sense, heritability could not be estimated since variation within RILs was not measured.

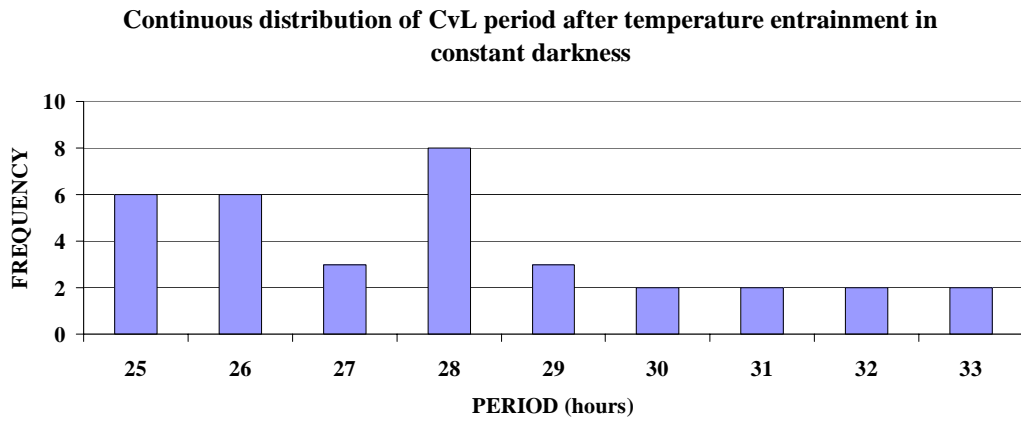


Figure 3.22 Continuous distribution of period of 34 CvL RILs after temperature entrainment in constant darkness

X-axis is period, measured in hours, and Y-axis represents number of CvL RILs with a certain period denoted as frequency.

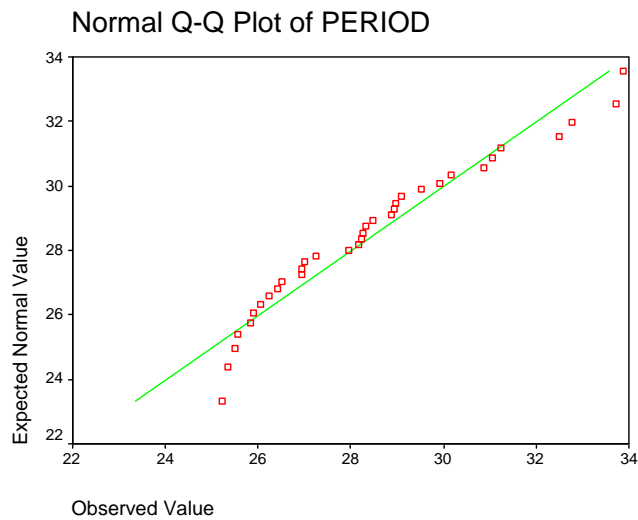


Figure 3.23 Normal Q-Q plot to test for normality of continuous distribution of period for 34 CvL Recombinant Inbred Lines

X-axis is the observed period, measured in hours and Y axis represents the expected period, measured in hours.

3.3.2 QTL mapping results of CvL in temperature cycles in constant darkness

The CvL lines transformed with *CCR2::LUC* were synchronized for seven days in temperature cycles of 12 hours at 22°C and 12 hours at 12°C under constant darkness. After application of luciferin in constant darkness conditions, the seedlings were free run in constant darkness and imaged. From all lines tested, only those that all the independent transformed lines gave exactly the same luciferase pattern were used for QTL mapping. In total thirty-nine lines were phenotypically characterized for clock period, and most of them were used for QTL detection after temperature cycles under constant light. For QTL mapping, initially, a nonparametric mapping using the Kruskal Wallis option of the MapQTL software was performed, due to the non normal distribution of the data (Figure 3.24). Kruskal Wallis considered a nonparametric equivalent to one-way ANOVA. For this test, it was assumed that the period has a continuous distribution, and was divided in an ordinal level of measurement. The period used for the QTL mapping ranges from 25 to 33 hours. For the mapping, the software first ranks the individuals by the period and then it classifies them according to their marker genotype.

In the Kruskal Wallis QTL mapping, a QTL at the first chromosome at 0-10cM was detected for probability of 0.01 and one or more QTL at 24-32cM for probability of 0.001. At the third chromosome, two QTLs, one at the 10-15cM for probability 0.01, and the bottom at 75-84cM for probability of 0.05, were detected. At the fourth chromosome, at 70-75cM a QTL was detected for 0.05 probability. At chromosome 5, from 100-110cM, another QTL was detected with a probability of 0.001. According to this analysis, and using a stringent threshold, two QTLs, at the first chromosome at 24-32cM, and at the fifth chromosome at 100-110cM, can be accounted as a main effect QTLs, whereas the others could be interaction QTLs. However, in this test, I could not test the effect of nearby QTLs, by selecting cofactors.

The different experimental set up used for the temperature entrainment in constant darkness would justify that period might not be normally distributed. Therefore, I performed IM and MQM mapping to compare with the Kruskal-Wallis test. Even after the IM and MQM were tried, QTLs were detected in the same

locations as with the Kruskal-Wallis test (Figure 3.25). Only at two chromosomes QTLs exceeded the LOD threshold of 2.9. In the first chromosome one or more main QTLs can be located at 24-32cM. GI colocalizes to this locus. At the bottom end of chromosome five, a main QTL was also detected at 100-110 cM. A candidate gene for this locus could be *TOCI*, *PRR3*, or *SRR1*. At chromosome 1 at 0-10cM, and in chromosome 3 at 0-10cM, two QTLs, although they did not exceed the LOD threshold, had large effects on the phenotype. These two could be considered as interacting QTLs. Further statistic analysis for the allelic interactions will be tested in session 3.3.3.

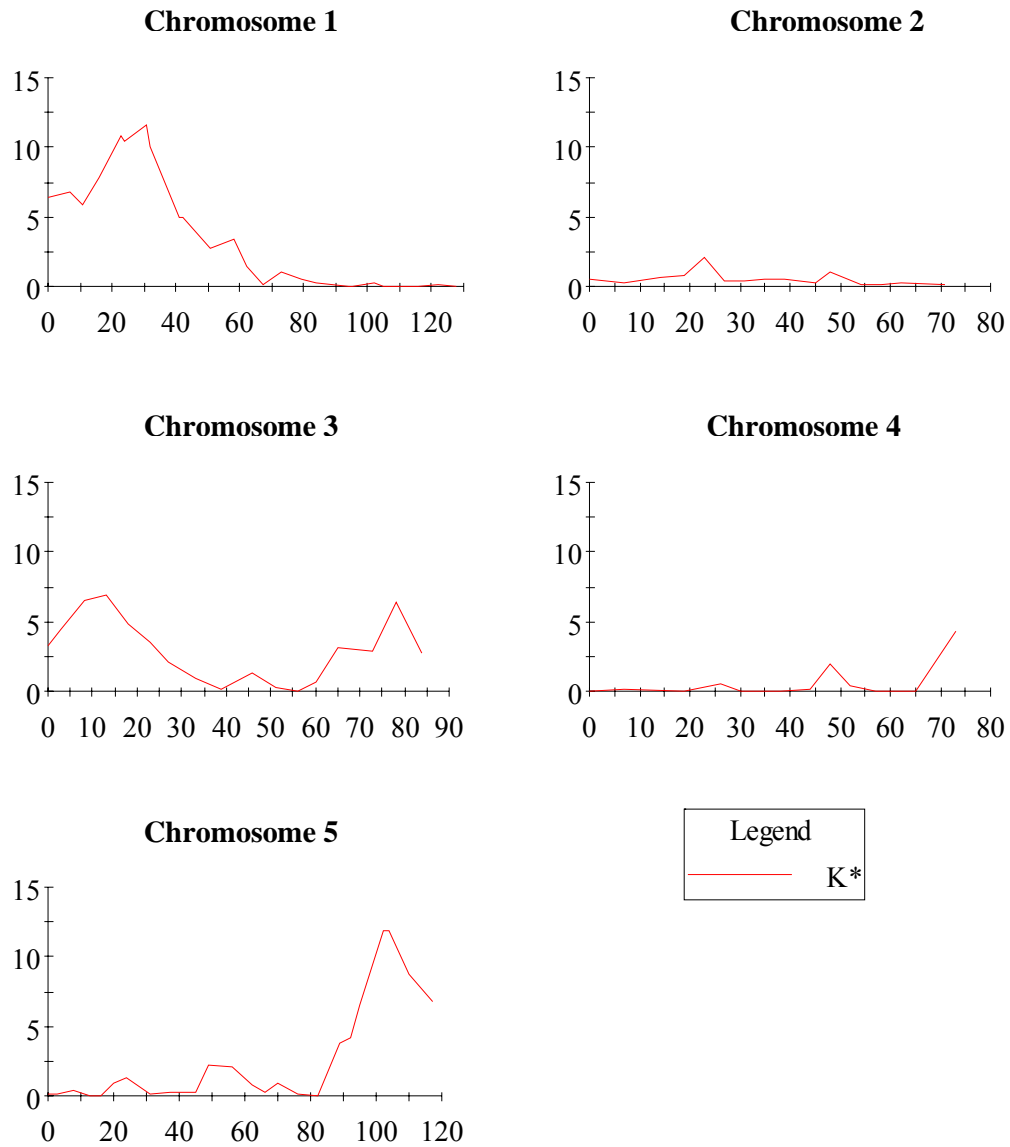


Figure 3.24 Kruskal Wallis application of MapQTL for QTL detection after entrainment to temperature cycles in constant darkness of the CvL population

X axis represents the chromosome location, measured in cM, and Y axis represents the LOD score.

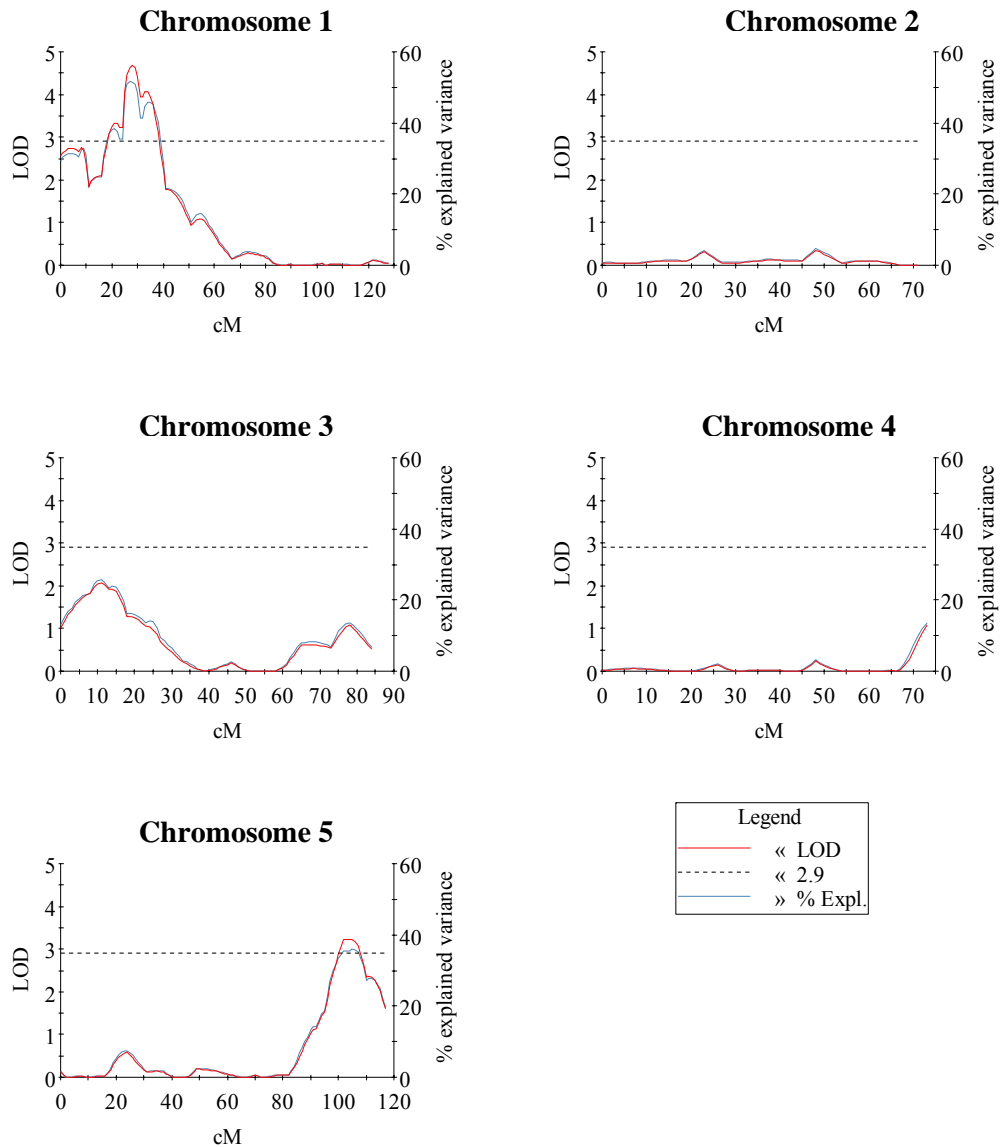


Figure 3.25 MQM output of MapQTL for QTL detection after entrainment to temperature cycles in constant darkness of the CvL population

X axis represents the chromosome location measured in cM, and the left Y axis represents the LOD score, whereas the right Y axis represents the % of explained variance. This percentage is a measure of the effect of the QTL that supplies to the phenotype. The dotted line represents the LOD score threshold. It was set to 2.9 after calculation of 1000 permutations, for 95% significance level.

3.3.3 Allelic interactions in CvL after the temperature entrainment in constant darkness

Allelic interactions were tested for the QTLs identified in the CvL population after temperature entrainment under constant light. Although in the QTL mapping several QTL appear, when tested through Univariate analysis then only two of them were the most significant. The main effect loci were the same in the first chromosome, but could be different for the fifth chromosome. Specifically, the *Ler* allele of the first chromosome QTL at the locus CH.160L-Col was 3.29 hours longer than the *Cvi* allele (Figure 3.26, Table 3.12). Additionally, the *Cvi* allele of the fifth chromosome QTL at the HH.143C locus has a longer period of 3.15 hours than the *Ler* allele (Figure 3.27, Table 3.12). Both QTLs were highly significant for $P=0.004$ (Table 3.12). Although MQM mapping possible interacting QTLs were indicated, in the statistic analysis turned out that there was no significant QTL interactions. The above described results are recapitulated in Table 3.12.

To conclude, the two main QTLs after temperature entrainment in constant darkness co-localized to some of the main QTLs identified after temperature entrainment under constant light. However, after temperature entrainment under constant light, an additional main QTL was found that was the only main QTL identified in the light-dark entrainment. Since in the natural world, light-dark and temperature changes occur together during the 24 hours cycle, temperature entrainment under constant light represents the integrative model that incorporates both the effects of the light-dark and temperature entrainment. To further compare the phenotype after the two temperature entrainment protocols, it appeared that the free-running period (FRP) due to the two QTLs found in constant darkness was longer than the FRP of the respective QTLs found in the constant light (Figures 3.3 and 3.22). Additionally, the allelic differences of the FRP due to either QTL were larger in constant darkness than under constant light, as they described by the additive effect (Figures 3.10, 3.11, 3.26, 3.27).

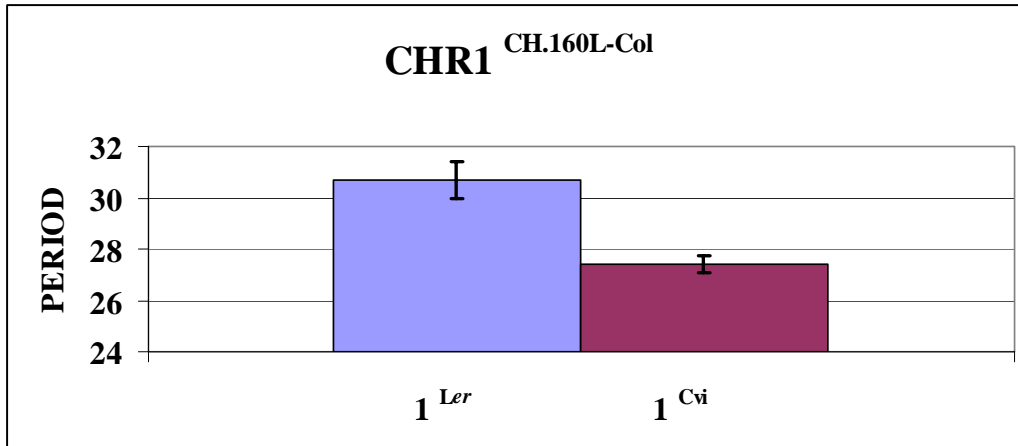


Figure 3.26 Period variation due to allelic variation of the main effect QTL at the first chromosome at locus CH.160L-Col identified for temperature entrainment in constant darkness in the CvL population

In X-axis the number represents the chromosome number and the superscripted *Ler* and *Cvi* are designated for the Landsberg *erecta* and Cape verde islands allele respectively. Bars represent standard error.

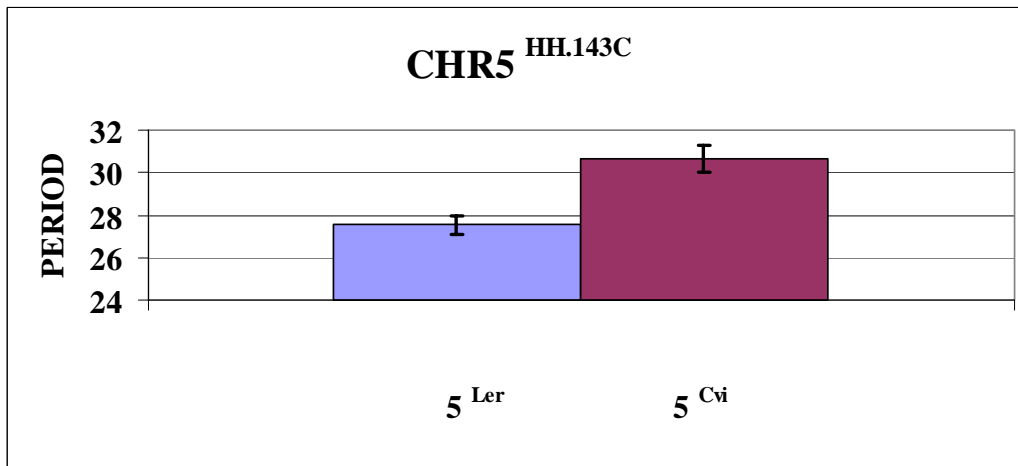


Figure 3.27 Period variation due to allelic variation of the main effect QTL at the first chromosome at locus HH.143C identified for temperature entrainment in constant darkness in the CvL population

In X-axis the number represents the chromosome number and the superscripted *Ler* and *Cvi* are designated for the Landsberg *erecta* and Cape verde islands allele respectively. Bars represent standard error.

Trait	Environment	Marker	Chromosome	Position (cM)	F	P value	2a (h)
PERIOD	TMP in DD						
		CH.160L-Col	I	31	6.833	0.004	3.29
		HH.143C	V	102	9.636	0.004	3.15

Table 3.12 Concentrated results for the QTL identified in the *Cvi/Ler* population after temperature entrainment in constant darkness

Marker, chromosome and position describe the exact location of the QTL identified. F is the value of the F-test calculated by ANOVA. P value is the probability value. <0.001 indicates highly significant QTLs. 2a is the additive effect of the QTL calculated as the difference of the two alleles, and it is measured in hours. TMP in DD denotes temperature cycles in constant darkness

4 GENERATION OF NEW RILS COLLECTIONS

INTRODUCTION

RILs are useful genetic resources to exploit the genetic variation between the two parental strains and map loci that account for any continuous phenotypic variation between these parents. In many cases, the phenotypic variation cannot be explained by a single locus. In contrast, different allelic combinations between various loci and their genetic interaction determine the variation on the phenotype. Natural-variation studies have revealed several loci that were not revealed in mutagenesis screens (Koorneef et al., 2004). Therefore, constructed RILs have become a robust alternative tool for mapping genes.

Natural variation has been used to map genetic variation that controls continuous traits. Flowering time and circadian rhythmicity are two such traits (Alonso-Blanco et al., 1998; Swarup et al., 1999). So far, ecotype-specific variation was found to control both traits (Swarup et al., 1999; Johanson et al., 2000; El-Din El-Assal et al., 2001; Michael et al., 2003b). Flowering time is regulated by internal and external factors. The external factors involve environmental cues, such as light and temperature. These two cues regulate flowering time through different pathways. As an example, prolong treatment to chilling cold ultimately induces flowering time through the vernalization pathway (Amasino, 2005). The central gene of this pathway is the repressor *Flowering Locus C (FLC)* (Michaels and Amasino, 1999). After extended cold temperatures, the expression of *FLC* is suppressed, and thereby, flowering is induced. Natural variation at the *FLC* locus has been detected repeatedly (Gazzani et al., 2003; Shindo et al., 2005). As a separate example, light information is mediated through the photoperiodic pathway, upstream of which is the circadian clock (Davis, 2002; Yanovsky and Kay, 2002). A major determinant of the photoperiodic pathway is a circadian regulated gene named *CONSTANS (CO)* (Putterill et al., 1995; Suarez-Lopez et al., 2001). *CO* induces the expression of a downstream gene named *Flowering locus T (FT)* (An et al., 2004). Up to now, no QTL has been identified at the *CO* or *FT* locus, suggesting that neither mediates natural-allelic variation of photoperiodism.

In addition to flowering time, environmental changes in light and temperature also set the circadian clock (Barak et al., 2000; McClung, 2006). In Chapter 3, natural

variation was exploited with regard to temperature versus light-dark entrainment of the circadian oscillator. For this, two pre-existing RILs populations were used. Generally, RILs are constructed by crossing two accessions that were originated from distinct environments. This has the advantage that the accessions have been selected differentially and QTL mapping will reveal these naturally selected variants. However, if the parental accessions are not commonly used, then the QTL fine mapping, phenotypic confirmation, and complementation will be progressively slowed down. To overcome these caveats, I describe here the creation of six new RIL populations using the four most popular accessions used in *A. thaliana* genetic studies. In this chapter, exploitation of natural variation of one RIL population controlling flowering time and circadian rhythmicity will be described. Their correlation will be noted.

4.1 Generation of new Recombinant Inbred Lines (nRILS)

The new sets of RILs were generated from pairwise crosses between the four most commonly used *A. thaliana* lab accessions, named Columbia (Col), Wassilewskija (WS), Landsberg *erecta* (*Ler*), and C24. Particularly, two accessions, WS and *Ler*, were harboring *CCR2::LUC*, and those were used as pollen donor in pairwise crosses. WS *CCR2::LUC* was respectively crossed to Col, C24, or *Ler*, whereas *Ler CCR2::LUC* was respectively crossed to Col, WS, and C24 (see 2.2.2.3). These F1s were backcrossed to the maternal parent and from 96 BC1 lines, 6 lines were selected for long, and six for short period, by assaying *CCR2::LUC* rhythms. Period was defined here as the time difference between the second and third peak of *CCR2* rhythms. These BC1 lines were self-fertilized. The BC1F2 progeny went through a second selection. Each BC1F2 line was selected for 8 out of 96 progeny. This resulted in 48 extremely short period (SP) lines such as 19-23 hours, and 48 lines with very long period (LP) from 26-32 hours. This was to my knowledge the first time that RILs were constructed in a non-random way. Therefore, it will be of interest to study segregation distortion (SD) based on phenotypic selection, and especially, to study whether the undertaken selection for *CCR2::LUC* rhythms affected other circadian regulated traits, such as hypocotyl elongation, and flowering time. This is partially tested below.

The new RILs (nRILs) have several significant advantages over other pre-existing RILs that could potentially improve their use for circadian-rhythm assays. The first advantage is that all lines were generated by crossing an accession bearing *CCR2::LUC* to a wild-type accession. In this case, *CCR2::LUC* was inserted in the same position in the genome in resultant RIL. In this way, phenotypic variation due to the positional effects of the T-DNA insertion was minimized. The lines in Chapter 3 suffer from this position effect disadvantage. The second advantage is that about 90% of the available genetic resources in the *A. thaliana* community exist in these four accessions. This eases the effort to map these lines, and in the future, should reduce the time needed to clone QTLs identified for a diverse natural-variation studies. The third advantage is that the RILs generated by a reciprocal cross can be used to study maternal effects of any given trait. This is particularly true for the population generated by the *Ler* x WS and WS x *Ler*.

The RIL population generated by the cross between C24 to WS exhibited flowering-time variation (see 4.3). It was particularly interesting to map loci responsible for this remarkable phenotypic variation. Additionally, this RIL was assayed for circadian rhythmicity in light-dark and this was compared to temperature entrainment. Flowering time is partially controlled by the circadian clock. Therefore it was of interest to compare the maps of these two traits in the same population and to determine whether the traits co-segregate. What follows is the evaluation of the C24WS RIL.

4.2 Determination of the genotype WSC24 RIL lines

The C24WS RILs were genotyped across five chromosomes with markers that were polymorphic for genomic sequence repeats found on the genome of *A. thaliana*. The criterion was to have evenly distributed markers across the genome. Therefore markers that were around 5 Mb apart were selected. A genetic map for each line was constructed by genotyping the RILs with 34 markers distributed in all five chromosomes. The genotype of all 85 lines is shown in Appendix 1. Twenty-five percent of the genome of each RIL was expected to be WS, and the remaining seventy-five percent was expected to be C24, since the F1 lines were backcrossed to C24. However, I found that some lines deviated from the expected ratios. There are genomic regions that a C24 allele was overrepresented. Especially, the SP-selected lines showed such overrepresentation of the C24 allele versus the WS allele all over

chromosome 1 (Table 4.1). Over representation of WS allele was observed at the top of chromosome 3. Since this was observed in all lines, one plausible explanation here is that this is the location of the *CCR2::LUC* T-DNA insertion, from the WS pollen donor.

Chromosome 1	C24 allele	WS allele	Total LP selected lines		C24 allele	WS allele	Total SP selected lines
NGA59	33	10	43		38	4	42
NGA63	29	14	43		38	4	42
MSAT1-10	24	19	43		36	6	42
SO392	21	22	43		36	6	42
T27K12	23	20	43		38	4	42
CIW1	23	20	43		36	6	42

Table 4.1 Allelic frequencies at various loci in the first chromosome for the long and short period selected lines

The frequency of C24 and WS alleles of six markers at chromosome one were assayed. Total LP corresponds to the total number of long-period-selected lines, whereas total SP to the total number of short-period-selected lines. Note that approximately 10% of the SP lines have a WS allele at a given marker.

4.3 Determination of two continuous traits in the C24WS RILS

4.3.1 Flowering-time assays of C24WS RIL under inductive long days

The RIL set generated by the cross of WS to C24 exhibited remarkable flowering-time variation. Flowering time is a continuous trait, and as such, QTL studies can be readily performed. For this, I measured flowering-time within the WSC24 RILs under long days in greenhouse-controlled conditions (see 2.2.6). Flowering time was assayed as total leaf number (TLN). Eight plants per RIL were measured and the averaged TLN per RIL was used for QTL mapping. The averaged TLN per RIL was rounded to the closest higher-integer number (Table 4.1). In total, 85 RIL lines were assayed. This resulted in about 680 plants being scored. In five RILs, less than eight plants were assayed due to reduced germination, therefore they were not included in the QTL mapping. Lines 1-43 were those selected for SP, whereas lines 44-85 were those selected for LP, as described in 4.1. The LP-selected lines exhibited the later-flowering phenotypes, whereas the SP-selected lines exhibited the earliest flowering-time phenotypes (Table 4.2). Thus, the selection of the clock resulted in phenotypic consequences.

The flowering-time phenotype described in Table 4.2 was then grouped in 6 interval classes and plotted against frequency (Figure 4.1). More than 50% of all lines flowered with fewer than twenty leaves. Interestingly, the extremely late-flowering lines were those selected for long period. The general trend as observed in Figure 4.1 is that LP-selected lines flowered later than the SP-selected lines.

RIL NAME	TLN		RIL NAME	TLN		RIL NAME	TLN
1	14		30	12		59	38
2	36		31	11		60	42
3	45		32	11		61	11
4	24		33	13		62	39
5	32		34	10		63	12
6	44		35	11		64	7
7	12		36	9		65	6
8	12		37	11		66	13
9	21		38	9		67	12
10	14		39	24		68	10
11	15		40	18		69	5
12	22		41	33		70	7
13	20		42	35		71	12
14	34		43	22		72	23
15	53		44	13		73	34
16	22		45	25		74	13
17	22		46	10		75	29
18	10		47	19		76	11
19	23		48	10		77	15
20	-		49	14		78	36
21	15		50	11		79	20
22	7		51	9		80	11
23	13		52	10		81	14
24	33		53	22		82	13
25	13		54	11		83	-
26	10		55	13		84	13
27	-		56	10		85	-
28	6		57	7	WS		8
29	6		58	8	C24		13

Table 4.2 Flowering time variation of the WSC24 RIL collection grown in 16 hours light::8 hours darkness in greenhouse

RIL NAME corresponds to the arbitrary name as given by me for the WSC24 population, TLN is the total leaf number measured by at least eight plants per experiment. Plants were shown twice within 2 weeks interval during November-December 2007. – indicates the lack of TLN data

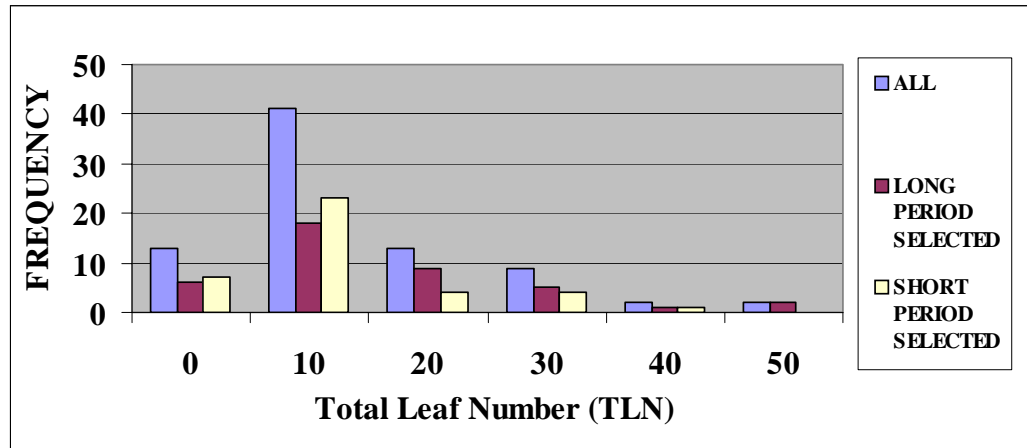


Figure 4.1 The continuous distribution of total leaf number for 80 out of 85 C24WS Recombinant Inbred Lines

X-axis is the total leaf number and Y axis represents number of C24WS RILs with a certain total leaf number (TLN). TLN was binned in 10 leaves interval as of 0-9. Note that there is a trend for LP lines being later flowering.

4.3.1.1 QTL mapping for flowering-time variation

QTL mapping was performed for the measured TLN. I performed QTL mapping in three different ways, based on the observation that the latest-flowering plants correlated with those selected for LP, whereas the earliest-flowering genotypes correlated with those selected for SP (Figure 4.1). In the first mapping test, I included only the LP-selected C24WS RIL lines. In the second mapping test, I included only the SP-selected C24WS RIL lines. And in the third mapping test, I included all of the C24WS RIL lines. In this way, three maps would be generated from phenotypically selected circadian data.

The QTL mapping for TLN of the LP-selected lines resulted in the detection of three main QTLs, and an interacting QTL (Figure 4.2). The main QTL was at chromosome 1 at the locus NGA59. Known genes in this interval are the circadian clock gene *LHY*, and two photoreceptor genes *CRY2* and *PHYA*. Most likely, this QTL would be *CRY2* since a natural variant already was found in Cvi accession (El-Din El-Assal et al., 2001). This QTL explains more than 30% of the TLN phenotype. Another QTL was localized at chromosome 4 at locus *FRI*. An obvious candidate gene was *FRIGIDA*, a gene that is an activator of *FLC* (Shindo et al., 2005). The QTL at this locus explains less than 30 % of the flowering variation. The third main QTL was at chromosome 5 between NGA158 and NGA106. At this region *FLC*, is localized. An interaction QTL was localized at chromosome 1 at locus SO392. This QTL interacted strongly with the presumed *FLC* QTL. Several known flowering time genes co-localized at the proximity of the presumed *FLC* QTL, including *CONSTANS*, *HUA2* (Suarez-Lopez et al., 2001; An et al., 2004; Doyle et al., 2005). This QTL explains more than 40% of the phenotype. Fine mapping will determine which is the underlying QTL.

The QTL mapping for the SP-selected lines did not result in a QTL at the top of chromosome 1 (Figure 4.3). Three main QTLs were detected at the fifth chromosome at the loci NGA106, MSAT5.14, and NGA76 (Figure 4.3). A case with three nearby QTLs suggests that the middle QTL is a ‘ghost’. Its detection could be due to large genetic effects of two other QTLs. The percentage of the explained variance of the non ‘ghost’ QTLs could be different. The possibility that the middle QTL is not a real will be tested later by statistic analysis (4.3.1.2.2). Another main QTL, although it did not exceed the LOD threshold, was found at the chromosome 4 at the locus *FRI*. In this QTL mapping assay, the LOD score was found to greatly vary

across the five chromosomes. Specifically, the LOD score at chromosomes 1 and 3 was 6.4 and 6.6. In contrast at the chromosomes 2, 4, and 5, the LOD score was 2.0, 2.3 and 3.3, respectively. This could be explained that at chromosome 1, a great segregation distortion was evident for the lines selected for short period (Table 4.1). Moreover, at chromosome 3 at the NGA162, all lines were WS. This could suggest that this was the location that the T-DNA was inserted, since WS was the accession that bears the *CCR2::LUC* construct; all lines harbor the LUC construct, and thus, there must be a genomic interval homozygous for WS in all RILs. In this case, the LOD score of the QTL identified at the locus *FRI* is 4.0, and therefore, was considered main QTL. The same consideration as to QTL found at locus *FRI* could be taken for a QTL found at chromosome 5 at the locus NGA76. Therefore, flowering time in the selected SP lines is controlled by the same but also different QTLs compared to the LP lines.

The mapping that included all RILs resulted in the detection of QTLs at the genomic locations that were described separate for long or short period selected lines (Figure 4.4). The LOD score again varied across chromosomes, an effect observed in the QTL mapping performed for the SP-selected lines. The first chromosome QTL just exceeded the genome-wide LOD threshold. This QTL confers less than 20% of the phenotypic variation. The QTL at *FRI* locus had a similar effect with the first chromosome QTL. At the fifth chromosome, two QTLs were detected at NGA106 and MSAT5.14 loci. Both QTLs had a LOD score that exceeded 15, and each explained around 50% of the phenotype. A QTL localized at SO392 locus at the first chromosome might be an interacting QTL. Interactions between QTLs will be described in the following session.

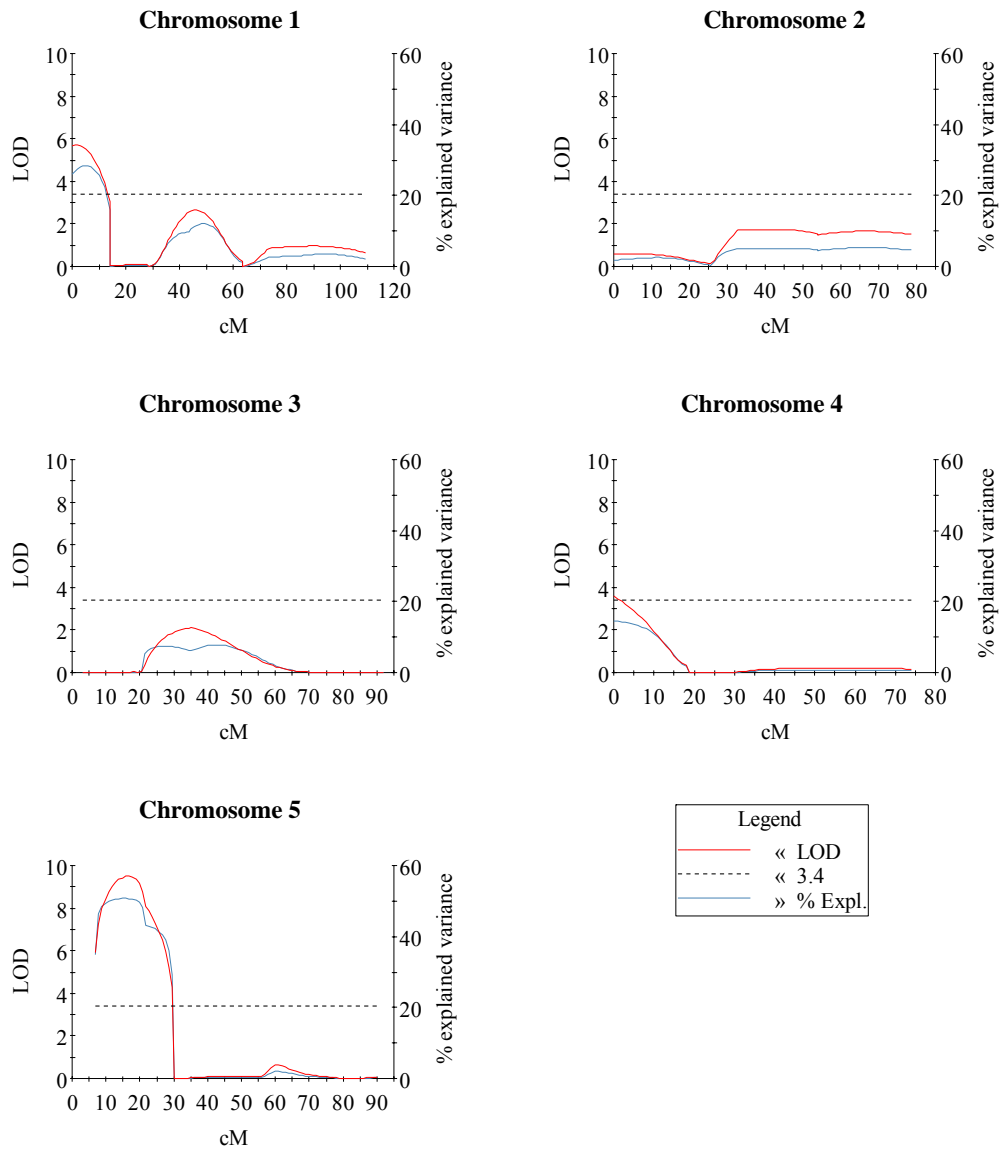


Figure 4.2 MapQTL for flowering time under long days of the long period selected C24WS RIL lines

X axis represents the chromosome location, measured in cM, left Y axis represents the LOD score, and right Y axis represents the % of explained variance. This percentage is a measure of the effect of the QTL that supplies to the phenotype. The dotted line represents the LOD score threshold. It was set to 3.4 after calculation of 1000 permutations, for 95% significance level.

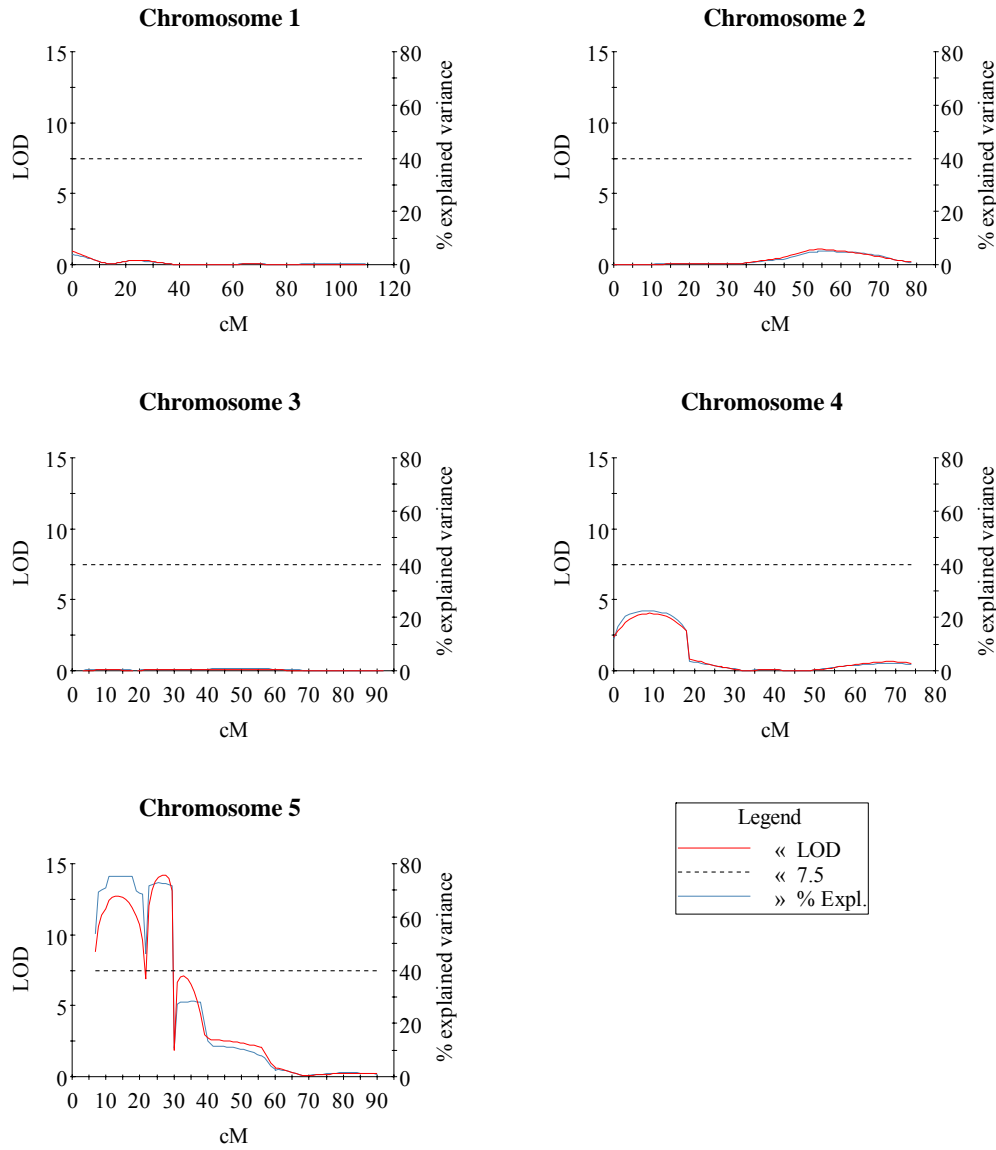


Figure 4.3 MapQTL for flowering time under long days of the short period selected C24WS RIL lines

X axis represents the chromosome location, measured in cM, left Y axis represents the LOD score, and right Y axis represents the % of explained variance. This percentage is a measure of the effect of the QTL that supplies to the phenotype. The dotted line represents the LOD score threshold. It was set to 7.5 after calculation of 1000 permutations, for 95% significance level.

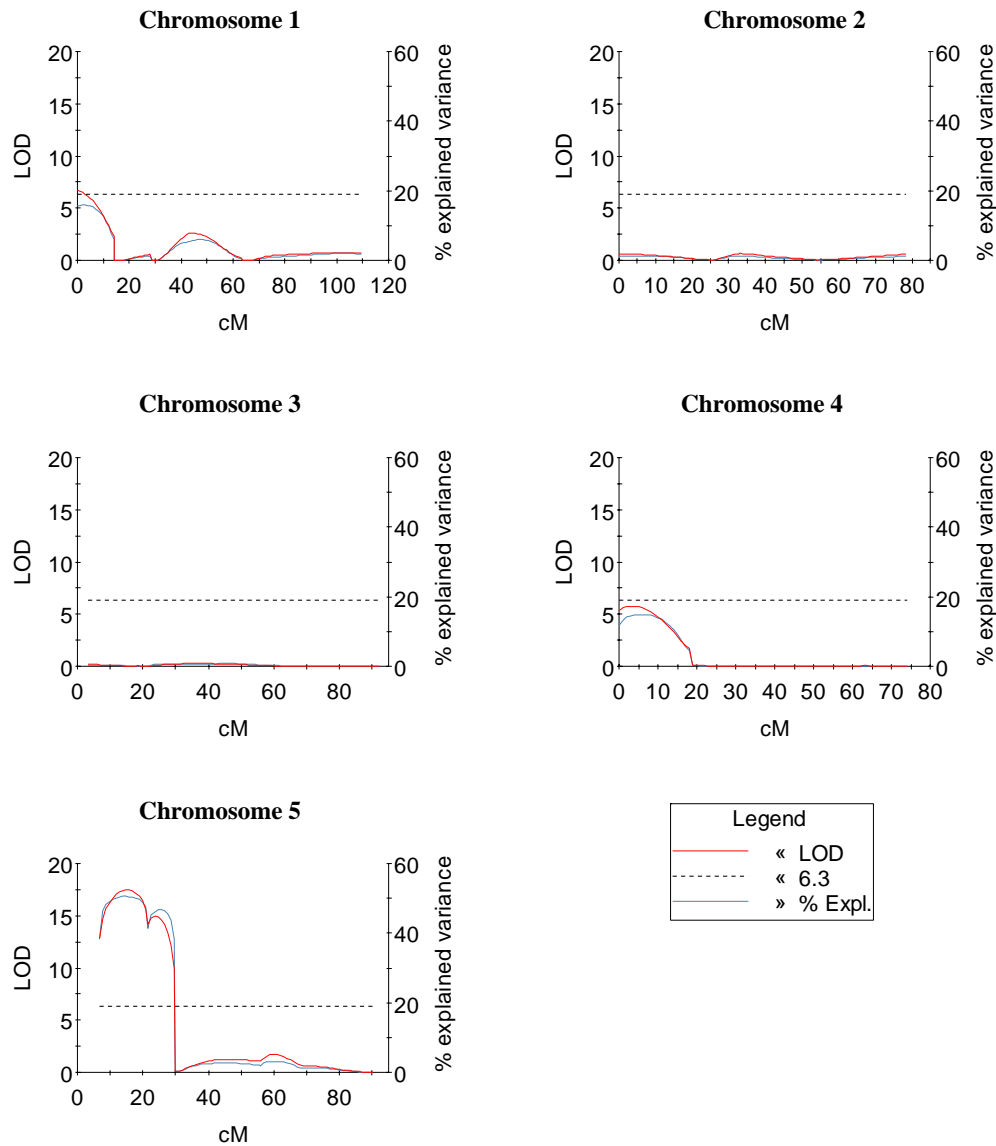


Figure 4.4 MapQTL for flowering time under long days of the total number of C24WS RIL lines

X axis represents the chromosome location, measured in cM, left Y axis represents the LOD score, and right Y axis represents the % of explained variance. This percentage is a measure of the effect of the QTL that supplies to the phenotype. The dotted line represents the LOD score threshold. It was set to 6.3 after calculation of 1000 permutations, for 95% significance level.

4.3.1.2 Allelic interactions

In the previous session, detection was hypothesized of an uncertain QTL at the locus MSAT 5.14, during the QTL mapping for the SP-selected lines. Therefore, I tested this ambiguous locus using statistical methods. Additionally, I determined the additive effects of each QTL by deducing the effect of the two allelic forms of each locus, and the allelic effects of interacting QTLs, to find epistatic relationships among different allelic combinations. The allelic relationships of the respective QTLs identified, and their additive effect on flowering time, are represented in the following graphs (Figures 4.5-4.17). All the above described analysis was performed by SPSS through GLM Univariate, where TLN was used as a dependent variable, and markers, and marker interactions were used as factors. The title on each graph represents the QTL location at which chromosome and the superscripted letter represent marker name where the QTL was identified. C24 and WS are the allelic forms of each QTL. In case of QTL interactions, the first code letter stands for the first QTL, the second letter code stands for the second QTL. Figures 4.5-4.8 represent QTLs identified for the LP-selected lines, Figures 4.9-4.12 for the SP-selected lines, and Figures 4.13-4.17 for all selected lines. An extensive description of allele specific effects of each QTL or interactions of QTL for each selection will be described below.

4.3.1.2.1 Allelic interactions for LP-selected lines

Three main QTL and an interaction were confirmed during statistic analysis for the LP-selected lines. The QTL at chromosome 1 at NGA59 locus was found to be highly significant for $P=0.0001$, and it has an additive effect of 12 leaves provided by the WS allele (Figure 4.5). The QTL at locus FRI was highly significant for $P=0.002$ (Table 4.3). Its additive effect was 11 leaves conferred by the C24 allele (Figure 4.6). The third main QTL localized at the locus NGA106 at the fifth chromosome has an additive effect of 10 leaves due to the WS allele, and is the most significant of all for $P<0.0001$ (Figure 4.7, Table 4.3). Only one interaction was statistically confirmed for the LP-selected lines. This interaction was between a QTL at locus SO392 and a QTL at locus NGA106 (Figure 4.8). This interaction was significant for $P<0.004$ (Table 4.3). The interaction of the C24 allele of the SO392 locus with the WS allele of the NGA106 locus displays an extremely late-flowering phenotype (33 leaves).

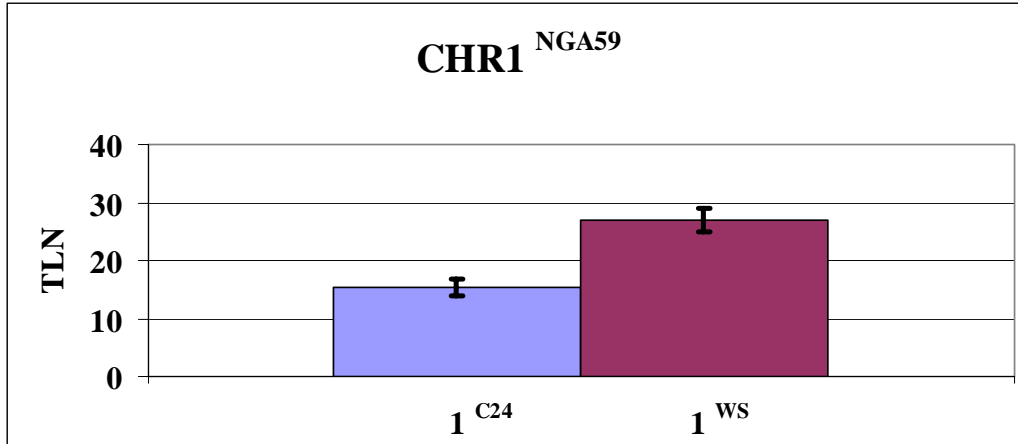


Figure 4.5 Flowering time variation in the long period selected lines due to allelic variation of the first chromosome QTL at locus NGA59

In X-axis the number represents the chromosome number and the superscripted C24 and WS are designated for the C24 and Wassilewskija allele respectively. Bars represent standard error.

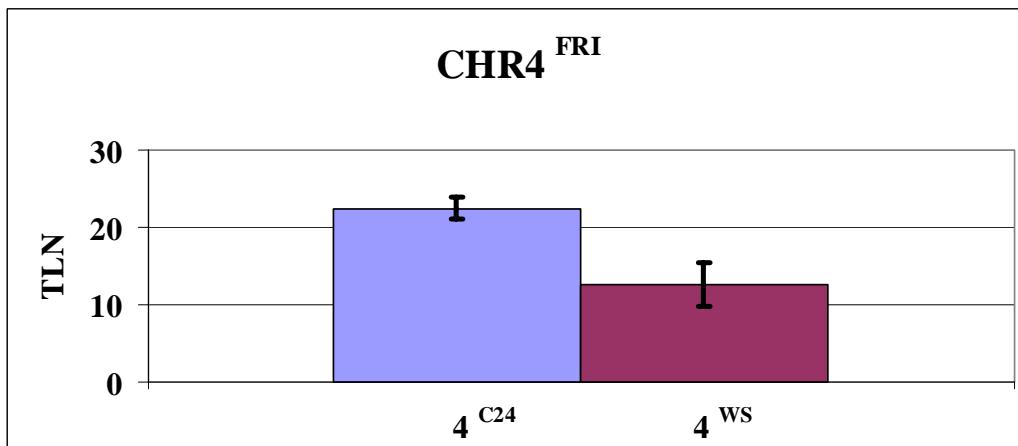


Figure 4.6 Flowering time variation in the long period selected lines due to allelic variation of the fourth chromosome QTL at locus FRI

In X-axis the number represents the chromosome number and the superscripted C24 and WS are designated for the C24 and Wassilewskija allele respectively. Bars represent standard error.

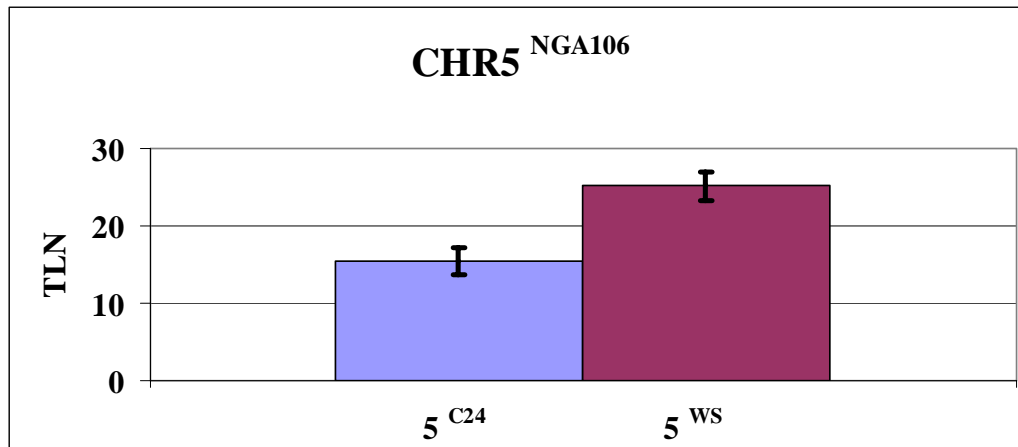


Figure 4.7 Flowering time variation in the long period selected lines due to allelic variation of the fifth chromosome QTL at locus NGA106

In X-axis the number represents the chromosome number and the superscripted C24 and WS are designated for the C24 and Wassilewskija allele respectively. Bars represent standard error.

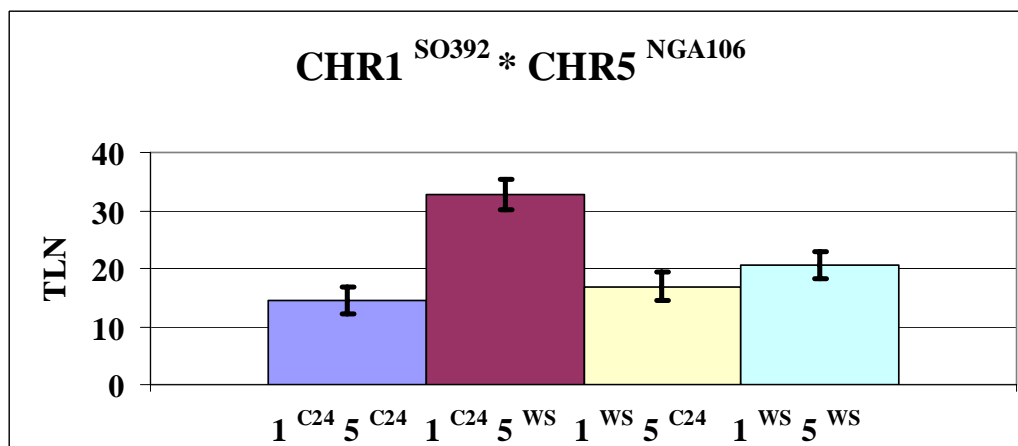


Figure 4.8 Flowering time variation in the long period selected lines due to interaction of two QTLs at chromosome 1 at locus SO392 and chromosome 5 at locus NGA106

In X-axis the number represents the chromosome number and the superscripted C24 and WS are designated for the C24 and Wassilewskija allele respectively. Bars represent standard error.

4.3.1.2.2 Allelic interactions for SP-selected lines

The identified QTLs for the SP-selected lines were further statistically analyzed for significance using the GLM Univariate model. Although four QTL were identified by the QTL analysis, only three of them, and an interaction, were confirmed during statistic analysis. The presence of the QTL at the fifth chromosome at MSAT5.14 was not confirmed by statistic analysis. In contrast, the QTLs at the loci NGA106 and NGA76 at the fifth chromosome were highly significant for $P < 0.0001$ (Table 4.3). Their additive effect was 10 and 13 leaves, respectively, and this provided by the WS allele (Figures 4.9, 4.10). The QTL at locus FRI was highly significant for $P < 0.0001$ (Table 4.3). Its additive effect was 15 leaves conferred by the C24 allele (Figure 4.11). This interaction was between a QTL at locus FRI and a QTL at locus NGA76 (Figure 4.12). This interaction was significant for $P < 0.0001$ (Table 4.3). The interaction of the C24 allele of the FRI locus with the WS allele of the NGA76 locus displays an extremely late-flowering phenotype (34 leaves). As it turns out, the QTL at MSAT5-14 was not identified by the statistical analysis either as main or as interacting QTL.

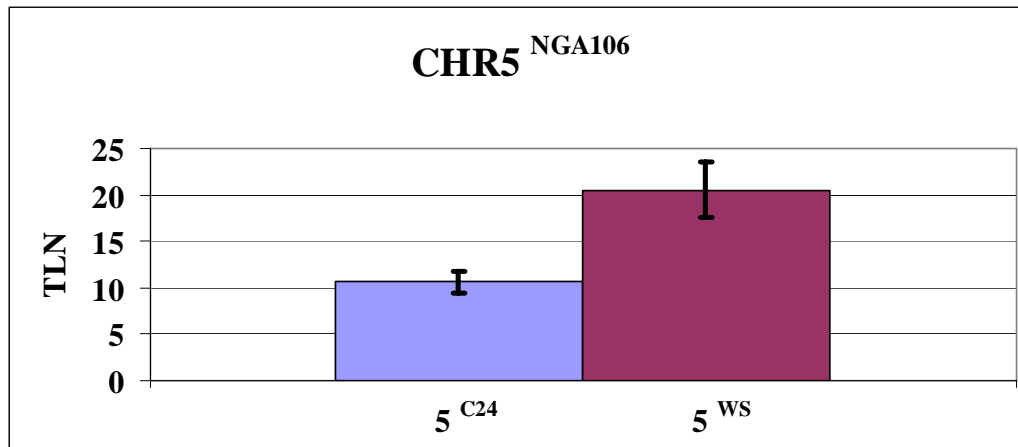


Figure 4.9 Flowering time variation in the short-period selected lines due to allelic variation of the fifth chromosome QTL at locus NGA106

In X-axis the number represents the chromosome number and the superscripted C24 and WS are designated for the C24 and Wassilewskija allele respectively. Bars represent standard error.

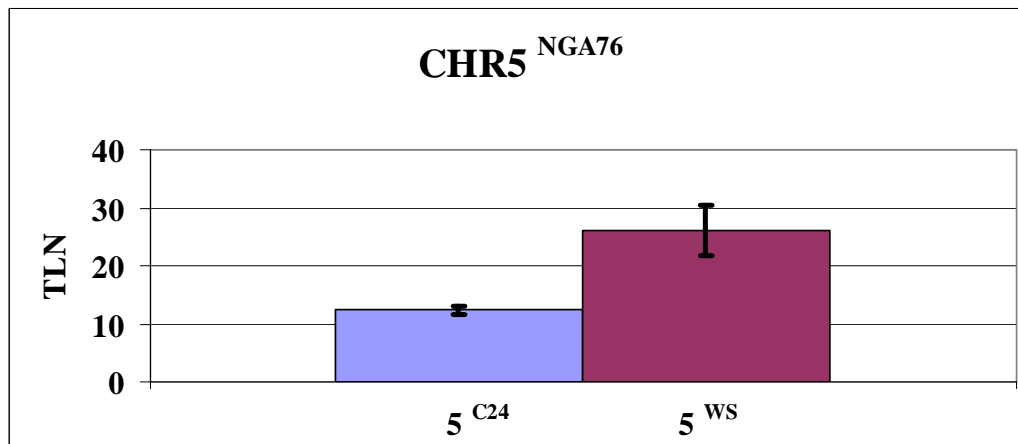


Figure 4.10 Flowering time variation in the short-period selected lines due to allelic variation of the fifth chromosome QTL at locus NGA76

In X-axis the number represents the chromosome number and the superscripted C24 and WS are designated for the C24 and Wassilewskija allele respectively. Bars represent standard error.

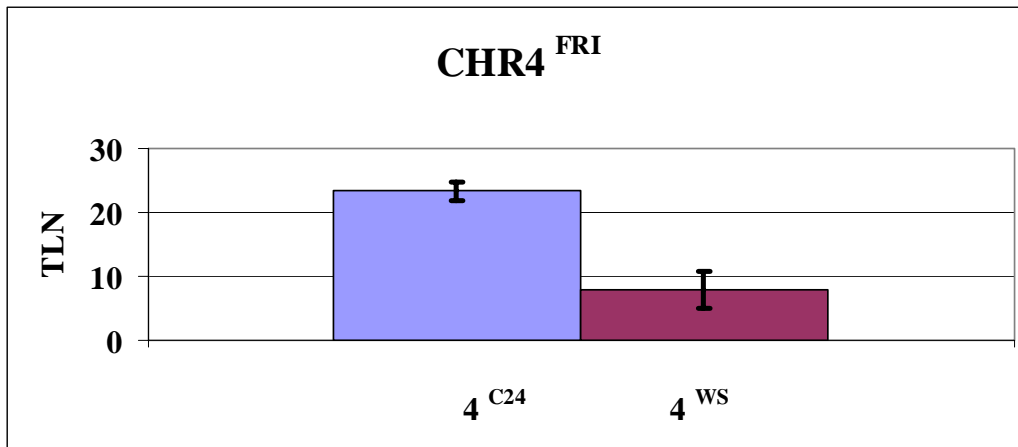


Figure 4.11 Flowering time variation in the short-period selected lines due to allelic variation of the fourth chromosome QTL at locus FRI

In X-axis the number represents the chromosome number and the superscripted C24 and WS are designated for the C24 and Wassilewskija allele respectively. Bars represent standard error.

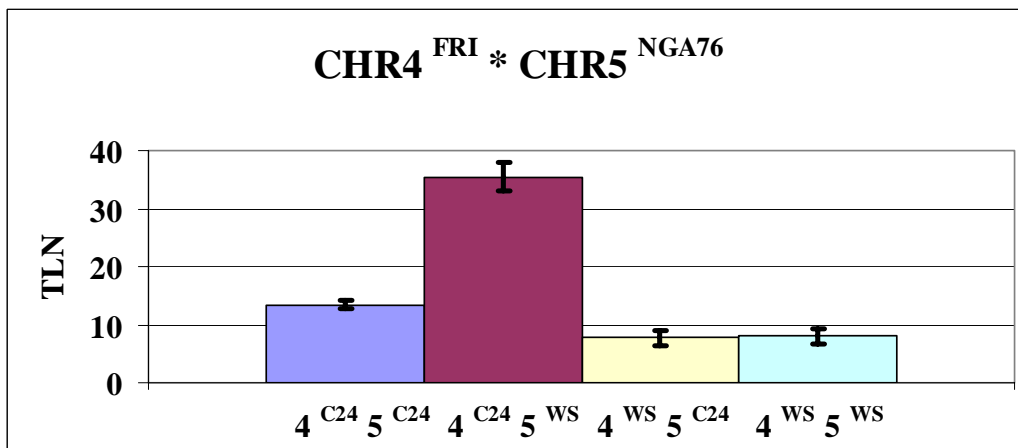


Figure 4.12 Flowering time variation in the short-period selected lines due to interaction of two QTLs at chromosome 4 at locus FRI and chromosome 5 at locus NGA76

In X-axis the number represents the chromosome number and the superscripted C24 and WS are designated for the C24 and Wassilewskija allele respectively. Bars represent standard error.

4.3.1.2.3 Allelic interactions for all C24WS lines

The QTL mapping analysis resulted in the identification of several QTLs that were found during the QTL mapping for either the SP- or LP-selected lines. I performed various GLM Univariate analyses to determine which loci and which interactions were highly statistically significant. Three main QTL were found to be highly significant and two interactions were found to be significant. The QTL at the locus NGA106, at the fifth chromosome, was highly significant for $P < 0.0001$ (Table 4.3). Its additive effect was 10 leaves provided by the WS allele (Figure 4.13). The QTL at locus FRI was another highly significant for $P < 0.0001$ (Table 4.3). Its additive effect was 11 leaves conferred by the C24 allele (Figure 4.14). The QTL identified at the locus NGA59 at the first chromosome was also highly significant for $P < 0.0001$ (Table 4.3). The additive effect was 11 leaves provided by the WS allele (Figure 4.15). One interaction was found between a QTL at locus SO392 and a QTL at locus NGA76 (Figure 4.16). A second interaction was found between a QTL at locus FRI and a QTL at locus NGA106 (Figure 4.17). The first interaction was significant for $P = 0.002$, whereas the second for $P < 0.05$ (Table 4.3). The interaction of the WS allele of the QTL at the SO392 with the C24 allele of the QTL at the NGA76 locus exhibits a late-flowering phenotype with 29 leaves (Figure 4.16). The interaction of the C24 allele of the FRI locus with the WS allele of the NGA106 locus displays an extremely late-flowering phenotype with 34 leaves (Figure 4.17). Therefore, the first chromosome QTL that was also identified in the QTL mapping performed for all lines was due to the phenotypic selection.

Collectively, in this chapter I described that the flowering-time variation in the C24WS is due to several QTLs and their interaction. Excitingly, this variation depended on previous circadian selection. Thus, the clock can control flowering-time variation through the use of natural-allelic interactions. The variation in the LP vs. SP-period selected lines was conferred by the same, and also by different QTLs. The QTL at the first chromosome at locus NGA59 was found exclusively in the LP-selected lines, whereas the QTL at the locus NGA76 at the fifth chromosome was detected only for the SP- selected lines. This again emphasizes the effect selection of the clock can lead to specific developmental consequences. The QTL identified at the loci FRI and NGA106 probably correspond to the genes *FRI* and *FLC*. This will be described more fully in Chapter 6.

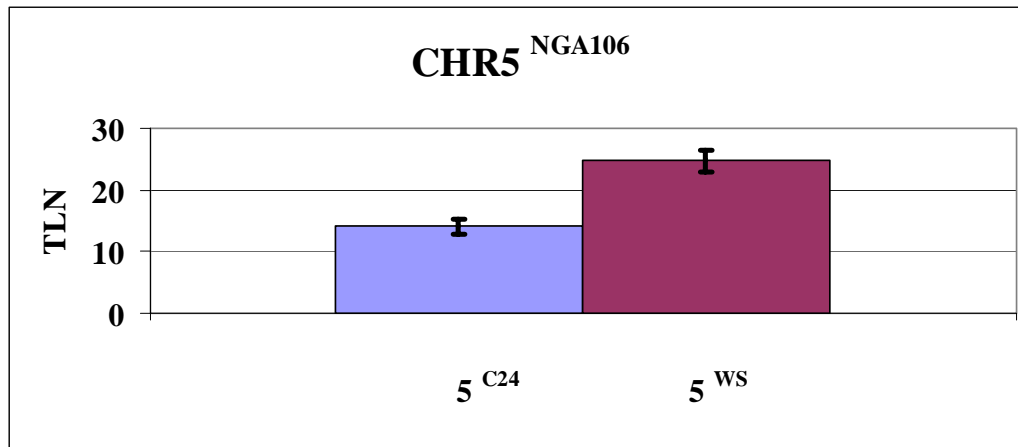


Figure 4.13 Flowering time variation in all RILs of the C24WS population due to allelic variation of the fifth chromosome QTL at locus NGA106

In X-axis the number represents the chromosome number and the superscripted C24 and WS are designated for the C24 and Wassilewskija allele respectively. Bars represent standard error.

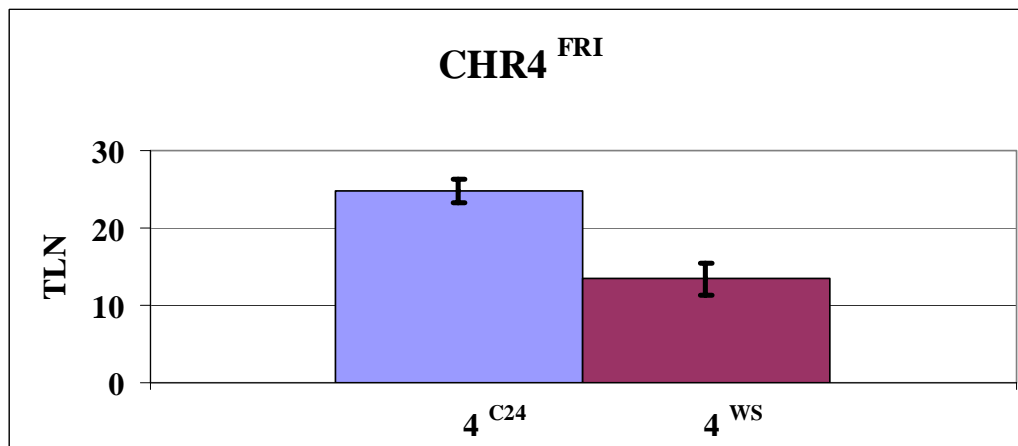


Figure 4.14 Flowering time variation in all RILs of the C24WS population due to allelic variation of the fourth chromosome QTL at locus FRI in the C24WS population

In X-axis the number represents the chromosome number and the superscripted C24 and WS are designated for the C24 and Wassilewskija allele respectively. Bars represent standard error.

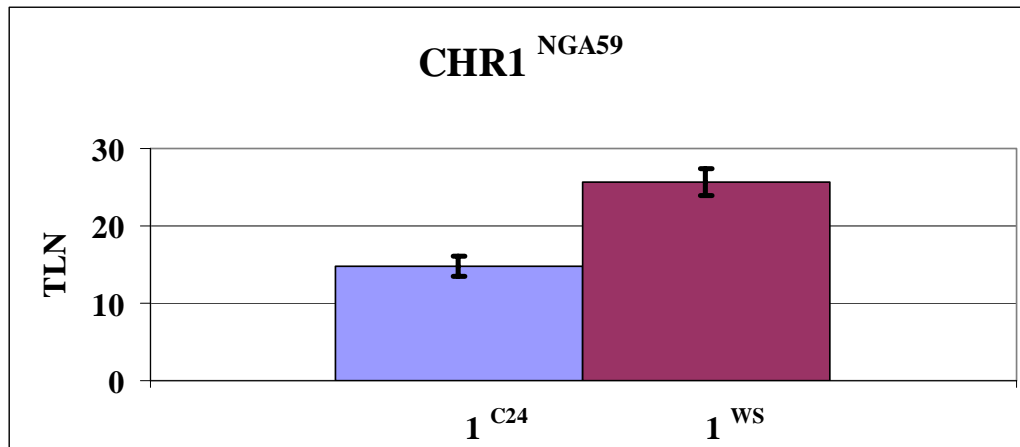


Figure 4.15 Flowering time variation in all RILs of the C24WS population due to allelic variation of the first chromosome QTL at locus NGA59

In X-axis the number represents the chromosome number and the superscripted C24 and WS are designated for the C24 and Wassilewskija allele respectively. Bars represent standard error.

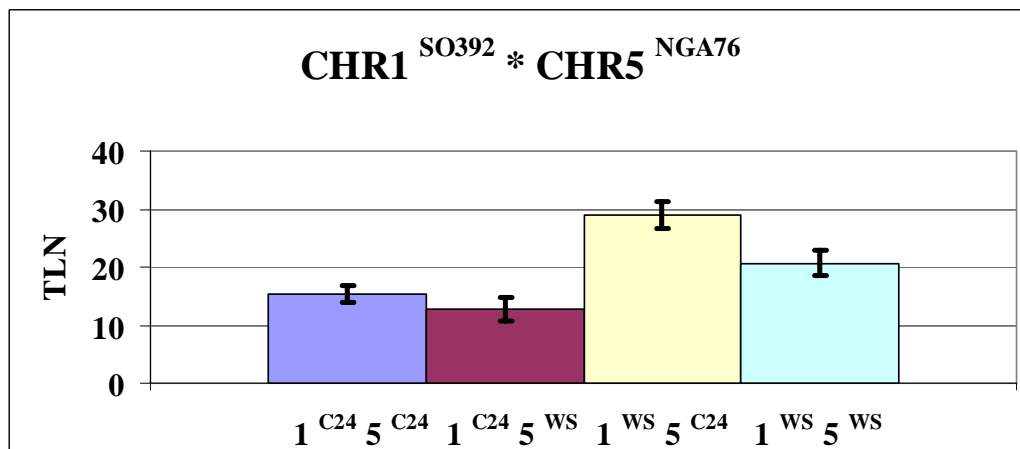


Figure 4.16 Flowering time variation in all RILs of the C24WS population due to interaction of two QTLs at chromosome 1 at locus SO392 and chromosome 5 at locus NGA76

In X-axis the number represents the chromosome number and the superscripted C24 and WS are designated for the C24 and Wassilewskija allele respectively. Bars represent standard error.

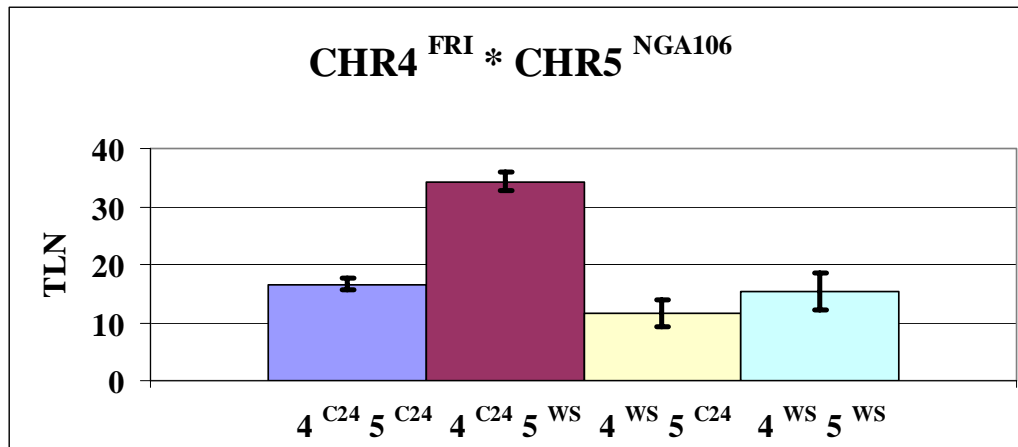


Figure 4.17 Flowering time variation in all RILs of the C24WS population due to interaction of two QTLs at chromosome 4 at locus FRI and chromosome 5 at locus NGA106

In X-axis the number represents the chromosome number and the superscripted C24 and WS are designated for the C24 and Wassilewskija allele respectively. Bars represent standard error.

Trait	RILs	h ²	Marker	Chromosome	Position (cM)	F	P value	2a (#leaves)
TLN	LP	0.90						
			NGA59	I	0	26.828	<0.0001	12
			FRI	IV	0	11.083	0.002	11
			NGA106	V	20	25.223	<0.0001	10
			SO392 * NGA106	I*V	50 * 20	6.561	0.004	-
TLN	SP	0.91						
			FRI	IV	0	102.648	<0.0001	15
			NGA106	V	20	12.392	=0.0001	10
			NGA76	V	40	55.190	<0.0001	13
			FRI * NGA76	IV*V	0*40	36.881	<0.0001	-
TLN	ALL	0.72						
			NGA59	I	0	41.412	<0.0001	12
			FRI	IV	0	43.029	<0.0001	11
			NGA106	V	20	12.748	<0.0001	10
			SO392 * NGA76	I*V	50 * 40	5.242	0.002	-
			FRI * NGA106	I*V	0*20	5.432	0.02	-

Table 4.3 Concentrated results for the QTL identified in the C24WS population for flowering time in inductive long days

h² denotes the heritability of the trait for a specific environment. Marker, chromosome and position describe the exact location of the QTL identified. F is the value of the F-test calculated by ANOVA. P value is the probability value. <0.001 indicates very highly significant QTLs. 2a is the additive effect of the QTL calculated as the difference of the two alleles, and it is measured in number of leaves. LP stands for long period, SP stands for short period, and ALL for lines including SP and LP.

4.3.2 Circadian rhythm assays under light-dark and temperature cycles

The generated C24WS population was assayed for *CCR2* period after light-dark entrainment of 12 hours light::12 hours darkness, and in temperature entrainment of 12 hours at 22°C::12 hours at 16°C before they would free-run under constant light conditions. To date, about 50% of the total number of C24WS RILS has been assayed. Most of the lines displayed low intraline variation (Table 4.3). The otherwise high intraline variation could be explained by the presence of a segregating QTL or by allelic interaction among QTL combinations of the respective RILs. SP- and LP-selected lines were evenly included in the preliminary QTL mapping. The RILs assayed, thus far for *CCR2* rhythmicity, after two entrainment protocols, were overlay plotted to identify the period variation within RILs after the different entrainments (Figure 4.18). The overlay plot indicated that there is enormous period variation as measured per RIL line after the two entrainments. Such large period variation was not observed in the CvL or BxS population assayed under the same conditions (see Chapter 3.1.2 and 3.2.2).

For the light-dark entrainment, the averaged period of each RIL line was used for QTL mapping. This resulted in a main QTL at the second chromosome at locus RGA (Figure 4.19). An interacting QTL at the second chromosome at locus MSAT2.41 enhances the effect of this QTL, but suppresses the effect of the fifth chromosome at locus JV 61/62. The RGA located QTL is novel, whereas the QTL at locus MSAT2.41 is in the interval that includes *ELF3*.

In addition to the light-dark entrainment, RILs were synchronized to temperature cycles for period measurements in subsequent free-running conditions. The period measured after temperature entrainment is showed in Table 4.3. Preliminary data will be described for the averaged period of individuals of the approximately same RILs lines. Data will be compared to the light-dark entrainment. Surprisingly, no QTL exceeds the LOD threshold (Figure 4.20). However, at the locus JV61/62 at the fifth chromosome the explained variance exceeds 20%, whereas at the first chromosome at the locus MSAT1.10, and at the second chromosome at the locus RGA the explained variances exceed 15%. For the resolution of these QTLs, more lines will need to be assayed.

Collectively, a remarkable period variation of *CCR2* for most respective RILS after two entrainment protocols was observed (Figure 4.18). Such large variation was not observed in CvL or BxS RILs after the two entrainments. The preliminary QTL mapping of C24WS of 34 RILS that were selected for both SP and LP after the light-dark entrainment resulted in the detection of a main QTL at the second chromosome at locus RGA. Two QTL at the loci MSAT2.41 and JV61/62 modify the effect of the main QTL. However, the preliminary QTL mapping of the same RILS after temperature entrainment did not result in any main QTL. The genome wide LOD score for both QTL mapping were calculated 2.4.

C24WS RIL	LD PERIOD	TMP PERIOD
1	31.02	28.75
2	31.16	26.84
4	29.61	28.10
5	30.81	27.62
9	29.40	28.35
10	31.21	31.09
11	29.44	26.26
12	29.07	29.22
13	29.46	28.98
14	33.17	29.69
15	33.70	31.70
16	30.87	29.06
19	30.71	28.40
23	27.98	25.67
24	30.23	26.08
25	27.61	26.99
26	31.16	28.31
28	31.36	26.00
29	33.22	28.90
57	26.18	25.31
59	30.14	28.64
60	30.50	27.95
61	29.29	30.50
62	28.77	27.35
72	27.19	26.79
73	27.78	25.88
75	27.64	26.33
76	28.67	27.94
78	27.75	27.73
79	28.01	26.47
80	31.16	28.51
81	32.02	26.25
82	31.43	26.88
84	31.54	27.88

Table 4.4 The free-running period of the C24WS RIL collection after light-dark entrainment under constant 22°C (LD) or after entrainment in temperature cycles of 12 hours at 22°C followed by 12 hours at 16°C under constant light (TMP)

LD period corresponds to averaged period after light-dark entrainment. TMP period corresponds to averaged period after temperature entrainment.

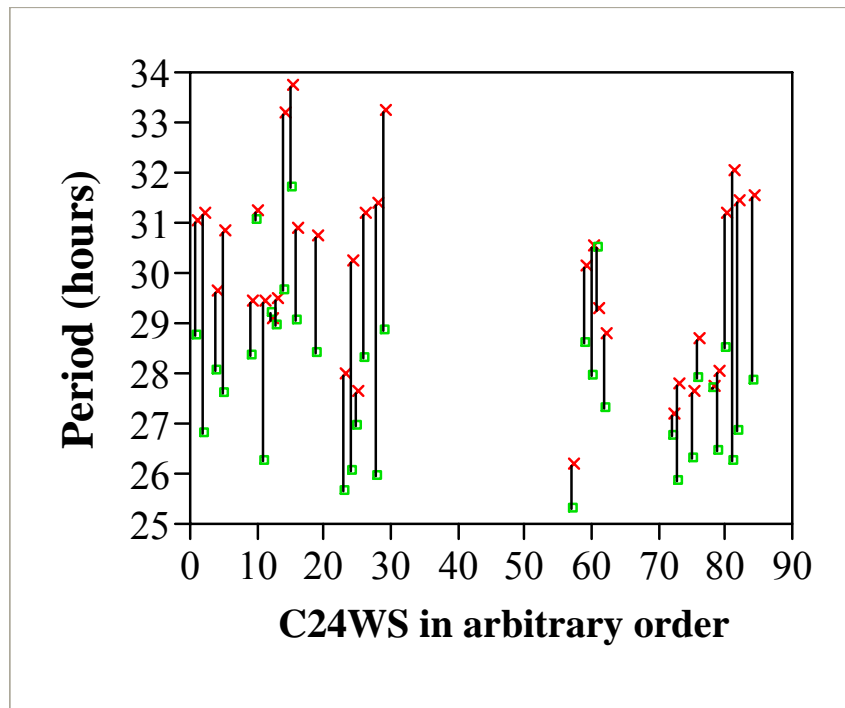


Figure 4.18 Period differences of rhythmic plants within genotypes of the C24WS RIL collection of temperature-entrained versus light-dark entrained plants

X axis represents the C24WS RIL number, and Y axis represents period. \square represents the period of temperature entrained plants, \times represents the period of the light-dark entrained plants.

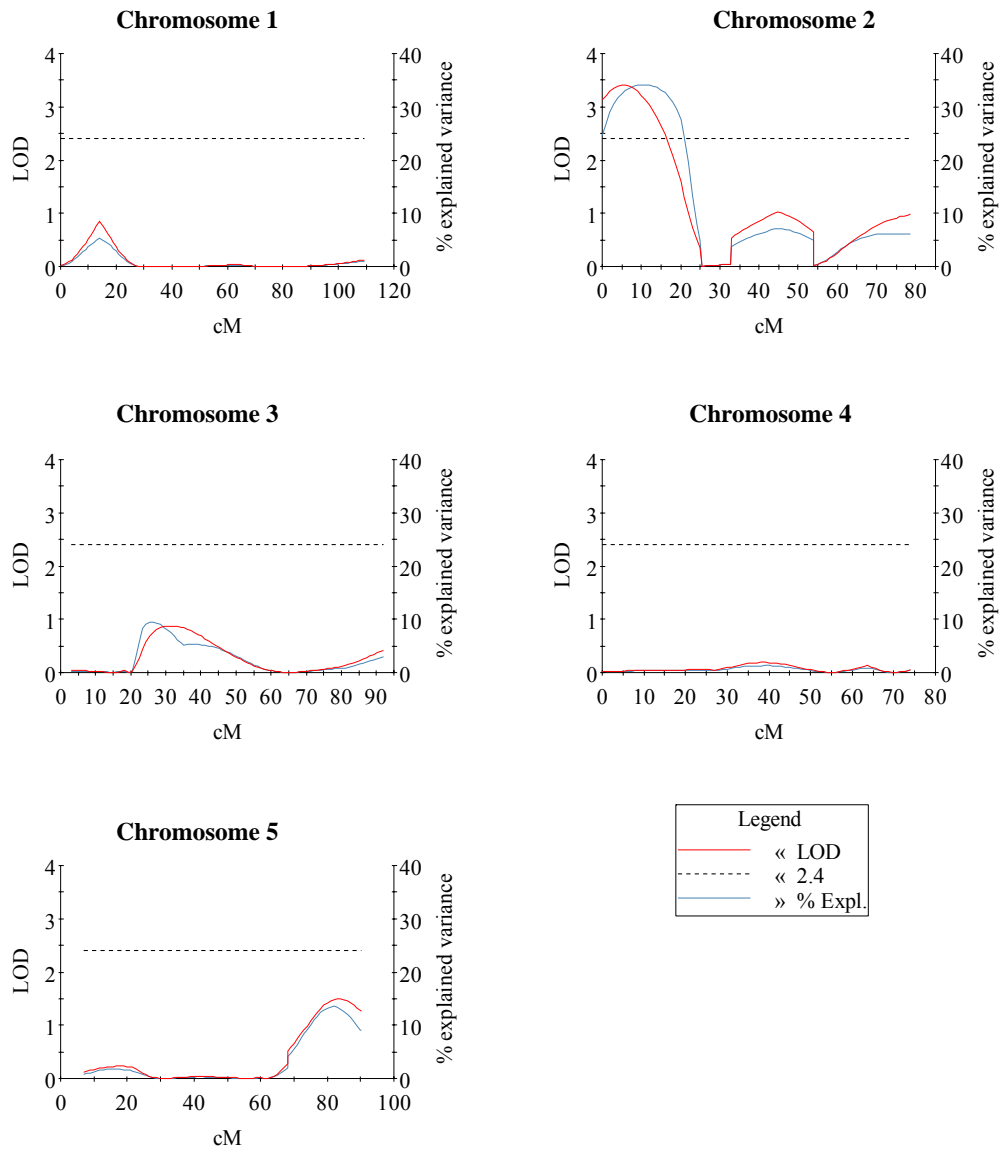


Figure 4.19 MapQTL for the light-dark entrainment of the C24WS population

X axis represents the chromosome location, measured in cM, left Y axis represents the LOD score, and right Y axis represents the % of explained variance. This percentage is a measure of the effect of the QTL that supplies to the phenotype. The dotted line represents the LOD score threshold. It was set to 2.4 after calculation of 1000 permutations, for 95% significance level.

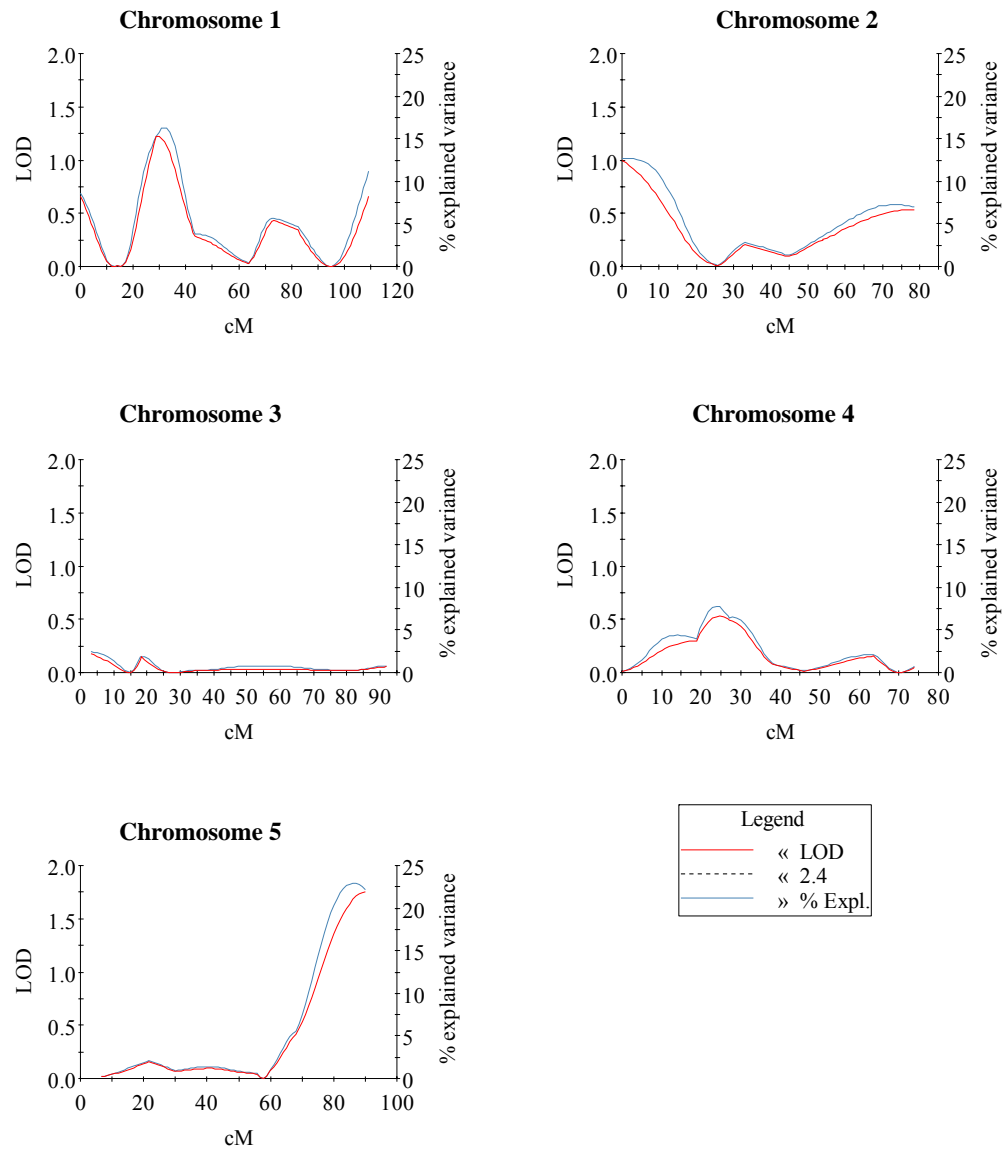


Figure 4.20 MapQTL for the temperature entrainment of the C24WS population

X axis represents the chromosome location, measured in cM, left Y axis represents the LOD score, and right Y axis represents the % of explained variance. This percentage is a measure of the effect of the QTL that supplies to the phenotype. The dotted line represents the LOD score threshold. It was set to 2.4 after calculation of 1000 permutations, for 95% significance level.

4.4 Conclusions-Remarks

In this chapter, the generation of six new RILs that were selected for short and long period of *CCR2* after light-dark entrainment was preliminary described. One of the RILs was genotyped using 34 SSLPs and microsatellites markers. Phenotypic assessment of this RIL population for flowering time and period control of *CCR2* after light-dark and temperature entrainment was also described. Eighty five lines from this single RIL set were assayed for flowering time under inductive long days. TLN was used to map QTL. Three main QTLs were found from these flowering-time assays. Variation at the marker loci FRI, NGA106, and NGA59, and their interaction were described as being the basis of the flowering-time variation of this RIL population. Additionally, 34 lines were assayed for circadian period of *CCR2* after light-dark and temperature entrainment. QTL mapping performed for these 34 genotypes from this RIL population resulted in one main QTL for the light-dark entrainment, whereas no QTL was detected for the temperature entrainment. The period data are preliminary, and more QTL are expected after the complete collection should be assayed. The LOD score for the QTL mapping of these 34 lines was approximately the same for all chromosomes, whereas the LOD score for the total 85 lines is distorted for chromosomes 1, 3 and 5. It is noted that the LOD score as calculated for the QTL mapping of flowering time of the same 34 lines that were used for the period QTL mapping resulted in almost equal LOD score across all chromosomes (data not shown). This suggests that some of the remaining 50 lines were responsible for the distortion of the LOD score. The LOD score distortion could be connected to the underlying segregation distortion in the RILS, due to the phenotypic selection that was performed during the generation of the RILS. Thus far, for the three traits no common QTL was identified.

5 PHYSIOLOGICAL ANALYSIS OF VARIOUS CLOCK MARKERS

INTRODUCTION

Our understanding of the *A. thaliana* circadian clockwork is based on data of light-dark entrained plants (Locke et al., 2006; Zeilinger et al., 2006; Ding et al., 2007b). The physiological existence of a second oscillator was revealed. Here, Salome *et al.* analyzed the resetting effect of temperature pulses on *TOC1* expression, and on two output genes of the clock. Temperature pulses caused the same phase advances and delays on *TOC1* and on *CAB2*, but were different in consequence to *CAT3* phase. Therefore, the presence of a second oscillator that responds preferentially to temperature was suggested (Michael et al., 2003a). Interestingly, these authors also suggested that *TOC1* is part of the light-dark entrained oscillator. Up to now, the genetic architecture of the temperature-entrained oscillator has not yet to be resolved.

Ding *et al.*, have reported that the *cca1 lhy toc1* triple mutant shows residual rhythmicity for a cycle after temperature entrainment, suggesting that these core-oscillator genes are part of the temperature-entrained clockwork. These cannot be the only components of the temperature-entrained oscillator given the partial rhythmic behavior of this triple mutant (Ding, 2007). Additionally, absence of both *PRR7* and *PRR9*, members of the TOC1 family, exhibits an arrhythmic phenotype after temperature entrainment, suggesting that these two genes are either part of the temperature-entrainment pathway, or part of the temperature-entrained oscillator (Salome and McClung, 2005). To conclude, performed assays in temperature entrainment have revealed that at least two genes *PRR7* and *PRR9* are essential for the oscillator function. Since these two genes are functional in the *cca1 lhy toc1* triple mutant, their presence could explain the residual rhythmicity of the triple mutant. A detailed physiological characterization of the oscillator is required for any further genetic conclusions to be drawn.

In this chapter, various physiological experiments using temperature-entrainment protocols will be described and these will be contrasted to that of light-dark entrainment. For these experiments, I used transformed WS plants with various clock-transcriptional-luciferase-reporters, including *CAB2*, *CCA1*, *LHY*, *TOC1*, *GI*,

CCR2, *ELF3*, and *ELF4*. The three genes, *LHY*, *GI*, and *TOC1* were selected, because they were candidate genes from the QTL mapping of the CvL RIL after light-dark or temperature entrainment (see 3.1.3). *CAB2* and *CCR2* were selected as they are two outputs of the clock that can be monitored to provide useful conclusions about the oscillator. Especially, *CCR2* was of interest because its transcriptional kinetics were studied for the natural-variation project (see following subchapters). *CCA1*, *ELF3*, and *ELF4* were selected as they are major clock genes with diverse functions within the oscillator mechanism. All these transgenic plants were synchronized to four different entrainment protocols (see 2.2.7). Additionally, the same reporter constructs were synchronized under light-dark and temperature T-cycles. T cycles are cycles with length other than 24 hours, such as daily cycles of 20 or 28 hours length. In this way, I could determine whether rhythmicity at the transcriptional level was driven by photo-signaling events or entrained by the clock. To further define the role of *TOC1* and *GI* under light, versus temperature entrainment, *CCR2::LUC* molecular kinetics were assayed in the several conditions in the loss of function mutants *gi-11*, *toc1-4*, and the double mutant *gi-11 toc1-4*. These collective experiments provided a first glimpse at the differential effects of environmental entrainment.

5.1 Light vs. temperature entrainment of various clock markers

To define the differences of light versus temperature entrainment, and thereby characterize the effect of temperature entrainment on the oscillator, I synchronized transgenic plants bearing promoter luciferase constructs of various circadian clock genes to either light dark or temperature cycles of 24 hours and measured luminescent rhythmicity. My interest was to find both whether and how photoperiod length or thermo period length impact on the oscillator, as defined by the circadian parameters. For this, I entrained plants to equal and unequal portions of light-versus-darkness or warm-versus-cool. Specifically, plants were entrained under light-dark cycles of 14 hours light::10 hours darkness or 10 hours light::14 hours darkness, and separately in temperature cycles of 14 hours warm::10 hours cool or 10 hours warm::14 hours cool. Here, the effect of light or warm duration will be described with the comparison of two genes, *GI* and *CCR2*. These genes have the same phase profile, as determined by the first peak of the free run, under a wide range of conditions.

The first peak in free-run conditions reflects the phase status of the oscillator dependent on the entrainment conditions. *GI* responds differentially to entrainment of 14 hours light/warm::10 hours darkness/cool cycles compared to 10 hours light/warm::14 hours darkness/cool cycles. In light-dark cycles, the first peak of *GI::LUC* was relative to the dusk signal (Figure 5.1). This suggests that *GI* measures photoperiod length and sets its phase accordingly. However, after temperature cycles, *GI* was expressed in the same phase irrespective of the preceding cool signal duration (Figure 5.1). Therefore, the peak of *GI* expression did not measure thermoperiod length. The second peak of *GI::LUC* clearly showed a stable phase difference between short light/warm duration compared to long light/warm duration (Figure 5.1). This suggested that photoperiod or thermoperiod length might affect periodicity. This was extensively explored in Chapter 3. The overall rhythmicity of *GI::LUC* over time suggested that its period is shorter after the temperature entrainment, as compared to after the light-dark entrainment. In contrast to *GI*, *CCR2* had the same first-peak profile after all four entrainment conditions, which is in agreement with the notion that is output of the core oscillator (Figure 5.2).

The dusk-expressed gene *TOC1* was found to have a completely different profile than the dusk expressed *GI*. The first peak of *TOC1* occurred at the same time after light-dark entrainment irrespective of the light duration. The same stood after temperature entrainment (Figure 5.3). So, it is clear that the length of the entrainment cues, either light or temperature, did not have an effect on this first *TOC1* parameter. Strikingly, the two entrainment cues affected differentially other circadian parameters of *TOC1*. Irrespective to daylength, temperature entrainment caused a later phase and shorter period of *TOC1*, compared to light-dark entrainment (Figure 5.3). The shorter-period phenotype after temperature entrainment compared to after light-dark entrainment was a key finding described in 3.1.2 and 3.2.2. All these collective findings lead me to suggest that *TOC1* mediates information of differing entraining cues. *TOC1* expression after temperature entrainment was more robust compared to after light-dark entrainment. From the profiles, one could assume that dawn sets the clock, perhaps through *GI*, and temperature fine tunes the circadian system through *TOC1* (Figure 5.1 and 5.3).

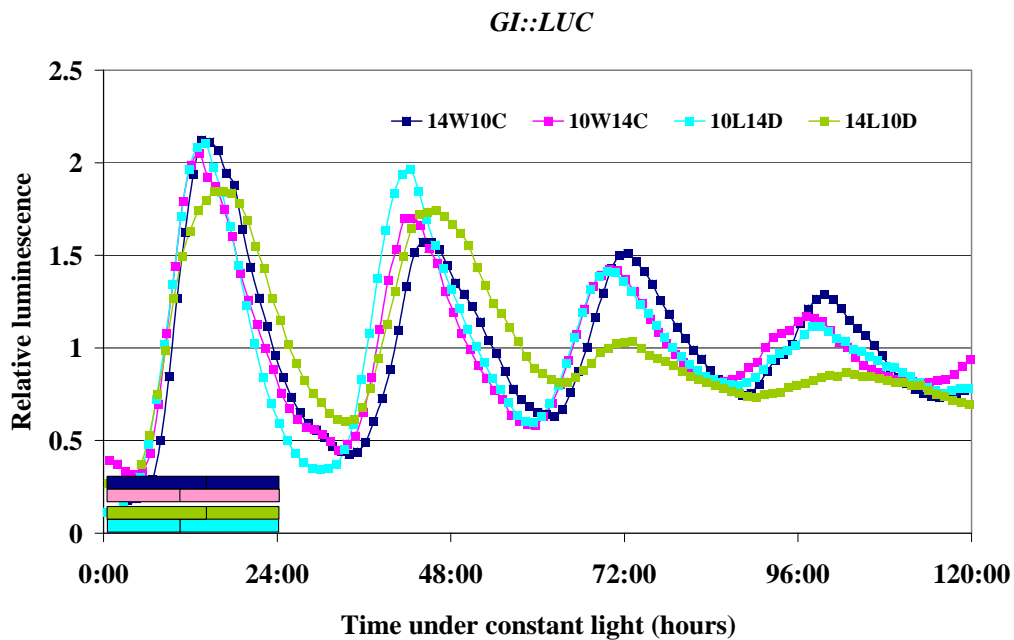


Figure 5.1 *GI::LUC* rhythms after light-dark entrainment to 14 hours light::10 hours darkness, 10 hours light::14 hours darkness, and temperature entrainment to 14 hours warm::10 hours cool, 10 hours warm::14 hours cool.

Relative luminescence is the ratio of luminescence measured at one time point divided by the average luminescence over the time course of the experiment. The solid colored bars represent light or warm temperature period and the shaded colored bars represent dark and cool temperature period. Blue bar represents 14 hours light::10 hours darkness, pink bar represents 10 hours light::14 hours darkness, yellow bars represent temperature entrainment to 14 hours warm::10 hours cool, and light blue bar 10 hours warm::14 hours cool. Note that the four hour phase shift of *GI* expression after the light-dark entrainment is dependent on the preceding photoperiod.

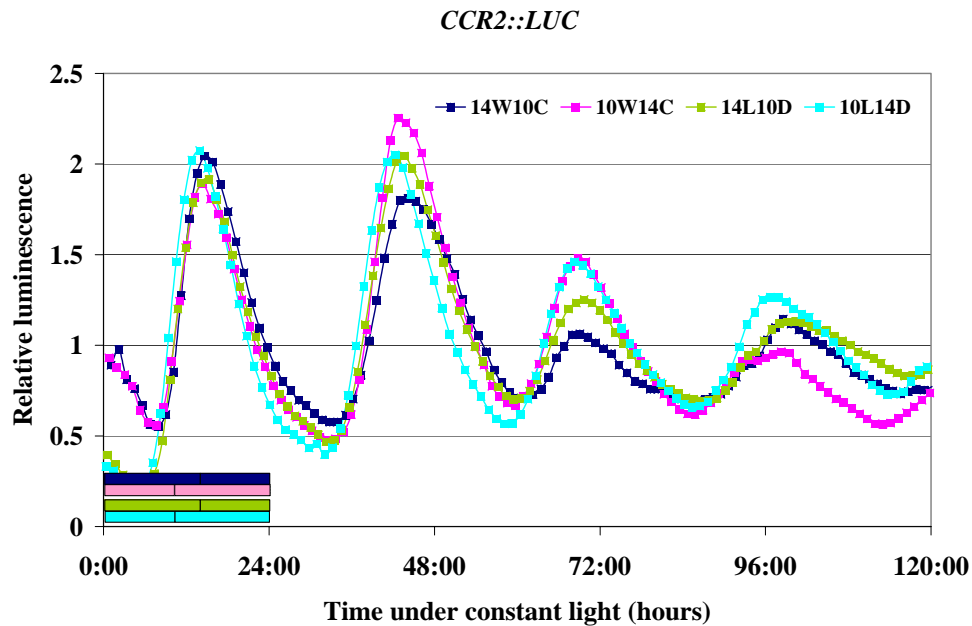


Figure 5.2 *CCR2::LUC* rhythms after light-dark entrainment to 14 hours light::10 hours darkness, 10 hours light::14 hours darkness, and temperature entrainment to 14 hours warm::10 hours cool, 10 hours warm::14 hours cool.

Relative luminescence is the ratio of luminescence measured at one time point divided by the average luminescence over the time course of the experiment. The solid colored bars represent light or warm temperature period and the shaded colored bars represent dark and cool temperature period. Blue bar represents 14 hours light::10 hours darkness, pink bar represents 10 hours light::14 hours darkness, yellow bars represent temperature entrainment to 14 hours warm::10 hours cool, and light blue bar 10 hours warm::14 hours cool.

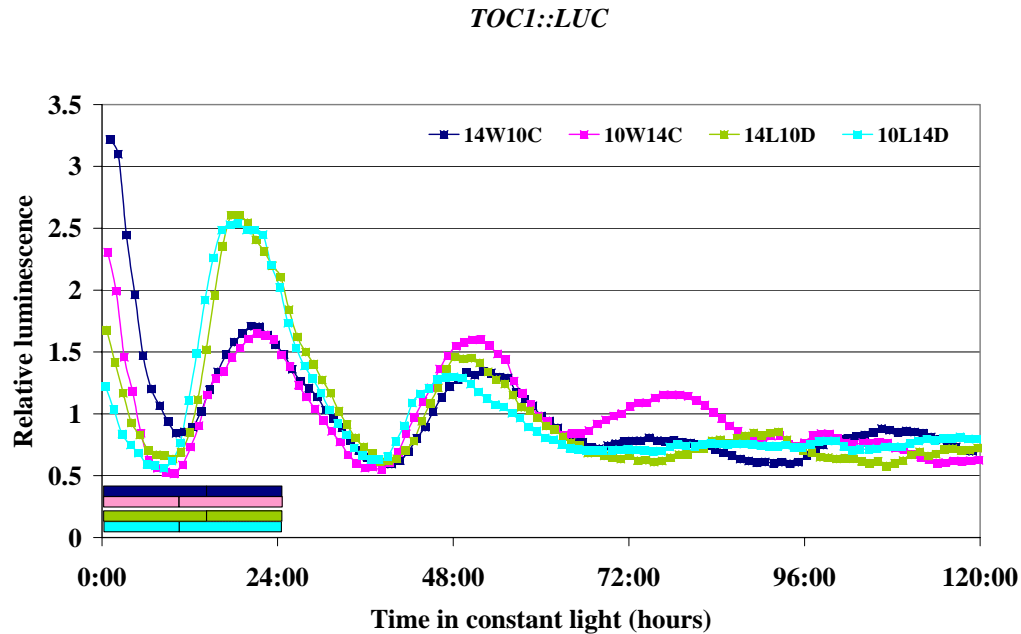


Figure 5.3 *TOC1::LUC* rhythms after light-dark entrainment to 14 hours light::10 hours darkness, 10 hours light::14 hours darkness, and temperature entrainment to 14 hours warm::10 hours cool, 10 hours warm::14 hours cool.

Relative luminescence is the ratio of luminescence measured at one time point divided by the average luminescence over the time course of the experiment. The solid colored bars represent light or warm temperature period and the shaded colored bars represent dark and cool temperature period. Blue bar represents 14 hours light::10 hours darkness, pink bar represents 10 hours light::14 hours darkness, yellow bars represent temperature entrainment to 14 hours warm::10 hours cool, and light blue bar 10 hours warm::14 hours cool.

5.2 IN-OUT of phase experiments of various clock reporter genes

In nature, light and temperature parallel their changes roughly at the same daily time over the time course of a day-night cycle of one day. Therefore, I was interested to dissect the effect of these synchronous changes on the entrainment of the oscillator. To interrogate these conditions, plants bearing the luciferase constructs were entrained in 12 hours light::12 hours darkness and in temperature cycles of 12 hours at 22°C and 12 hours at 12°C, with 6 hours shift between the two entrainment protocols, where temperature cycles are either IN-phase, if cold to warm transition coincides with light, or OUT-of-phase, if this transition coincides with darkness. The basic idea of using these conditions was to map whether some clock genes show preferential response to either of these two entrainments, and if possible, to make hypothesis about the underlying oscillator state in response to these physiological perturbations.

The time of the transfer from entraining to free run conditions could potentially have an effect on the phase. The transfer time can be different for the tested entrainment protocols. For example, when plants were entrained only to a single entrainment protocol, such as only light-dark or only temperature cycles, then they were transferred to free-run conditions just before onset of lights or warm temperature. But when plants were grown to the IN-OUT of phase protocol, then there were several options as to when to transfer to the free-run conditions, *e.g.* before the onset of lights or before the onset of warm/cold temperatures during the day period of the light-dark entrainment. Interestingly, the choice of different times of free run for the IN-OUT of phase plants resulted in different phase responses (Figure 5.4). When plants were transferred to free run just before the dark-to-light transition, for all three entrainment protocols, the circadian pattern of all clock genes tested, which were *CCA1*, *LHY*, *CCR2*, *GI*, *ELF3*, and *ELF4*, was the same, as shown in Figure 5.4 for the *CCA1* (for the others, data not shown). For all tested transcriptional reporters, the light-dark entrained plants, and the IN phase plants have the same phase, as indicated by the first peak. However, the OUT of phase plants displayed advancement in phase of six hours (Figure 5.4). This suggested that when in the presence of light, temperature is gated by the clock, but warm temperatures in darkness resulted in strong effect on the expression of several clock genes, and thereby the oscillator.

However, when plants were transferred to the free-run conditions just before the temperature transition, in the middle of the light period, then the IN phase plants showed a delay in phase of six hours compared to the light-dark entrained plants (Figure 5.4). This suggested a memory effect of the preceding entrainment that can be called anticipation.

The transcriptional profile of *TOCI* was different than *CCA1*. Interestingly, when *TOCI::LUC* bearing plants were transferred to the free-running conditions, just before the dark to light transition, while grown in the IN entrainment protocol, a phase delay of 6 hours was observed (Figure 5.5). The IN phase plants, at that time point, were in the middle of the cold part of the cycle, and they experienced a change of 10°C. The phase shift in *TOCI* expression caused by the 10°C difference in temperature suggested that *TOCI* transcription was preferential to temperature than to light entrainment. The opposite preference to entrainment was observed in *CCA1*, *LHY*, and *GI*. These latter genes could be part of the light-dark entrained oscillator. Taken together, the results shown in Figures 5.3 and 5.5 revealed that *TOCI* not only entrains to temperature cycles, but is the physiological thermal target of the clock after the warm-cool entrainment.

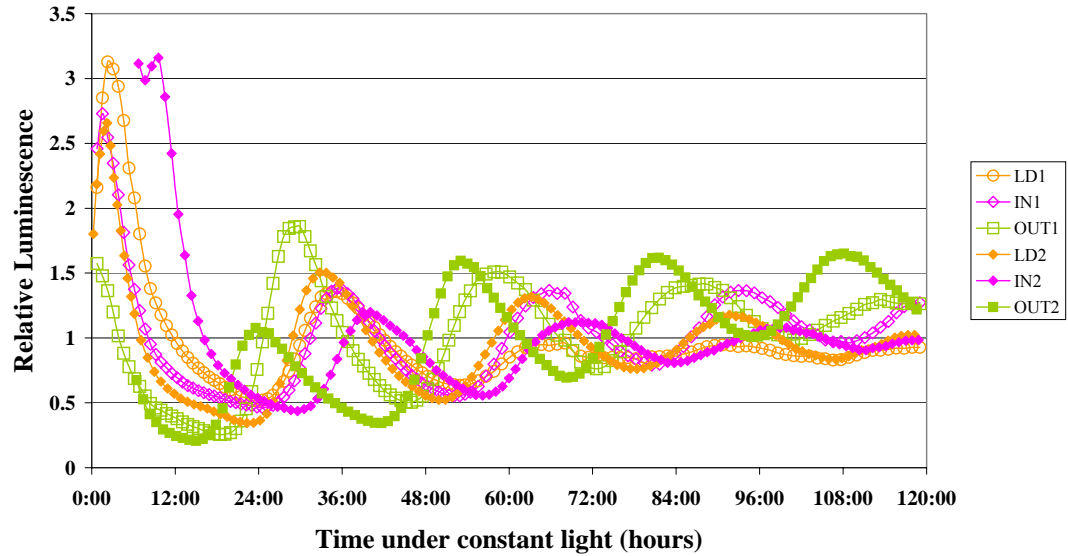
CCA1::LUC

Figure 5.4 *CCA1::LUC* rhythms after the light-dark entrainment (LD) and synchronous entrainment of light dark and temperature cycles, where IN denotes onset of warm temperatures in the middle of the light period and OUT the onset of cool temperatures in the middle of the light period.

1 and 2 denote two independent experiments starting just before lights on, or just before the different temperature transitions during the light period. Time 0 is the time when lights were turned on. Relative luminescence is the ratio of luminescence measured at one time point divided by the average luminescence over the time course of the experiment. Note that *CCA1* phase is shifted by 6 hours only during the OUT phase and not during IN phase (experiment 1), whereas a memory effect was indicated for *CCA1* (experiment 2).

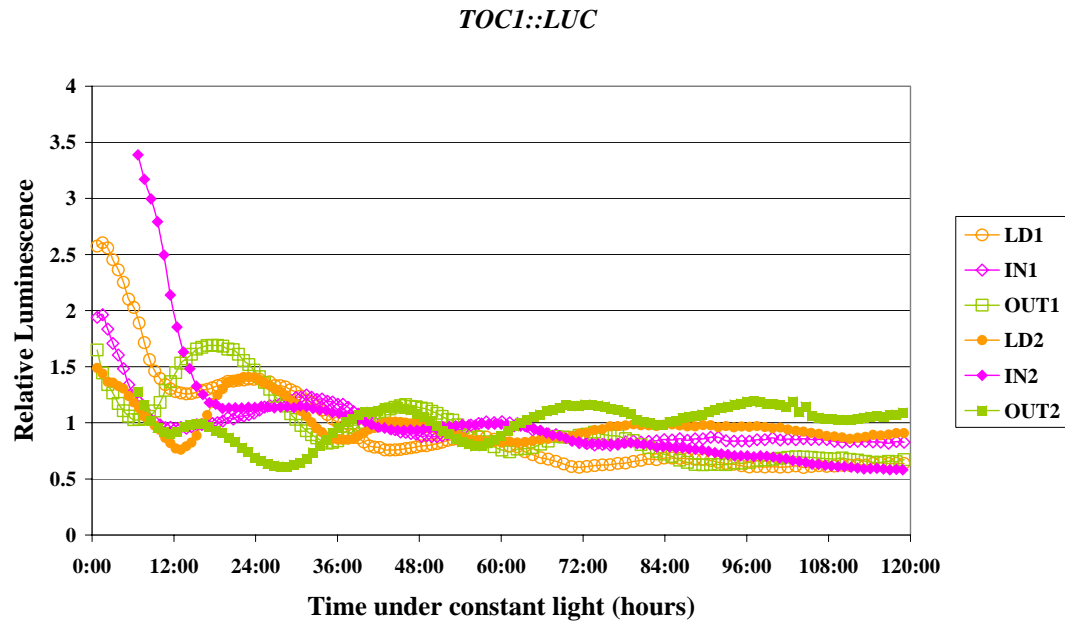


Figure 5.5 *TOC1::LUC* rhythms after the light-dark entrainment (LD) and synchronous entrainment of light-dark and temperature cycles, where IN denotes onset of warm temperatures in light period and OUT the onset of cool temperatures in light period.

1 and 2 denote two independent experiments. Time 0 is the time when lights turned on. Relative luminescence is the ratio of luminescence measured at one time point divided by the average luminescence over the time course of the experiment. Note that *TOC1* phase is the same after the IN and OUT for both experiments, irrespective of the time transfer to free-running conditions.

5.3 Light vs. temperature: driven or entrained rhythms

In the previous section, differential response to light compared with temperature cycles was described for a set of the clock-reporter genes. To determine whether light and/or temperature drove rhythmicity due to entrainment of the underlying circadian oscillator or through direct response to the environmental signal, transgenic plants bearing the promoter reporter were synchronized to non-24-hour-cycles, or else called T-cycles, of light-dark or warm to cool. The synchronizing conditions were 14 hours of light::14 hours of darkness, 10 hours of light::10 hours of darkness for the light-dark entrainment, in constant 22°C, and 14 hours of warm::14 hours of cool, 10 hours of warm::10 hours of cool, under constant light, for the temperature entrainment. I choose these conditions, because they could be compared in two different ways to the conditions used in Chapter 5.1. First, the conditions used in Chapter 5.1 were of 24-hour cycle length, which was an intermediate length compared to 20 hours or 28 hours used for the T-cycle. Second, the first peak of luciferase expression reported for various circadian promoters could be compared to the amount of time of light/dark or warm/cool in the conditions of Chapter 5.1.

In the IN-OUT experiments, it was found that from all circadian promoters tested that *TOC1* was the only clock gene whose expression was shifted, by six hours, when ambient temperature was changed by 10 degrees; this was just before lights on (Figure 5.5). Furthermore, the period of *TOC1* after temperature entrainment was found to be shorter compared to the period after light-dark entrainment, whereas, the phase of *TOC1*, as determined by the first peak, was later after temperature entrainment, compared to after light-dark entrainment (Figure 5.3). The above cannot discriminate whether *TOC1* expression was driven or entrained by temperature cycles. To address this, I entrained the plants to non circadian cycles, as such of 20 or 28 hours length and then bioluminescence was measured in constant light free-running conditions. After the 14 hours light::14 hours darkness, *TOC1* phase peaked at the light to dark transition, whereas in the 10 hours light::10 hours darkness, *TOC1* phase peaked at the end of dark period (Figure 5.6). The first peak after entrainment to 20 hours cycle was identical to that of 10 hours light::14 hours darkness (Figure 5.3). This probably suggests that light period determined *TOC1* expression under 24 or 20 hour cycles. The subsequent peaks after the 28-hour cycle were observed in the dark

period of the cycle, with peak phase being shifted. This is characteristic of entrained rhythms. So, *TOC1* differentially entrained to T-cycles of various lengths of light-dark cycles. After temperature cycles of 20-hour cycle, peak expression of *TOC1* was displayed at the end of the subjective cool period. An acute peak was observed just after the transfer from entrainment to free-run conditions, as a response to temperature change from 12°C to 22°C (Figure 5.6). The same acute peak was observed after the transfer from 28 hours temperature cycle to free-run conditions. In the latter case, *TOC1* was not rhythmic over the first 28 hours (Figure 5.6). This arrhythmicity was because there was no oscillation in luminescence, and not because of variations. Normal rhythmicity was restored after these 28 hours (Figure 5.6). All data suggested that *TOC1* expression was driven by the 28-hour cycle, but entrained by the 20-hour cycle, irrespective of the environmental signal. In previous studies, mutant alleles of *toc1* displayed short-period phenotypes in free run constant-light conditions. There is probably an adaptive significance to the response of *TOC1* that was entrained by light-dark and temperature cycles up to 24 hours, and not in 28-hour cycles. However, to obtain any concrete conclusions, future experiments with entrain plants to intermediate T-cycles would be required. To date, this has not been done.

CCR2 entrained to both in light-dark and temperature T-cycles. The peak expression of *CCR2* was during day for the 28 hours of T-cycles after light dark and temperature entrainment, whereas in short T-cycles of both protocols, *CCR2* was expressed in the early evening, as it was found for the circadian protocols (Figure 5.7). The difference between the peaks after temperature entrainment or light-dark entrainment equals four hours, which was as much a difference as in the light/warm period length (Figure 5.7). A different pattern was observed for the subsequent peaks. After the temperature entrainment, all *CCR2* peaks coincided, whereas after the light-dark entrainment, there was a stable phase shift (Figure 5.7). In the long T-cycles, the expression of *CCR2* was always preceded lights-off, whereas in short days the peak expression always was after the onset of darkness. This suggested that under the long cycles, in light-dark, entrainment *CCR2* expression was driven, because all peaks of *CCR2* expression falls onto the end of the light period. The subsequent peaks after temperature entrainment coincide, suggesting that *CCR2* was entrained by temperature.

GI displayed the same expression pattern as did the *CCR2*, concerning the first peak after the four protocols. In long T-cycles, *GI* peaked its expression during day

time, whereas in short T-cycles it was expressed in the early evening (Figure 5.8). The difference between the two peaks was 4 hours, as much as the difference of the light period of the short and long T-cycles (Figure 5.8). The subsequent peaks of *GI* after temperature cycles coincided, with the peaks after long T-cycles observed from warm to cool transition, while after short cycles the peak expression was observed in does not. This suggested that temperature drove the expression of *GI* after 28 hours cycle. In contrast, light dark entrained *GI* expression after 28-hour cycle.

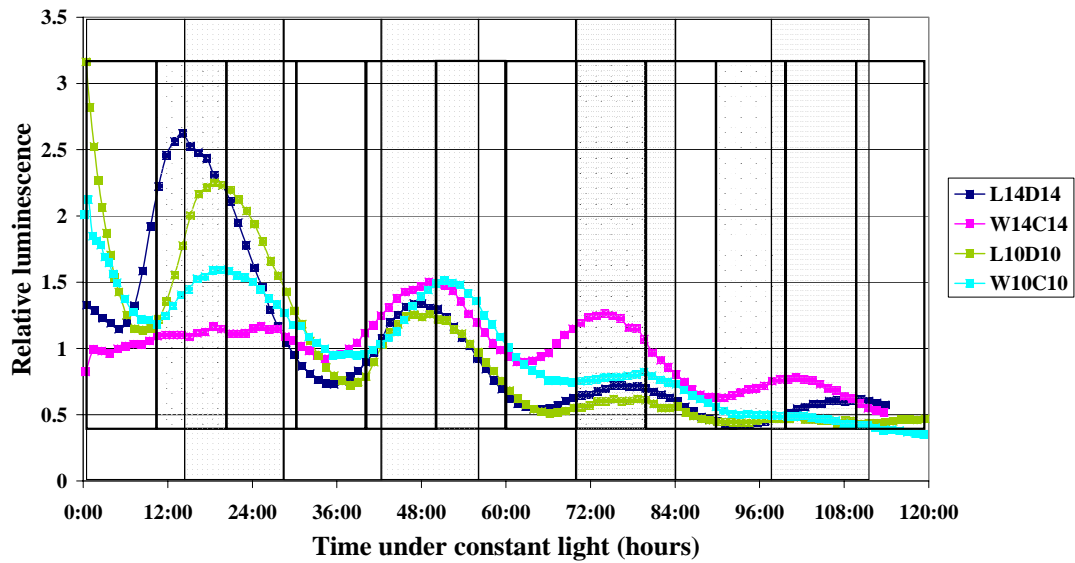
TOC1::LUC

Figure 5.6 *TOC1::LUC* rhythms after entrainment in T-cycles of 14 hours of light::14 hours of darkness, 10 hours of light::10 hours of darkness for the light-dark entrainment, and 14 hours of warm::14 hours of cool, 10 hours of warm::10 hours of cool for the temperature entrainment.

White-long boxes represent 14 hours of light or warm temperatures, and grey-shaded-long boxes represent 14 hours of darkness or cool temperatures. White-short boxes represent 10 hours of light or warm temperatures, and white-short-dotted boxes represent 10 hours of darkness or cool temperatures. In the legend, L stands for light, D stands for darkness, W stands for warm temperatures, C for cool temperatures. Numbers next to the letters stand for hours.

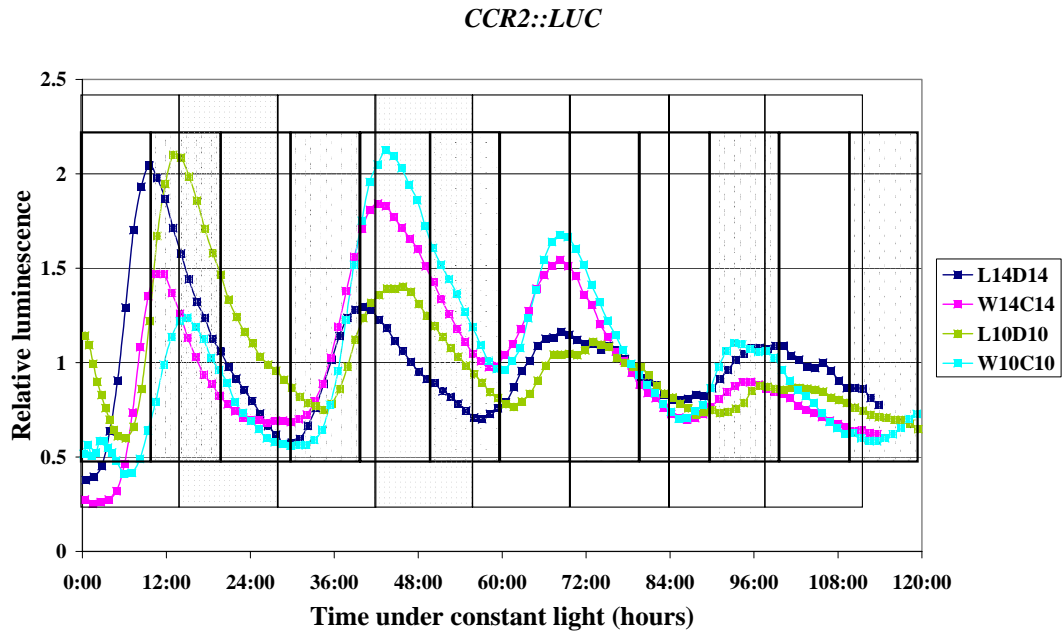


Figure 5.7 *CCR2::LUC* rhythms after entrainment in T-cycles of 14 hours of light::14 hours of darkness, 10 hours of light::10 hours of darkness for the light-dark entrainment, and 14 hours of warm::14 hours of cool, 10 hours of warm::10 hours of cool for the temperature entrainment.

White-long boxes represent 14 hours of light or warm temperatures, and grey-shaded-long boxes represent 14 hours of darkness or cool temperatures. White-short boxes represent 10 hours of light or warm temperatures, and white-short-dotted boxes represent 10 hours of darkness or cool temperatures. In the legend, L stands for light, D stands for darkness, W stands for warm temperatures, C for cool temperatures. Numbers next to the letters stand for hours.

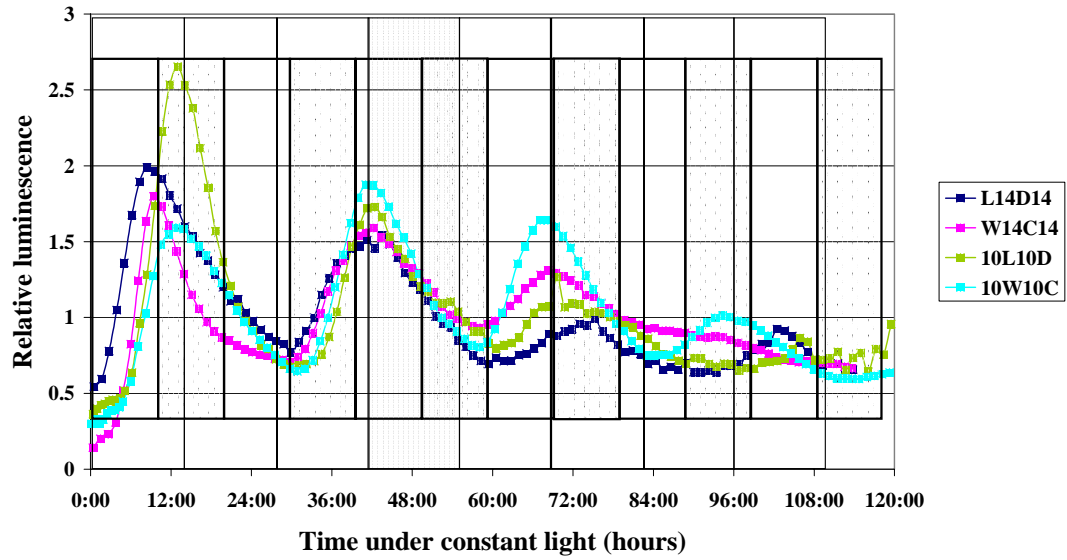
GI::LUC

Figure 5.8 *GI::LUC* rhythms after entrainment in T-cycles of 14 hours of light::14 hours of darkness, 10 hours of light::10 hours of darkness for the light-dark entrainment, and 14 hours of warm::14 hours of cool, 10 hours of warm::10 hours of cool for the temperature entrainment.

White-long boxes represent 14 hours of light or warm temperatures, and grey-shaded-long boxes represent 14 hours of darkness or cool temperatures. White-short boxes represent 10 hours of light or warm temperatures, and white-short-dotted boxes represent 10 hours of darkness or cool temperatures. In the legend, L stands for light, D stands for darkness, W stands for warm temperatures, C for cool temperatures. Numbers next to the letters stand for hours.

5.4 Study of *GI* and *TOC1* under light and temperature entrainment

To study the genetic requirements of *TOC1* and *GI* in environmental entrainment differences, the mutant alleles of *gi-11* and of *toc1-21* in WS background, bearing the *CCR2::LUC* reporter, were used in circadian experiments after light-dark and after temperature entrainment. The single mutants were crossed to each other resulted the double mutant *gi-11 toc1-21* was compared to circadian assays to find possible genetic relationships of these to evening genes. *CCR2::LUC* expression in these backgrounds was assayed in 24-hour cycles that were divided in 14h or 10 hours light/warm and 10h or 14h dark/cool, respectively. *CCR2::LUC* was selected as reporter, because *CCR2* was not environmentally responsive under these conditions, as described in Figure 5.2. The length of the light or warm period did not phase shift the *CCR2* expression (Figure 5.2). Therefore, the expression of the reporter marker would be due to the genetic effect of the mutations.

The genetic requirement of *GI* was tested in different photo-and thermo-period lengths as performed previously in Chapter 3.1, by assaying *CCR2* rhythmicity. The *CCR2::LUC* phase in the *gi-11* mutant was the same as the wild type, with concern to the response to the length of the warm to cool (Figures 5.2 and 5.9). Therefore, it can be concluded that *GI* did not play a role to detect the different warm/cool length, confirming the *GI::LUC* data described before (Figure 5.1). However, after light-dark entrainment, the *CCR2* phase in the *gi-11* mutant was delayed compared to *CCR2* in the wild-type background (Figures 5.2 and 5.9). Additionally, the phase of *CCR2* in *gi-11* was differential for the different photoperiod length (Figure 5.9). This suggested that *GI* was important for light-dark entrainment, and it was involved in day-length measurement.

Similarly to *GI*, the genetic requirement of *TOC1* was tested under different photoperiod and thermoperiod lengths by monitoring *CCR2* expression. In the *toc1-21* allele, *CCR2::LUC* displayed an early phase and a short period, compared to the wild type (Figure 5.2 and 5.10). This was the case after either temperature or light-dark entrainment (Figure 5.10). Therefore, *TOC1* was required for proper expression of *CCR2* after both light-dark and temperature entrainment. As far as the length of the warm-to-cool and light-to-dark, there was no difference between the *toc1-21* and the

wild type. This suggests that *TOC1* did not respond to day-length or thermo-length measurement, which supports the findings of *TOC1::LUC* under the same conditions (Figures 5.3 and 5.10).

To determine whether there is a genetic interaction between *TOC1* and *GI*, the luciferase expression driven by the *CCR2* promoter was measured in the double mutant *gi-11 toc1-21*, under the same conditions as that of the single mutants. *CCR2* in the double mutant exhibited the early-phase phenotype similar to the *toc1-21* mutant (Figure 5.10 and 5.11). Additionally, the double mutant displayed early phase of *CCR2* after temperature entrainment, compared to the light-dark entrainment (Figure 5.11). This effect was described in the *CCR2* transcriptional rhythms of the *gi-11* mutant (Figure 5.9). Moreover, the double mutant was less robust in its *CCR2* rhythm than either single mutant (Figures 5.9-5.11). After the light-dark entrainment, irrespective of the daylength, the double mutant was found to be rhythmic for one cycle and then gradually became arrhythmic to intermediate levels of *CCR2* expression (Figure 5.11). After temperature entrainment, *CCR2* expression levels went through a complete cycle, then there was a continuous, but gradual, expression increase for two cycles, and then a decrease for the next two cycles in a continuous gradual manner. In both cases, the phenotype was found to be more severe than that of either single mutant. By comparing the *CCR2* expression shown in Figures 5.9-5.11, the pattern of the double mutant after the light-dark and temperature was similar to that seen in *toc1-21*, as noted by the opposite triangle or by the star. There was no obvious circadian pattern of *CCR2* of the double mutant in response to day-or thermo-length. All the above suggested that there is a genetic interaction of *TOC1* and *GI* after temperature entrainment, since the phase of *CCR2* is earlier than any single mutant. Thus, both *GI* and *TOC1* participated in entrainment.

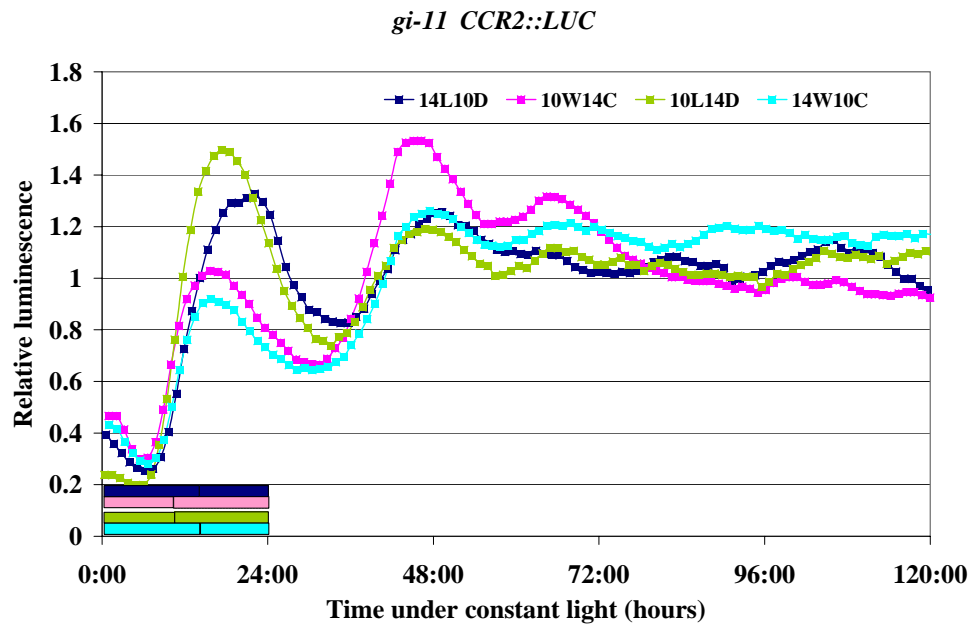


Figure 5.9 *CCR2::LUC* rhythms in the *gi-11* mutant after light-dark entrainment to 14 hours light::10 hours darkness, 10 hours light::14 hours darkness, and temperature entrainment to 14 hours warm::10 hours cool, 10 hours warm::14 hours cool

Relative luminescence is the ratio of luminescence measured at one time point divided by the average luminescence over the time course of the experiment. The solid colored bars represent light or warm temperature period and the shaded colored bars represent dark and cool temperature period. Blue bar represents 14 hours light::10 hours darkness, pink bar represents 10 hours light::14 hours darkness, yellow bars represent temperature entrainment to 14 hours warm::10 hours cool, and light blue bar 10 hours warm::14 hours cool.

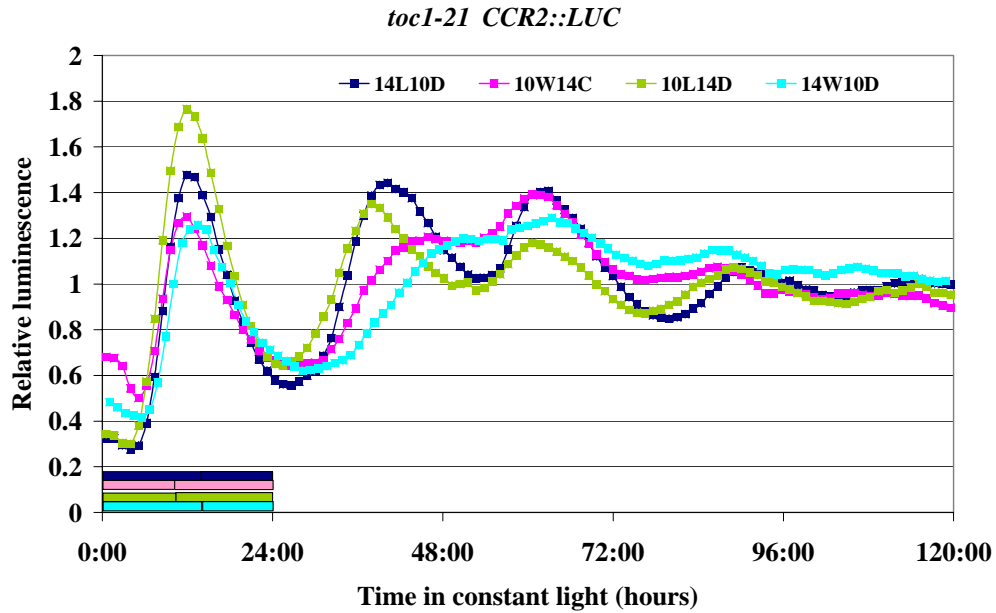


Figure 5.10 *CCR2::LUC* rhythms in the *toc1-21* mutant after light-dark entrainment to 14 hours light::10 hours darkness, 10 hours light::14 hours darkness, and temperature entrainment to 14 hours warm::10 hours cool, 10 hours warm::14 hours cool.

Relative luminescence is the ratio of luminescence measured at one time point divided by the average luminescence over the time course of the experiment. The solid colored bars represent light or warm temperature period and the shaded colored bars represent dark and cool temperature period. Blue bar represents 14 hours light::10 hours darkness, pink bar represents 10 hours light::14 hours darkness, yellow bars represent temperature entrainment to 14 hours warm::10 hours cool, and light blue bar 10 hours warm::14 hours cool.

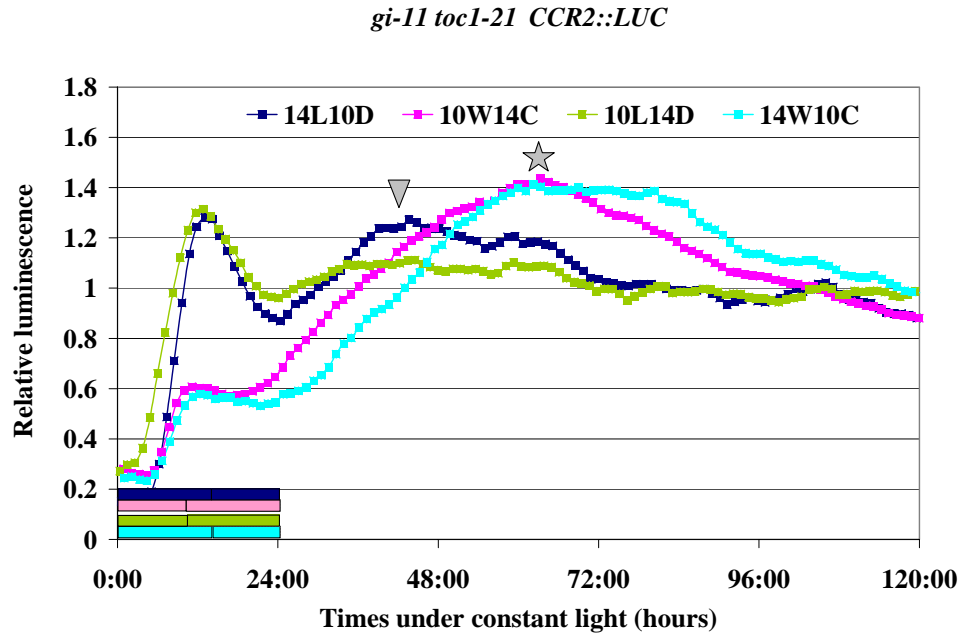


Figure 5.11 *CCR2::LUC* rhythms in the double mutant *gi-11 toc1-21* after light-dark entrainment to 14 hours light::10 hours darkness, 10 hours light::14 hours darkness, and temperature entrainment to 14 hours warm::10 hours cool, 10 hours warm::14 hours cool.

Relative luminescence is the ratio of luminescence measured at one time point divided by the average luminescence over the time course of the experiment. Star points the third peak of *CCR2* expression after temperature cycles, and opposite triangle points the second peak of *CCR2* expression after light-dark cycles.

5.5 Light vs. temperature: driven or entrained rhythms

To determine the genetic architecture of temperature entrainment and explore the role of *TOC1* and *GI* and their potential genetic interaction under temperature entrainment, the mutant alleles of *TOC1* and *GI* were synchronized in T-cycles of 14 hours light/warm::14 hours darkness/cool and 10 hours light/warm::10 hours darkness/cool. *CCR2* rhythmicity was used to marker the effect of the two gene mutations after the entrainment protocols.

In *gi-11*, *CCR2* expression after temperature entrainment of 20-hour cycles tended to be arrhythmic, in contrast to the *CCR2* expression after light-dark entrainment of 20-hours cycles, which was rhythmic with a short period (Figure 5.12). However, the phase of *CCR2* in *gi-11* after the 20 hour light dark cycle was delayed compared to the wild type, whereas after the 20 hour of temperature cycles was identical to the wild type (Figures 5.7 and 5.12). The phase of *CCR2* after 20-hour cycles was at the beginning of the dark/cool, whereas after the 28-hour cycles the phase was peaked at the end of the light/warm period (Figure 5.12). The phase of *CCR2* in the *gi-11* background was the same observed in the wild type after all entrainment protocols except for the 14 hours light::14 hours darkness, which was delayed by four hours (Figures 5.7 and 5.12). However, after the second cycle, *CCR2* expression was dampened (Figure 5.12). These results supported the notion that *GI* is part of light-dark entrainment.

In the *toc1-21* mutant, *CCR2* expression was different concerning the different cycle lengths, irrespective of the entraining signal (Figure 5.13). Furthermore, after both long cycles, *CCR2* expression peaked during day/warm part of the cycle, whereas after both short cycles, it peaked during the night/cool (Figure 5.13). The phase of *CCR2* in the *toc1-21* was the similar to the wild type for the short-cycle length protocols, whereas in the long cycles of both light-dark and temperature entrainment, the phase of *CCR2* in the *toc1-21* mutant was displayed earlier compared to the wild type of about 2 hours (Figures 5.7 and 5.13). Furthermore, under temperature entrainment in long cycle *CCR2* became arrhythmic (Figure 5.13). *toc1-21* displayed short period of *CCR2* under all protocols compared to the wild type (Figures 5.7 and 5.13). This differential response to temperature suggested that *TOC1* is involved in both light-dark and temperature entrainment.

In the *gi-11 toc1-21* double mutant, *CCR2* was severely affected towards arrhythmicity (Figure 5.14). Regarding the effect of the various T-cycles in the phase of *CCR2*, that was variable. After the 28-hour light-dark T-cycles, the first peak was intermediate of both *toc1-21* and *gi-11*, although it was similar to the wild type. This is because the phase of *CCR2* in *toc1-21* was advanced and the phase in *gi-11* was delayed compared to the wild type. After the long T-cycles the two genes displayed differential response to the different entraining signals. In the short light-dark cycles, the phase of *CCR2* in the double mutant was the same to the phase of *toc1-21*, however the subsequent response was arrhythmic as observed in *gi-11* and not short period as in *toc1-21*. In the 28 hour warm-cool cycle, *CCR2* phase and expression pattern over the five day experiment was similar to the response after the 10 hours warm::14 hours cool cycles (Figures 5.11 and 5.14). The two protocols have 14 hours of cool period, and this could be the reason why the same response is observed. All the data indicated that *GI* and *TOC1* interact despite their ability to detect various aspects of entrainment.

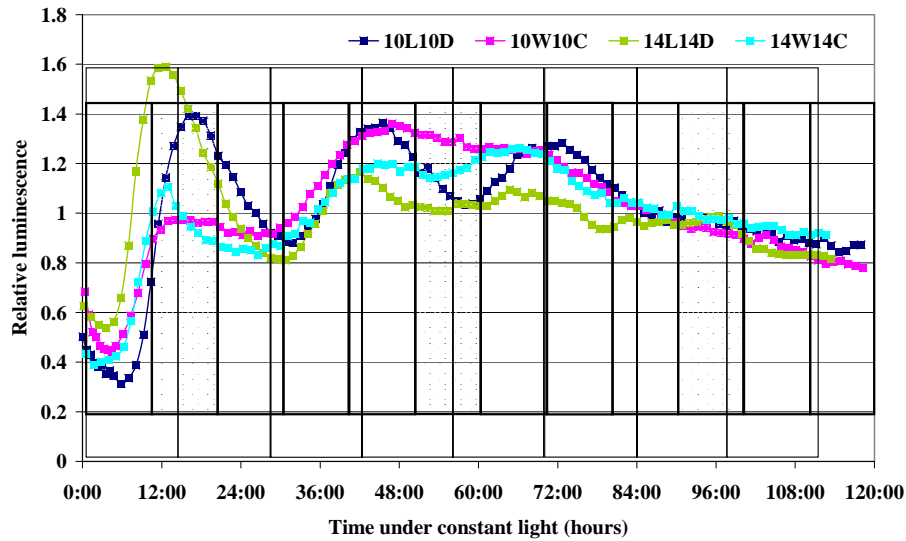
gi-11 CCR2::LUC

Figure 5.12 *CCR2::LUC* rhythms in *gi-11* after entrainment in T-cycles of 14 hours of light::14 hours of darkness, 10 hours of light::10 hours of darkness for the light-dark entrainment, and 14 hours of warm::14 hours of cool, 10 hours of warm::10 hours of cool for the temperature entrainment.

White-long boxes represent 14 hours of light or warm temperatures, and grey-shaded-long boxes represent 14 hours of darkness or cool temperatures. White-short boxes represent 10 hours of light or warm temperatures, and white-short-dotted boxes represent 10 hours of darkness or cool temperatures. In the legend, L stands for light, D stands for darkness, W stands for warm temperatures, C for cool temperatures. Numbers next to the letters stand for

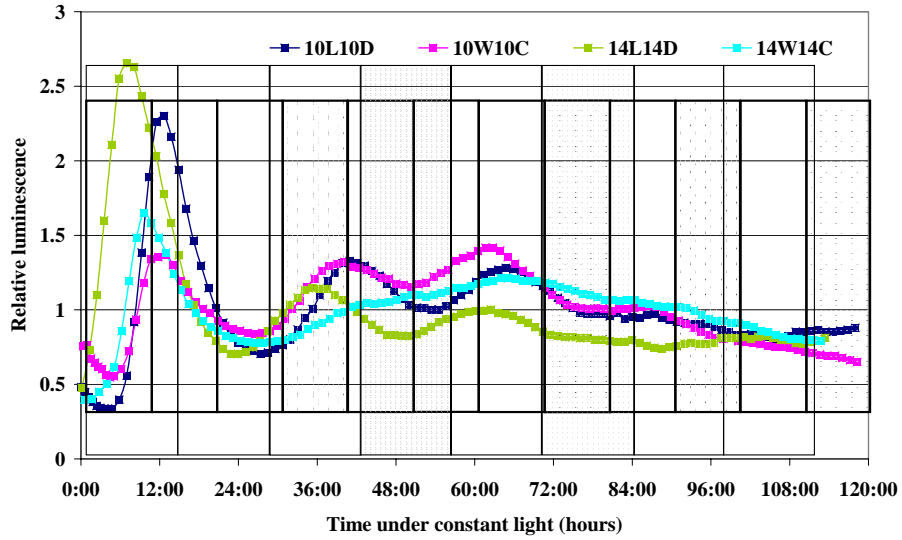
toc1-21 CCR2::LUC

Figure 5.13 *CCR2::LUC* rhythms in *toc1-21* after entrainment in T-cycles of 14 hours of light::14 hours of darkness, 10 hours of light::10 hours of darkness for the light-dark entrainment, and 14 hours of warm::14 hours of cool, 10 hours of warm::10 hours of cool for the temperature entrainment.

White-long boxes represent 14 hours of light or warm temperatures, and grey-shadowed-long boxes represent 14 hours of darkness or cool temperatures. White-short boxes represent 10 hours of light or warm temperatures, and white-short-dotted boxes represent 10 hours of darkness or cool temperatures. In the legend, L stands for light, D stands for darkness, W stands for warm temperatures, C for cool temperatures. Numbers next to the letters stand for hours.

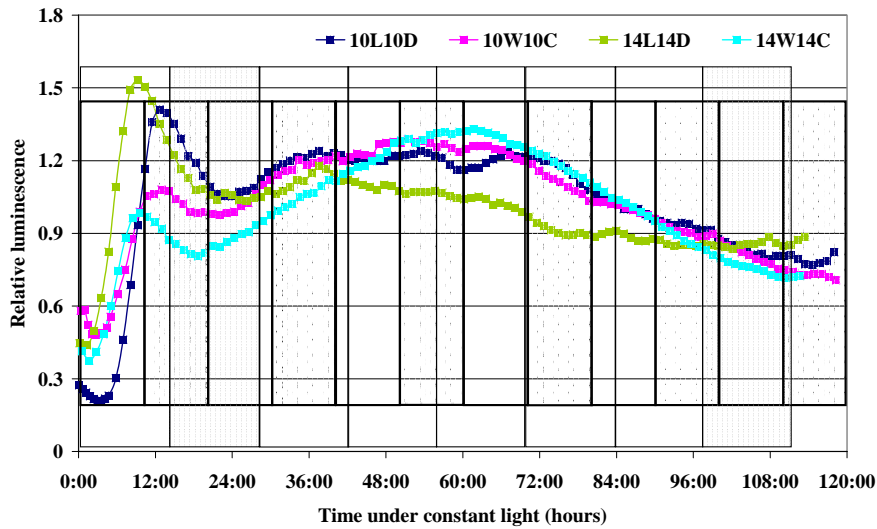
gi-11 toc1-21 CCR2::LUC

Figure 5.14 *CCR2::LUC* rhythms in *toc1-21* after entrainment in T-cycles of 14 hours of light::14 hours of darkness, 10 hours of light::10 hours of darkness for the light-dark entrainment, and 14 hours of warm::14 hours of cool, 10 hours of warm::10 hours of cool for the temperature entrainment.

White-long boxes represent 14 hours of light or warm temperatures, and grey-shadowed-long boxes represent 14 hours of darkness or cool temperatures. White-short boxes represent 10 hours of light or warm temperatures, and white-short-dotted boxes represent 10 hours of darkness or cool temperatures. In the legend, L stands for light, D stands for darkness, W stands for warm temperatures, C for cool temperatures. Numbers next to the letters stand for hours.

5.6 Conclusions-Remarks

The clock synchronizes to the ambient environment by detecting changes in entraining cues, such as light and temperature. The changes of those cues can be variable in duration, and in amplitude between the two states of the cues. My interest was to identify how the known circadian genes respond to such changes. For this, I assayed the transcriptional kinetics of various clock-regulated promoters by assaying luciferase-reporter expression. From these physiological experiments, the resultant conclusions are described below.

To test for photoperiod or thermo-period dependent responses, various clock-regulated reporters were entrained in temperature and light-dark cycles of 24 hours length. However, the length of light or warm was not equal to the length of dark or cool. From these results, it was concluded that *GI* can measure photoperiod length but not thermo-period length (Figure 5.1). However, by assaying phase of all circadian promoters, it was found that none of any of the tested markers, including neither *GI*, not *TOC1*, was able to track thermo-period length (data not shown, Figures 5.2 and 5.3). *GI* and *TOC1* therefore detect different aspects of the environment.

A differential response of various clock reporters to light versus temperature entrainment was found. During the light period of entrainment, temperature did not affect the phase of most tested reporters (Figure 5.4, data not shown). This suggests that temperature effects on entrainment were gated by light. When warm temperatures occurred in the middle of the dark period of the cycle, the phase of all reporter genes was shifted (Figure 5.4, data not shown). In the absence of light, temperature changes affected phase. In this case, the oscillations of all genes tested were more robust than that of the light-dark entrained plants. However, the only component of the known circadian oscillator that responds to temperature changes during the light period was *TOC1* (Figure 5.5). *TOC1* expression responded to temperature changes during the light and the dark period.

To determine whether the observed rhythms in the INOUT of phase experiments (see 2.2.7) was driven or due to entrainment, seedlings were synchronized to cycles of 20 or 28 hour length. *GI* and *CCR2* entrain to light-dark and temperature cycles as indicated by the first peaks. The long T-cycles peaks preceded by four hours the respective of short T-cycles. The last is an indication of entrained rhythms. Furthermore, the subsequent peaks fell in the same phase irrespective of

cycle length, and the time of these peaks coincide with the circadian peaks, as observed for the entrainment after 10 hours of light::14 hours of darkness. This suggested that under free-run, no matter the preceding entrainment, the clock was ultimately set to the circadian component of the cycle. Genes that follow this trend are part of the circadian machinery. *TOC1* is a key component in terms of temperature entrainment. In long T-cycles of temperature, *TOC1* expression for the first day was constant at intermediate levels of peak and trough. After the first 28 hours, rhythmicity of *TOC1* was restored to the circadian pattern (Figure 5.6). This response probably suggests that *TOC1* is specific for entrainments up to 24 hours, and not more. In the short T-cycles of temperature entrainment, *TOC1* peaked in late evening (Figure 5.6), consistent with data that were described for 24 hours entrainment. It would be interesting to assay *toc1-21* mutant in such entrainment.

To confirm the physiological responses of the *TOC1* and *GI* in genetic terms, *CCR2* expression was tested in the *gi-11*, and *toc1-21* single mutants, and the *gi-11 toc1-21* double mutant and compared to the *CCR2* expression in wild type background. The mutant and wild type seedlings were synchronized to different photoperiod and thermoperiod, of 24 hours, protocols. Genetic analysis confirmed the role of *GI* in photoperiod measurement (Figures 5.2 and 5.9). Additionally, the differential response of *TOC1* after light-dark and temperature cycles was also confirmed (Figures 5.2 and 5.10).

The *gi-11* and *toc1-21* mutants and the double mutant were entrained in 20-or 28-hour cycles of equal period of light/warm and dark/cool. In these conditions, I could test for the genetic requirement of *TOC* and *GI* under these conditions. *CCR2* phase in single and double mutants were observed during the light/warm part of the cycle after the 28-hour cycles, whereas after the 20-hour cycle *CCR2* phase was observed in the dark/cool phase. *CCR2* phase in the *gi-11* after temperature entrainment irrespective to cycle length was the same compared to the *CCR2* phase in the wild type (Figures 5.7 and 5.12). This suggested that *GI* did not entrain to temperature cycles. In general, the phase of *CCR2* in the *toc1-21* was much earlier in both 28-and 20-hour cycles of both entraining signals compared to the phase of *CCR2* in the *gi-11*. This suggested that both *TOC1* and *GI* had differential effects on *CCR2* expression. Furthermore, after the temperature entrainment in 28-hour cycles, *CCR2* expression was arrhythmic after one cycle, whereas in all other conditions tested, including temperature entrainment in 20-hour cycles, was rhythmic with short period.

This confirmed that *TOCI* was the gene of the oscillator that is able to measure temperature cycle length, and entrained to temperature.

6 GENERAL CONCLUSIONS AND DISCUSSION

6.1 CONCLUSIONS - FUTURE PERSPECTIVES

The circadian clock is an internal-timing mechanism that is highly adaptive to the daily environmental changes. Successive changes in light and temperature are able to reset the oscillator (McClung, 2006). The most prominent signal studied is light (Davis and Millar, 2001). Mathematical modeling predicted that the core oscillator of light-dark entrained *A. thaliana* seedlings is comprised of three interconnected feedback loops (Locke et al., 2006; Zeilinger et al., 2006). This basic loop generates the 24-hour rhythmicity of the oscillating mechanism, whereas the morning and evening loops are fine tune rhythmicity in a temporal specific manner. However, only limited studies on the role of temperature cycles to the circadian oscillator existed before this thesis work.

To define the role of temperature and to identify genetic components that mediate temperature input to the plant-circadian oscillator, I exploited the variation of the circadian rhythmicity of *CCR2::LUC* in two existing RILs populations (Chapter 3). Transformed lines of those two RILs populations were entrained in light-dark and temperature cycles, and measured for *CCR2* period under constant light conditions. Statistic analysis revealed that the averaged period per line after light-dark entrainment was longer as compared to temperature entrainment. This was true for both RIL populations (3.1.2, 3.2.2). Interestingly, period analysis of entrainment in the two different protocols resulted in the identification of both QTL at the same and different genomic intervals (3.1.3, 3.2.3). This suggests that the natural-allelic variation that exists for both light and temperature inputs are mediated effects on the oscillator. A QTL at the first chromosome was found to be specific to temperature entrainment (3.1.3). *GI* localizes to that interval. Further fine mapping of this QTL should eventually reveal whether the QTL is *GI* or is a previously uncharacterized locus.

The above populations have the caveat that to map circadian-rhythmicity QTLs, I needed to transform each RIL line within the population. For this, I generated hundreds of individual transgenics for each RIL harboring *CCR2::LUC* (Chapter 3). The disadvantage of this approach was that the T-DNA insertion was random and

aspects of the observed phenotype could have been moderately affected by the insertion site of the *CCR2::LUC* transgene. To avoid such disadvantage for future QTL mapping, I also generated six new RILs by pairwise crosses of the four most commonly used accessions (Chapter 4). Two of the accessions harbored the *CCR2::LUC* reported that was crossed to wild-type accessions. Selection of 48 lines with short period and 48 lines with long period of *CCR2* was realized at the BC1 and at the BC1F2 generations. In Chapter 4, one RIL was extensively described. This population was generated by the cross of WS, bearing *CCR2::LUC*, to C24 (4.1). First, the resultant RILs were assayed for flowering-time variation and circadian rhythmicity (4.3). Next a genetic map of the population was generated (4.2). I found that the flowering time of the short or long period selected lines was selected by loci at the same and different positions, and interactions amongst the detected QTLs. *FRI* and *FLC* are candidate genes for the fourth and fifth chromosome QTL found in all lines (4.3.1.1). A third QTL was identified at the first chromosome after QTL mapping of the long-period selected lines to co-localize with the *CRY2* (4.3.1.1). Additionally, preliminary results of assessment of circadian rhythmicity showed that a QTL for light-dark entrainment were detected from 0-20cM at the second chromosome (4.3.2). No main QTL was detected for period of *CCR2* after temperature entrainment in the described population.

The role of temperature entrainment to the circadian clock was further defined by physiological experiments. For this, transcriptional kinetics properties of several clock-controlled genes were assayed (Chapter 5). In this study, it was found that *GI* tracks photoperiod, whereas *TOCI* was the only tested promoter able to synchronize preferentially to temperature cycles, compared to light-dark cycles. This suggests that dawn, as measured by *GI*, sets the circadian clock, and temperature, through *TOCI*, fine tunes circadian clock (5.1-5.3). The role of *GI* and *TOCI* in light-dark and temperature entrainment, respectively, was confirmed by genetic studies (5.4, 5.5).

Genetic analysis of temperature entrainment using natural variation

In this thesis, the main aim was to characterize how temperature synchronizes the circadian oscillator of *A. thaliana*. This was performed as a comparison to light-dark entrainment. Two different pre-existing RILs sets –CvL and BxS- were exploited for characterizing the periodicity of *CCR2* rhythmicity, as reported by luciferase

expression (Chapter 3). Both populations were entrained in two protocols, and these were 12 hours at light::12 hours at darkness in constant temperature at 22°C, for light-dark entrainment, and in 12 hours at 22°C::12 hours at 16°C under constant light, for temperature entrainment (3.1 and 3.2). Additionally, the CvL RIL was tested in the same temperature cycle conditions, but under constant darkness (3.3).

The first conclusion drawn after the entrainment to light-dark and temperature cycles was that in both populations the period of *CCR2* after the temperature entrainment was statistically-significantly shorter compared to the period of *CCR2* after light-dark entrainment, as shown in sections 3.1.2 and 3.2.2. Since this was observed in both RILs, and in the new RILs set (C24WS) (Chapter 4), this suggested that varying period length after the two different entrainment protocols is probably of an adaptive value. The nature of this adaptive value could be that whilst light and dark dominantly entrain the oscillator, the additional effect of thermal changes fine-tune this response.

The second conclusion drawn from the *CCR2* periodicity studies after light-dark and temperature entrainment was that different entrainment protocols resulted in the detection of QTLs that are mediated by natural-allelic variation at both the same and different loci positions. This was shown to be true in both RIL populations tested (see 3.1.4 and 3.2.4). A detailed description and possible implications of the identified QTLs per RIL and per separate entrainment protocol on the period phenotype follows.

The first RIL population assayed for periodicity was the CvL. Specifically, for the light-dark entrainment, one main QTL at the locus BH.107 at the fifth chromosome was identified, and it explained about 50% of the phenotype. The additive effect of the Cvi allele was 0.838 hours as compared to the *Ler* allele. A QTL at this approximate location has been found in past studies (Edwards et al., 2005). From known circadian modulators, *FLC* localizes close to this area and it was shown that an *flc* mutant displayed period phenotype (Salathia et al., 2006). Therefore *FLC* could be candidate gene for this locus, especially as Cvi allele of *FLC* is strong, and such alleles were previously shown to lengthen period (Salathia et al., 2006). It was also shown that *Ler* carries a weak *FLC* (Gazzani et al., 2003).

At the first chromosome at the PW4 locus, another main QTL was identified for light-dark entrainment (3.1.3). The *Ler* allele of this QTL displayed a longer period of 1.131 hours compared to the Cvi allele, which displayed a 25.5 hours period under constant light free-running conditions (3.1.4). A known clock gene named *LHY*

is localized within this interval. *LHY* is a light-induced gene that forms feedback loops with other core oscillator components (Kim et al., 2003a). It is an attractive hypothesis that *LHY* plays a role in the light input to the oscillator. It is not known if the allelic status of *LHY* varies between *Cvi* and *Ler*. Perhaps a more plausible candidate gene for this locus within the defined interval would be *CRY2*. *CRY2* mediates blue-light input to the clock (Yanovsky et al., 2001). Moreover, its expression is under the control of the circadian clock (Toth et al., 2001). It was found that a single amino-acid change in the *Cvi* allele of *CRY2* was responsible for daylength-insensitive flowering, whereas the *Ler* allele of *CRY2* displayed a late flowering phenotype under short days (El-Din El-Assal et al., 2001). Therefore, it would be exciting to determine whether the same polymorphism accounts for periodicity, as well as for flowering-time variation.

Another QTL at the locus CC.262C at the bottom of the fifth chromosome was identified for the light-dark entrainment (3.1.3). Statistical analysis confirmed the existence of this QTL and its highly significant interaction with the QTL identified at the PW4 locus. Several candidate clock genes are localized at the proximity of this locus. *SRR1*, *PRR3*, and *TOC1* are candidate genes for this QTL. *SRR1* was found to be a component of PHYB signaling (Staiger et al., 2003b). Previous natural-variation studies showed that *PRR3* and *SRR1*, but not *TOC1*, might account for a phase QTL detected after entrainment to light-dark entrainment in 12 hours light::12 hours darkness in the CvL collection (Darrah et al., 2006). It was somewhat expected that *TOC1* will not be a candidate gene, since it is an evening-expressed gene that, until now, there has been no evidence of *TOC1* directing light activation. Moreover, this is partially confirmed by mathematical models according to which it was predicted that light activation of *TOC1* is mediated through an unknown ‘Y’ factor (Locke et al., 2005).

Additional interacting QTLs after light-dark entrainment were identified (3.1.3). One such interacting QTL was found at about 60-65cM at the first chromosome. This is a novel QTL. Although QTL mapping showed that this QTL greatly reduces the effect the fifth chromosome QTL at the locus BH.107L, such an interaction was not confirmed by the statistical analysis. This is probably due to the different assumptions of the applied statistical tests. A fourth chromosome interaction QTL was found that enhances the effect of the first chromosome identified QTLs and reduces the effect of the QTL at the fifth chromosome at the CC.262C locus.

However, such an interaction was not confirmed by statistic analysis. Collectively, previously known QTLs were confirmed, and new QTLs were identified for the light-dark entrainment. As well, the epistatic nature of clock QTLs was revealed.

For period QTLs after temperature entrainment, a main QTL in the CvL collection was identified on chromosome 1 at the CH.160L-Col locus (3.1.3). It was highly statistically significant and the *Ler* allele conferred a longer-period phenotype of about 1.1 hours compared to the *Cvi* allele (3.1.4). *GI* remains a candidate gene since it is still localized within a newly generated NILs during my QTL cloning (see below). Other approaches taken to map the first chromosome QTL at the locus Ch.160L-Col will be described in the future perspectives section.

A QTL at the third chromosome was found to have strong interaction with the main QTLs identified after temperature entrainment in the CvL collection (3.1.3). This QTL displayed a positive effect on both the QTL at the chromosome 1 at the CH.160L-Col, and on the QTL at the bottom of chromosome 5 (3.1.4). This QTL is novel and was not previously identified from other circadian studies. Statistic analysis showed that it strongly interacts with a QTL at the PW4 locus, although no QTL, interacting or main, for the temperature entrainment was found at the PW4 locus. This discrepancy could be due to the different test assumptions.

At chromosome five, three separable period QTLs after temperature entrainment were identified in the CvL collection. Two of them were located at the beginning of chromosome, at the AD.292L and at the BH.107L loci, respectively. The QTL at the locus AD.292L increased the effect of the first chromosome QTL at the CH.160L-Col, but it decreased the effect of the fifth chromosome QTL at the locus BH.107L. The *PRR7* gene is localized close to the QTL at the locus AD.292L. Previously, it was shown that *PRR7* is entrained by temperature (Salome and McClung, 2005). An interaction between *PRR7* and *GI*, in case these are the loci at the fifth and first chromosome, respectively, has not yet been shown. At the CC.262C locus, a main QTL was identified. This QTL was also detected after the light-dark entrainment as described above. Collectively, numerous epistatic interactions were revealed.

To remove the confounding effect of light in temperature entrainment, the CvL RILs were synchronized to temperature cycles in constant darkness and then free run in constant darkness at 22°C for period measurements. The aim was to assay periodicity in exactly the same RILs as the ones assayed under the constant light and

temperature cycles. QTL mapping of *CCR2* period after this entrainment resulted in two main QTLs (3.3.2). These QTLs were at the CH.160L-Col and HH.143C loci. Interestingly, these two QTLs were also identified after temperature entrainment under constant light. In the latter entrainment, a third QTL was also identified at the fifth chromosome at the BH.107L locus. At this locus, the main QTL for the light-dark entrainment was detected. This suggests that during temperature entrainment under constant light conditions, both light and temperature entrainment cues, light and temperature, are effective in allowing the detection of the identified QTLs.

In past natural-variation studies, the CvL collection has been used to map period, phase, and amplitude QTLs for temperature compensation, photoperiod, or light dark entrainment (Swarup et al., 1999). Swarup *et al.* measured the period phenotype of leaf movement in the 48 Cvi/Ler after light-dark entrainment (Swarup et al., 1999). Three QTLs were identified for period variation of leaf movement. The first chromosome QTL named *ESPRESSO* (*ESP*) co-localized with the one I identified for the temperature entrainment. *GI* remains a candidate for this locus. Two QTLs were also identified by Swarup *et al.* on the chromosome five, named *ANDANTE* (*AND*) and *RALENTANDO* (*RAL*). The *AND* QTL was found to be localized at the top of chromosome five, whereas the *RAL* QTL was localized at the bottom of chromosome five (Swarup et al., 1999). These two QTLs do not co-localize with the QTLs I identified for the light-dark or temperature entrainment (3.1.3). In the Col/Ler RIL set tested by Swarup *et al.*, two QTLs at the fifth chromosome, but none at the first chromosome were identified. A second publication mapped QTL by assessing period, phase, and amplitude of leaf movement rhythms in 76 Col/Ler RIL (Michael et al., 2003b). Especially for period, two QTLs were identified on the first chromosome. This discrepancy between the two publications might be observed due to the different number of the RILS assayed.

In another QTL experiment from the Millar group, Edwards *et al.* performed temperature compensation experiments scoring period, phase, and amplitude of leaf movement in 30 Col/Ler and 48 Ler/Cvi RILs in three different ambient temperature environments (Edwards et al., 2005). Several period QTLs were identified, with many of them co-localizing for the different RILS populations. Many interesting findings were described. Different period QTLs were found to be involved in temperature compensation at various temperatures. On the first chromosome, two period QTL at the loci PW4 and CH.160L-Col were identified for 12°C and 27°C, respectively.

Interestingly, at the PW4 locus, I also identified a QTL for the light-dark entrainment, whereas in the locus CH.160L-Col, I identified a QTL for temperature entrainment. Since temperature has a dual role in regard to the oscillator, as that of compensation and entrainment, it would be interesting to test if the QTL at the locus CH.160L-Col is involved in both processes. On the fifth chromosome, four different period QTL were mapped by Edwards *et al.* within the Cvi/Ler population (Edwards *et al.*, 2005). The only potential co-localization with the QTLs I identified is restricted to the QTL previously named PerCv5d. PerCv5d colocalizes with the QTL I identified after the temperature entrainment in constant darkness at the HH.143C locus (3.3.2). Additionally, amplitude QTLs were also detected for the temperature compensation, but surprisingly no phase QTL was identified. This probably suggests that period and phase are under different genetic control regarding leaf movement.

Darrah *et al.*, exploited natural variation of *CAB2* phase after entrainment in three different photoperiod environments in 47 CvL RILs. The three photoperiod environments consisted of 3 hours light::21 hours darkness (short photoperiod), 12 hours light::12 hours darkness (intermediate photoperiod), and 21 hours light::3 hours darkness (long photoperiod). In total, four QTLs were identified. For the short photoperiods, a QTL on chromosome 1 close to the CH.160L-Col locus, and another QTL on the fifth chromosome at the FD.207L locus were identified. QTL fine mapping suggested that the first chromosome QTL is novel and does not correspond to *GI* (Darrah *et al.*, 2006). Two QTLs were identified for the intermediate photoperiod, on the second chromosome at the ERECTA locus, and on the fifth chromosome at the HH.122C/120L locus. No QTLs were detected for the entrainment in long photoperiod. The two QTLs at the chromosome 5 did not co-localize with any of the QTL I identified. To conclude, of all the past publications, my findings share more similarities to the Edwards *et al.* results.

To confirm that my findings of the light-dark and temperature entrainment of the CvL collection were adaptive, I extended my experiments to a second RIL population, named BxS, that was generated by accessions different than those used for the generation of the CvL RIL. The parental strains of the BxS population were Bayreuth-0 and Shakdara (Loudet *et al.*, 2002). Strikingly, although the BxS population was synchronized to the same protocols as CvL, different QTLs were detected. Two main QTL at the same loci were mapped for the two different entrainments. Specifically, the two QTL were located at the second chromosome at

MSAT 2.41 locus and at the fourth chromosome at the locus MSAT 4.37 (3.2.3). The second chromosome QTL was detected after both entrainments, whereas the fourth chromosome was less significant for the temperature entrainment.

The second chromosome QTL co-localizes to an interval that contains *ELF3*. *ELF3* functions to gate light to the oscillator (McWatters et al., 2000). However, this gene has not yet been implicated in temperature entrainment. However, Tajima *et al.*, has shown that extensive natural variation in the polyglutamine repeats of *ELF3* exist within 60 accessions (Tajima, 2007). Possibly, the variation in the repeats may play a role in the interactions of *ELF3* with other partner proteins. Whether the Bay-0 or Shakdara accessions have different repeats in *ELF3* is as of yet not published.

A fourth chromosome QTL in the BxS population was found, and it is novel since it does not co-localize with any known circadian gene. Collectively, in Chapter 3 two RIL collections were assayed in light-dark and temperature cycles. It was found that temperature and light-dark entrainment controlled by both the same and different QTLs. Furthermore, different QTLs were detected for each collection, suggesting that circadian clock is a highly adaptive to environment.

Temperature entrainment QTL fine mapping future perspectives

Thus far, the fine mapping of the QTL at the locus CH.160L-Col, paralleled to phenotypic assays, led to a defined genomic region in a NIL background. This region is close to, and includes, *GI*. In the case of the CvL population, NILS were constructed by introgression of Cvi alleles into *Ler* genome (Keurentjes et al., 2007). I backcrossed four of the original NILs that had a Cvi introgression at the first chromosome to *Ler* bearing *CCR2::LUC* in order to generate an informative population to fine map the QTLs detected for temperature entrainment by assaying circadian rhythmicity of *CCR2*. To elucidate whether the first chromosome QTL is *GI*, these four NILs were crossed to *gi-3* mutant bearing *CCR2::LUC*. This mutation is in *Ler* background and displayed a short-period phenotype (Koornneef et al., 1991). Several F1 lines of each NIL cross over the mutation were assayed for rhythmicity of *CCR2*, and were scored as to whether they had restored the mutant phenotype. The F1 crosses of *gi-3* to two separate NILs with introgressions of Cvi in part of chromosome 1, including smaller and larger area around *GI* were compared to NILS that had introgression of Cvi in part of the chromosome 1, but at the *GI* locus, they were *Ler*.

As the control, the Cvi and the *Ler* accessions were crossed to *gi-3* mutant. The NILs lines that introgressed a Cvi allele of *GI* restored the mutant phenotype of *gi-3* in the tested F1 lines. The NILs with *LerGI* also restored the phenotype. So, both the Cvi and *Ler* alleles of *GI* were found to be functional and could recover the mutant phenotype of *gi-3*. However, the NILs that Cvi*GI* introgressed displayed shorter period after temperature entrainment than after light-dark entrainment, compared to the *LerGI*. The F1 of Cvi accession crossed to *gi-3* displayed a shorter-period phenotype, compared to the Cvi accession. This suggested that *GI* and a QTL not at *GI* locus interacted in these F1 lines. However, the F1 of the two parental accessions was not created. This would be the control for the Cvi accession crossed to *gi-3*. So to conclude, the *gi-3* mutant phenotype is restored by NILs that contain Cvi*GI* and *LerGI*. However, the presence of interacting QTLs within the NILs cannot be excluded. Further fine mapping would be useful to determine whether the QTL is *GI* or an interaction that modifies *GI* activity.

In section 3.1.4, interallelic epistatic interactions for light-dark and temperature entrainment were described. In the temperature entrainment studies, a genetic interaction between two main QTLs was found, one at the first chromosome at locus CH.160L-Col and that at the fifth chromosome QTL at locus CC.262C (3.1.4). To assay for this interaction, NILs isolated during my QTL mapping of the first chromosome QTL, containing a small region of Cvi, could be crossed to NILS that contain a Cvi introgression at the QTL of the fifth chromosome. F2 seedlings from this cross could be assayed for circadian rhythmicity to determine the allele-specific interactions between these two QTLs. The interaction of the *Ler* allele of the first chromosome QTL with the Cvi allele of the fifth chromosome QTL displayed a long-period phenotype, and thus, this epistatic interaction should be easily identifiable. After identification of the genes that create these QTLs, complementation tests to available mutants could be realized in QTL confirmation. Further characterization of gene function in various physiological protocols should then be assayed.

Molecular genetic characterization of non-randomly generated RILS

Assessment of luciferase activity driven by circadian promoters in two pre-existed RIL populations led to the detection of several QTLs (Chapter 3). To avoid positional effects due to the insertion of the reporter construct, multiple progeny seedlings from 2 to 4 independent transformants per RIL were assayed for circadian rhythmicity. To minimize such an effect for future circadian experiments, six new RILs were constructed during this PhD by pairwise crosses of the four most commonly used *A.thaliana* accessions, named Columbia, Landsberg *erecta*, C24, and Wassilewskija (Chapter 4). Two of the accessions, WS and *Ler*, were bearing the *CCR2::LUC*, were crossed to the remaining three accessions. Therefore, in all lines within each RIL population *CCR2::LUC* was inserted at the same genomic region. In total, per each RIL population, 48 lines were selected for long period and 48 lines for short period of *CCR2*, after light-dark entrainment. Four RIL populations were taken to the BC1F7 generation. Generation of a dense genetic map for each population will be required. For two of the populations, those generated by the cross of C24WS and ColWS, a preliminary genetic map was constructed. Both RIL populations were genotyped with SSLPs and CAPS markers (2.1.5). The C24WS RIL population was genotyped using 34 markers spread across the five chromosomes (4.2). These maps facilitated the QTL identification and described SD from selection.

In Chapter 4, QTL mapping was described in C24WS for two circadian clock controlled traits, flowering time and circadian period of *CCR2*. The parental accessions WS and C24 were both early flowering, bolting at around 8 and 13 leaves, respectively (Table 4.2). However, extensive flowering-time variation was observed in my generated RILs, from 5 to 53 leaves (Table 4.2). For the flowering-time variation, three QTLs were identified that accounted for more than 70 % of the total phenotypic variation. In the long-period selected lines, three QTLs were identified, whereas in the short-period selected lines two QTLs were identified. The two QTLs mapped in the long-period selected lines were the same as those identified in the short-period selected lines, and thus, only three total QTLs were detected for flowering time in the C24WS collection. The two common QTL were localized at the beginning of the fourth chromosome at the locus *FRI*, and at the fifth chromosome between the loci NGA158 and NGA106. In between of these markers *FLC* is located. Thus, *FRI* and *FLC* are strong candidates for these QTLs. Shindo *et al.*, assessed

natural variation on both genes in 192 accessions, including C24 and WS (Shindo et al., 2005). These accessions originate from different latitudes. Specifically, C24 was collected from 35-40N, whereas WS was collected at 50-55N. Since both parents are early flowering, then it is the allelic interactions that define the late-flowering phenotype of some RILS. Additive effects and allelic interactions between the QTLs were shown (4.3.1.2). The C24 allele of the *FRI* QTL is later flowering than the WS allele, whereas the WS allele of *FLC* is later flowering than that of the C24 allele. It was previously described that the *FRI* gene is an activator of *FLC*, a major repressor of flowering time (Michaels and Amasino, 1999). The interaction of C24 allele of *FRI* with the WS allele of *FLC* displayed a late-flowering phenotype compared to the rest allelic combination interactions (4.3.1.2.3). It is known that C24 has a strong *FRI* allele and weak *FLC* allele, whereas the WS has a weak *FRI* allele and a strong *FLC* allele (Gazzani et al., 2003). Thus, I expected these genes would be mapped and their interaction would be found to confer flowering-time variation, this was the case (4.3.1.2.3).

The third flowering time QTL in C24WS was identified on chromosome one at the NGA59 locus. This QTL was first found in the long-period selected lines, and also in 'all lines included.' The WS allele delayed flowering compared to the C24 allele. The *CRY2* gene is a candidate for this locus as it is located within this interval. In the past, *CRY2* was mapped in the CvL collection for conferring insensitivity in response to day-length (El-Din El-Assal et al., 2001). Photoperiod insensitivity was provided by the Cvi allele of *CRY2*. The photoperiod insensitive flowering time phenotype was expected because Cvi origin is from close to the Equator. In this environment, daylength does not drastically change as in other parts of the world. It is not known if C24 has a different *CRY2* sequence than WS.

Circadian rhythmicity after light-dark and temperature entrainment was assayed in the C24WS lines. To date, more than fifty percent of the lines have been assayed in constant light after entrainment to these light-dark and temperature-entrainment protocols. QTL mapping resulted in the identification of a QTL at the top arm of chromosome 2 for the light dark-entrainment. No common QTL was identified for the two traits tested in the C24WS collection. Interestingly, as was seen with CvL and BxS, the C24WS population was displayed a longer period after light-dark than temperature entrainment (3.1.3, 3.2.3, 4.4.2).

Future perspectives

Several RILs populations have been generated in a non random way during this PhD. Segregation distortion was observed on chromosomes 1, 3, and 5. This segregation distortion, together with the non-dense genetic map are the main causes for the high LOD scores generated from the MapQTL, especially for the short-period selected lines (4.2, 4.3). This then affected as well the MapQTL results for ‘all RILs.’ Therefore, it will be of interest in the future to study segregation distortion based on phenotypic selection, and especially, to study whether the undertaken selection for *CCR2::LUC* periodicity correlates with other circadian-regulated traits, such as hypocotyl elongation and flowering time. This would thereby determine the possibility of genetic co-segregation of these three traits. This correlated trait measurement will define if circadian selection coordinates physiology.

The best genetic resources to perform the above described experiments would be the C24WS and the reciprocal *Ler*WS RILs due to the flowering time and hypocotyl elongation variation that was observed in each collection, respectively. Additionally, in the reciprocal *Ler*WS RILs, one could determine maternal effects on the understudy phenotype. If a QTL will be found in all measured traits, such as circadian rhythmicity, hypocotyl elongation, and flowering time, this would suggest that the detected QTL is a common link for all traits. Such detection is somewhat expected since the circadian clock controls these processes, and therefore the three traits can be correlated. If true, this would in part explain why extensive natural variation in periodicity exists.

The QTL mapping for flowering-time variation in the C24WS population resulted in the detection of three main QTLs. For each QTL, a candidate gene exists. Natural variation has been described in the past for all three loci (El-Din El-Assal et al., 2001; Shindo et al., 2005). Generation of NILs at these loci should be initiated. Phenotypic confirmation should be followed by sequence analysis of candidate genes to reveal the polymorphism underlying the variation. It would be interesting to compare the variation of WS, and C24 for all candidates. Further experiments would be to run parallel flowering time experiments in short days and long days, as well as in vernalization and non-vernalization conditions, to map flowering time QTLs for these four environments. Since *FLC* is a strong candidate for the late-flowering phenotype under long days, and it is known that prolonged low temperatures that

result in vernalization treatment down-regulate the expression of *FLC*, I would expect that on average the C24WS collection will generally flower earlier after vernalization treatment. Additionally, flowering-time assays of plants grown under short days could be used to define whether the first chromosome QTL accounts for photoperiod-dependent flowering time variation. This might be expected, as *CRY2* is candidate for this QTL.

Physiological analysis of various clock markers

The results of the Chapter 3 suggested that QTLs co-localized with known circadian genes, such as *GI*, *TOC1*, *LHY*, *ELF3*, mediate temperature entrainment. Therefore, I decided to map the transcriptional kinetics of these promoters, as well as the outputs *CAB2*, *CCR2*, *ELF4*, and *CCA1*, under various physiological experiments to assess their entrainability. Temperature entrainment was of interest and it was contrasted to results after light-dark entrainment. Luciferase activity driven by various promoters was assayed in different daylength and thermo-length protocols (Chapter 5). From these results, it was concluded that *GI* promoter was the only one of those tested that was able to discriminate photoperiod length (5.1). However, none of the tested promoters was able to discriminate thermo-period length. Detection of thermo-period or photoperiod through the *TOC1* promoter was not observed (5.1). Interestingly, there was a distinct pattern for luciferase activity driven by the *TOC1* promoter after the different entrainment protocols (5.1). *TOC1* displayed a later phase and shorter period after temperature entrainment compared to after light-dark entrainment. This suggested that light and temperature regulate *TOC1* transcription, in a differential manner. The delayed-phase phenotype after temperature entrainment, compared to light-dark entrainment, was also observed for *LHY* (5.1). Thus, *TOC1* and *LHY* are regulated by temperature differentially compared to other clock genes. Whether this is a reciprocal regulation remains to be elucidated.

In nature, changes in light and temperature often take place at the same time. However to map the differential effect of the two signals and the preference of these genes to either input, I subjected the transgenic plants to desynchronizing entrainment protocols, where temperature cycles were 6 hours delayed (IN) or advanced (OUT) compared to the onset of lights in the light-dark cycle (5.2). When plants were

transferred to continuous light just before the warm-to-cool or cool-to-warm transition, which was in the middle of the light period, the phase of all promoters was shifted, advanced or delayed by six hours, suggesting that they anticipate for the temperature change (5.2). Interestingly, when seedlings were transferred to continuous light just before lights on, all clock promoters responded to temperature only in the OUT protocol, as determined by six hours advanced phase shift compared to the light-dark entrainment (5.2). However, *TOCI* was the only clock promoter of those tested that was reset during the middle of IN protocol by advancing its phase by 6 hours (5.2). These results collectively suggested that temperature changes were gated by light during the day. This could mean that light was a stronger entrainment signal than temperature during subjective day time. In the absence of light, temperature dominated clock resetting (5.2). Here, *TOCI* could be the thermal target of the clock. So, at this point it is not clear whether the *TOCI* response that was 6 hours phase shifted was entrained or driven. There are a couple of approaches that could resolve this discrepancy.

To determine whether temperature entrains *TOCI*, I performed non 24-hour cycles of light-dark and temperature entrainment. In nature, plants would never experience a cycle length other than 24 hours. Therefore, entrainment in such conditions would be certainly enlighten the determination of entrainment. I chose to synchronize to cycle lengths of 20 and 28 hours, using equal portions of light/warm and dark/cool, because I could compare the 20 or 28 hours cycle to the 24 hours photoperiod or thermo period results obtained in Chapter 5.1, in terms of cycle length or light/warm period length. The general trend was that the peak expression of the transcriptional rhythms of the 28 hours cycle was earlier than that of the 20 hours cycles. The difference in phase was an indication of entrained rhythms and not driven (Pittendrigh, 1976). All promoters displayed a phase difference of four hours between the different cycle lengths, as defined by the first peak. However, the subsequent peaks of *GI*, *TOCI*, *CCA1*, and *CCR2* were not identical. A detailed analysis of these expression profiles follows.

GI entrained in 20 hour and 28 hour cycles of both light-dark and temperature entrainment, as indicated by the first peak. After the 28-hour cycle, *GI* expression peaked 5 hours before dusk/cool, whereas after the 20-hour cycle peak expressed 3 hours after dusk/cool (5.3). However, from the second and subsequent peaks it seemed that temperature entrainment had the same effect irrespective of the cycle

length. Importantly, in free running under constant light, after being entrained at 28-hour temperature cycles, its expression peaked was at the subjective warm to cool transition (5.3). This response indicated a driven response due to temperature. After light-dark entrainment to both 20- and 28-hour cycle *GI* expression peaked at different phases, suggesting that *GI* entrained to light-dark cycle (5.3).

TOC1 after light-dark entrainment displayed different phase regarding the different T-cycles, and after the second peak, both light-dark entrainments displayed the same profile. This was similar to the *GI* response (5.3). However, the phase of *TOC1* expression peak after 28-hour cycles was at the transition from light to dark (5.3). After the 20-hour cycles *TOC1* expression peaked at the end of the dusk period. Therefore, *TOC1* tracks to the light-dark cycles. Strikingly, *TOC1* expression displayed an acute response soon after transfer from the temperature T-cycles to constant light conditions (5.3). This acute response could be explained by the temperature change during the transfer from cold to warm. The phase of *TOC1* after temperature entrainment to 20-hour cycles was the same after light-dark entrainment to 20-hour cycles. Unexpectedly, after temperature entrainment to 28-hour cycles, *TOC1* expression was arrhythmic at intermediate expression for the first cycle, as defined by peak and trough levels (5.3). In subsequent cycles rhythmicity was restored. This response after the 28 hours cycles in temperature entrainment was unique and never found before neither in *A. thaliana* nor in any other circadian-clock model organisms (Liu, 2003; Glaser and Stanewsky, 2005).

Both *GI* and *TOC1* were genetically tested under the photoperiod and thermoperiod protocol, as was described in 5.1 (5.4). This was done to test whether the observed response of *GI* and *TOC1* promoter to photoperiod and thermoperiod protocols was could be genetically confirmed. For this, *CCR2* expression was monitored after photoperiod and thermoperiod protocols in the *gi-11*, *toc1-21*, and the double mutant *gi-11 toc1-21*. Clearly, *CCR2* expression peaked later after entrainment to different photoperiod protocols compared to the wild-type. In contrast *CCR2* expression in the mutants peaked the same with wild-type after temperature entrainment. These results confirmed that *GI* measured photoperiod and not thermoperiod, whereas *TOC1* was not able to measure photoperiod or thermoperiod (5.4).

The effect of the *gi-11* and *toc1-21* mutants in the *CCR2* expression was also tested under the various T-cycles protocols (5.5). The expression of *CCR2* was

arrhythmic after one cycle, compared to the wild-type (5.5). *CCR2* phase in single and double mutants were observed during the light/warm part of the cycle after the 28-hour cycles, whereas after the 20-hour cycle *CCR2* phase was observed in the dark/cool phase (5.5). *CCR2* phase in the *gi-11* after temperature entrainment irrespective to cycle length was the same compared to the *CCR2* phase in the wild type (5.5). This suggested that *GI* did not entrain to temperature cycles. In general, the phase of *CCR2* in the *toc1-21* was much earlier in both 28-and 20-hour cycles of both entraining signals compared to the phase of *CCR2* in the *gi-11* (5.5). This suggested that both *TOC1* and *GI* had differential effects on *CCR2* expression. Moreover, it was suggested that *TOC1* responds to both light-dark and temperature entrainment, whereas *GI* responds only to light-dark entrainment and not temperature entrainment. Different evening genes thus appear to be differentially sensitive to environmental entrainment.

Future perspectives

TOC1 expression varied compared to other clock genes and displayed a physiological response under any tested protocol (5.1-5.3). It would be interesting to further define the temperature-regulated physiological responses of *TOC1*. So far, the responses of *TOC1* to entrainment in T-cycles indicated that *TOC1* could be entrained to 24 hours and to less than 24 hours protocols, but cannot be entrained to more than 24 hours. For this, one could test intermediate T-cycle to refine the phase of the various clock promoters. Additionally, it would be interesting to monitor the expression pattern of all clock promoters tested in this study, during entrainment in 28 or 20-hour cycles. Though, it is important to note that since luciferase is an enzyme, temperature changes affect its activity.

Mathematical modeling has predicted that the *A. thaliana* circadian oscillator of light-dark entrained plants is comprised by three loops (Locke et al., 2006). Two genes of the morning loop model, *PRR9* and *PRR7*, were shown to have an effect in temperature entrainment (Salome and McClung, 2005). Moreover the triple mutant of *cca1 lhy toc1* was found to be rhythmic for a day, and then it becomes arrhythmic (Ding et al., 2007b). All data so far have indicated that all known core-clock genes are either actively involved in temperature entrainment or their expressions patterns are temperature regulated (Salome and McClung, 2005; Ding et al., 2007b). One such

temperature regulated gene was shown to be *GI*. Therefore, it would be fruitful to generate the quadruple mutant of *cca1 lhy toc1 gi*, with all the respective double and triple combinations, and assay their entrainability to temperature. According to the three-feedback-loop model, *PRR9* and *PRR7* and an unknown *X* factor are proposed to remain functional (Locke et al., 2006; Zeilinger et al., 2006). Additionally, it would be useful to generate another quadruple mutant, in which *PRR9*, *PRR7*, *TOC1*, *GI* would be non functional. Here, the only functional clock genes would be *CCA1*, *LHY*, and *GI*. According to the predicted model, this quadruple tests the other arm of the oscillator. Studies on these two quadruple mutants might then explain the majority of the core-clock machinery. Eventually, all these generated genetic materials should be tested after various temperature-entrainment protocols, such as those performed in Chapter 5. Currently, experiments on the *toc1-21*, *gi-11* and their double mutant were carried out under the same entrainment protocols, such as INOUT entrainment protocols (Chapter 5). This double mutant was particularly interesting, as *GI* and *TOC1* were found to be reciprocally regulated (Martin-Tryon et al., 2007). Furthermore, *GI* negatively regulates *TOC1*, in an indirect manner, since in blue light *GI* stabilizes *ZTL* protein, which in turn mediates *TOC1* degradation (Mas et al., 2003; Kim et al., 2007b). Whether this supposedly light-requiring mechanism is regulated by temperature will also need to be determined.

In the IN protocol, the response of *TOC1* was observed upon transfer from dark to light while being in the middle of the cool part of the temperature cycle (5.3). It would be interesting to monitor the status of *TOC1* over time in the IN protocol. For this, seedling bearing *TOC1::LUC* would be transferred to free-run conditions at different phases of the entraining cycle. This would be particularly interesting for *TOC1*, because one could determine whether the physiological response displayed in the INOUT experiments was phase dependent. Applying these conditions to the double, triple and quadruple mutants of *cca1 lhy toc1 gi*, and *prp7 prp9 toc1 gi*, one could determine when the oscillator stops, and which genes were essential for temperature entrainment. Eventually, all developed knowledge would lead towards the physiological and genetic understanding of temperature effects in terms of entrainment.

6.2 DISCUSSION

In this PhD thesis, the temperature effect on the entrainment of the *A. thaliana* circadian clock was studied. Quantitative genetics and physiological experiments led to the conclusion that temperature inputs were mediated by a partially overlapping gene set as that determined for light-dark entrainment. In physiological experiments performed, it was shown that *TOC1* responds to light and also temperature changes, whereas *GI* responded only to light. A novel function for *GI* was also revealed in that it tracks photoperiod. Genetic analysis confirmed these functions. Both genes were candidates for the quantitative variation of *CCR2* period found in the CvL RIL. Natural selection regarding clock genes was observed in another two RIL collections. It was found that different QTLs were detected in different RILs, suggesting that circadian clock is an adaptive mechanism under strong environmental selection.

In chapter 3, it was shown that light-dark entrainment and temperature entrainment were controlled by a variety of QTL, which in the majority were common for both protocols. This was somewhat expected, since in nature, both inputs temporally coincide. Therefore genes might have been selected to mediate both inputs. Natural variation present in a given accession could have been strongly selected for the specific environmental conditions. To test this, two RILs collections were tested that they were generated from four different parental strains. The RILs were synchronized to the same conditions (conditions that none of the parental accessions was selected on). Different QTLs for each RIL population were identified for both entrainments (3.1.3, 3.2.3). This was a strong indication that circadian clock is a mechanism under selective pressure. Furthermore, in both RILs there was not much difference on the components that genetically control circadian rhythmicity in response to the different entrainments. Strong allelic interactions between the QTLs were described (3.1.4, 3.2.4). These different interactions could partially define the response to the two different entrainments. Furthermore, period shortening after temperature entrainment compared to light-dark entrainment, was observed in both RIL populations (3.1.1, 3.2.1). This practically means that the temperature entrainment protocol was effectively used for mapping. Moreover, the biological significance of this observation was that temperature fine tuned the light-dark entrained oscillator.

In addition to the preexisting RILS, one of the RIL populations generated during this thesis was also assayed after light-dark and temperature entrainment (4.1). Here, preliminary data supported the conclusion drawn by the existing two RILs (Chapter 3) that circadian rhythmicity in regard to the different inputs was mediated by the known and novel loci. Additionally, this new population was scored for flowering time, since extensive variation was observed (4.3). This trait is controlled by rhythmic external and internal cues. External cues such as photoperiod and ambient temperature induce flowering (McClung, 2006). The physiological promotion of flowering after prolonged exposure to extended low temperatures is called vernalization, and *FLC* is the central gene of this pathway (Amasino, 1996, 2005). Upon cold induction, *FLC* is repressed. This repression is an irreversible process in *A. thaliana*, leading to flowering. Upstream of *FLC*, a gene called *FRIGIDA* (*FRI*) induces *FLC* expression. Extensive natural variation have been found in both *FRI* and *FLC* (Shindo et al., 2005). In an assay of 192 accessions, *FRI* and *FLC* alleles were characterized in terms of flowering time (Shindo et al., 2005). It was shown that the parents of the C24WS RIL belong in different groups of *FRI* and *FLC* (Shindo et al., 2005). According to these publications, WS accession has a weak *FRI* and a strong *FLC*, whereas the C24 accession has a strong *FRI* but a weak *FLC*. Therefore it was expected that the extensive variation of this RIL would be observed due to the allelic interactions of these QTLs. This was found and was confirmed by statistical analysis (Table 4.3, Figure 4.17). Other QTLs that may account for the flowering-time variation in the C24WS, could be *FLF* and *FLG* (Alonso-Blanco et al., 1998). It was shown that the Cvi allele of these two loci account for late-flowering time (Alonso-Blanco et al., 1998).

A. thaliana is a facultative long day plant. This means that flowering is induced in response to long days versus short days (Searle and Coupland, 2004). Light perception is mediated by photoreceptors. Depending on light quality, three classes of photoreceptors exist. Red light is perceived by phytochromes (PHYs), and blue light by cryptochromes (CRYs) (McClung et al., 1989). The red and blue spectrum of light have opposite effects on flowering time, since loss-of-function of PHYB causes early flowering phenotype, whereas loss of function of CRY2 causes late-flowering phenotype (Mockler et al., 1999). This suggested that CRY2 promotes early flowering whereas PHYB represses early flowering. Furthermore, functional interaction between CRY2 and PHYB lead to the suggestion that they probably

mediate in the control of flowering time (Mas et al., 2000). The differential flowering phenotype can be explained by the effect of these two genes on a photoperiod inductive gene. This gene is called *CONSTANS* (Valverde et al., 2004). Valverde *et al.*, proposed that *PHYB* promotes degradation of *CO* in the morning, and *CRY2* stabilizes *CO* protein by antagonizing *PHYB* during evening. Furthermore an allelic variant of *CRY2* in the Cvi accession, was found to confer insensitivity to photoperiod due to an amino acid change (El-Din El-Assal et al., 2001). This amino acid change was found only in the Cvi-0 accession (El-Din El-Assal et al., 2001). Regarding my findings reported in Chapter 4, I found a QTL localized at the proximity of *CRY2*. As it was shown, extensive nucleotide variation at *CRY2* locus exists (Olsen et al., 2004). Based on the nucleotide diversity found in 95 accessions the haplotype structure of *CRY2* was divided in two highly differentiated haplogroups. According to polymorphisms WS belongs to the same haplogroup as *Ler*. The second parental strain of the C24WS collection (C24) was not studied in the work of Olsen *et al.* If the QTL at the first chromosome is *CRY2* then there should be variation between the alleles of C24 and WS. This could be tested by sequencing *CRY2* and comparing this to the existed data from WS. Further characterization of this QTL by constructing NILs could be pursued.

A potential problem, but also a great opportunity, is to study how the selection of the *CCR2* periodicity might have affected other circadian-regulated processes. The first chromosome QTL identified in the long-period selected lines as well as in ‘all lines’ in the C24WS collection suggested that this QTL was selected due to the phenotypic selection taken, while generating the RILs (4.1). Therefore, I would expect that a QTL at this locus would also be identified for the light-dark entrainment. The selection resulted in segregation distortion that was observed on the chromosome 1 (4.2). The segregation distortion in chromosome 3 was probably due to the T-DNA insertion of the *CCR2::LUC*, therefore QTL mapping at that area would be impossible since there is no allelic segregation. In case of a detected QTL at that genomic area, one must be skeptic that this is not a real QTL.

In Chapter 5, physiological and genetic experiments confirmed that *GI* and *TOC1* serve in different aspects of entrainment. I found that *GI* functions in photoperiod measurement at the transcriptional level (5.1). Additionally, the *TOC1* promoter was the only one of those tested that responded to temperature changes in the presence of light. For example, *CCA1/LHY* did not (5.2). In the past, it was

published that two oscillators exist based on temperature effects on *TOC1*, *CAB2*, and *CAT3* expression (Michael et al., 2003a). *TOC1* and *CAB2* display the same expression pattern and this was different from *CAT3*. Therefore, it was suggested that *TOC1* responds to light-dark entrainment, whereas *CAT3* to temperature entrainment (Michael et al., 2003a). Regarding my data, two hypotheses can be formed. The first hypothesis is that thermal entrainment is gated by light. Here, the gate acts on *TOC1*. If the feedback loop between *TOC1* and *CCA1/LHY* is still functional under the synchronous light-dark and temperature entrainment, then *CCA1/LHY* would suppress *TOC1* during day/warm period, and therefore the temperature regulation of *TOC1* would be ineffective. As soon as *TOC1* rises and *CCA1/LHY* protein levels decrease, then temperature can be input information to the clock mediated by *TOC1*. Moreover, the OUT experiments performed in Chapter 5 support the notion that warm temperatures can set the clock, since in the OUT experiments all clock promoters tested displayed a phase shift regarding the cool to warm transition, and the opposite transition was not observed (5.2). This suggests that warm temperatures had a similar effect to light, concerning the resetting of the oscillator. This is expected because in nature, light and warm temporally coincide. Alternatively, it was possible that *TOC1* was part of another oscillator that is primarily for temperature entrainment. Since *PRR9* and *PRR7* were shown to be required for entrainment by temperature, they might form a loop with *TOC1*. In that case, one can ask if *TOC1* still remains interlocked with *CCA1/LHY*. The quadruple mutants of *cca1 lhy tocl gi* and *toc1 gi prr9 prr7* that could be generated will be useful resources in direct clock assays to provide answers from all genetic perspective.

The transcriptional regulation of *TOC1* by temperature, to my knowledge, is the only one that has been reported in model organism. For example, in *Neurospora*, *FRQ* is regulated by temperature at post-transcriptional level (Liu et al., 1997; Liu, 2003). Temperature-dependent alternative splicing of the *FRQ* mRNA leads to two proteins forms, the long and the short. The temperature-dependent transcriptional regulation of *TOC1* could be determined by promoter analysis at the primary sequence.

Moreover, it was shown that in presence of blue light, *GI* protein stabilizes *ZTL* protein, a negative regulator of *TOC1* (Kim et al., 2007b) Therefore, *GI* protein, indirectly, affects *TOC1* protein accumulation. In temperature cycles, *TOC1* was found to be transcriptionally regulated by temperature, as it was observed under white

light (Chapter 5). It is of interest to test whether there is any temperature-dependent interaction between *TOC1*, to *GI* or to *ZTL*. Further, temperature entrainment in various monochromatic light quality assays would be define any light-dependent temperature regulation of *TOC1*.

Temperature changes are probably perceived at the membranes. It was shown that fatty acid desaturases seems to be involved in temperature sensing in the membranes (Los and Murata, 2000; Vaultier et al., 2006). So far, potential involvement of these enzymes to the temperature entrainment of the oscillator has not been shown. Furthermore, cytosolic calcium ion concentration is known to be modified by temperature. A recent study showed that these oscillations are an output of the circadian clock, in a light-quality dependent manner (Xu et al., 2007). Furthermore, light maintains robust rhythmicity of cytosolic calcium, but a cue other than light can elevate calcium levels during night (Xu et al., 2007). Since temperature is gated by light, it is of interest to determine whether temperature is the signal that elevates calcium levels during evening. An exciting hypothesis would be that calcium changes can mediate temperature information to the oscillator and thereby the oscillator would entrain to temperature.

Xu *et al.*, have shown that the cytosolic calcium was affected by *CCA1*, *LHY*, *ZTL*, *ELF3*, and *TOC1* (Xu et al., 2007). However, two different alleles of *toc1* mutant, *toc1-1* and *toc1-2* showed different phenotypes in *AEQUORIN* (*AEQ*) oscillations. *AEQ* was used as a reporter in this case for the calcium oscillations. *toc1-1* mutant was found to control differentially *CAB2* expression and cytosolic calcium (Xu et al., 2007). The period of *CAB2* oscillations was 21 hours whereas the period of *AEQ* oscillations, was similar to wild type. Additionally the *toc1-2* mutant displayed short period phenotype for both calcium oscillations and *CAB2* expression (Xu et al., 2007). The discrepancy of the two alleles probably is due to the mutation site. The *toc1-2* allele is alternatively spliced at the end of the first exon, which resulted in a truncated protein of 59 amino acids and therefore is a near loss of function allele, whereas the *toc1-1* allele has an amino acid change in the CCT domain, and clearly has some activity. It would be interesting to test the period of *CAB2* and *CCR2* expression in both mutant backgrounds after temperature entrainment. These experiments would serve as a link for temperature and calcium oscillations. Is it that temperature information goes to the oscillator indirectly via calcium due to these cell biology changes or actually temperature entrains the oscillator directly?

Temperature regulates the circadian machinery in two different ways. Changes in temperature synchronize the oscillator by delaying or advancing the phase of the rhythm. However, circadian rhythms are also temperature compensated, indicating that the pace of the rhythm does not change by temperature increases or decreases. Clearly, additional insights in these two processes are needed to understand the temperature effect on the circadian oscillator. As an example, in *Drosophila*, it was shown that both temperature entrainment and temperature compensation are mediated by the same gene products that are also involved in the light-dark entrainment (Glaser and Stanewsky, 2005; Ruoff et al., 2005; Kaushik et al., 2007). This suggests that the circadian machinery organization in entrainment by both signals, light and temperature, and the mechanism of entrainment by these two signals, is not very different. However, it was shown that in some neurons, temperature entrainment is mediated preferentially over light entrainment, suggesting that different oscillators might contribute to the differential regulation of the two signals.

In *A.thaliana*, it was shown that distinct oscillators exist in different tissues of intact plants (Thain et al., 2002). This was further supported by *CAB2* rhythms; in leaves that were entrained in antiphase, *CAB2* rhythms persisted in opposite phase under constant conditions. Furthermore, in the *toc1* mutant, *CAB2* expression and cytosolic calcium oscillations oscillated with different period indicating that multiple independent oscillators exist in different cell types that can remain uncoupled. In addition, two circadian oscillators were distinguished by differential response to temperature sensitivity (Michael et al., 2003a). Whether *TOC1* is part of only the temperature entrained oscillator remains to be elucidated. I showed that *TOC1* was the only gene that temperature phase shifts resulted in change in the transcription rate. The collective impact of this PhD thesis is that it serves as an entry point to the quantitative understanding of temperature entrainment of the *A. thaliana* circadian clock. This field hold promises to be a very exciting area for future discoveries.

7 REFERENCES

- Alabadi, D., Yanovsky, M.J., Mas, P., Harmer, S.L., and Kay, S.A.** (2002). Critical role for CCA1 and LHY in maintaining circadian rhythmicity in *Arabidopsis*. *Curr Biol* **12**, 757-761.
- Alabadi, D., Oyama, T., Yanovsky, M.J., Harmon, F.G., Mas, P., and Kay, S.A.** (2001). Reciprocal regulation between TOC1 and LHY/CCA1 within the *Arabidopsis* circadian clock. *Science* **293**, 880-883.
- Alonso-Blanco, C., Mendez-Vigo, B., and Koornneef, M.** (2005). From phenotypic to molecular polymorphisms involved in naturally occurring variation of plant development. *Int J Dev Biol* **49**, 717-732.
- Alonso-Blanco, C., El-Assal, S.E., Coupland, G., and Koornneef, M.** (1998). Analysis of natural allelic variation at flowering time loci in the Landsberg erecta and Cape Verde Islands ecotypes of *Arabidopsis thaliana*. *Genetics* **149**, 749-764.
- Alonso-Blanco, C., Peeters, A.J.M., Koornneef, M., Lister, C., Dean, C.** (1998). Development of an AFLP based linkage map of *Ler*, *Col* and *Cvi Arabidopsis thaliana* ecotypes and construction of a *Ler/Cvi* recombinant inbred line population. *Plant Journal* **14**, 259-271.
- Amasino, R.M.** (1996). Control of flowering time in plants. *Curr Opin Genet Dev* **6**, 480-487.
- Amasino, R.M.** (2005). Vernalization and flowering time. *Curr Opin Biotechnol* **16**, 154-158.
- An, H., Roussot, C., Suarez-Lopez, P., Corbesier, L., Vincent, C., Pineiro, M., Hepworth, S., Mouradov, A., Justin, S., Turnbull, C., and Coupland, G.** (2004). *CONSTANS* acts in the phloem to regulate a systemic signal that induces photoperiodic flowering of *Arabidopsis*. *Development* **131**, 3615-3626.
- Aronson, B.D., Johnson, K.A., Loros, J.J., and Dunlap, J.C.** (1994). Negative feedback defining a circadian clock: autoregulation of the clock gene frequency. *Science* **263**, 1578-1584.
- Ashmore, L.J., and Sehgal, A.** (2003). A fly's eye view of circadian entrainment. *J Biol Rhythms* **18**, 206-216.
- Balasubramanian, S., Sureshkumar, S., Agrawal, M., Michael, T.P., Wessinger, C., Maloof, J.N., Clark, R., Warthmann, N., Chory, J., and Weigel, D.** (2006). The *PHYTOCHROME C* photoreceptor gene mediates natural variation in flowering and growth responses of *Arabidopsis thaliana*. *Nat Genet* **38**, 711-715.
- Barak, S., Tobin, E.M., Andronis, C., Sugano, S., and Green, R.M.** (2000). All in good time: the *Arabidopsis* circadian clock. *Trends Plant Sci* **5**, 517-522.
- Bastow, R., Mylne, J.S., Lister, C., Lippman, Z., Martienssen, R.A., and Dean, C.** (2004). Vernalization requires epigenetic silencing of *FLC* by histone methylation. *Nature* **427**, 164-167.
- Blazquez, M.A., Ahn, J.H., and Weigel, D.** (2003). A thermosensory pathway controlling flowering time in *Arabidopsis thaliana*. *Nat Genet* **33**, 168-171.

- Boothroyd, C.E., Wijnen, H., Naef, F., Saez, L., and Young, M.W.** (2007). Integration of light and temperature in the regulation of circadian gene expression in *Drosophila*. *PLoS Genet* **3**, e54.
- Bretzl, H.** (1903). *Botanische Forschungen des Alexanderzuges*. (Leipzig, Germany:: B.G. Teubner).
- Buenning, E.** (1931). Untersuchungen ueber die autonomen tagesperiodischen Bewegungen der Primaerblaetter von *Phaseolus multiflorus*. *Jahrb. Wiss. Bot.* **75**, 439-480.
- Busza, A., Murad, A., and Emery, P.** (2007). Interactions between circadian neurons control temperature synchronization of *Drosophila* behavior. *J Neurosci* **27**, 10722-10733.
- Cao, S., Ye, M., and Jiang, S.** (2005). Involvement of GIGANTEA gene in the regulation of the cold stress response in *Arabidopsis*. *Plant Cell Rep* **24**, 683-690.
- Carpenter, C.D., Kreps, J.A., and Simon, A.E.** (1994). Genes encoding glycine-rich *Arabidopsis thaliana* proteins with RNA-binding motifs are influenced by cold treatment and an endogenous circadian rhythm. *Plant Physiol* **104**, 1015-1025.
- Chen, M., Chory, J., and Fankhauser, C.** (2004). Light signal transduction in higher plants. *Annu Rev Genet* **38**, 87-117.
- Cheng, P., Yang, Y., Gardner, K.H., and Liu, Y.** (2002). PAS domain-mediated WC-1/WC-2 interaction is essential for maintaining the steady-state level of WC-1 and the function of both proteins in circadian clock and light responses of *Neurospora*. *Mol Cell Biol* **22**, 517-524.
- Chinnusamy, V., Ohta, M., Kanrar, S., Lee, B.H., Hong, X., Agarwal, M., and Zhu, J.K.** (2003). ICE1: a regulator of cold-induced transcriptome and freezing tolerance in *Arabidopsis*. *Genes Dev* **17**, 1043-1054.
- Clough, S.J., and Bent, A.F.** (1998). Floral dip: a simplified method for *Agrobacterium*-mediated transformation of *Arabidopsis thaliana*. *Plant J* **16**, 735-743.
- Collett, M.A., Dunlap, J.C., and Loros, J.J.** (2001). Circadian clock-specific roles for the light response protein WHITE COLLAR-2. *Mol Cell Biol* **21**, 2619-2628.
- Correa, A., Lewis, Z.A., Greene, A.V., March, I.J., Gomer, R.H., and Bell-Pedersen, D.** (2003). Multiple oscillators regulate circadian gene expression in *Neurospora*. *Proc Natl Acad Sci U S A* **100**, 13597-13602.
- Covington, M.F., Panda, S., Liu, X.L., Strayer, C.A., Wagner, D.R., and Kay, S.A.** (2001). ELF3 modulates resetting of the circadian clock in *Arabidopsis*. *Plant Cell* **13**, 1305-1315.
- Crosthwaite, S.K., Loros, J.J., and Dunlap, J.C.** (1995). Light-induced resetting of a circadian clock is mediated by a rapid increase in frequency transcript. *Cell* **81**, 1003-1012.
- Darrah, C., Taylor, B.L., Edwards, K.D., Brown, P.E., Hall, A., and McWatters, H.G.** (2006). Analysis of phase of LUCIFERASE expression reveals novel circadian quantitative trait loci in *Arabidopsis*. *Plant Physiol* **140**, 1464-1474.
- Davis, S.J.** (2002). Photoperiodism: the coincidental perception of the season. *Curr Biol* **12**, R841-843.
- Davis, S.J., and Millar, A.J.** (2001). Watching the hands of the *Arabidopsis* biological clock. *Genome Biol* **2**, REVIEWS1008.
- de Mairan, J.** (1729). *Observation Botanique*. *Hist. Acad. Roy. Sci.*

- Denault, D.L., Loros, J.J., and Dunlap, J.C.** (2001). WC-2 mediates WC-1-FRQ interaction within the PAS protein-linked circadian feedback loop of *Neurospora*. *Embo J* **20**, 109-117.
- Devlin, P.F., and Kay, S.A.** (2000). Cryptochromes are required for phytochrome signaling to the circadian clock but not for rhythmicity. *Plant Cell* **12**, 2499-2510.
- Devlin, P.F., Kay, S.** (2001). Circadian photoreception. *Annu Rev Physiol* **63**, 677-694.
- Diernfellner, A., Colot, H.V., Dintsis, O., Loros, J.J., Dunlap, J.C., and Brunner, M.** (2007). Long and short isoforms of *Neurospora* clock protein FRQ support temperature-compensated circadian rhythms. *FEBS Lett* **581**, 5759-5764.
- Diernfellner, A.C., Schafmeier, T., Merrow, M.W., and Brunner, M.** (2005). Molecular mechanism of temperature sensing by the circadian clock of *Neurospora crassa*. *Genes Dev* **19**, 1968-1973.
- Ding, Z., Millar, A.J., Davis, A.M., and Davis, S.J.** (2007a). TIME FOR COFFEE encodes a nuclear regulator in the *Arabidopsis thaliana* circadian clock. *Plant Cell* **19**, 1522-1536.
- Ding, Z., Doyle, M.R., Amasino, R.M., and Davis, S.J.** (2007b). A complex genetic interaction between *Arabidopsis thaliana* TOC1 and CCA1/LHY in driving the circadian clock and in output regulation. *Genetics* **176**, 1501-1510.
- Dodd, A.N., Salathia, N., Hall, A., Kevei, E., Toth, R., Nagy, F., Hibberd, J.M., Millar, A.J., and Webb, A.A.** (2005). Plant circadian clocks increase photosynthesis, growth, survival, and competitive advantage. *Science* **309**, 630-633.
- Domagalska, M.A., Schomburg, F.M., Amasino, R.M., Vierstra, R.D., Nagy, F., and Davis, S.J.** (2007). Attenuation of brassinosteroid signaling enhances FLC expression and delays flowering. *Development* **134**, 2841-2850.
- Dowson-Day, M.J., and Millar, A.J.** (1999). Circadian dysfunction causes aberrant hypocotyl elongation patterns in *Arabidopsis*. *Plant J* **17**, 63-71.
- Doyle, M.R., Bizzell, C.M., Keller, M.R., Michaels, S.D., Song, J., Noh, Y.S., and Amasino, R.M.** (2005). HUA2 is required for the expression of floral repressors in *Arabidopsis thaliana*. *Plant J* **41**, 376-385.
- Doyle, M.R., Davis, S.J., Bastow, R.M., McWatters, H.G., Kozma-Bognar, L., Nagy, F., Millar, A.J., and Amasino, R.M.** (2002). The ELF4 gene controls circadian rhythms and flowering time in *Arabidopsis thaliana*. *Nature* **419**, 74-77.
- Dunlap, J.C., and Loros, J.J.** (2004). The *neurospora* circadian system. *J Biol Rhythms* **19**, 414-424.
- Dunlap, J.C., Loros, J.J., Aronson, B.D., Merrow, M., Crosthwaite, S., Bell-Pedersen, D., Johnson, K., Lindgren, K., and Garceau, N.Y.** (1995). The genetic basis of the circadian clock: identification of *frq* and *FRQ* as clock components in *Neurospora*. *Ciba Found Symp* **183**, 3-17; discussion 17-25.
- Edwards, K.D., Lynn, J.R., Gyula, P., Nagy, F., and Millar, A.J.** (2005). Natural allelic variation in the temperature-compensation mechanisms of the *Arabidopsis thaliana* circadian clock. *Genetics* **170**, 387-400.
- Edwards, K.D., Anderson, P.E., Hall, A., Salathia, N.S., Locke, J.C., Lynn, J.R., Straume, M., Smith, J.Q., and Millar, A.J.** (2006). FLOWERING LOCUS C mediates natural variation in the high-temperature response of the *Arabidopsis* circadian clock. *Plant Cell* **18**, 639-650.

- El-Din El-Assal, S., Alonso-Blanco, C., Peeters, A.J., Raz, V., and Koornneef, M.** (2001). A QTL for flowering time in *Arabidopsis* reveals a novel allele of *CRY2*. *Nat Genet* **29**, 435-440.
- Emery, P., So, W.V., Kaneko, M., Hall, J.C., and Rosbash, M.** (1998). *Drosophila* clock and light-regulated cryptochrome, is a major contributor to circadian rhythm resetting and photosensitivity. *Cell* **95**, 669-679.
- Emery, P., Stanewsky, R., Helfrich-Forster, C., Emery-Le, M., Hall, J.C., and Rosbash, M.** (2000). *Drosophila* *CRY* is a deep brain circadian photoreceptor. *Neuron* **26**, 493-504.
- Fankhauser, C., and Staiger, D.** (2002). Photoreceptors in *Arabidopsis thaliana*: light perception, signal transduction and entrainment of the endogenous clock. *Planta* **216**, 1-16.
- Farre, E.M., Harmer, S.L., Harmon, F.G., Yanovsky, M.J., and Kay, S.A.** (2005). Overlapping and distinct roles of *PRR7* and *PRR9* in the *Arabidopsis* circadian clock. *Curr Biol* **15**, 47-54.
- Fowler, S.G., Cook, D., and Thomashow, M.F.** (2005). Low temperature induction of *Arabidopsis* *CBF1*, *2*, and *3* is gated by the circadian clock. *Plant Physiol* **137**, 961-968.
- Franklin, K.A., and Whitelam, G.C.** (2004). Light signals, phytochromes and cross-talk with other environmental cues. *J Exp Bot* **55**, 271-276.
- Froehlich, A.C., Liu, Y., Loros, J.J., and Dunlap, J.C.** (2002). White Collar-1, a circadian blue light photoreceptor, binding to the frequency promoter. *Science* **297**, 815-819.
- Gardner, G.F., and Feldman, J.F.** (1980). The *frq* locus in *Neurospora crassa*: a key element in circadian clock organization. *Genetics* **96**, 877-886.
- Gazzani, S., Gendall, A.R., Lister, C., and Dean, C.** (2003). Analysis of the molecular basis of flowering time variation in *Arabidopsis* accessions. *Plant Physiol* **132**, 1107-1114.
- Gilmour, S.J., Zarka, D.G., Stockinger, E.J., Salazar, M.P., Houghton, J.M., and Thomashow, M.F.** (1998). Low temperature regulation of the *Arabidopsis* *CBF* family of AP2 transcriptional activators as an early step in cold-induced *COR* gene expression. *Plant J* **16**, 433-442.
- Glaser, F.T., and Stanewsky, R.** (2005). Temperature synchronization of the *Drosophila* circadian clock. *Curr Biol* **15**, 1352-1363.
- Glossop, N.R., Lyons, L.C., and Hardin, P.E.** (1999). Interlocked feedback loops within the *Drosophila* circadian oscillator. *Science* **286**, 766-768.
- Gong, Z., Lee, H., Xiong, L., Jagendorf, A., Stevenson, B., and Zhu, J.K.** (2002). RNA helicase-like protein as an early regulator of transcription factors for plant chilling and freezing tolerance. *Proc Natl Acad Sci U S A* **99**, 11507-11512.
- Gould, P.D., Locke, J.C., Larue, C., Southern, M.M., Davis, S.J., Hanano, S., Moyle, R., Milich, R., Putterill, J., Millar, A.J., and Hall, A.** (2006). The molecular basis of temperature compensation in the *Arabidopsis* circadian clock. *Plant Cell* **18**, 1177-1187.
- Green, R.M., and Tobin, E.M.** (1999). Loss of the circadian clock-associated protein 1 in *Arabidopsis* results in altered clock-regulated gene expression. *Proc Natl Acad Sci U S A* **96**, 4176-4179.
- Hadi, M.Z., Kemper, E., Wendeler, E., Reiss, B.** (2002). Simple and versatile selection of *Arabidopsis* transformants. *Plant Cell Rep* **21**, 130-135.

- Hall, A., Bastow, R.M., Davis, S.J., Hanano, S., McWatters, H.G., Hibberd, V., Doyle, M.R., Sung, S., Halliday, K.J., Amasino, R.M., and Millar, A.J. (2003). The TIME FOR COFFEE gene maintains the amplitude and timing of Arabidopsis circadian clocks. *Plant Cell* **15**, 2719-2729.
- Halliday, K.J., Salter, M.G., Thingnaes, E., and Whitelam, G.C. (2003). Phytochrome control of flowering is temperature sensitive and correlates with expression of the floral integrator FT. *Plant J* **33**, 875-885.
- Hardin, P.E. (2000). From biological clock to biological rhythms. *Genome Biology* **1**, 1-5.
- Hardin, P.E., Hall, J.C., and Rosbash, M. (1990). Feedback of the Drosophila period gene product on circadian cycling of its messenger RNA levels. *Nature* **343**, 536-540.
- Hardin, P.E., Krishnan, B., Houl, J.H., Zheng, H., Ng, F.S., Dryer, S.E., and Glossop, N.R. (2003). Central and peripheral circadian oscillators in Drosophila. *Novartis Found Symp* **253**, 140-150; discussion 150-160.
- Harmer, S.L., Hogenesch, J.B., Straume, M., Chang, H.S., Han, B., Zhu, T., Wang, X., Kreps, J.A., and Kay, S.A. (2000). Orchestrated transcription of key pathways in Arabidopsis by the circadian clock. *Science* **290**, 2110-2113.
- Hazen, S.P., Schultz, T.F., Pruneda-Paz, J.L., Borevitz, J.O., Ecker, J.R., and Kay, S.A. (2005). LUX ARRHYTHMO encodes a Myb domain protein essential for circadian rhythms. *Proc Natl Acad Sci U S A* **102**, 10387-10392.
- Heintzen, C., Nater, M., Apel, K., and Staiger, D. (1997). AtGRP7, a nuclear RNA-binding protein as a component of a circadian-regulated negative feedback loop in Arabidopsis thaliana. *Proc Natl Acad Sci U S A* **94**, 8515-8520.
- Hicks, K.A., Millar, A.J., Carre, I.A., Somers, D.E., Straume, M., Meeks-Wagner, D.R., and Kay, S.A. (1996). Conditional circadian dysfunction of the Arabidopsis early-flowering 3 mutant. *Science* **274**, 790-792.
- Initiative, A.G. (2000). Analysis of the genome sequence of the flowering plant Arabidopsis thaliana. *Nature* **408**, 796-815.
- Jander, G., Norris, S.R., Rounsley, S.D., Bush, D.F., Levin, I.M., and Last, R.L. (2002). Arabidopsis map-based cloning in the post-genome era. *Plant Physiol* **129**, 440-450.
- Johanson, U., West, J., Lister, C., Michaels, S., Amasino, R., and Dean, C. (2000). Molecular analysis of FRIGIDA, a major determinant of natural variation in Arabidopsis flowering time. *Science* **290**, 344-347.
- Kaneko, M., and Cahill, G.M. (2005). Light-dependent development of circadian gene expression in transgenic zebrafish. *PLoS Biol* **3**, e34.
- Kaushik, R., Nawathean, P., Busza, A., Murad, A., Emery, P., and Rosbash, M. (2007). PER-TIM interactions with the photoreceptor cryptochrome mediate circadian temperature responses in Drosophila. *PLoS Biol* **5**, e146.
- Keurentjes, J.J., Bentsink, L., Alonso-Blanco, C., Hanhart, C.J., Blankestijn-De Vries, H., Effgen, S., Vreugdenhil, D., and Koornneef, M. (2007). Development of a near-isogenic line population of Arabidopsis thaliana and comparison of mapping power with a recombinant inbred line population. *Genetics* **175**, 891-905.
- Kikis, E.A., Khanna, R., and Quail, P.H. (2005). ELF4 is a phytochrome-regulated component of a negative-feedback loop involving the central oscillator components CCA1 and LHY. *Plant J* **44**, 300-313.

- Kim, J.Y., Song, H.R., Taylor, B.L., and Carre, I.A.** (2003a). Light-regulated translation mediates gated induction of the Arabidopsis clock protein LHY. *Embo J* **22**, 935-944.
- Kim, T.S., Logsdon, B.A., Park, S., Mezey, J.G., and Lee, K.** (2007a). Quantitative Trait Loci for the Circadian Clock in *Neurospora crassa*. *Genetics* **177**, 2335-2347.
- Kim, W.Y., Geng, R., and Somers, D.E.** (2003b). Circadian phase-specific degradation of the F-box protein ZTL is mediated by the proteasome. *Proc Natl Acad Sci U S A* **100**, 4933-4938.
- Kim, W.Y., Fujiwara, S., Suh, S.S., Kim, J., Kim, Y., Han, L., David, K., Putterill, J., Nam, H.G., and Somers, D.E.** (2007b). ZEITLUPE is a circadian photoreceptor stabilized by GIGANTEA in blue light. *Nature* **449**, 356-360.
- Knight, H., Trewavas, A.J., and Knight, M.R.** (1996). Cold calcium signaling in Arabidopsis involves two cellular pools and a change in calcium signature after acclimation. *Plant Cell* **8**, 489-503.
- Konopka, R.J., and Benzer, S.** (1971). Clock mutants of *Drosophila melanogaster*. *Proc Natl Acad Sci U S A* **68**, 2112-2116.
- Koornneef, M., Hanhart, C.J., and van der Veen, J.H.** (1991). A genetic and physiological analysis of late flowering mutants in *Arabidopsis thaliana*. *Mol Gen Genet* **229**, 57-66.
- Koornneef, M., Alonso-Blanco, C., and Vreugdenhil, D.** (2004). Naturally occurring genetic variation in *Arabidopsis thaliana*. *Annu Rev Plant Biol* **55**, 141-172.
- Kreps, J.A., and Simon, A.E.** (1997). Environmental and genetic effects on circadian clock-regulated gene expression in Arabidopsis. *Plant Cell* **9**, 297-304.
- Kuno, N., Geir Moeller, S., Shinomura, T., Xu, X., Chua, N.** (2003). The Novel MYB protein EPR1 is a Component of a Slave Circadian Oscillator in Arabidopsis. *Plant Cell*.
- Lahiri, K., Vallone, D., Gondi, S.B., Santoriello, C., Dickmeis, T., and Foulkes, N.S.** (2005). Temperature regulates transcription in the zebrafish circadian clock. *PLoS Biol* **3**, e351.
- Lee, B.H., Henderson, D.A., and Zhu, J.K.** (2005). The Arabidopsis cold-responsive transcriptome and its regulation by ICE1. *Plant Cell* **17**, 3155-3175.
- Lee, K., Loros, J.J., and Dunlap, J.C.** (2000). Interconnected feedback loops in the *Neurospora* circadian system. *Science* **289**, 107-110.
- Lee, K., Dunlap, J.C., and Loros, J.J.** (2003). Roles for WHITE COLLAR-1 in circadian and general photoperception in *Neurospora crassa*. *Genetics* **163**, 103-114.
- Liu, X.L., Covington, M.F., Fankhauser, C., Chory, J., and Wagner, D.R.** (2001). ELF3 encodes a circadian clock-regulated nuclear protein that functions in an Arabidopsis PHYB signal transduction pathway. *Plant Cell* **13**, 1293-1304.
- Liu, Y.** (2003). Molecular mechanisms of entrainment in the *Neurospora* circadian clock. *J Biol Rhythms* **18**, 195-205.
- Liu, Y., Garceau, N.Y., Loros, J.J., and Dunlap, J.C.** (1997). Thermally regulated translational control of FRQ mediates aspects of temperature responses in the *neurospora* circadian clock. *Cell* **89**, 477-486.
- Locke, J.C., Southern, M.M., Kozma-Bognar, L., Hibberd, V., Brown, P.E., Turner, M.S., and Millar, A.J.** (2005). Extension of a genetic network model

- by iterative experimentation and mathematical analysis. *Mol Syst Biol* **1**, 2005 0013.
- Locke, J.C., Kozma-Bognar, L., Gould, P.D., Feher, B., Kevei, E., Nagy, F., Turner, M.S., Hall, A., and Millar, A.J.** (2006). Experimental validation of a predicted feedback loop in the multi-oscillator clock of *Arabidopsis thaliana*. *Mol Syst Biol* **2**, 59.
- Lopez-Olmeda, J.F., Sanchez-Vazquez, F.J.** (2006). Light and temperature cycles as zeitgebers of zebrafish (*Danio rerio*) circadian activity rhythms. *Chronobiology International* **23**, 537-550.
- Los, D.A., and Murata, N.** (2000). Regulation of enzymatic activity and gene expression by membrane fluidity. *Sci STKE* **2000**, PE1.
- Loudet, O., Chaillou, S., Camilleri, C., Bouchez, D., and Daniel-Vedele, F.** (2002). Bay-0 x Shahdara recombinant inbred line population: a powerful tool for the genetic dissection of complex traits in *Arabidopsis*. *Theor Appl Genet* **104**, 1173-1184.
- Makino, S., Matsushika, A., Kojima, M., Yamashino, T., and Mizuno, T.** (2002). The APRR1/TOC1 quintet implicated in circadian rhythms of *Arabidopsis thaliana*: I. Characterization with APRR1-overexpressing plants. *Plant Cell Physiol* **43**, 58-69.
- Maloof, J.N., Borevitz, J.O., Dabi, T., Lutes, J., Nehring, R.B., Redfern, J.L., Trainer, G.T., Wilson, J.M., Asami, T., Berry, C.C., Weigel, D., and Chory, J.** (2001). Natural variation in light sensitivity of *Arabidopsis*. *Nat Genet* **29**, 441-446.
- Martin-Tryon, E.L., Kreps, J.A., and Harmer, S.L.** (2007). GIGANTEA acts in blue light signaling and has biochemically separable roles in circadian clock and flowering time regulation. *Plant Physiol* **143**, 473-486.
- Mas, P., Devlin, P.F., Panda, S., and Kay, S.A.** (2000). Functional interaction of phytochrome B and cryptochrome 2. *Nature* **408**, 207-211.
- Mas, P., Kim, W.Y., Somers, D.E., and Kay, S.A.** (2003). Targeted degradation of TOC1 by ZTL modulates circadian function in *Arabidopsis thaliana*. *Nature* **426**, 567-570.
- McClung, C.R.** (2006). *Plant Circadian Rhythms*. *Plant Cell* **18**, 792-803.
- McClung, C.R., Fox, B.A., and Dunlap, J.C.** (1989). The *Neurospora* clock gene frequency shares a sequence element with the *Drosophila* clock gene period. *Nature* **339**, 558-562.
- McWatters, H.G., Bastow, R.M., Hall, A., and Millar, A.J.** (2000). The ELF3 zeitnehmer regulates light signalling to the circadian clock. *Nature* **408**, 716-720.
- McWatters, H.G., Kolmos, E., Hall, A., Doyle, M.R., Amasino, R.M., Gyula, P., Nagy, F., Millar, A.J., and Davis, S.J.** (2007). ELF4 is required for oscillatory properties of the circadian clock. *Plant Physiol* **144**, 391-401.
- Medina, J., BARGUES, M., Terol, J., Perez-Alonso, M., and Salinas, J.** (1999). The *Arabidopsis* CBF gene family is composed of three genes encoding AP2 domain-containing proteins whose expression is regulated by low temperature but not by abscisic acid or dehydration. *Plant Physiol* **119**, 463-470.
- Merrow, M., Brunner, M., and Roenneberg, T.** (1999). Assignment of circadian function for the *Neurospora* clock gene frequency. *Nature* **399**, 584-586.
- Merrow, M., Boesl, C., Ricken, J., Messerschmitt, M., Goedel, M., Roenneberg, T.** (2006). Entrainment of the *Neurospora* circadian clock. *Chronobiology International* **23**, 71-80.

- Michael, T.P., and McClung, C.R.** (2002). Phase-specific circadian clock regulatory elements in Arabidopsis. *Plant Physiol* **130**, 627-638.
- Michael, T.P., Salome, P.A., and McClung, C.R.** (2003a). Two Arabidopsis circadian oscillators can be distinguished by differential temperature sensitivity. *Proc Natl Acad Sci U S A* **100**, 6878-6883.
- Michael, T.P., Salome, P.A., Yu, H.J., Spencer, T.R., Sharp, E.L., McPeck, M.A., Alonso, J.M., Ecker, J.R., and McClung, C.R.** (2003b). Enhanced fitness conferred by naturally occurring variation in the circadian clock. *Science* **302**, 1049-1053.
- Michael, T.P., Mockler, T.C., Breton, G., McEntee, C., Byer, A., Trout, J.D., Hazen, S.P., Shen, R., Priest, H.D., Sullivan, C.M., Givan, S.A., Yanovsky, M., Hong, F., Kay, S.A., and Chory, J.** (2008). Network Discovery Pipeline Elucidates Conserved Time-of-Day-Specific cis-Regulatory Modules. *PLoS Genet* **4**, e14.
- Michaels, S.D., and Amasino, R.M.** (1999). FLOWERING LOCUS C encodes a novel MADS domain protein that acts as a repressor of flowering. *Plant Cell* **11**, 949-956.
- Millar, A.J.** (2004). Input signals to the plant circadian clock. *J. Exp. Bot.* **55**, 277-283.
- Millar, A.J., Carre, I.A., Strayer, C.A., Chua, N.H., and Kay, S.A.** (1995). Circadian clock mutants in Arabidopsis identified by luciferase imaging. *Science* **267**, 1161-1163.
- Mockler, T.C., Guo, H., Yang, H., Duong, H., and Lin, C.** (1999). Antagonistic actions of Arabidopsis cryptochromes and phytochrome B in the regulation of floral induction. *Development* **126**, 2073-2082.
- Murtas, G., and Millar, A.J.** (2000). How plants tell the time. *Curr Opin Plant Biol* **3**, 43-46.
- Mylne, J.S., Barrett, L., Tessadori, F., Mesnage, S., Johnson, L., Bernatavichute, Y.V., Jacobsen, S.E., Fransz, P., and Dean, C.** (2006). LHP1, the Arabidopsis homologue of HETEROCHROMATIN PROTEIN1, is required for epigenetic silencing of FLC. *Proc Natl Acad Sci U S A* **103**, 5012-5017.
- Nagy, F., and Schafer, E.** (2002). Phytochromes control photomorphogenesis by differentially regulated, interacting signaling pathways in higher plants. *Annu Rev Plant Biol* **53**, 329-355.
- Neff, M.M., Turk, E., Kalishman, M.** (2002). Web-based primer design for single nucleotide polymorphism analysis. *Trends in Genetics* **18**, 613-.
- Olsen, K.M., Halldorsdottir, S.S., Stinchcombe, J.R., Weinig, C., Schmitt, J., and Purugganan, M.D.** (2004). Linkage disequilibrium mapping of Arabidopsis CRY2 flowering time alleles. *Genetics* **167**, 1361-1369.
- Onai, K., and Ishiura, M.** (2005). PHYTOCLOCK 1 encoding a novel GARP protein essential for the Arabidopsis circadian clock. *Genes Cells* **10**, 963-972.
- Pando, M.P., and Sassone-Corsi, P.** (2002). Unraveling the mechanisms of the vertebrate circadian clock: zebrafish may light the way. *Bioessays* **24**, 419-426.
- Pittendrigh, C.S., Daan, S.** (1976). A functional analysis of circadian pacemakers in nocturnal rodents. IV. Entrainment: Pacemaker as clock. *J. Comp. Physiol.* **106**, 291-331.
- Pittendrigh, C.S., Minis, D.H.** (1964). The entrainment of circadian oscillations by light and their role as photoperiodic clocks. *Am. Nat.* **98**, 261-322.

- Plautz, J.D., Straume, M., Stanewsky, R., Jamison, C.F., Brandes, C., Dowse, H. B., Hall, J.C., Kay, S.A.** (1997). Quantitative analysis of *Drosophila* period Gene Transcription in Living Animals. *J Biol Rhythms* **12**, 204.
- Plautz, J. D., K., M., Hall, J.C., Kay, S.F.** (1997). Independent photoreceptive circadian clocks throughout *Drosophila*. *Science* **278**, 1632-1635.
- Putterill, J., Robson, F., Lee, K., Simon, R., and Coupland, G.** (1995). The *CONSTANS* gene of *Arabidopsis* promotes flowering and encodes a protein showing similarities to zinc finger transcription factors. *Cell* **80**, 847-857.
- Ramos, A., Perez-Solis, E., Ibanez, C., Casado, R., Collada, C., Gomez, L., Aragoncillo, C., and Allona, I.** (2005). Winter disruption of the circadian clock in chestnut. *Proc Natl Acad Sci U S A* **102**, 7037-7042.
- Rensing, L., and Monnerjahn, C.** (1996). Heat shock proteins and circadian rhythms. *Chronobiol Int* **13**, 239-250.
- Ruoff, P., Christensen, M.K., and Sharma, V.K.** (2005). *PER/TIM*-mediated amplification, gene dosage effects and temperature compensation in an interlocking-feedback loop model of the *Drosophila* circadian clock. *J Theor Biol* **237**, 41-57.
- Salathia, N., Davis, S.J., Lynn, J.R., Michaels, S.D., Amasino, R.M., and Millar, A.J.** (2006). *FLOWERING LOCUS C*-dependent and -independent regulation of the circadian clock by the autonomous and vernalization pathways. *BMC Plant Biol* **6**, 10.
- Salome, P.A., and McClung, C.R.** (2005). *PSEUDO-RESPONSE REGULATOR 7* and *9* are partially redundant genes essential for the temperature responsiveness of the *Arabidopsis* circadian clock. *Plant Cell* **17**, 791-803.
- Sawyer, L.A., Hennessy, J.M., Peixoto, A.A., Rosato, E., Parkinson, H., Costa, R., and Kyriacou, C.P.** (1997). Natural variation in a *Drosophila* clock gene and temperature compensation. *Science* **278**, 2117-2120.
- Schmid, K.J., Rosleff-Soerensen, T., Stracke, R., Toerjek, O., Altmann, T., Mitchell-Olds, T., Weisshaar, B.** (2003). Large-Scale Identification and Analysis of Genome-Wide-Single-Nucleotide Polymorphisms for Mapping in *Arabidopsis thaliana*. *Genome Research* **13**, 1250-1257.
- Searle, I., and Coupland, G.** (2004). Induction of flowering by seasonal changes in photoperiod. *Embo J* **23**, 1217-1222.
- Searle, I., He, Y., Turck, F., Vincent, C., Fornara, F., Krober, S., Amasino, R.A., and Coupland, G.** (2006). The transcription factor *FLC* confers a flowering response to vernalization by repressing meristem competence and systemic signaling in *Arabidopsis*. *Genes Dev* **20**, 898-912.
- Sehgal, A., Rothenfluh-Hilfiker, A., Hunter-Ensor, M., Chen, Y., Myers, M.P., and Young, M.W.** (1995). Rhythmic expression of *timeless*: a basis for promoting circadian cycles in period gene autoregulation. *Science* **270**, 808-810.
- Shindo, C., Aranzana, M.J., Lister, C., Baxter, C., Nicholls, C., Nordborg, M., and Dean, C.** (2005). Role of *FRIGIDA* and *FLOWERING LOCUS C* in determining variation in flowering time of *Arabidopsis*. *Plant Physiol* **138**, 1163-1173.
- Somers, D.E., Devlin, P.F., and Kay, S.A.** (1998a). Phytochromes and cryptochromes in the entrainment of the *Arabidopsis* circadian clock. *Science* **282**, 1488-1490.

- Somers, D.E., Webb, A.A., Pearson, M., and Kay, S.A.** (1998b). The short-period mutant, *toc1-1*, alters circadian clock regulation of multiple outputs throughout development in *Arabidopsis thaliana*. *Development* **125**, 485-494.
- Staiger, D., Zecca, L., Wiczyk, K., Kirk, D.A., Apel, K., and Eckstein, L.** (2003a). The circadian clock regulated RNA-binding protein AtGRP7 autoregulates its expression by influencing alternative splicing of its own pre-mRNA. *Plant J* **33**, 361-371.
- Staiger, D., Allenbach, L., Salathia, N., Fiechter, V., Davis, S.J., Millar, A.J., Chory, J., and Fankhauser, C.** (2003b). The *Arabidopsis* SRR1 gene mediates phyB signaling and is required for normal circadian clock function. *Genes Dev* **17**, 256-268.
- Stanewsky, R., Kaneko, M., Emery, P., Beretta, B., Wager-Smith, K., Kay, S.A., Rosbash, M., and Hall, J.C.** (1998). The *cryb* mutation identifies cryptochrome as a circadian photoreceptor in *Drosophila*. *Cell* **95**, 681-692.
- Stitt, M., and Hurry, V.** (2002). A plant for all seasons: alterations in photosynthetic carbon metabolism during cold acclimation in *Arabidopsis*. *Curr Opin Plant Biol* **5**, 199-206.
- Strand, A., Hurry, V., Henkes, S., Huner, N., Gustafsson, P., Gardestrom, P., and Stitt, M.** (1999). Acclimation of *Arabidopsis* leaves developing at low temperatures. Increasing cytoplasmic volume accompanies increased activities of enzymes in the Calvin cycle and in the sucrose-biosynthesis pathway. *Plant Physiol* **119**, 1387-1398.
- Strayer, C., Oyama, T., Schultz, T.F., Raman, R., Somers, D.E., Mas, P., Panda, S., Kreps, J.A., and Kay, S.A.** (2000). Cloning of the *Arabidopsis* clock gene *TOC1*, an autoregulatory response regulator homolog. *Science* **289**, 768-771.
- Suarez-Lopez, P., Wheatley, K., Robson, F., Onouchi, H., Valverde, F., and Coupland, G.** (2001). *CONSTANS* mediates between the circadian clock and the control of flowering in *Arabidopsis*. *Nature* **410**, 1116-1120.
- Swarup, K., Alonso-Blanco, C., Lynn, J.R., Michaels, S.D., Amasino, R.M., Koornneef, M., and Millar, A.J.** (1999). Natural allelic variation identifies new genes in the *Arabidopsis* circadian system. *Plant J* **20**, 67-77.
- Sweeney, B.M.** (1987). *Rhythmic phenomena in plants*, 2nd edition, Academic Press.
- Tajima, T., Oda, A., Nakagawa, M., Kamada, H., Mizoguchi, T.** (2007). Natural variation of polyglutamine repeats of a circadian clock gene *ELF3* in *Arabidopsis*. *Plant Biotechnology* **24**, 237-240.
- Thain, S.C., Murtas, G., Lynn, J.R., McGrath, R.B., and Millar, A.J.** (2002). The circadian clock that controls gene expression in *Arabidopsis* is tissue specific. *Plant Physiol* **130**, 102-110.
- Toerjek, O., Berger, D., Meyer, R.C., Muessig, C., Schmid, K. J., Rosleff-Soerensen, T., Weisshaar, B., Mitchell-Olds, T., Altmann, T.** (2003). Establishment of a high-efficiency SNP-based framework marker set for *Arabidopsis*. *Plant Journal* **36**, 122-140.
- Toth, R., Kevei, E., Hall, A., Millar, A.J., Nagy, F., and Kozma-Bognar, L.** (2001). Circadian clock-regulated expression of phytochrome and cryptochrome genes in *Arabidopsis*. *Plant Physiol* **127**, 1607-1616.
- Valverde, F., Mouradov, A., Soppe, W., Ravenscroft, D., Samach, A., and Coupland, G.** (2004). Photoreceptor regulation of *CONSTANS* protein in photoperiodic flowering. *Science* **303**, 1003-1006.
- van Doorn, W.G., and Van Meeteren, U.** (2003). Flower opening and closure: a review. *J Exp Bot* **54**, 1801-1812.

- Vaultier, M.N., Cantrel, C., Vergnolle, C., Justin, A.M., Demandre, C., Benhassaine-Kesri, G., Cicek, D., Zachowski, A., and Ruelland, E.** (2006). Desaturase mutants reveal that membrane rigidification acts as a cold perception mechanism upstream of the diacylglycerol kinase pathway in *Arabidopsis* cells. *FEBS Lett* **580**, 4218-4223.
- Wang, Z.Y., and Tobin, E.M.** (1998). Constitutive expression of the CIRCADIAN CLOCK ASSOCIATED 1 (CCA1) gene disrupts circadian rhythms and suppresses its own expression. *Cell* **93**, 1207-1217.
- Waterhouse, J., Reilly, T., Atkinson, G., Edwards, B.** (2007). Jet lag: trends and coping strategies. *The Lancet* **369**, 1117-.
- Werner, J.D., Borevitz, J.O., Warthmann, N., Trainer, G.T., Ecker, J.R., Chory, J., and Weigel, D.** (2005). Quantitative trait locus mapping and DNA array hybridization identify an FLM deletion as a cause for natural flowering-time variation. *Proc Natl Acad Sci U S A* **102**, 2460-2465.
- Whitmore, D., Foulkes, N.S., and Sassone-Corsi, P.** (2000). Light acts directly on organs and cells in culture to set the vertebrate circadian clock. *Nature* **404**, 87-91.
- Xu, X., Hotta, C.T., Dodd, A.N., Love, J., Sharrock, R., Lee, Y.W., Xie, Q., Johnson, C.H., and Webb, A.A.** (2007). Distinct Light and Clock Modulation of Cytosolic Free Ca²⁺ Oscillations and Rhythmic CHLOROPHYLL A/B BINDING PROTEIN2 Promoter Activity in *Arabidopsis*. *Plant Cell* **19**, 3474-3490.
- Yanovsky, M.J., and Kay, S.A.** (2002). Molecular basis of seasonal time measurement in *Arabidopsis*. *Nature* **419**, 308-312.
- Yanovsky, M.J., Mazzella, M.A., and Casal, J.J.** (2000). A quadruple photoreceptor mutant still keeps track of time. *Curr Biol* **10**, 1013-1015.
- Yanovsky, M.J., Mazzella, M.A., Whitelam, G.C., and Casal, J.J.** (2001). Resetting of the circadian clock by phytochromes and cryptochromes in *Arabidopsis*. *J Biol Rhythms* **16**, 523-530.
- Yu, W., Zheng, H., Houl, J.H., Dauwalder, B., and Hardin, P.E.** (2006). PER-dependent rhythms in CLK phosphorylation and E-box binding regulate circadian transcription. *Genes Dev* **20**, 723-733.
- Zeilinger, M.N., Farre, E.M., Taylor, S.R., Kay, S.A., and Doyle, F.J., 3rd.** (2006). A novel computational model of the circadian clock in *Arabidopsis* that incorporates PRR7 and PRR9. *Mol Syst Biol* **2**, 58.

APPENDIX 1

The genotype of 85 C24WS RILs as determined by scoring 34 SSLP, SSR and CAPS markers.

For each marker locus a denoted C24 genome, b denoted WS genome, h denoted heterozygotes, and minus sign denoted not determined.

Marker	1	2	3	4	5	6	7	8	9	10	11	12
NGA59	a	a	b	b	a	b	a	a	a	a	a	a
NGA63	a	a	b	b	b	b	a	a	b	b	a	b
MSAT1.10	a	a	b	b	b	b	b	a	b	b	a	a
ATHS0392	a	a	a	b	a	a	a	a	b	b	a	b
T27K12	b	b	b	a	b	a	a	a	b	-	a	b
CIW1	a	a	a	a	a	a	a	a	b	b	a	b
NGA128	a	a	a	a	a	a	a	a	b	b	a	b
NGA111	a	a	a	a	a	a	a	a	b	a	b	b
RG A	b	b	b	b	a	b	a	a	a	a	a	a
MSAT2.28	a	b	b	h	a	b	a	a	a	a	a	a
MSAT2.11	a	b	b	b	a	b	a	a	a	a	a	a
MSAT2.41	a	b	b	b	a	b	a	a	a	a	a	a
NGA361	a	a	b	b	a	b	a	a	a	a	a	a
MSAT2.22	a	b	b	a	a	b	a	a	a	a	a	a
NGA172	b	a	b	b	b	b	b	b	b	b	b	a
NGA162	b	b	b	b	b	b	b	b	b	b	b	b
MSAT3.19	b	b	b	b	b	b	b	b	b	b	b	h
MSAT3.28	a	a	a	a	b	a	a	a	a	a	a	a
NGA6	a	a	a	a	a	a	a	a	a	a	a	a
FRI	a	a	a	a	a	a	a	a	a	a	a	a
T3H13	a	a	a	a	a	a	a	b	b	a	a	b
MSAT4.16	a	a	a	a	a	a	a	b	b	a	a	b
MSAT4.15	a	a	a	a	a	a	a	b	a	a	b	b
CIW7	a	a	a	a	a	a	a	a	a	a	b	b
MSAT4.12	a	a	a	a	a	a	a	a	a	a	b	b
MSAT4.28	b	a	a	a	a	a	a	a	b	a	b	b
NGA158	a	b	b	a	a	b	a	a	a	a	a	a
NGA106	a	b	b	a	a	b	a	a	a	a	a	a
MSAT5.14	a	a	b	a	h	a	a	a	a	a	a	a
NGA76	-	-	b	-	b	-	-	-	-	-	-	-
MSAT5.22	b	a	b	h	b	a	a	a	a	a	a	a
ATHS0191	b	a	b	b	b	a	a	a	a	a	a	a
MSAT5.9	b	a	b	b	b	a	a	a	a	a	a	a
JV61/62	a	a	a	a	a	a	a	b	b	b	a	a

Marker	13	14	15	16	17	18	19	20	21	22	23	24
NGA59	a	b	a	h	b	b	b	a	b	a	a	a
NGA63	b	b	a	b	b	b	b	a	b	a	a	a
MSAT1.10	b	b	a	b	b	b	b	b	b	a	a	a
ATHS0392	a	b	a	b	b	b	b	b	a	a	b	b
T27K12	a	b	a	b	a	a	a	a	a	b	b	b
CIW1	b	b	a	b	a	a	a	a	a	b	b	b
NGA128	b	b	a	b	a	a	a	a	a	b	b	b
NGA111	a	a	a	a	a	a	a	a	a	a	b	b
RGA	a	b	b	a	a	b	b	b	b	a	a	a
MSAT2.28	a	a	a	a	a	a	-	b	b	a	a	a
MSAT2.11	a	a	b	a	a	a	b	a	b	a	a	a
MSAT2.41	a	a	b	a	a	a	b	a	b	a	a	a
NGA361	a	a	b	a	a	a	a	a	b	a	a	a
MSAT2.22	a	a	b	a	b	a	b	b	b	a	a	a
NGA172	a	a	-	a	a	a	a	a	a	b	b	a
NGA162	b	b	b	a	b	b	b	b	b	b	b	b
MSAT3.19	b	b	b	b	b	b	b	b	b	b	a	b
MSAT3.28	a	b	b	b	a	b	b	b	b	b	b	b
NGA6	a	b	b	a	b	a	b	a	a	b	b	b
FRI	a	a	a	a	b	a	a	a	b	b	a	a
T3H13	a	a	a	a	a	a	a	a	a	b	a	a
MSAT4.16	a	a	a	a	a	a	a	a	a	b	b	b
MSAT4.15	b	a	a	a	a	a	a	a	a	a	a	a
CIW7	b	a	a	a	a	a	a	a	a	a	a	a
MSAT4.12	b	a	a	a	a	a	a	a	a	a	a	a
MSAT4.28	b	-	-	-	-	-	-	-	-	a	a	a
NGA158	a	b	b	a	b	b	a	a	a	a	a	b
NGA106	a	b	b	a	b	a	a	a	a	a	b	b
MSAT5.14	a	b	b	a	a	a	b	a	a	a	b	b
NGA76		b	b	-	b	-	b	-	-	-	b	-
MSAT5.22	a	b	b	a	b	a	b	a	a	b	b	a
ATHS0191	a	b	b	a	b	a	b	a	a	b	a	a
MSAT5.9	a	b	b	b	b	b	b	a	a	b	a	a
JV61/62	a	b	b	b	a	b	b	a	b	b	a	a

Marker	25	26	27	28	29	30	31	32	33	34	35	36
NGA59	a	a	-	a	a	a	a	a	a	a	a	a
NGA63	a	a	a	a	a	a	a	a	a	a	a	a
MSAT1.10	a	a	a	a	a	a	a	a	a	a	a	a
ATHS0392	a	b	a	b	b	a	a	a	a	b	a	b
T27K12	b	a	a	a	b	a	a	a	a	a	a	b
CIW1	b	a	a	b	b	a	a	a	b	a	a	b
NGA128	b	a	b	b	b	a	a	a	b	a	a	b
NGA111	b	-	b	b	b	-	-	-	-	-	-	-
RGA	a	b	b	a	b	a	a	a	a	a	a	a
MSAT2.28	a	b	b	b	b	a	a	a	a	a	a	a
MSAT2.11	a	b	a	b	a	a	a	a	a	a	a	a
MSAT2.41	a	b	a	b	a	a	a	a	a	a	a	a
NGA361	a	b	a	b	a	a	a	a	a	a	a	a
MSAT2.22	a	b	a	b	a	a	a	a	a	a	a	a
NGA172	b	b	b	a	b	b	b	b	a	b	b	b
NGA162	b	b	b	b	b	b	b	b	b	b	b	b
MSAT3.19	a	b	b	b	b	b	a	b	b	b	b	b
MSAT3.28	b	a	b	b	b	b	b	a	a	a	a	a
NGA6	b	b	b	b	b	b	b	a	a	b	a	a
FRI	a	a	b	b	b	a	a	a	a	a	a	a
T3H13	a	a	a	b	a	a	a	a	a	a	a	a
MSAT4.16	a	a	b	a	a	-	-	-	-	-	-	-
MSAT4.15	a	a	a	a	a	b	a	b	a	b	a	a
CIW7	a	a	a	a	a	b	a	b	a	b	b	a
MSAT4.12	a	a	a	a	a	b	a	a	b	a	b	a
MSAT4.28	a	a	b	b	b	b	a	a	a	a	a	a
NGA158	a	a	a	b	b	a	a	a	a	a	a	a
NGA106	b	a	a	b	b	a	a	a	a	a	a	a
MSAT5.14	b	a	a	b	b	a	a	a	a	a	a	a
NGA76	b	-	-	b	-	-	-	-	-	-	-	-
MSAT5.22	b	a	a	b	a	a	a	a	a	a	a	a
ATHS0191	b	b	a	a	a	a	a	a	a	a	a	a
MSAT5.9	b	b	b	b	a	a	a	a	a	a	a	a
JV61/62	b	b	b	b	b	a	a	a	a	a	a	a

Marker	37	38	39	40	41	42	43	44	45	46	47	48
NGA59	a	a	a	a	a	a	a	a	a	a	a	a
NGA63	a	a	a	a	a	a	a	a	b	a	b	a
MSAT1.10	a	b	a	b	b	a	b	a	b	a	b	b
ATHS0392	b	b	a	b	b	a	b	a	b	b	a	b
T27K12	b	b	b	a	b	a	b	-	-	-	-	-
CIW1	b	b	b	b	b	a	b	a	a	a	a	a
NGA128	b	b	b	a	b	a	b	-	-	-	-	-
NGA111	-	-	-	-	-	-	-	-	-	-	-	-
RGA	a	a	a	a	a	a	a	a	a	a	a	a
MSAT2.28	a	a	a	a	a	a	a	-	-	-	-	-
MSAT2.11	a	a	a	a	a	a	a	a	a	a	a	a
MSAT2.41	a	a	a	a	a	a	a	a	a	a	a	b
NGA361	a	a	a	a	a	a	a	a	a	a	a	b
MSAT2.22	a	a	a	a	a	a	a	a	a	a	a	b
NGA172	b	b	b	a	b	b	b	b	b	b	a	b
NGA162	b	b	b	b	b	b	b	b	b	b	b	b
MSAT3.19	b	b	b	b	b	b	b	a	b	b	b	b
MSAT3.28	b	-	a	b	a	a	a	a	a	a	b	b
NGA6	a	a	a	b	a	a	a	a	a	a	b	b
FRI	a	a	a	a	a	a	a	a	a	a	a	a
T3H13	a	a	a	a	a	a	a	a	a	a	a	a
MSAT4.16	-	-	-	-	-	-	-	a	a	a	a	a
MSAT4.15	a	a	a	a	a	a	a	a	a	a	a	a
CIW7	a	a	a	a	a	a	a	a	a	a	a	a
MSAT4.12	a	b	a	a	a	a	a	a	-	-	-	-
MSAT4.28	b	a	a	a	a	a	a	a	a	a	a	a
NGA158	a	a	b	b	b	a	b	a	a	a	a	a
NGA106	a	a	b	h	b	b	b	a	a	a	a	a
MSAT5.14	a	a	b	b	b	b	b	a	a	a	a	a
NGA76	-	-	b	b	b	b	b	-	-	-	-	-
MSAT5.22	a	a	a	a	a	a	a	a	a	a	a	a
ATHS0191	a	a	a	a	a	a	a	a	a	a	a	b
MSAT5.9	a	a	a	a	a	a	a	b	b	a	a	a
JV61/62	a	a	a	a	a	a	a	b	b	b	b	b

Marker	49	50	51	52	53	54	55	56	57	58	59	60
NGA59	a	a	a	a	a	a	a	a	a	a	a	a
NGA63	a	a	a	a	a	a	a	a	a	a	a	a
MSAT1.10	a	a	a	b	b	a	b	a	a	a	a	a
ATHS0392	a	b	a	-	a	a	b	a	a	a	a	a
T27K12	-	-	-	-	-	-	-	-	-	-	-	-
CIW1	a	a	a	a	b	a	b	a	a	b	a	a
NGA128	-	-	-	-	-	-	-	-	-	-	-	-
NGA111	-	-	-	-	-	-	-	-	-	-	-	-
RGA	a	a	a	b	b	b	b	b	a	h	b	a
MSAT2.28	-	-	-	-	-	-	-	-	-	-	-	-
MSAT2.11	a	a	a	b	a	a	a	b	a	b	b	a
MSAT2.41	a	a	b	b	b	b	b	b	a	b	b	a
NGA361	a	a	b	b	a	a	a	b	a	b	b	a
MSAT2.22	a	a	b	b	b	b	b	b	a	a	b	a
NGA172	b	b	b	b	b	b	b	b	b	b	a	b
NGA162	b	b	b	b	b	b	b	b	b	b	b	b
MSAT3.19	a	b	b	b	b	b	b	b	b	b	a	b
MSAT3.28	a	b	b	a	a	a	a	a	b	b	b	a
NGA6	a	b	a	a	a	a	a	a	b	b	b	a
FRI	a	a	a	a	a	a	a	a	b	b	a	a
T3H13	a	a	a	a	a	a	a	a	b	b	a	b
MSAT4.16	a	a	a	a	a	a	a	a	h	b	b	b
MSAT4.15	a	a	a	-	a	a	a	a	h	b	b	b
CIW7	a	a	a	a	a	a	a	a	a	b	b	b
MSAT4.12	-	-	a	b	a	a	a	a	b	a	b	b
MSAT4.28	a	a	a	b	h	b	a	a	a	a	b	b
NGA158	a	a	a	a	b	a	a	a	a	b	b	b
NGA106	a	a	a	-	a	a	a	a	a	b	b	b
MSAT5.14	a	a	a	a	a	a	a	a	a	a	b	a
NGA76	-	-	-	-	-	-	-	-	-	-	b	b
MSAT5.22	a	a	a	a	a	a	a	a	a	h	b	b
ATHS0191	b	b	b	a	a	a	a	a	a	h	b	b
MSAT5.9	b	b	b	a	a	a	a	a	a	b	b	b
JV61/62	b	b	a	a	a	a	a	a	a	a	a	a

Marker	61	62	63	64	65	66	67	68	69	70	71	72
NGA59	a	a	a	a	a	a	a	a	a	a	a	b
NGA63	a	a	a	a	a	a	a	a	a	a	a	a
MSAT1.10	a	a	a	a	a	a	a	a	a	a	a	a
ATHS0392	a	a	a	a	a	a	a	a	a	a	a	a
T27K12	-	-	-	-	-	-	-	-	-	-	-	-
CIW1	b	b	b	a	a	a	a	a	a	a	a	a
NGA128	-	-	-	-	-	-	-	-	-	-	-	-
NGA111	-	-	-	-	-	-	-	-	-	-	-	-
RGA	b	a	b	a	a	a	a	a	a	a	a	a
MSAT2.28	-	-	-	-	-	-	-	-	-	-	-	-
MSAT2.11	b	a	b	a	a	a	a	a	b	b	-	a
MSAT2.41	b	a	b	a	b	a	b	a	b	b	a	b
NGA361	b	a	b	a	b	a	a	a	b	b	b	-
MSAT2.22	b	b	b	a	b	a	b	a	a	a	-	a
NGA172	b	b	b	a	a	a	a	a	a	a	a	a
NGA162	b	b	b	b	b	b	b	b	b	b	b	b
MSAT3.19	b	b	b	b	b	b	b	b	a	b	b	b
MSAT3.28	b	b	b	b	b	b	a	a	b	a	b	a
NGA6	b	b	b	b	b	b	a	a	b	a	b	a
FRI	b	a	a	b	b	a	b	a	b	b	a	a
T3H13	a	a	a	b	b	a	a	a	a	b	a	a
MSAT4.16	a	a	a	b	b	a	a	a	a	b	a	a
MSAT4.15	a	a	a	a	a	b	b	b	a	b	a	a
CIW7	a	a	a	a	a	b	a	b	a	b	a	a
MSAT4.12	a	a	a	a	a	b	b	b	a	b	a	b
MSAT4.28	b	a	a	b	a	b	b	b	a	a	b	b
NGA158	a	b	a	a	a	a	a	a	a	a	a	b
NGA106	a	b	a	a	a	a	a	a	a	a	a	h
MSAT5.14	a	b	a	a	a	a	a	a	a	a	a	h
NGA76	-	b	-	b	b	-	b	-	-	b	-	b
MSAT5.22	a	b	b	b	b	a	b	a	a	b	a	b
ATHS0191	a	b	b	b	b	a	b	a	a	b	a	b
MSAT5.9	a	b	b	b	b	a	a	b	a	b	a	a
JV61/62	-	a	a	b	b	a	b	a	a	b	a	a

Marker	73	74	75	76	77	78	79	80	81	82	83	84	85
NGA59	a	b	b	a	a	a	b	a	a	a	a	a	a
NGA63	a	a	b	a	a	a	b	a	a	a	a	a	a
MSAT1.10	a	a	a	a	a	a	a	a	a	a	a	a	a
ATHS0392	a	a	a	a	a	a	a	a	a	a	a	a	a
T27K12	-	-	-	-	-	-	-	-	-	-	-	-	-
CIW1	a	a	a	a	a	a	a	a	a	a	a	a	a
NGA128	-	-	-	-	-	-	-	-	-	-	-	-	-
NGA111	-	-	-	-	-	-	-	-	-	-	-	-	-
RGA	a	a	a	a	a	a	a	a	b	b	a	b	b
MSAT2.28	-	-	-	-	-	-	-	-	-	-	-	-	-
MSAT2.11	a	a	a	a	a	a	a	a	a	a	a	a	a
MSAT2.41	a	b	h	b	a	a	b	a	a	a	a	a	a
NGA361	-	-	-	-	-	-	-	-	-	-	-	-	-
MSAT2.22	a	b	a	b	a	a	b	a	a	a	a	a	a
NGA172	a	a	a	a	a	a	a	b	b	a	a	b	a
NGA162	b	b	b	b	b	b	b	b	b	b	b	b	b
MSAT3.19	b	a	b	b	b	a	b	a	b	b	b	b	b
MSAT3.28	a	a	a	a	a	a	a	a	a	b	b	a	b
NGA6	a	a	a	a	a	a	a	a	a	a	-	a	b
FRI	a	a	a	a	a	a	a	a	a	a	a	a	a
T3H13	b	a	a	b	b	a	a	a	a	a	b	a	a
MSAT4.16	b	a	a	b	b	a	a	a	b	a	b	a	a
MSAT4.15	b	a	a	a	b	b	a	b	b	a	-	a	b
CIW7	b	a	a	a	a	b	a	b	b	a	b	b	b
MSAT4.12	a	a	b	a	b	b	a	a	a	a	a	a	a
MSAT4.28	a	a	b	a	h	a	b	a	a	a	a	a	a
NGA158	b	a	h	a	a	b	a	a	a	a	a	a	a
NGA106	b	a	h	b	a	b	a	a	a	a	a	a	a
MSAT5.14	b	a	h	-	a	b	a	a	a	a	a	a	a
NGA76	b	-	b	-	-	b	-	-	-	-	-	-	-
MSAT5.22	b	a	b	a	a	b	a	a	a	a	a	a	a
ATHS0191	b	a	b	a	a	b	a	-	-	-	-	-	-
MSAT5.9	a	a	a	a	a	a	a	a	a	a	a	a	a
JV61/62	a	a	a	a	a	a	a	a	a	a	a	a	a

ACKNOWLEDGMENTS

This thesis was collaboration between the group of Dr. Seth Davis at the Max Planck Institute fuer Zuchtungsforchung, in Cologne, and the group of Prof. Dr. Ferenc Nagy at the Biological Research Center in Szeged. My warmest thank you goes to my thesis committee members Prof. Dr. Wolfgang Werr, for being the Committee Chairman, Prof. Dr. George Coupland and Prof. Dr. Ute Hoecker for being my thesis examiners. Thanks to Dr. Michael Bartch for being 'beisitzer' for my defense.

I would like to express my deepest gratitude to Dr. Seth Jon Davis for accepting me to work at his lab. Thank you for the guidance that was broadly offered at any point was asked. Special thanks for letting me work independent and deciding freely the project directions taken, and thereby develop my scientific skills. I am very grateful to you for stressing me to write, while I was still working in the lab. That said, regarding working hours, I have not found my limits yet. Like you say: **work harder!!!**

Next, I am indebted to Ferenc Nagy for accepting this to be a collaborative project. Moreover, I am very grateful to Ferenc that always finding time to help me on whatever problem I was facing.

I am also grateful to M. Koornneef for advising and providing genetic resources.

Many thanks to our administrative technician Amanda for the help provided whenever asked, and the endless support during the last stressful weeks.

My warmest thanks to Elsebeth for her help, especially, regarding advices on thesis formatting, gathering information about thesis submission. Most of all, I thank Elsebeth for the 'adventurous' tea experiences!!!

Many thanks to Elsebeth, Zhaojun, Gosia, Alfredo, Eva, Chiarina, and Sarah for the innumerable little favours, advises, questions, and the friendly atmosphere in the lab.

I am grateful to Roxana for helping me with the formatting, for going outs and for the fun that we had together.

I am grateful to Rebecca and Karolin for helping me with the german bureaucracy.

My deepest thank you goes to my husband for the endless support, encouragement patience, and understanding through out my PhD studies.

Θα ήθελα να εκφράσω την βαθύτερη ευγνωμοσύνη μου και τα αμέτρητα ευχαριστώ μου στους αγαπημένους μου γονείς, και αδέρφια, για την αμέριστη συμπαράσταση, και υπομονή καθώς και την περισσή αγάπη που με περιέβαλαν όλα αυτά τα χρόνια.

ERKLÄRUNG

„Ich versichere, dass ich die von mir vorgelegte Dissertation selbständig angefertigt, die benutzten Quellen und Hilfsmittel vollständig angegeben und die Stellen der Arbeit –einschließlich Tabellen, Karten und Abbildungen –, die anderen Werken im Wortlaut oder dem Sinn nach entnommen sind, in jedem Einzelfall als Entlehnung kenntlich gemacht habe; dass diese Dissertation noch keiner anderen Fakultät oder Universität zur Prüfung vorgelegen hat; dass sie – abgesehen von unten angegebenen Teil-publicationen – noch nicht veröffentlicht worden ist sowie, dass ich eine solche Veröffentlichung vor Abschluss des Promotionsverfahrens nicht vornehmen werde. Die Bestimmungen dieser Promotionsordnung sind mir bekannt. Die von mir vorgelegte Dissertation ist von Prof. Dr. George Coupland betreut worden.“

Max-Planck-Institut für Züchtungsforschung,
Köln 19 February 2008,

Eleni Boikoglou

TAGUNGEN

Poster Präsentationen:

Boikoglou, E., Davis, A., Nagy, F., Davis, S.J.: Natural Variation Studies For Circadian Clock Input Components In *Arabidopsis thaliana*
International Plant Photobiology Meeting, Paris, April 2006

Boikoglou, E., Davis, A., Nagy, F., Davis, S.J.: Natural Variation Studies For Circadian Clock Input Components In *Arabidopsis thaliana*
17th International Conference on Arabidopsis Research, Madison, Wisconsin, Juni 2006

LEBENS LAUF

Persoenlicher Informationen

Name: Boikoglou
Vorname: Eleni

Geburtstag: 20 May 1976
Geburtsort: Thessaloniki, Griechenland
Nationalitaet: Griechisch

Ausbildung

Juni 1994	Schulabschluss nach der 12 Klasse, N.Triglia Halkidiki
Jan 1997- Apr 2001	Studium die Pflanzen Produktion (BSc), Technologische Bildungsinstitut, Thessaloniki, Griechenland. Diplomarbeit: <i>Determination of bud differentiation in olive trees.</i> Betreuer: Prof. Dr. A. Roubos
Apr 2001- Dec 2002	Sekretaerin (Teilzeitarbeit), genossenschaftliche Landwirtschaft, N. Triglia Halkidiki
Feb 2002- Jul 2002	Auslandsaufenthalt in der Arbeitsgruppe von D.A.M. van der Kop, Genetwister Technologies B.V., Wageningen, The Netherlands. Arbeit: <i>Optimization of particle bombardment in horticultural species</i>
Sep 2002- Aug2004	Studium der Pflanzen Biotechnologie (MSc), Wageningen University, Wageningen, The Netherlands. Diplomarbeit: <i>Localisation of LHP1 in Arabidopsis thaliana roots</i> Betreuer: Prof. Dr. Ton Bisseling
Oct 2004	Beginn der Doktorarbeit am Max-Planck-Institut fuer Zuechtungsforschung, Koeln, in der Arbeitsgruppe von Dr. Seth J. Davis